Journal of Ophthalmology

Ocular Angiogenesis

Guest Editors: Juliana L. Dreyfuss, Ricardo J. Giordano, and Caio V. Regatieri

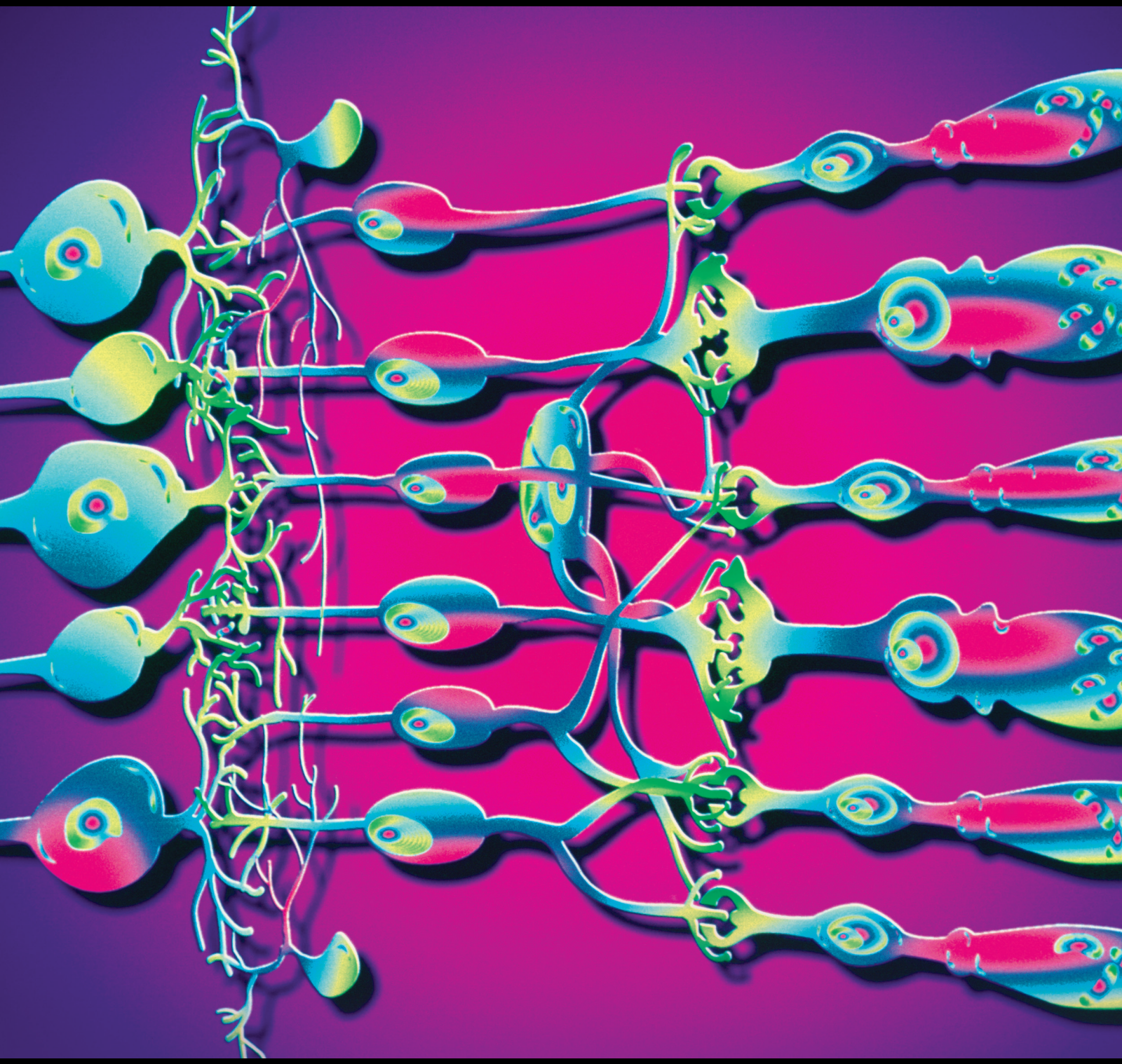

Ocular Angiogenesis

Journal of Ophthalmology

Ocular Angiogenesis

Guest Editors: Juliana L. Dreyfuss, Ricardo J. Giordano, and Caio V. Regatieri

Editorial Board

Contents

Hindawi Publishing Corporation
Journal of Ophthalmology
Volume 2015, Article ID 892043, 2 pages
http://dx.doi.org/10.1155/2015/892043

Editorial

Ocular Angiogenesis

Juliana L. Dreyfuss,[1,2] Ricardo J. Giordano,[3] and Caio V. Regatieri[4,5]

[1]*Department of Health Informatics, Federal University of São Paulo, Paulista School of Medicine, 04023-062 São Paulo, SP, Brazil*
[2]*Department of Biochemistry, Federal University of São Paulo, Paulista School of Medicine, 04039-032 São Paulo, SP, Brazil*
[3]*Department of Biochemistry, University of São Paulo, 05508-000 São Paulo, SP, Brazil*
[4]*Department of Ophthalmology, Federal University of São Paulo, Paulista School of Medicine, 04023-062 São Paulo, SP, Brazil*
[5]*Department of Ophthalmology, Tufts University School of Medicine, Boston, MA 02111, USA*

Correspondence should be addressed to Juliana L. Dreyfuss; jdreyfuss@unifesp.br

Received 22 June 2015; Accepted 5 July 2015

This special issue shows the continuing efforts to understand the molecular biology and the development of new treatments and diagnostic tools for ocular angiogenesis. In this issue we bring novel research and discuss challenges in developing therapeutics for ocular neovascular diseases, angiogenesis and its role in ocular diseases, and the mechanisms leading to progressive vessel dysfunction and blindness.

This issue shows papers describing clinical and experimental studies of ocular angiogenesis (OA), showing advances in molecular biology and new insights into retinal, corneal, and choroidal neovascularization and imaging techniques, besides current concepts in the treatment of ocular angiogenesis. This special issue promotes new ideas, inspires discussion of the concepts presented in the issue, increases the understanding of mechanisms that control the dynamic process of angiogenesis in the eye, and brings together the available information of new types of treatments.

Angiogenesis has fundamental importance in disease and health. It is the formation of new blood vessels from preexisting vasculature. Angiogenesis is a complex process constituting multiple steps. Extracellular matrix degrading enzymes secreted by activated endothelial cells degrade the basement membrane, allowing the migration and proliferation of these cells, resulting in the formation of solid endothelial cell capillary tubes. Pathologic angiogenesis in the eye can lead to severe visual impairment. The ocular angiogenesis can occur in retina, choroid, and cornea. The ocular angiogenesis is related to a broad spectrum of disorders such as wet age-related macular degeneration (AMD), diabetic retinopathy, retinal artery or vein occlusion, retinopathy of prematurity (ROP), neovascular glaucoma, and corneal neovascularization secondary to infectious or inflammatory processes.

Ocular neovascularization is an intricate process controlled by myriad angiogenic agents such as growth factors, cytokines, and extracellular matrix components. Angiogenesis is regulated by a balance between endogenous proangiogenic and antiangiogenic factors. And the diseases where ocular angiogenesis occurs require disruption of such balance; thus, the angiogenic switch must be turned "on" for neovascularization progression.

The proangiogenic growth factors implicated in pathologic vessel formation in ocular diseases are fibroblast growth factor (FGF), platelet-derived endothelial growth factor (PDGF), and vascular endothelial growth factor (VEGF), among others. The antiangiogenic factors are pigment epithelium-derived factor (PEDF), endostatin, and thrombospondin, among others. Identification of these angiogenesis regulators has enabled the development of novel therapeutic approaches for many ocular disorders.

Recent clinical studies regarding the intravitreal injection of monoclonal antibodies anti-VEGF (ranibizumab and bevacizumab) have shown excellent results in the treatment of degenerative and vascular chorioretinal diseases. Diagnostic imaging tools have played an increasingly important role in eye care in recent years.

Advances in fundus imaging make assessment of peripheral neovascularization in many chorioretinal diseases possible, such as diabetic retinopathy and retinal vein occlusion. The technology has unveiled new insights into the role of peripheral pathology in retinal vascular, degenerative, and inflammatory diseases.

Additionally, new techniques in optical coherence tomography have improved the axial image resolution and image acquisition and the ability to allow the detection of individual retinal layers and lesion components. With spectral domain it is possible to identify retinal new vessels in wet age-related macular degeneration using OCT angiography. The next step will be the swept source OCT development, which will make the blood flow measurements possible. The study by W. Chen et al. investigates the aqueous levels of pigment epithelium-derived factor (PEDF) and macular choroidal thickness in individuals with high myopia. The authors noticed a significant correlation between aqueous PEDF levels and macular choroidal thickness in patients without angiogenesis but no association with the group of patients with pathological angiogenesis. It would be interesting to expand these association studies to include vascular endothelial growth factor and assess whether the balance between VEGF and PEDF levels could predict disease progression and resistance to anti-VEGF therapy. Another study by S. Rusnak et al. shows that the concentrations of IL-6, TGF-β1, and VEGF correlate with the severity of proliferative diabetic retinopathy and were particularly high in patients with refractive neovascular glaucoma. IL-6 is a multifunctional cytokine with pro- and anti-inflammatory properties and TGF-β1 is an interesting therapeutic target for ocular angiogenesis. Their results reinforce these findings and also suggest that, in patients with neovascular glaucoma refractory to treatment, IL-6 and TGF-β1 may have a potential use in patient stratification and in determining personalized medical needs.

The mechanisms and new experimental treatments for corneal neovascularization are investigated and presented in this issue. K. Tomoyose et al. show that the loss of TRP vanilloid subtype 1 (TRPV1), the capsaicin receptor, did not affect VEGF-dependent neovascularization in cell culture. On the other hand, lack of TRPV1 inhibited neovascularization in mouse corneal stroma following cauterization. The study performed by J. Yoshida et al. shows the inhibition of corneal neovascularization by subconjunctival injection of Fc-endostatin in rabbit corneas. The endostatin is an angiogenesis inhibitor, a fragment of collagen XVIII, and the Fc-endostatin was developed by fusing endostatin to the Fc region of an IgG molecule. The subconjunctival injection of this antiangiogenic molecule showed to be efficient and safe in rabbit model.

The role of stromal cells in angiogenesis is also addressed in this special issue. The role of molecules in pericytes and anti-VEGF therapy in fibroblasts is shown in this issue. Pericytes are contractile cells that interact with endothelial cells stabilizing the newly formed vessel. These cells modulate vascular permeability and blood flow and can regulate angiogenesis modulating endothelial proliferation, differentiation, and migration. The study by L. Chen et al. shows the protective effect of apelin (an endogenous ligand of G protein-coupled receptor APJ) from apoptosis due to chemical hypoxia induced in rat retinal pericytes. The study performed by L. Lytvynchuk et al. shows the antiproliferative, apoptotic, and autophagic activity of anti-VEGFs on fibroblasts cultures. These effects upon fibroblasts may explain the cellular response and the etiology of choroidal neovascularization involution after treatment with anti-VEGFs.

This special issue additionally presents very interesting clinical studies. R. Mastropasqua et al. reveal that optical coherence tomography-angiography is a noninvasive dyeless method to image the retinal microcirculation; the images provided distinct vascular patterns for different diseases. It provides detailed images of retinal vascular plexuses and quantitative data of pathologic structures. P. Calvo et al. analyzed the visual outcome in 51 patients with wet age-related macular degeneration depending on the number of ranibizumab injections after 3 years of follow-up. The best outcomes were found in stable wet AMD patients that received ≥ 7 ranibizumab intravitreal injections in 3 years. Following the same treatment modality for wet AMD, anti-VEGF therapy using ranibizumab, A. García-Layana et al. compile data showing the comparison of different regimens of intravitreal injections and their outcomes. Finally, but not less interestingly, S. D. Nicoara et al. show the outcomes of bevacizumab treatment of retinopathy of prematurity. They recorded no complications subsequent to the intravitreal injections of bevacizumab with no late retinal detachment. In addition the study shows a very high ROP regression rate after one intravitreal bevacizumab injection.

We expect that the present volume on ocular angiogenesis may provide useful information to understand the mechanisms and new therapies and diagnostic tools for ocular angiogenesis to the readers.

Juliana L. Dreyfuss
Ricardo J. Giordano
Caio V. Regatieri

Hindawi Publishing Corporation
Journal of Ophthalmology
Volume 2015, Article ID 137136, 8 pages
http://dx.doi.org/10.1155/2015/137136

Research Article

Inhibition of Corneal Neovascularization by Subconjunctival Injection of Fc-Endostatin, a Novel Inhibitor of Angiogenesis

Junko Yoshida,[1] Robert T. Wicks,[2] Andrea I. Zambrano,[1] Betty M. Tyler,[2] Kashi Javaherian,[3] Rachel Grossman,[2] Yassine J. Daoud,[1] Peter Gehlbach,[1] Henry Brem,[1,2,4] and Walter J. Stark[1]

[1] *Wilmer Eye Institute, Johns Hopkins University School of Medicine, Baltimore, MD 21287, USA*
[2] *Department of Neurosurgery, Johns Hopkins University School of Medicine, Baltimore, MD 21231, USA*
[3] *Center of Cancer Systems Biology, St. Elizabeth's Medical Center, Tufts University School of Medicine, Boston, MA 02111, USA*
[4] *Departments of Oncology and Biomedical Engineering, Johns Hopkins University School of Medicine, Baltimore, MD 21205, USA*

Correspondence should be addressed to Betty M. Tyler; btyler@jhmi.edu

Received 19 August 2014; Revised 16 December 2014; Accepted 12 January 2015

Academic Editor: Juliana L. Dreyfuss

We assessed the antiangiogenic effects of subconjunctival injection of Fc-endostatin (FcE) using a human vascular endothelial growth factor-induced rabbit corneal neovascularization model. Angiogenesis was induced in rabbit corneas through intrastromal implantations of VEGF polymer implanted 2 mm from the limbus. NZW rabbits were separated into groups receiving twice weekly subconjunctival injections of either saline; 25 mg/mL bevacizumab; 2 mg/mL FcE; or 20 mg/mL FcE. Corneas were digitally imaged at 5 time points. An angiogenesis index (AI) was calculated (vessel length (mm) × vessel number score) for each observation. All treatment groups showed a significant decrease in the vessel length and AI compared to saline on all observation days ($P < 0.001$). By day 15, FcE 2 inhibited angiogenesis significantly better than FcE 20 ($P < 0.01$). There was no significant difference between FcE 2 and BV, although the values trended towards significantly increased inhibition by BV. BV was a significantly better inhibitor than FcE 20 by day 8 ($P < 0.01$). FcE was safe and significantly inhibited new vessel growth in a rabbit corneal neovascularization model. Lower concentration FcE 2 exhibited better inhibition than FcE 20, consistent with previous FcE studies referencing a biphasic dose-response curve. Additional studies are necessary to further elucidate the efficacy and clinical potential of this novel angiogenesis inhibitor.

1. Background

To maintain transparency, the cornea is an avascular tissue. Infectious and inflammatory processes, however, can induce new vessel growth causing corneal neovascularization, which leads to scarring, edema, and blindness [1]. Corneal neovascularization affects an estimated 4.1% of all patients presenting to general ophthalmology offices in the US [2]. It also contributes to worsening prognosis after penetrating keratoplasty (PK). A meta-analysis has shown a significantly higher risk of corneal graft rejection with increased number of corneal quadrants affected by neovascularization prior to keratoplasty [3].

Corneal neovascularization is thought to occur through the imbalance of angiogenic and antiangiogenic protein factors. Vascularized human corneas have been shown to have significant upregulation of vascular endothelial growth factor (VEGF), matrix metalloproteinases (MMP), and basic fibroblastic growth factor (bFGF) [4]. Bevacizumab (BV) (Avastin, Genentech, Inc., San Francisco, CA) is a monoclonal antibody that targets human VEGF (VEGF) and has been studied as a potentially potent therapy for corneal neovascularization. Antiangiogenic monotherapy with a drug such as BV, which targets VEGF alone, however, may not provide the best long-term therapy since inhibition of one antiangiogenic factor can result in the upregulation of others leading to

acquired drug resistance [5]. In addition, lymphangiogenesis has been identified as an important process involved in the pathogenesis of corneal graft rejection. Endostatin, in contrast to bevacizumab, has been identified as a potent inhibitor of both neovascularization and lymphangiogenesis [6–8].

Another potential deficiency of BV therapy is its association with systemic side effects seen during trials of its use in age-related macular degeneration, including bleeding, hypertension, and stroke [9–12]. Thus, an angiogenesis inhibitor that blocks multiple promoters of angiogenesis with few systemic side effects is desired.

Endostatin promised such potential. As a 20 kDa fragment of collagen XVIII, it modifies 12% of the human genome in order to downregulate angiogenesis with few systemic side effects [13–15]. By affecting multiple angiogenic pathways simultaneously [16], endostatin may allow for a much lower possibility of drug resistance. In contrast to the noted hypertension found with BV use in human studies [17, 18], endostatin was noted to decrease systolic blood pressure by almost 10 mmHg when dosed daily in animal studies [19]. Endostatin was initially studied in preclinical models of corneal neovascularization and tumor models [20, 21]. Despite high expectations, human endostatin had a limited response in phase I and II human cancer clinical trials largely due to two deficiencies. First, the half-life of endostatin in circulation was only 42.3 minutes. Second, approximately 50% of the recombinant human endostatin used in the clinical trials lacked four amino acids at the NH_2 terminus, which resulted in a nonfunctional molecule due to an inability to bind zinc [22].

In order to engineer a more stable form of endostatin, Fc-endostatin (FcE) was developed by fusing endostatin to the Fc region of an IgG molecule [22]. The presence of the Fc portion increases the half-life to greater than one week and conserves the molecule's zinc affinity. This increase in half-life is similar to the role of the Fc domain in BV, which increases the molecule's half-life to weeks rather than hours [23]. FcE was recently shown to be effective in a rodent model of high-grade glioma using various delivery methodologies [24].

We set out to evaluate the safety and antiangiogenic efficacy of subconjunctival injection of FcE using a rabbit VEGF-induced corneal neovascularization model. This paper is the first published assessment of FcE as a potential therapy for corneal neovascularization.

2. Methods

2.1. Animals. Eight male New Zealand White rabbits, each weighing 4.5 to 6.5 kg (Robinson Industry Farms, Mocksville, NC) were used. Care and treatment of all rabbits were in strict agreement with the Association for Research in Vision and Ophthalmology (ARVO) Statement for the Use of Animals in Ophthalmic and Vision Research and with the approval of the Johns Hopkins University Animal Care and Use Committee. Rabbits were housed in standard animal facilities, one animal per cage, and given free access to food and Baltimore City water.

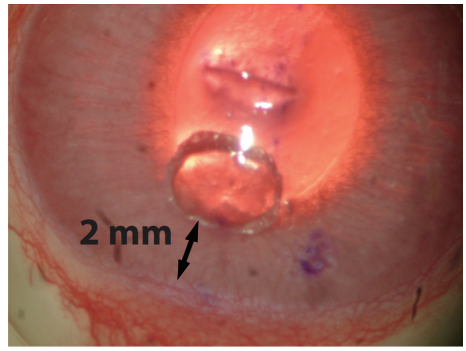

Figure 1: VEGF-induced corneal neovascularization model. Each human vascular endothelial growth factor (VEGF) polymer was inserted into surgically created corneal micropockets. Two micropockets, at 6 and 12 o'clock, were made from the midline incision. One VEGF polymer was placed at the end of each micropocket at a distance of 2 mm from the limbus.

2.2. Anesthesia. For intracorneal implantations and subsequent operative microscope examinations the animals were anesthetized with a mixture of xylazine 10 mg/kg (Butler Schein, Dublin, OH) and ketamine 2 mg/kg (Butler Schein, Dublin, OH). The ocular surface was anesthetized with topical 0.5% proparacaine hydrochloride (Alcaine, Alcon, Fort Worth, TX). Pain control was provided, as needed, with subcutaneous injection of buprenorphine HCL 0.1 mg/kg (Bedford Labs, Bedford, OH).

2.3. VEGF Polymer Preparation. Ethylene-vinyl acetate copolymer (40% vinyl acetate by weight, Elvax 40P) (Du Pont Co., Wilmington, DE) was prepared as previously described [19]. Briefly, human VEGF (Peprotech, Rocky Hill, NJ) was incorporated into the ethylene-vinyl acetate copolymer (EVAc) matrix. EVAc (130 mg) was dissolved in methylene chloride (1.8 mL) and VEGF (20 μg) was added. The mixture was poured into cylindrical glass molds measuring 5 mm × 220 mm and placed in −20°C for 48 hours and the methylene chloride was allowed to passively evaporate. The VEGF polymer was then cut into uniform pellets of size 1 mm × 1 mm × 0.5 mm. The VEGF amount per implanted polymer pellet totaled 770 ng.

2.4. VEGF-Induced Corneal Neovascularization Model. We use a corneal angiogenesis model as previously described by Sefton et al. [25]. Rabbits were placed under general anesthesia and topical 0.5% proparacaine hydrochloride was applied to the corneal surface. 5% povidone-iodine was applied on the ocular surface for antisepsis. At the center of the cornea, a 2 mm horizontal incision was placed to the midstromal level using the bevel of a 16 gauge needle (BD, Franklin Lakes, NJ). Two micropockets were made from the incision towards 6 and 12 o'clock by dissecting the corneal stroma with an iris spatula (Figure 1). One VEGF polymer was placed at the end of each micropocket 2 mm apart from the limbus. A total of 32 VEGF polymer pellets were placed (2 pellets per cornea, one at 6 o'clock and one at 12 o'clock). The surgery day was referred to as day 0.

Rabbits were separated into 4 groups (8 pellets per group). Each eye received a subconjunctival injection, one half of each dose was injected at 6 and 12 o'clock in proximity to each VEGF polymer, with either 0.125 mL of 0.9% normal saline (NS), 0.1 mL of 25 mg/mL BV, 0.125 mL of 20 mg/mL human FcE (FcE 20) (Bio X Cell, West Lebanon, New Hampshire), or 0.125 mL of 2 mg/mL human FcE (FcE 2). A volume of 0.125 mL of FcE was used in order to approximate the mg concentration of BV 25 mg/mL. Subconjunctival injections were performed twice weekly starting on the day of surgery: days 0, 5, 8, and 12.

2.5. Corneal Neovascularization Evaluation. Corneal neovascularization was assessed via operative microscopy (Carl Zeiss, Germany) on days 0, 5, 8, 12, and 15. The corneas were digitally imaged, and the images were analyzed using ImageJ software (NIH.gov). To have a single standardized value that incorporated both vessel length and number of vessels, we calculated an angiogenesis index (AI), as previously described by Tamargo et al. [26]. Briefly, the number of new vessels associated with each VEGF polymer was given a numbered score: 0 = no vessels, 1 =< 10 vessels, 2 =≥ 10 vessels with a visible iris, and 3 =≥ 10 vessels with no visible iris. Neovessel length was assessed as distance from the limbus to the leading edge of the new vessels in millimeters (mm). AI was then calculated as

$$\text{AI} = \text{vessel length (mm)} \times \text{vessel number score}. \quad (1)$$

Given that the greatest vessel length achievable was 2 mm (distance to the VEGF polymer from the limbus) and the highest vessel number score was 3, the AI ranged from 0 to 6.

2.6. Histological Evaluation of Corneas. All rabbits were sacrificed after the last observation on day 15. Both eyes of all rabbits were enucleated and placed in 10% formalin. After fixation in formalin, corneas were removed and cut in half at the midline, one VEGF polymer pellet in each half. All cornea halves were embedded in paraffin with the cornea-sclera border facing down, sectioned, and stained with hematoxylin and eosin (H&E). The extent of neovascularization was analyzed and photographed using digital, light microscopy (BX41, Olympus, Japan; Diagnostic Instruments, Inc., Sterling Heights, MI).

2.7. Statistical Analysis. Total sample size was 32 with measurements of neovascularization taken on days 5, 8, 12, and 15. Vessel length and AI values recorded throughout the observation period were analyzed for statistical significance using a repeated measures 2-way analysis of variance (2-way ANOVA). Post hoc analysis was performed using the Bonferroni test to correct for multiple comparisons (Graphpad Prism 5.0, CA).

3. Results

3.1. Analysis of Corneal Neovascularization. Neovascularization was analyzed with respect to both vessel length and AI. The representative images taken on days 0, 8, and 15 before and after treatment with BV and FcE are shown in Figure 2. Figure 3 displays the mean vessel length for each treatment group. While NS control developed corneal vessels nearly 2 mm length, all treatment groups had a statistically significant decrease in vessel length compared to NS on all observation days ($P < 0.001$). FcE 2 significantly decreased vessel length more than FcE 20 on days 12 and 15 ($P < 0.05$). BV inhibited vessel length significantly more than FcE 2 on days 12 and 15 ($P < 0.05$). BV decreased vessel length significantly more than FcE 20 on days 8, 12, and 15 ($P < 0.01$).

Corneal neovascularization was then analyzed by calculating AI (Figure 4). AI provided a more comprehensive analysis of the neovascularization as it reflects a more direct assessment of neovessel density. All treatment groups showed a significant decrease in the AI compared to NS on all observation days ($P < 0.001$). FcE 2, when compared to NS, decreased AI by a factor of 8.0-fold, 7.0-fold, 8.8-fold, and 6.8-fold on days 5, 8, 12, and 15, respectively. FcE 20, when compared to NS, decreased AI by a factor of 68-fold, 2.7-fold, 3.6-fold, and 2.4-fold at days 5, 8, 12, and 15, respectively. BV decreased AI compared to NS by a factor of 138-fold on day 15, with no vessel growth at days 5, 8, and 12. A significant difference in AI was not found between BV and FcE 2 during the study period, although BV appeared to have a nonsignificant qualitative improvement over FcE 2 during the study period. BV was found to have a significantly smaller AI than FcE 20 on days 8, 12, and 15 ($P < 0.01$). By day 15, AI of FcE 2 was significantly smaller than FcE 20 ($P < 0.01$). No obvious side effects were observed topically or systemically from either FcE or BV.

3.2. Analysis of Cornea Histology. The cornea sections within the NS group showed the greatest corneal neovascularization with a relative increase in both vessel number and vessel circumference when compared with the treatment groups (Figure 5). New vessels were observed within both the superficial and deep stroma. Corneas from the BV treated group had the fewest number of new vessels. The neovascularization present in the BV group was primarily isolated to the superficial stroma and showed a relative decrease in circumference. FcE corneal sections revealed decreased neovascularization, with decreased vessel circumference, when compared with NS but a greater amount than corneas within the BV group. There was no notable histological difference between the neovascularization that occurred in the FcE 2 group and the FcE 20 group.

4. Discussion

Subconjunctival injection of FcE was found to be well tolerated and to significantly decrease corneal neovascularization in a rabbit model of VEGF-induced neovascularization. Although BV inhibited the corneal neovascularization best in this model, no statistical difference was identified between FcE 2 and BV. FcE 20 had an early decrease in neovascularization noted on day 5, but this benefit was less than that noted by FcE 2 on day 8. Both BV and FcE 2 significantly inhibited corneal neovascularization better than FcE 20. No corneal

Figure 2: Representative photos of each treatment group on days 0, 8, and 15 after implantation of human vascular endothelial growth factor (VEGF) polymer within the corneal stroma micropocket. Treatment drugs were delivered via subconjunctival injection on days 0, 5, 8, 12, and 15. No statistical difference was noted between bevacizumab (BV) and Fc-endostatin 2 mg/mL (FcE 2). BV was found to significantly decrease neovascularization when compared with Fc-endostatin 20 mg/mL (FcE 20) by day 8. FcE 2 was found to significantly decrease neovascularization compared with FcE 20 by day 15.

ulcers, edema, infection, or conjunctival necrosis was noted as a result of either the subconjunctival injection of FcE or BV.

The purpose of this study was as a proof of concept to determine the safety and relative efficacy of FcE in inhibiting corneal neovascularization. We chose to use a VEGF-induced corneal neovascularization model and as a positive control BV, a monoclonal antibody to VEGF, was used. In the short time course of this study, BV inhibited

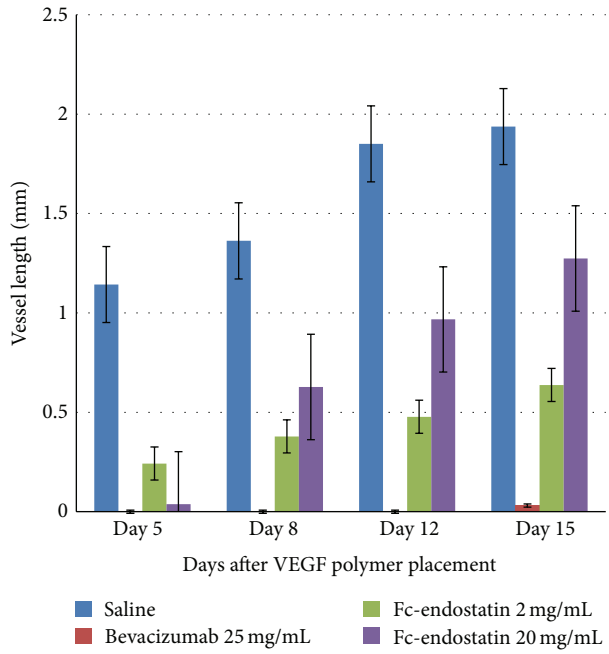

Figure 3: Inhibition of human vascular endothelial growth factor- (VEGF-) induced corneal neovascularization in rabbit. Mean vessel length ± standard error of the mean (SEM) of new vessels in control and treatment groups (BV: bevacizumab; FcE: Fc-endostatin).

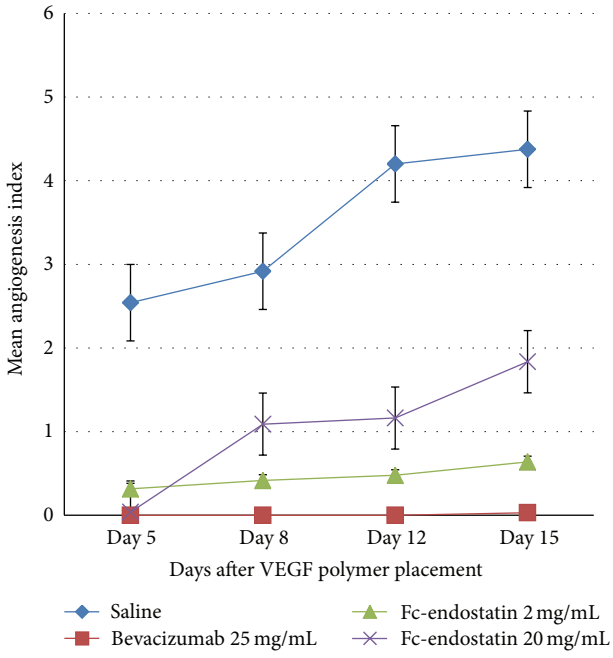

Figure 4: Inhibition of human vascular endothelial growth factor- (VEGF-) induced corneal neovascularization in rabbit. Mean angiogenesis index (AI) ± standard error of the mean (SEM) of new vessels in control and treatment groups (BV: bevacizumab; FcE: Fc-endostatin).

the corneal neovascularization the most, as expected. Human FcE, however, was found to be noninferior to BV, representing an important finding. FcE may be more effective than BV on a multicytokine angiogenesis model given its known multitargeted antiangiogenic effect.

FcE 2 was found to outperform the higher concentration FcE 20 by the completion of the experiment on day 15. Initially, FcE 20 had an impressive decrease in neovascularization on day 5, but this effect had weaned by day 15. This finding had been described by Celik et al., who noted the antitumor activity of endostatin to have a biphasic dose-response curve [22, 27]. Efficacy is found to proportionally increase until an optimal dose is reached with higher doses resulting in decreased response. A biphasic dose-response curve has been noted in studies of other antiangiogenic cytokines such as interferon-α (IFN-α) [27, 28] and the diabetes medication rosiglitazone, a known tumor cell angiogenesis inhibitor [29]. FcE has also been demonstrated to have a similar pattern of activity [30]. Further dose response analysis will need to be performed within the corneal neovascularization model to fully characterize the dose-response relationship.

Several limitations to the current study should be taken into account. The first limitation comes as a result of the corneal neovascularization model selected that allows for the controlled release of VEGF and does not entirely mimic the natural proangiogenic environment in which corneal neovascularization develops within a damaged cornea. Additional studies utilizing other models such as the mechanical limbal injury-induced corneal neovascularization model [31], alkali-induced corneal neovascularization model [31, 32], and the corneal micropocket tumor implantation model [26] should be considered in future experiments. Secondly, the study was not designed to determine the most optimal dose of FcE or the cause of the biphasic dose response. Additional studies to determine the mechanism of inhibition and establish a complete dose-response curve are warranted. A third limitation of the current study is that long-term efficacy of FcE was not assessed. Further preclinical research would need to be completed prior to pursuing human trials into FcE as a potential novel inhibitor of corneal neovascularization.

5. Conclusions

FcE is a novel antiangiogenic compound shown to significantly inhibit new vessel growth in a rabbit corneal neovascularization model. Lower concentration FcE 2 exhibited better inhibition than FcE 20—consistent with previous FcE studies referencing a biphasic dose-response curve. The FcE 2 concentration was found to be noninferior to BV in this VEGF model. Because of its known multitargeted, antiangiogenic properties, FcE holds great promise for future clinical efficacy. Further studies are necessary to elucidate the clinical potential and optimal dosing of this novel inhibitor of corneal neovascularization.

Abbreviations

VEGF: Human vascular endothelial growth factor
BV: Bevacizumab

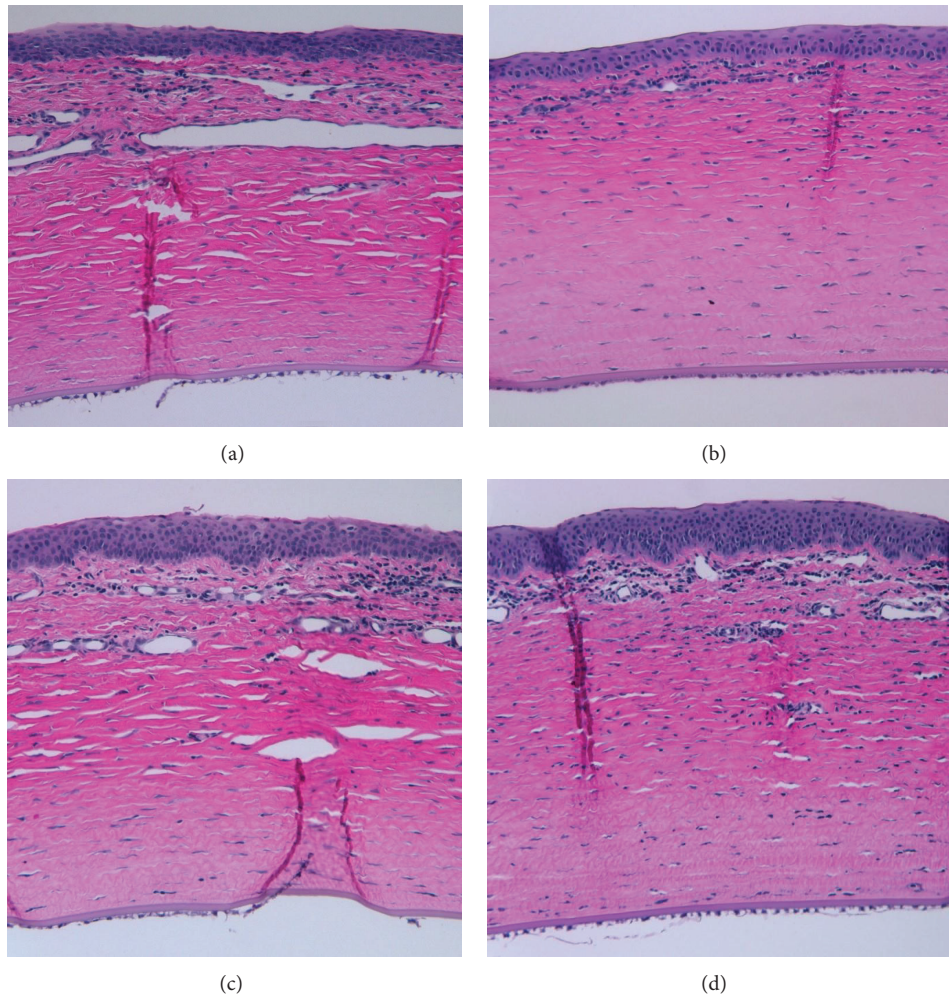

Figure 5: Corneal histology. On day 15, all eyes were enucleated and fixed in formalin. After fixation in formalin, corneas were removed, embedded in paraffin, and stained with hematoxylin and eosin (H&E). Pictured are H&E stained slices taken at the cornea-sclera border. The cornea epithelial surface is facing up. (a) Normal saline (group); (b) bevacizumab 25 mg/mL; (c) Fc-endostatin 2 mg/mL; and (d) Fc-endostatin 20 mg/mL.

FcE:	Fc-endostatin
EVAc:	Ethylene-vinyl acetate copolymer
FcE 20:	20 mg/mL human FcE
FcE 2:	2 mg/mL human FcE
AI:	Angiogenesis index.

Conflict of Interests

The authors declare that they have no competing interests.

Authors' Contribution

Junko Yoshida carried out study design, participated in polymer pellet synthesis and implantation, performed semiweekly injections and photography, drafted the paper, and assisted in critical revisions. Robert T. Wicks assisted with study design, participated in polymer pellet synthesis and implantation, performed semiweekly injections and photography, performed data analysis and interpretation, drafted the paper, and assisted in critical revisions. Andrea I. Zambrano assisted in polymer implantation, performed semiweekly injections and photography, performed data analysis, performed histology and photography, drafted the paper, and assisted in critical revisions. Betty M. Tyler carried out study design, participated in polymer design and synthesis, drafted the paper, and assisted in critical revisions. Kashi Javaherian assisted in study design and in synthesis of Fc-endostatin. Rachel Grossman assisted in study design and in drafting the paper. Yassine J. Daoud assisted in data analysis and interpretation and in drafting the paper and critical revisions. Peter Gehlbach assisted in study design and data interpretation. Henry Brem assisted in study design and methodology, in drafting the paper, and in critical revisions. Walter J. Stark assisted in study concept, in study design and methodology, in drafting the paper, and in critical revisions. All authors read and approved the final paper. Junko Yoshida and Robert T. Wicks contributed equally to the design and

execution of this study and composition of the paper and, therefore, equally share first authorship of this publication.

Acknowledgments

The authors would like to thank the Kwok Family Research Fund, Andreas Dracopoulos, and Ali and Peter Jennison for their generous support of this research. This work was also supported by the Research Scholar Grant 116293-RSG-08-119-01-CCE from the American Cancer Society (B. M. Tyler) as well as by the American Physicians Fellowship for Medicine in Israel (R. Grossman).

References

[1] D. Gupta and C. Illingworth, "Treatments for corneal neovascularization: a review," *Cornea*, vol. 30, no. 8, pp. 927–938, 2011.

[2] P. Lee, C. C. Wang, and A. P. Adamis, "Ocular neovascularization: an epidemiologic review," *Survey of Ophthalmology*, vol. 43, no. 3, pp. 245–269, 1998.

[3] B. Bachmann, R. S. Taylor, and C. Cursiefen, "Corneal neovascularization as a risk factor for graft failure and rejection after keratoplasty: an evidence-based meta-analysis," *Ophthalmology*, vol. 117, no. 7, pp. 1300.e7–1305.e7, 2010.

[4] J.-H. Chang, E. E. Gabison, T. Kato, and D. T. Azar, "Corneal neovascularization," *Current Opinion in Ophthalmology*, vol. 12, no. 4, pp. 242–249, 2001.

[5] A. Abdollahi, L. Hlatky, and P. E. Huber, "Endostatin: the logic of antiangiogenic therapy," *Drug Resistance Updates*, vol. 8, no. 1-2, pp. 59–74, 2005.

[6] X. Ma, Y. Yao, D. Yuan et al., "Recombinant human endostatin endostar suppresses angiogenesis and lymphangiogenesis of malignant pleural effusion in mice," *PLoS ONE*, vol. 7, no. 12, Article ID e53449, 2012.

[7] W. Zhuo, Y. Chen, X. Song, and Y. Luo, "Endostatin specifically targets both tumor blood vessels and lymphatic vessels," *Frontiers of Medicine in China*, vol. 5, no. 4, pp. 336–340, 2011.

[8] C. Cursiefen, L. Chen, M. R. Dana, and J. W. Streilein, "Corneal lymphangiogenesis: evidence, mechanisms, and implications for corneal transplant immunology," *Cornea*, vol. 22, no. 3, pp. 273–281, 2003.

[9] R. J. Campbell, C. M. Bell, J. M. Paterson et al., "Stroke rates after introduction of vascular endothelial growth factor inhibitors for macular degeneration: a time series analysis," *Ophthalmology*, vol. 119, no. 8, pp. 1604–1608, 2012.

[10] D. F. Martin, M. G. Maguire, S. L. Fine et al., "Ranibizumab and bevacizumab for treatment of neovascular age-related macular degeneration: two-year results," *Ophthalmology*, vol. 119, no. 7, pp. 1388–1398, 2012.

[11] T. Ueta, H. Mori, A. Kunimatsu, T. Yamaguchi, Y. Tamaki, and Y. Yanagi, "Stroke and anti-VEGF therapy," *Ophthalmology*, vol. 118, no. 10, pp. 2093–2093.e2, 2011.

[12] D. S. Boyer, J. S. Heier, D. M. Brown, S. F. Francom, T. Ianchulev, and R. G. Rubio, "A Phase IIIb study to evaluate the safety of ranibizumab in subjects with neovascular age-related macular degeneration," *Ophthalmology*, vol. 116, no. 9, pp. 1731–1739, 2009.

[13] M. S. O'Reilly, T. Boehm, Y. Shing et al., "Endostatin: an endogenous inhibitor of angiogenesis and tumor growth," *Cell*, vol. 88, no. 2, pp. 277–285, 1997.

[14] A. Abdollahi, P. Hahnfeldt, C. Maercker et al., "Endostatin's antiangiogenic signaling network," *Molecular Cell*, vol. 13, no. 5, pp. 649–663, 2004.

[15] J. Folkman, "Antiangiogenesis in cancer therapy—endostatin and its mechanisms of action," *Experimental Cell Research*, vol. 312, no. 5, pp. 594–607, 2006.

[16] T. Boehm-Viswanathan, "Is angiogenesis inhibition the Holy Grail of cancer therapy?" *Current Opinion in Oncology*, vol. 12, no. 1, pp. 89–94, 2000.

[17] J. C. Yang, L. Haworth, R. M. Sherry et al., "A randomized trial of bevacizumab, an anti-vascular endothelial growth factor antibody, for metastatic renal cancer," *The New England Journal of Medicine*, vol. 349, no. 5, pp. 427–434, 2003.

[18] H. Hurwitz, L. Fehrenbacher, W. Novotny et al., "Bevacizumab plus irinotecan, fluorouracil, and leucovorin for metastatic colorectal cancer," *The New England Journal of Medicine*, vol. 350, no. 23, pp. 2335–2342, 2004.

[19] S. B. Sunshine, S. M. Dallabrida, E. Durand et al., "Endostatin lowers blood pressure via nitric oxide and prevents hypertension associated with VEGF inhibition," *Proceedings of the National Academy of Sciences of the United States of America*, vol. 109, no. 28, pp. 11306–11311, 2012.

[20] Y. Yu, K. S. Moulton, M. K. Khan et al., "E-selectin is required for the antiangiogenic activity of endostatin," *Proceedings of the National Academy of Sciences of the United States of America*, vol. 101, no. 21, pp. 8005–8010, 2004.

[21] G. Pradilla, F. G. Legnani, G. Petrangolini et al., "Local delivery of a synthetic endostatin fragment for the treatment of experimental gliomas," *Neurosurgery*, vol. 57, no. 5, pp. 1032–1040, 2005.

[22] T.-Y. Lee, R. M. T. T. Sjin, S. Movahedi et al., "Linking antibody Fc domain to endostatin significantly improves endostatin half-life and efficacy," *Clinical Cancer Research*, vol. 14, no. 5, pp. 1487–1493, 2008.

[23] M. S. Gordon, K. Margolin, M. Talpaz et al., "Phase I safety and pharmacokinetic study of recombinant human anti-vascular endothelial growth factor in patients with advanced cancer," *Journal of Clinical Oncology*, vol. 19, no. 3, pp. 843–850, 2001.

[24] R. Grossman, B. Tyler, L. Hwang et al., "Improvement in the standard treatment for experimental glioma by fusing antibody Fc domain to endostatin: laboratory investigation," *Journal of Neurosurgery*, vol. 115, no. 6, pp. 1139–1146, 2011.

[25] M. V. Sefton, L. R. Brown, and R. S. Langer, "Ethylene-vinyl acetate copolymer microspheres for controlled release of macromolecules," *Journal of Pharmaceutical Sciences*, vol. 73, no. 12, pp. 1859–1861, 1984.

[26] R. J. Tamargo, R. A. Bok, and H. Brem, "Angiogenesis inhibition by minocycline," *Cancer Research*, vol. 51, no. 2, pp. 672–675, 1991.

[27] I. Celik, O. Sürücü, C. Dietz et al., "Therapeutic efficacy of endostatin exhibits a biphasic dose-response curve," *Cancer Research*, vol. 65, no. 23, pp. 11044–11050, 2005.

[28] J. W. Slaton, P. Perrotte, K. Inoue, C. P. N. Dinney, and I. J. Fidler, "Interferon-α-mediated down-regulation of angiogenesis-related genes and therapy of bladder cancer are dependent on optimization of biological dose and schedule," *Clinical Cancer Research*, vol. 5, no. 10, pp. 2726–2734, 1999.

[29] D. Panigrahy, S. Singer, L. Q. Shen et al., "PPARγ ligands inhibit primary tumor growth and metastasis by inhibiting angiogenesis," *The Journal of Clinical Investigation*, vol. 110, no. 7, pp. 923–932, 2002.

[30] K. Javaherian, T.-Y. Lee, R. M. T. T. Sjin, G. E. Parris, and L. Hlatky, "Two endogenous antiangiogenic inhibitors, endostatin and angiostatin, demonstrate biphasic curves in their antitumor profiles," *Dose-Response*, vol. 9, no. 3, pp. 369–376, 2011.

[31] W.-L. Chen, C.-T. Lin, N.-T. Lin et al., "Subconjunctival injection of bevacizumab (Avastin) on corneal neovascularization in different rabbit models of corneal angiogenesis," *Investigative Ophthalmology & Visual Science*, vol. 50, no. 4, pp. 1659–1665, 2009.

[32] L. D. Ormerod, A. Garsd, C. V. Reddy, S. A. Gomes, M. B. Abelson, and K. R. Kenyon, "Dynamics of corneal epithelial healing after an alkali burn. A statistical analysis," *Investigative Ophthalmology and Visual Science*, vol. 30, no. 8, pp. 1784–1793, 1989.

Hindawi Publishing Corporation
Journal of Ophthalmology
Volume 2015, Article ID 934963, 10 pages
http://dx.doi.org/10.1155/2015/934963

Research Article

Antiproliferative, Apoptotic, and Autophagic Activity of Ranibizumab, Bevacizumab, Pegaptanib, and Aflibercept on Fibroblasts: Implication for Choroidal Neovascularization

Lyubomyr Lytvynchuk,[1,2,3] Andrii Sergienko,[1] Galina Lavrenchuk,[4] and Goran Petrovski[2,3]

[1] *Professor Sergienko Eye Clinic, 47 A Pirogova Street, 21008 Vinnycia, Ukraine*
[2] *Department of Ophthalmology, Faculty of Medicine, Albert Szent-Györgyi Clinical Center, University of Szeged, Korányi fasor Ulica 10-11, 6720 Szeged, Hungary*
[3] *Stem Cells and Eye Research Laboratory, Department of Biochemistry and Molecular Biology, Faculty of Medicine, University of Debrecen, Egyetem Téren 1, 4032 Debrecen, Hungary*
[4] *State Institution "Research Center for Radiation Medicine of Academy of Medical Sciences of Ukraine", Laboratory of Cell Radiobiology, 53 Melnykova Street, 04050 Kyiv, Ukraine*

Correspondence should be addressed to Goran Petrovski; gokipepo@gmail.com

Received 12 October 2014; Accepted 26 March 2015

Academic Editor: Juliana L. Dreyfuss

Purpose. Choroidal neovascularization (CNV) is one of the most common complications of retinal diseases accompanied by elevated secretion of vascular endothelial growth factor (VEGF). Intravitreal anti-VEGFs (ranibizumab, bevacizumab, pegaptanib, and aflibercept) can suppress neovascularization, decrease vascular permeability and CNV size, and, thereby, improve visual function. The antiproliferative, apoptotic, and autophagic effect of anti-VEGF drugs on fibroblasts found in CNVs has not been yet explored. *Methods*. Concentration-dependent cellular effects of the four anti-VEGFs were examined in L929 fibroblasts over a 5-day period. The cell survival, mitotic and polykaryocytic indices, the level of apoptosis and autophagy, and the cellular growth kinetics were all assessed. *Results*. The anti-VEGFs could inhibit the survival, mitotic activity, and proliferation as well as increase the cellular heterogeneity, apoptosis, and autophagy of the fibroblasts in a dose-dependent manner. Cellular growth kinetics showed ranibizumab to be less aggressive, but three other anti-VEGFs showed higher antiproliferative and apoptotic activity and expressed negative cellular growth kinetics. *Conclusions*. The antiproliferative, apoptotic, and autophagic activity of anti-VEGFs upon fibroblasts may explain the cellular response and the etiology of CNV involution *in vivo* and serve as a good study model for CNV *in vitro*.

1. Introduction

The development of choroidal neovascularization (CNV) is one of the most sight threatening complications of different retinal diseases such as age-related macular degeneration, pathologic myopia, angioid streaks, and choroidal rupture. Foveal or extrafoveal location of CNV limits the use of lasers due to its potential side effects on the surrounding healthy tissue. The effectiveness of intravitreal administration of different antivascular endothelial growth factors (anti-VEGFs) is well known in the treatment of CNV of different origin [1–4]. The mechanism how intravitreal injections (IVIs) of such drugs work is complex and involves blocking of various types of VEGFs, decreased permeability of newly formed blood vessel walls, and reduced swelling of the retinal layers. Our optical coherence tomography (OCT) and fluorescein angiography (FA) performed before and after IVI of anti-VEGF drugs have revealed significant involution and decrease of CNV size (Figure 1).

The exact mechanism which leads to decrease of the CNV dimensions is not well understood. During recent years, a number of studies have published the impact of anti-VEGF drugs upon different cellular cultures *in vitro* [5–10]. Fibroblasts and myofibroblasts being among the most common

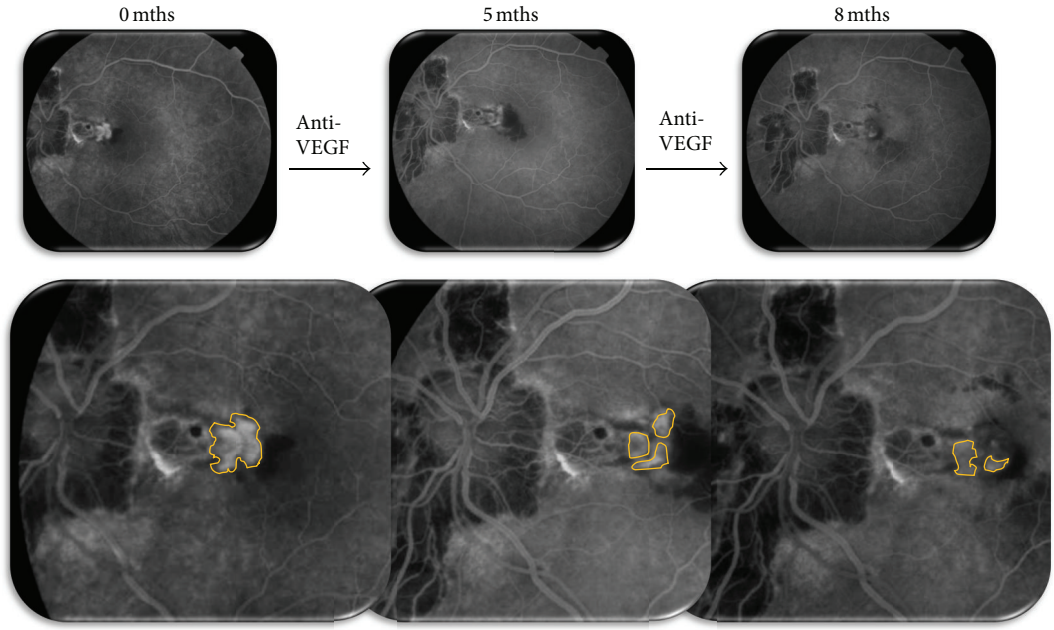

Figure 1: Choroidal neovascularization (CNV) dynamics after repeated anti-VEGF therapy (CNV size is circumscribed with yellow color; images shown are at the 40th second of fluorescein angiography).

cells found within the cellular matrix of CNVs and known to have high mitotic activity [7] have not been examined for their cellular effects upon anti-VEGF drug treatment. Our goal was to investigate the antiproliferative, apoptotic, and autophagic effects of anti-VEGF drugs on a fibroblast-like cell strain which can serve as *in vitro* model for CNV cellular matrix formation and to analyze the dose dependence regarding antiproliferative activity.

2. Materials and Methods

2.1. Cell Culture and Treatment Regimes. *In vitro* studies were performed using a fibroblast-like mouse cell strain L929 obtained from ATCC and cultivated according to conventional methods [11, 12] and nutrient medium composed of RPMI-1640 supplemented with fetal calf serum (10%) and gentamicin (10 mg/mL). Cultivation of the cell strain with different concentration of anti-VEGF drugs was performed as described below.

Ranibizumab (Lucentis, Novartis, Switzerland), a fragment of a human monoclonal antibody against VEGF-A, which is secreted by recombinant strain of *Escherichia coli* and its isoforms selectively bind to VEGF-A ($VEGF_{110}$, $VEGF_{121}$, and $VEGF_{165}$), was added to the culture 24 hours after fresh cell plating in concentrations of 12.5, 50, 125, and 250 μg/mL.

Bevacizumab (Avastin, Genetech/Roche, USA), a monoclonal antibody against VEGF, which is used off-label to treat various eye diseases in which increased concentration of VEGF is found and neovascularization is present, was added to the culture 24 hours after fresh cell plating at concentrations of 0.65, 3.13, 6.5, and 12.5 μg/mL.

Pegaptanib (Macugen, Pfizer, USA), a pegylated modified oligonucleotide that binds selectively and with high affinity to an extracellular $VEGF_{165}$, was added to the culture 24 hours after fresh cell plating at concentrations of 0.075, 0.15, 0.3, 0.75, and 1.5 μg/mL.

Aflibercept (Eylea, Bayer HealthCare, Germany), a fusion protein approved in the United States and Europe for the treatment of wet form of age-related macular degeneration, working by binding to circulating VEGF (subtypes VEGF-A and VEGF-B), as well as to placental growth factor (PGF), thus inhibiting growth of new blood vessels in the choriocapillaris [2], was added to the culture 24 hours after cell plating at concentrations of 0.04, 0.08, 0.2, 0.4, and 0.5 μg/mL.

Minimal drug concentrations were established according to the appearance of a multiplex of cellular effects (cellular proliferation, mitotic activity, polykaryocytic index, and apoptosis) and applied into the study, while maximal concentrations were determined with relevance and close approximation to the ones used in clinical practice (e.g., 0.5 mg/4 mL vitreous volume for ranibizumab; 1.25 mg/4 mL vitreous volume for bevacizumab; 0.3 mg/4 mL vitreous volume for pegaptanib; 2.0 mg/4 mL vitreous volume for aflibercept; all of the anti-VEGFs are used clinically at 1–3-month interval).

2.2. Cellular Vital Parameters. Different cellular responses were evaluated on a daily basis up to 5 days. The following cellular vital activity indices were evaluated: cellular growth/expansion and mitotic and polykaryocytic indices (PKI). For cultivation, 5×10^4 cells were added to the cell culture dishes covered by culture glass slides (size 16 × 8 mm) and filled up to 1 mL of medium and then left to form monolayers within 5 days. Anti-VEGFs were added to the cultures 24 hours after cell plating in different concentrations specified accordingly.

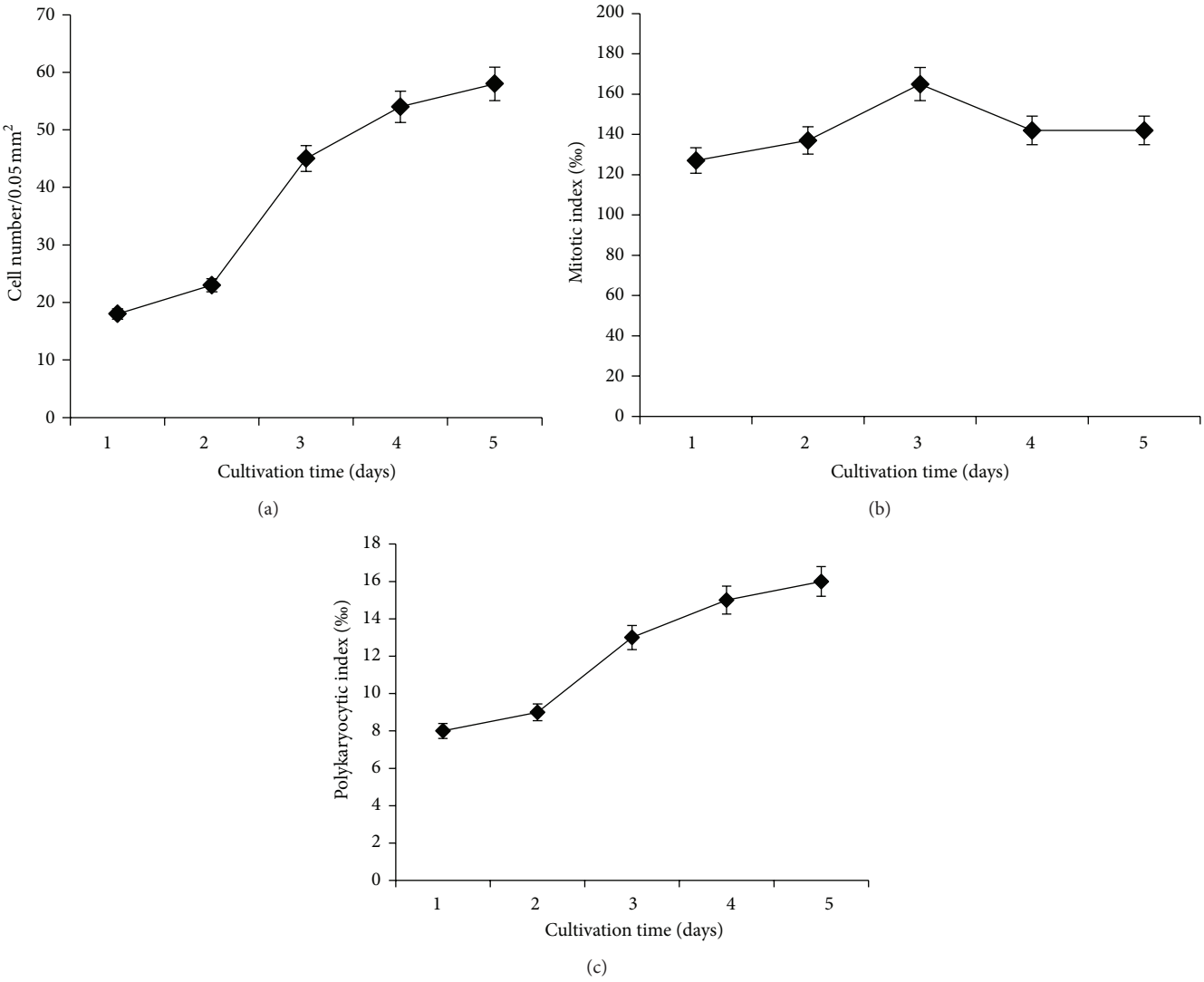

Figure 2: Kinetics of the cellular survival (a) and mitotic (b) and polykaryocytic indices (c) in untreated, control L929 cells.

The samples were fixed for analysis in 96% ethanol and then stained by hematoxylin and eosin (H&E). The total number of cells and the count of mitoses and polykaryocytes (2 or more nuclei) were determined under optical microscope (Axioscope, Germany) at 1000x magnification within a grid area of 0.05 mm^2. Mitotic index and PKI were adjusted to 1000 cells (‰). Parallely, cellular vital indices were evaluated within the intact cellular culture.

2.3. Detection of Apoptosis and Autophagy. The level of apoptosis was determined on the same cultures in which the cellular vital indices were analyzed. The cells were first washed in phosphate buffered saline (PBS) and then detached for 10 minutes in trypsin and suspended again in PBS. Consequently, centrifugation (1400 rpm, 5 min) and resuspension of the cells in propidium iodide (1 μg/mL) were performed. The level of apoptosis was determined according to the number of apoptotic cells in pre-G1 phase using ductal cytofluorimeter FACStar Plus (Becton Dickinson, USA).

Anti-LC3 polyclonal antibody was purchased from Novus Biologicals, USA (NB100-2220-0.1) for analysis of autophagy. Cell lysates were prepared from each condition after which equal amounts of protein were loaded onto the gel. Proteins were separated on a NuPAGE 15% Bis-Tris polyacrylamide gel and then transferred onto Immobilon-P Transfer Membrane (Millipore, IPVH00010). Membranes were blocked in Tris buffered saline containing 0.05% Tween-20 (TBS-T) and 5% nonfat dry milk (BioRad, 170-6435, 170-6531, and 100-04504-MSDS) for 1 hour. After blocking, membranes were probed overnight at 4°C with the anti-LC3 antibody in dilution buffer (TBS-T containing 1% nonfat dry milk), followed by 1-hour incubation with a peroxidase-conjugated rat anti-rabbit secondary antibody (Sigma, A6154) for 1 hour at room temperature. Peroxidase activity was detected with SuperSignal West Femto Maximum Sensitivity Chemiluminescent Substrate (Pierce, 34095) using a Lumi-Imager (Roche Diagnostics, Mannheim, Germany).

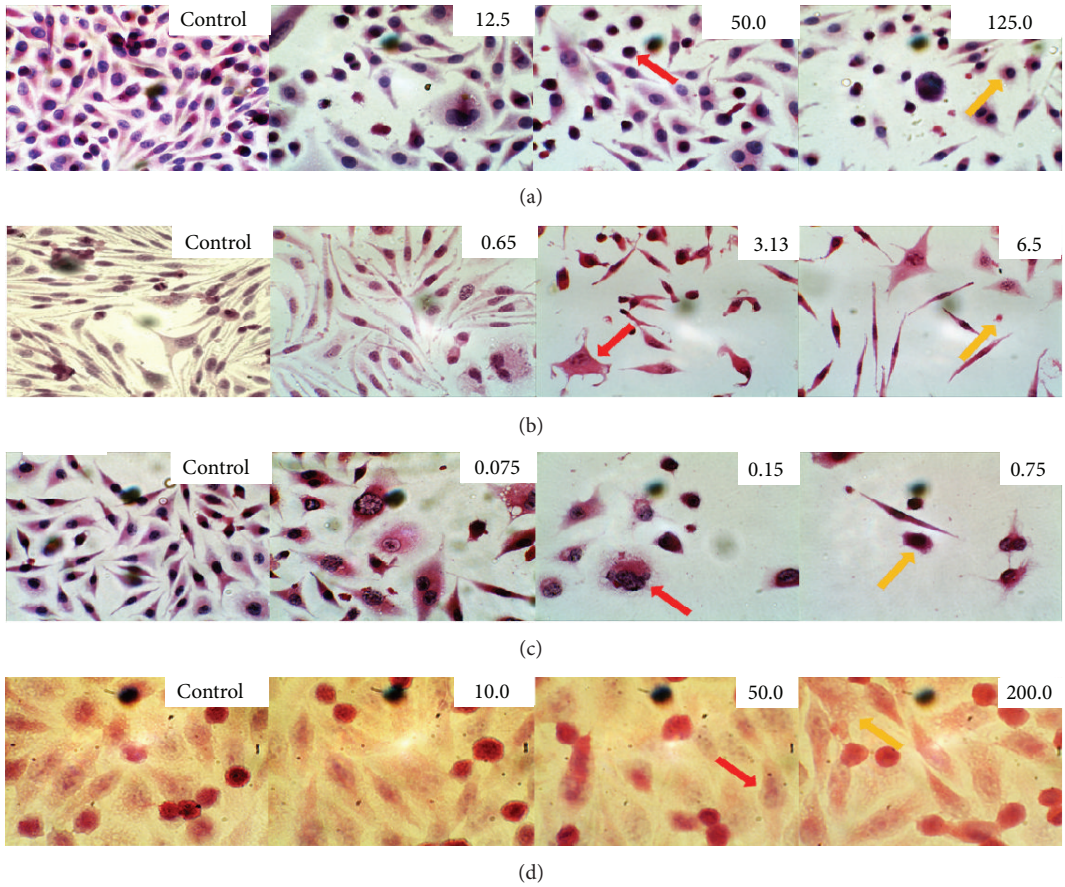

FIGURE 3: Cellular effects of ranibizumab (a), bevacizumab (b), pegaptanib (c), and aflibercept (d) on L929 cells. Cells shown are at Day 5 of various treatment concentrations (H&E staining, magnification ×1000).

2.4. Cellular Growth Kinetics. Proliferative activity of cells was determined according to their growth kinetics parameters: specific growth velocity (μ), population doubling time (t_d), and reproduction velocity (n) at Day 5 of the observation [13]. The specific growth velocity of the culture in phase of logarithmic growth was calculated using the formula $\mu = (\ln X - \ln X_o)t^{-1}$, where X is the cell quantity after certain time interval t (Day 5 of cultivation), X_o is the cell quantity on Day 1 of cultivation, and t is the time of observation (5 days of cultivation). Using specific growth velocity, population doubling time was calculated as $t_d = \ln 2/\mu = 0693\mu$. Reproduction velocity (n) was determined using the formula $n = 3.32 \log(X/X_o)$.

2.5. Statistical Analysis. Results were statistically analyzed by Student's t-test using Microsoft Excel and Biostat (Primer of Biostatistics, Version 4.03, by Stanton A. Glantz). $P < 0.05$ was considered significant. If not otherwise noted, all the experiments were performed three times independently.

3. Results

3.1. Morphological and Functional Characteristics of L929 Cells Treated by Anti-VEGFs. Under normal conditions, L929 cells form a dense cellular monolayer with the majority of the cells acquiring polygonal and spindle shape morphology. The cells have relatively large nuclei, light cytoplasmic vacuoles, and small granules with occasional di- and trinucleated cells found in the culture. On average, 2 to 5 cells at different stages of mitosis can be detected per visual field in the untreated culture, assuming round shape, small cytoplasm, and hyperchromatic nuclei due to condensation of the chromatin under mitosis. The intact cells have a characteristic proliferative activity that increases from Day 1 to Day 5 of cultivation (logarithmic growth phase), reaching growth plateau at Day 6 (stationary growth phase), when the density of the cellular monolayer becomes highest ($58.0 \pm 2.7/0.05\,\text{mm}^2$) (Figure 2(a)). Maximum mitotic activity is observed at Day 3 of cultivation (166.0 ± 7.5‰), with a decrease in the mitotic index at Day 4 due to contact inhibition and confluency of the cellular culture. The PKI in the intact control cells varies between 8 and 12‰.

Incubation of the L929 cells with ranibizumab at a concentration of 12.5 μg/mL leads to decreased density of the culture monolayer by 3 times (Figures 3(a) and 4(a)), which is caused by the appearance of increased number of cells with apoptotic features—decreased cytoplasm and condensed chromatin in the nucleus (Figures 3(a) (red arrow) and 4(d)). The treated cells assume mainly spindle-shape morphology, while their PKI increases by 54‰ (Figure 4(c)), a sign of cell

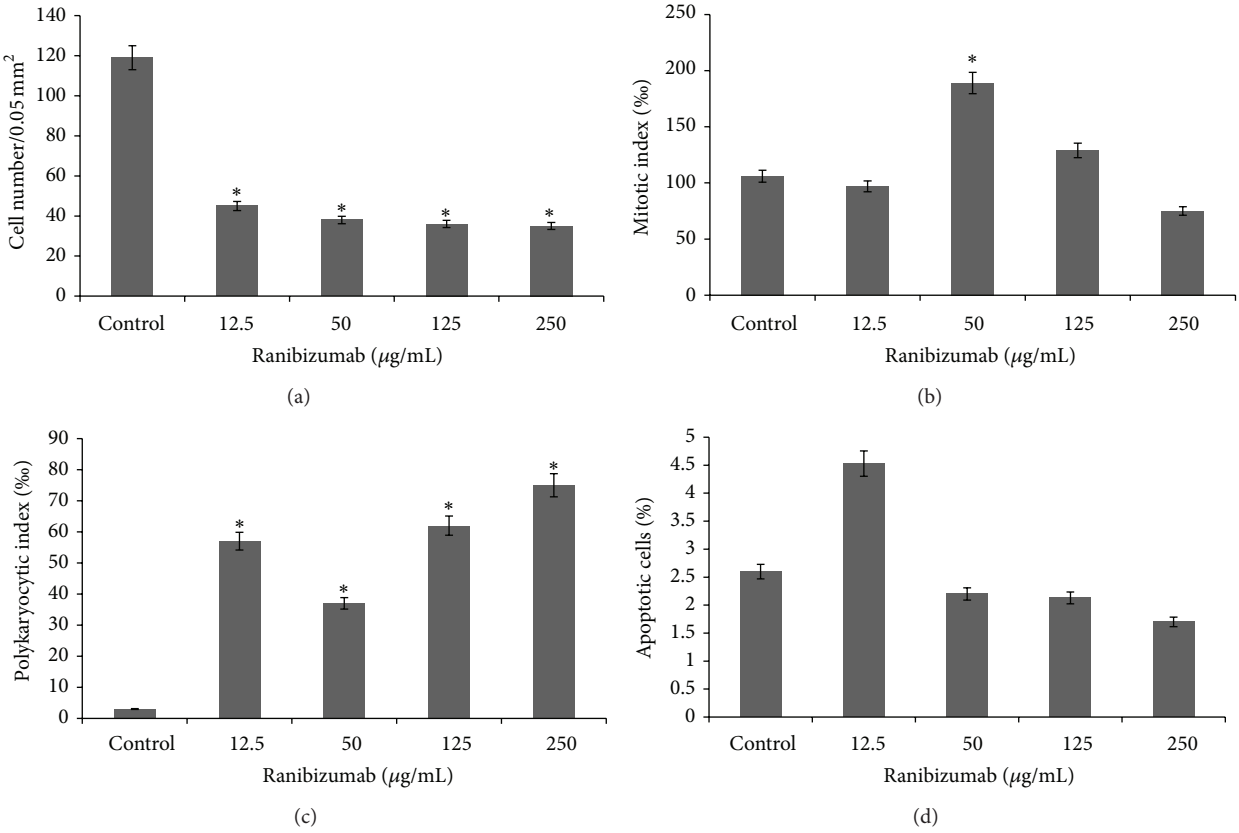

Figure 4: Kinetics of cellular proliferation (a), mitotic activity (b), polykaryocytic index (c), and apoptosis (d) in L929 cells treated by ranibizumab at different concentrations (data shown are at Day 5 of the treatment; $n = 3$, $^*P < 0.05$).

demise. At higher concentrations up to 125.0 μg/mL, the heterogeneity of the cell culture increases, with a predominant cellular morphology being round and polygonal (Figure 3(a) (yellow arrow)). The number of polykaryocytes markedly increases to 62‰, while the mitotic index remains relatively stable compared to the control (Figure 4(b)). Incubation of the L929 cells at a dose of 250 μg/mL results in severe degradation of the cellular structure and strong vacuolization of the cytoplasm.

Exposure to bevacizumab at concentration of 0.65 μg/mL induces no morphological changes in the L929 cells compared to the control (Figure 3(b)). Increasing the dose up to 3.13 μg/mL leads to an increase in the heterogeneity of cellular culture, with round and polygonal cellular morphology becoming more prominent (Figure 3(b) (red arrow)). A small number of mitotic cells with vacuolar cytoplasm can be observed compared to the control, while the number of polykaryocytes increases 6.3 times (Figure 5(c)), and the mitotic index and cell number decrease by 1.9 and 1.6 times, respectively, compared to the control (Figures 5(a) and 5(b)). At higher concentrations of bevacizumab (6.25 and 12.5 μg/mL), a severe degradation of cellular structure, with the cytoplasm becoming full of vacuoles, and a large number of apoptotic cells appear (38.0 ± 1.5 and 46.0 ± 2.2, resp.) (Figures 3(b) (yellow arrow) and 4(d)). A significant reduction in the cell density and mitotic activity as well as increase in the PKI is noticed at concentrations higher than 0.625 μg/mL ($P < 0.05$) (Figure 5(c)).

Incubation of cells with pegaptanib shows pronounced antiproliferative effects of the drug from its lowest dose (0.075 μg/mL) (Figure 6(a)) and an almost doubling of the apoptotic cells in the culture. This is manifested by a significant decrease in the cell number and mitotic activity compared to the controls ($P < 0.05$) (Figures 6(a) and 6(b)). Increasing the dose up to 1.5 μg/mL increases the antiproliferative effect which is manifested through a reduction in the density of the cells and the appearance of vacuoles in the cytoplasm (Figure 3(c) (red arrow)). Cells with signs of apoptosis also appear at higher concentrations (Figure 3(c) (yellow arrow)), but their number, paradoxically, is similar to that of the control cells (Figure 6(d)), while the number of mitoses and presence of polykaryocytes decreases and increases, respectively (Figures 6(b) and 6(c)).

Exposure to aflibercept causes not much morphological difference in the L929 cells compared to the control; for example, the cells remain predominantly polygonal and spindle shaped with centrally situated well-colored round or oval nuclei (Figure 3(d) (red arrow)). The cytoplasm has mesh structure and becomes slightly vacuolized under aflibercept treatment (Figure 3(d) (yellow arrow)), with many cells

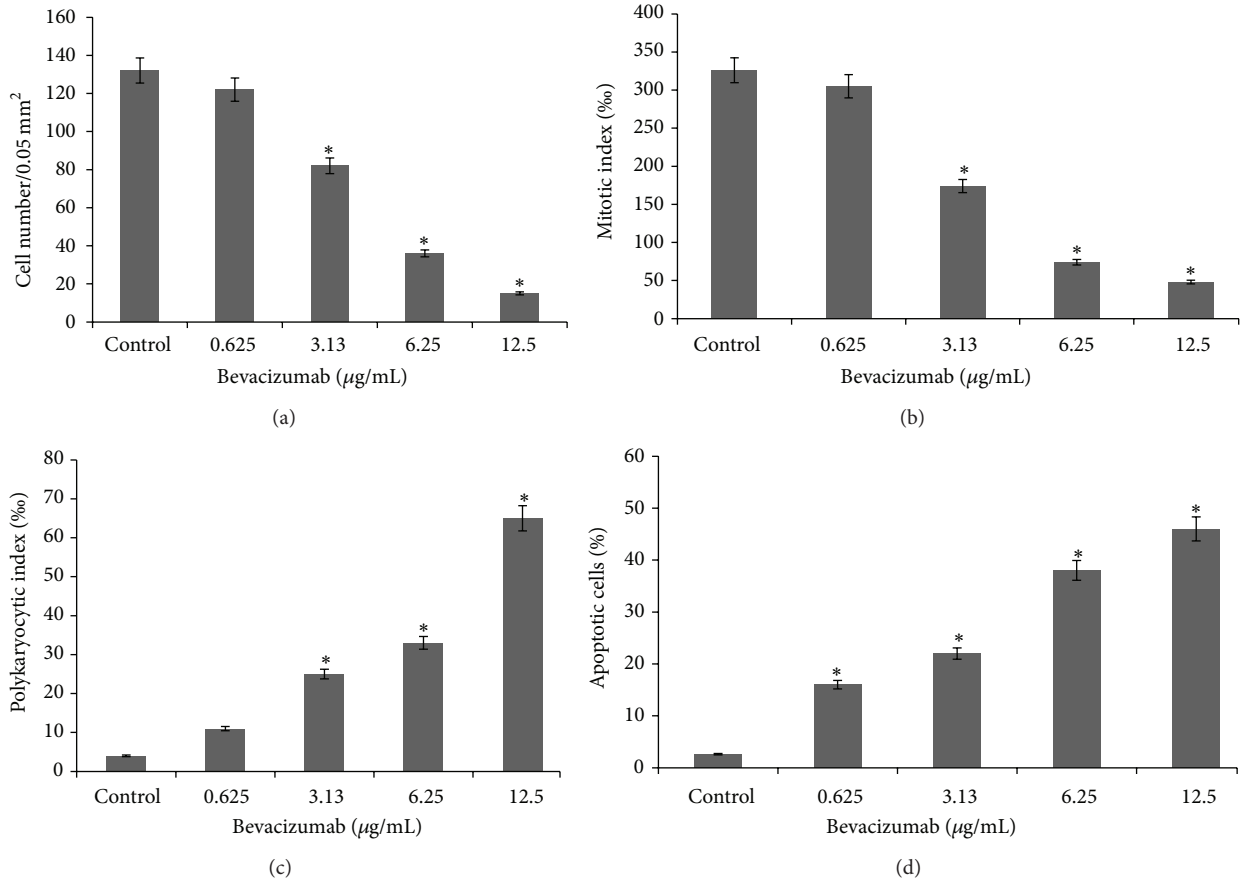

Figure 5: Kinetics of cellular proliferation (a), mitotic activity (b), polykaryocytic index (c), and apoptosis (d) in L929 cells treated by bevacizumab at different concentrations (data shown are at Day 5 of the treatment; $n = 3$, $^*P < 0.05$).

appearing at different stages of mitosis and, under certain concentrations, an entire absence of polykaryocytes' formation is seen compared to control (Figure 7(c)). The cell number is reduced by at least 1.6-fold with drug concentration of 10 μg/mL and by 2.2-fold when exposed to a maximum concentration of 200 μg/mL (Figure 7(a)). Interestingly, the mitotic index does not change compared to the control, which corresponds well to the morphological cellular stability observed (Figure 7(b)). Furthermore, complete lack of polykaryocytes is observed under certain concentrations (10 and 100 μg/mL) (Figure 7(c)). There is no statistical difference between PKI of control cells and under 50 or 200 μg/mL treatment with aflibercept ($P < 0.05$). The number of apoptotic cells (Figure 7(d)) increases and depends in a nonlinear manner on the drug concentration.

3.2. Cellular Growth Kinetics of L929 Cells under Different Treatments. Comparison of the cellular growth effect of different concentrations of anti-VEGF drugs is shown in Figure 8. According to the cellular growth kinetic parameters (specific growth velocity (μ), population doubling time (t_d), and cell reproduction velocity (n)), ranibizumab seems to be less aggressive compared to the rest of the anti-VEGFs studied, the cellular death being compensated by cellular reproduction in its case (Figure 8(a)) [13]. Minimal concentrations of bevacizumab cause faster cellular proliferation than death (Figure 8(b)); however, this turns around under higher concentrations, when generalized cell death through initiation of apoptosis occurs. The action of pegaptanib appears to be antiproliferative at lowest concentrations, while the balance between survival, reproductive activity, and death is shifted towards death at higher concentrations, meaning that the destruction in cellular culture runs faster than cellular mitosis (Figure 8(c)). Treatment by aflibercept (Figure 8(d)) causes statistically significant reduction in the cell number, in particular, concentrations of 50 to 200 μg/mL, while, at the same time, the population doubling time decreases (at 50 μg/mL), and the rate of cell proliferation increases. This indicates a shift of the balance of cellular growth and death in the culture towards death, and, according to the determination of number of apoptotic cells (Figure 8(d)), this death is mainly caused by apoptosis. Concentration of 200 μg/mL slows down the progression of cellular growth, which indicates linking of the reproductive death (pathologic mitosis) to apoptosis.

3.3. Induction of Autophagy by Ranibizumab and Bevacizumab in L929 Cells. The appearance of vacuoles in the cytoplasm of L929 cells under different treatments by ranibizumab and bevacizumab was further examined for the presence of autophagy. Both treatment modalities induce

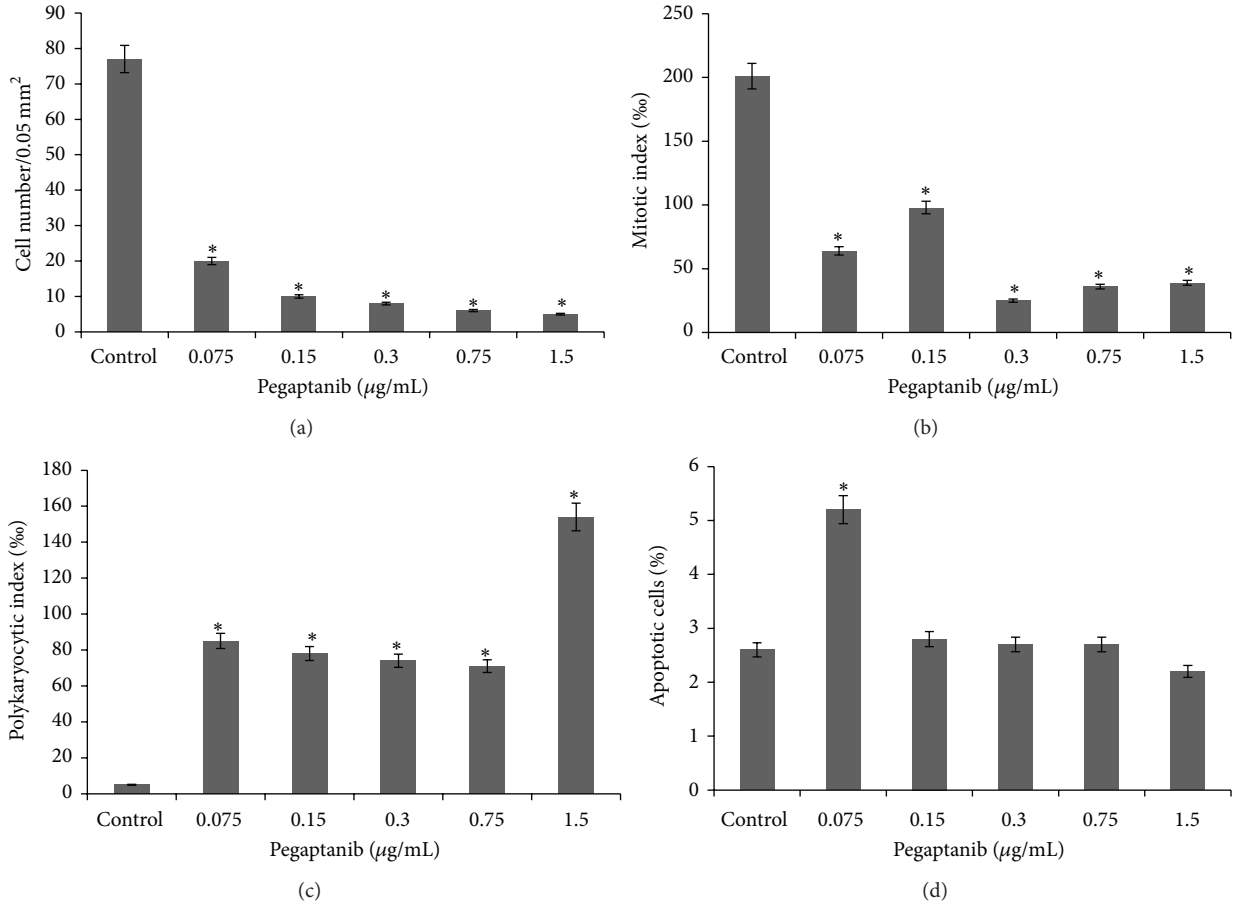

Figure 6: Kinetics of cellular proliferation (a), mitotic activity (b), polykaryocytic index (c), and apoptosis (d) in L929 cells treated by pegaptanib at different concentrations (data shown are at Day 5 of the treatment; $n = 3$, $^*P < 0.05$).

conversion of the cytoplasmic form of the myosin light chain kinase 3 (LC3) I into the autophagic vacuoles-bound LC3 II, with the highest concentrations of each drug inducing highest conversion of LC3 I to LC3 II (quantification data not shown) (Figure 9).

4. Discussion

Over the past decade, IVIs of anti-VEGF drugs take the leading place among the treatment modalities used for retinal diseases with increased production of VEGF [1–4]. However, only a few studies are dedicated to the side effects these drugs have on ocular tissues being exposed [5–10]. To our knowledge, this is the first study which compares antiproliferative action of ranibizumab, bevacizumab, pegaptanib, and aflibercept on fibroblast-like cells *in vitro* to elucidate the different dose-dependent properties and implications for CNV.

Our data show that all four anti-VEGFs demonstrate antiproliferative activity on the L929 cells over a 5-day study period. Starting from the lowest concentrations used, the heterogeneity of the cellular monolayer increases as a result of depression of mitosis and survival, while the number of apoptotic cells increases. Increasing the concentrations of each of the four anti-VEGFs results in exacerbation of the above-mentioned effects.

The growth kinetic analysis reveals concentration-dependent antiproliferative and apoptotic effects of all anti-VEGFs, except for ranibizumab, where higher cellular reproduction occurs with concentration increase, and, therefore, the concentration-dependent cellular growth is partially compensated by reproduction. The ranibizumab proves, therefore, to be less aggressive than other anti-VEGFs in regard to its antiproliferative activity.

A recent study compared the antiproliferative and cytotoxic effects of bevacizumab, pegaptanib, and ranibizumab on different ocular cells, except fibroblasts [8]. Ranibizumab reduced the cell proliferation by 44.1%, while bevacizumab and pegaptanib reduced it by 38.2% and 35.1%, respectively, when applied to choroidal epithelial cells (CECs), although the difference was not found to be statistically significant. A slight antiproliferative effect of bevacizumab and pegaptanib was also revealed on adult retinal pigment epithelium (ARPE19 cell line). Ranibizumab neither had the same effect on cell proliferation of ARPE19 cells nor did it have cytotoxicity on retinal ganglion cells (RGC5), CECs, and ARPE19 cells. It could also efficiently block migration, but not proliferation

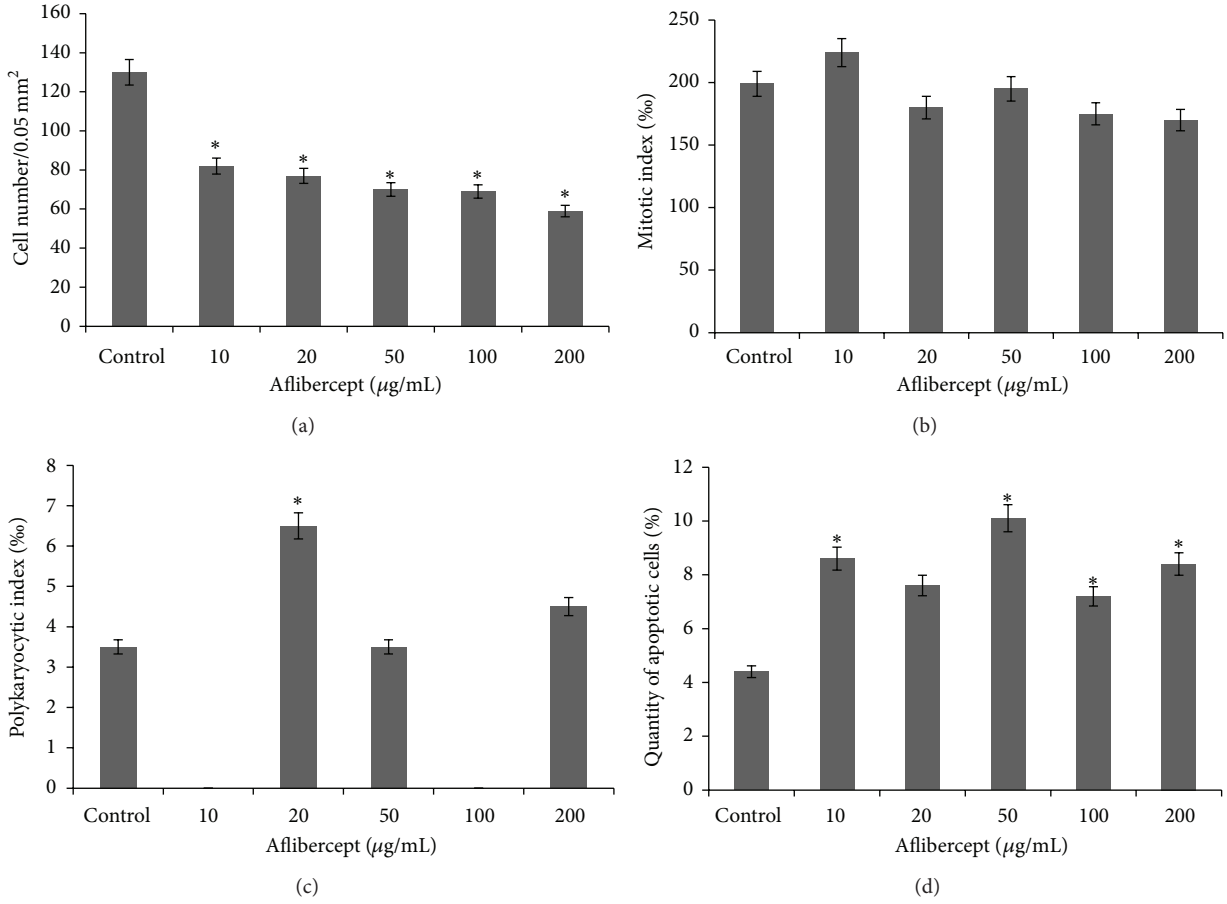

Figure 7: Kinetics of cellular proliferation (a), mitotic activity (b), polykaryocytic index (c), and apoptosis (d) in L929 cells treated by aflibercept at different concentrations (data shown are at Day 5 of the treatment; $n = 3$ $^*P < 0.05$).

induced by growth factor combinations, including VEGF in retinal endothelial cells.

Another study collated the effects of ranibizumab, pegaptanib, and bevacizumab on the different stages of angiogenesis using cultivation of drugs on human umbilical vein endothelial cells (HUVEC) [5]. According to the results, apoptosis of HUVEC was markedly increased by ranibizumab and bevacizumab. Clinically used doses of these drugs, but not pegaptanib, caused significantly reduced cellular proliferation without causing cytotoxic effects at all concentrations used. Finally, incubation of HUVEC with anti-VEGF drugs caused a decreased expression of the active form of the VEGF receptor-2, with bevacizumab causing 66% of control and ranibizumab and pegaptanib causing 86% decrease compared to the control.

A separate study compared the cytotoxicity and antiproliferative activity of aflibercept, bevacizumab, and ranibizumab on different ocular cells (ARPE19, RGC-5, and 661W) [7] and concluded that aflibercept does not affect cellular viability or induce apoptosis. Albeit aflibercept had slight upregulation and downregulation effects on certain VEGF-related factors, however, those were not significant when compared to bevacizumab and ranibizumab.

Our experimental study explored the cellular effects of four different anti-VEGFs on L929 cells as a model of the fibroblast-based cellular matrix of CNV *in vitro*. The results revealed their effect on the proliferative activity (survival, proliferative and mitotic activity, and apoptosis) and their hormesis; that is, small doses of the drugs (ranibizumab 12.5 μg/mL, bevacizumab 3.13 μg/mL, pegaptanib 0.15 μg/mL, and aflibercept 0.04 μg/mL) exhibited a pronounced antiproliferative effect on the cellular culture, while bevacizumab in all concentrations increased apoptosis of the L929 cells. Inhibition of the proliferation and increased heterogeneity of these cells under anti-VEGF treatment are a sign of reproductive cellular death.

When cultured with bevacizumab, pegaptanib, and aflibercept, the L929 cells showed marked dose-dependent effects which were manifested by an increase in the antiproliferative action with increasing dose. Inversely, ranibizumab caused compensation of the antiproliferative and apoptotic action by cellular proliferation in spite of increasing drug concentration. This compensation can probably be partially due to autophagy, which is a self-digestive or self-recycling mechanism found in cells.

The reasons why L929 cell strain was chosen in this study were the absence of background VEGF secretion, as well as exploring the alternative cellular effects of anti-VEGF drugs as an *in vitro* model for CNV. Indeed, the most highly proliferating cell types amid the cellular types in CNV are

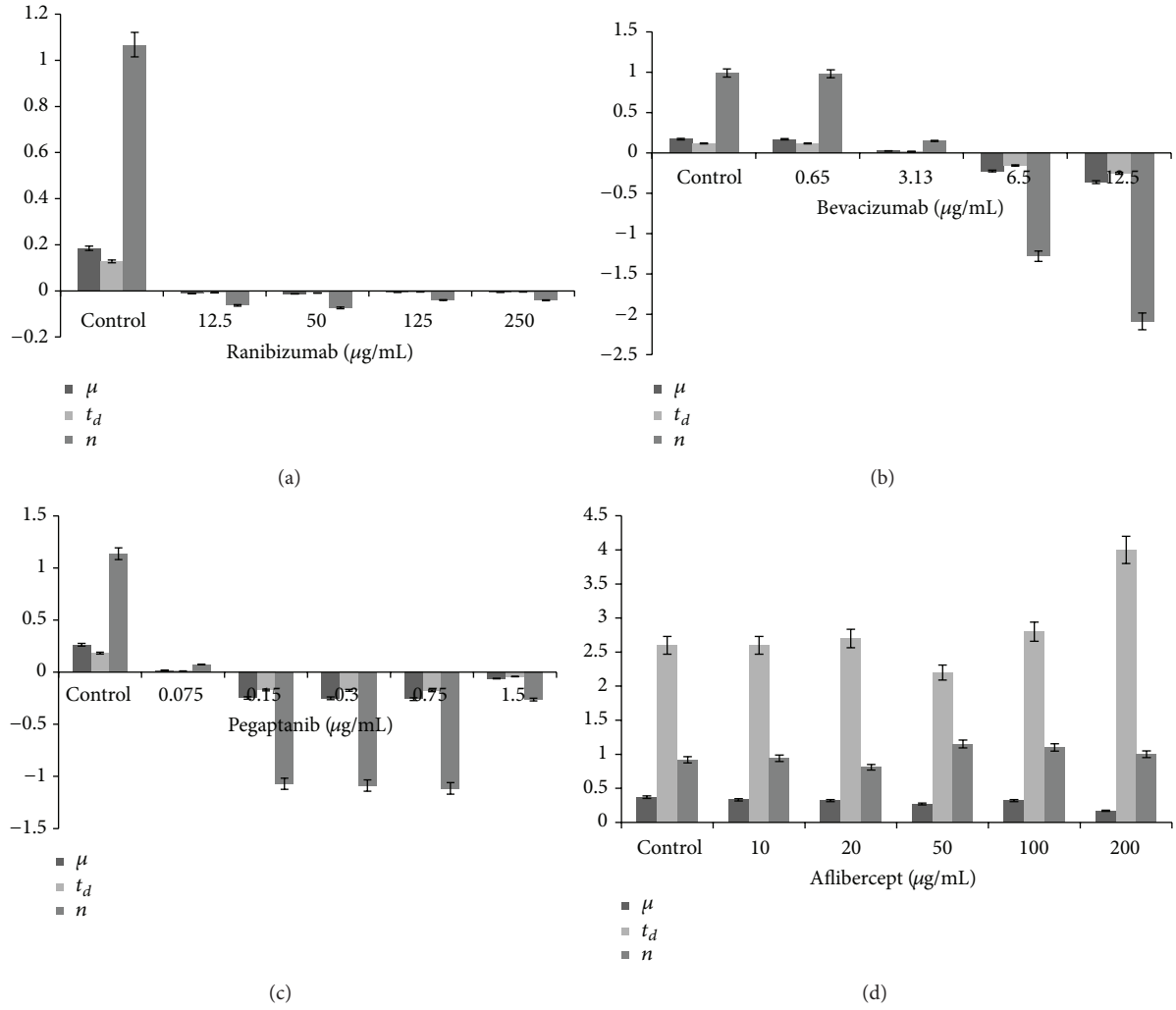

Figure 8: Comparison of the cellular growth kinetics in L929. Specific growth velocity (μ), population doubling time (t_d), and cell reproduction velocity (n) are shown under treatment with ranibizumab (a), bevacizumab (b), pegaptanib (c), and aflibercept (d) at different concentrations (data shown are at Day 5 of the treatment; $n = 3$).

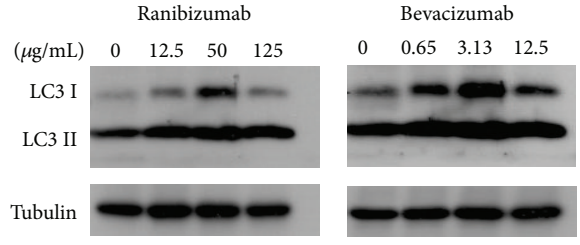

Figure 9: Induction of autophagy by ranibizumab and bevacizumab in L929 cells.

fibroblasts and myofibroblasts [14]. L929 cells have also been used as *in vitro* model for vital cell, allowing to judge cellular effects of different drugs upon vital, highly proliferating cells.

Although the data regarding presence of absence of VEGF receptors on the cellular membrane of fibroblast-like cells in CNV is missing, other studies have shown VEGF receptor presence on joint fibroblasts extracted from humans as well as expression of VEGF by inflammatory stimulation of fibroblast-like cells that infiltrate the joint in a collagen-induced arthritis [15]. An obvious limitation of this study is the resemblance of the *in vitro* findings to clinical conditions, for example, CNV.

Antiproliferative and apoptotic properties of anti-VEGF drugs on fibroblast-like cells can explain an alternative, beneficial mechanism of their action on such cells and myofibroblasts found in CNV [14]. Inhibition of the cellular survival and mitosis by ranibizumab, bevacizumab, pegaptanib, and aflibercept in different concentrations has to be taken into consideration while using them in patients. Only ranibizumab, amid all anti-VEGFs studied, exhibits the slightest antiproliferative activity which allows for compensation of apoptosis by increased proliferation. The complete absence of polykaryocytes revealed after cultivation with aflibercept at concentrations of 10 and 100 μg/mL may indicate the influence of the drug on the signal transfer from the membrane to the nucleus.

The identified properties of these drugs require further investigation of their action *in vitro* and *in vivo*. Additionally, further research pertaining to hormesis of anti-VEGFs needs to be performed to eliminate possible side effects on healthy retinal tissues.

Conflict of Interests

The authors declare that they have no competing interests.

Acknowledgments

The work has been supported by the Hungarian Scientific Research Fund (OTKA PD 101316) and TÁMOP-4.2.2A-11/1/KONV-2012-0023 Grant, project implemented through the New Hungary Development Plan and cofinanced by the European Social Fund.

References

[1] P. Biswas, S. Sengupta, R. Choudhary, S. Home, A. Paul, and S. Sinha, "Comparative role of intravitreal ranibizumab versus bevacizumab in choroidal neovascular membrane in age-related macular degeneration," *Indian Journal of Ophthalmology*, vol. 59, no. 3, pp. 191–196, 2011.

[2] D. J. Browning, P. K. Kaiser, P. J. Rosenfeld, and M. W. Stewart, "Aflibercept for age-related macular degeneration: a game-changer or quiet addition?" *American Journal of Ophthalmology*, vol. 154, no. 2, pp. 222–226, 2012.

[3] S. Grisanti and F. Ziemssen, "Bevacizumab: off-label use in ophthalmology," *Indian Journal of Ophthalmology*, vol. 55, no. 6, pp. 417–420, 2007.

[4] N. Kumaran, D. A. Sim, and A. Tufail, "Long-term remission of myopic choroidal neovascular membrane after treatment with ranibizumab: a case report," *Journal of Medical Case Reports*, vol. 3, article 84, 2009.

[5] Â. Carneirob, M. Falcão, A. Pirraco, P. Milheiro-Oliveira, F. Falcão-Reis, and R. Soaresa, "Comparative effects of bevacizumab, ranibizumab and pegaptanib at intravitreal dose range on endothelial cells," *Experimental Eye Research*, vol. 88, no. 3, pp. 522–527, 2009.

[6] S. Kaempf, S. Johnen, A. K. Salz, A. Weinberger, P. Walter, and G. Thumann, "Effects of bevacizumab (avastin) on retinal cells in organotypic culture," *Investigative Ophthalmology & Visual Science*, vol. 49, no. 7, pp. 3164–3171, 2008.

[7] S. Schnichels, U. Hagemann, K. Januschowski et al., "Comparative toxicity and proliferation testing of aflibercept, bevacizumab and ranibizumab on different ocular cells," *British Journal of Ophthalmology*, vol. 97, no. 7, pp. 917–923, 2013.

[8] M. S. Spitzer, E. Yoeruek, A. Sierra et al., "Comparative antiproliferative and cytotoxic profile of bevacizumab (Avastin), pegaptanib (Macugen) and ranibizumab (Lucentis) on different ocular cells," *Graefe's Archive for Clinical and Experimental Ophthalmology*, vol. 245, no. 12, pp. 1837–1842, 2007.

[9] M. S. Spitzer, B. Wallenfels-Thilo, A. Sierra et al., "Antiproliferative and cytotoxic properties of bevacizumab on different ocular cells," *British Journal of Ophthalmology*, vol. 90, no. 10, pp. 1316–1321, 2006.

[10] Y. Wang, D. Fei, M. Vanderlaan, and A. Song, "Biological activity of bevacizumab, a humanized anti-VEGF antibody in vitro," *Angiogenesis*, vol. 7, no. 4, pp. 335–345, 2004.

[11] L. P. Dyakonov, Ed., *Animal Cells in Culture (Methods and Application of Biotechnology)*, Sputnik, Moscow, Russia, 2009.

[12] H. Hay and J. Cohen, "Studies on the specificity of the L929 cell bioassay for the measurement of tumor necrosis factor," *Journal of Clinical and Laboratory Immunology*, vol. 29, pp. 151–155, 1989.

[13] I. Freshney, *Animal Cell Culture, A Practical Approach*, IRL Press Oxford, Washington, DC, USA, 1986.

[14] A. Scupola, L. Ventura, A. C. Tiberti, D. D'Andrea, and E. Balestrazzi, "Histological findings of a surgically excised myopic choroidal neovascular membrane after photodynamic therapy. A case report," *Graefe's Archive for Clinical and Experimental Ophthalmology*, vol. 242, no. 7, pp. 605–610, 2004.

[15] J. Lu, T. Kasama, K. Kobayashi et al., "Vascular endothelial growth factor expression and regulation of murine collagen-induced arthritis," *Journal of Immunology*, vol. 164, no. 11, pp. 5922–5927, 2000.

Hindawi Publishing Corporation
Journal of Ophthalmology
Volume 2015, Article ID 820605, 5 pages
http://dx.doi.org/10.1155/2015/820605

Clinical Study

Long-Term Visual Outcome in Wet Age-Related Macular Degeneration Patients Depending on the Number of Ranibizumab Injections

Pilar Calvo,[1,2] Beatriz Abadia,[1] Antonio Ferreras,[1,2] Oscar Ruiz-Moreno,[1,2] Jesús Leciñena,[1] and Clemencia Torrón[1,2]

[1]*Ophthalmology Department, Miguel Servet University Hospital, Isabel la Catolica 1-3, 50009 Zaragoza, Spain*
[2]*University of Zaragoza, Zaragoza, Spain*

Correspondence should be addressed to Pilar Calvo; xenatrance@yahoo.es

Received 2 December 2014; Revised 10 January 2015; Accepted 4 February 2015

Academic Editor: Caio V. Regatieri

Purpose. To analyse the visual outcome in wet age-related macular degeneration (AMD) patients depending on the number of ranibizumab injections. *Methods*. 51 naïve wet AMD patients were retrospectively recorded. Visual acuity (VA), central retinal thickness (CRT) measured with spectral domain (SD) optical coherence tomography (OCT), and number of intravitreal injections were compared at 6, 12, 18, 24, 30, and 36 months of follow-up. Kaplan-Meier survival rates (SRs) based on VA outcomes were calculated depending on the number of ranibizumab injections performed. *Results*. VA improved compared with baseline at 6 and 12 months ($P < 0.005$). No differences were found at 18, 24, 30, and 36 months ($P > 0.05$). CRT measured with Cirrus OCT decreased ($P < 0.001$) at all time points analysed. The mean number of injections received was 6.98 ± 3.69. At 36 months, Kaplan-Meier SR was 76.5% (the proportion of patients without a decrease in vision of more than 0.3 logMAR units). VA remained stable (≤0.01 logMAR units) or improved in 62.7%. Within this group, SR was 92.9% in those who received 7 or more injections versus 51.4% receiving <7 treatments ($P = 0.008$; log-rank test). *Conclusion*. Better VA outcomes were found in stable wet AMD patients after 3 years of follow-up if they received ≥7 ranibizumab injections.

1. Introduction

Intravitreal antivascular endothelial growth factor (anti-VEGF) agents are the treatment of choice for wet age-related macular degeneration (AMD). Multicentre studies such as the Minimally Classic/Occult Trial of the Anti-VEGF Antibody Ranibizumab in the Treatment of Neovascular AMD (MARINA) and Anti-VEGF Antibody for the Treatment of Predominantly Classic Choroidal Neovascularization (CNV) in AMD (ANCHOR) [1, 2] have shown that monthly intravitreal injections of ranibizumab over a 2-year period not only maintained but also improved best corrected visual acuity (BCVA), with a mean gain of 7.2 and 11.3 letters, respectively.

However, most centres have considerable difficulty maintaining this type of treatment schedule due to an ever-increasing patient load and stress on the patient and family members to attend monthly assessments, as well as the associated economic costs. Alternate regimens of treatment have evolved in an attempt to provide comparable results in terms of BCVA, but with a fewer number of injections.

The PIER and EXCITE trials, using a regimen of three monthly injections as a loading dose and then quarterly injections, failed to match the good results of BCVA [3, 4]. On the other hand, those based on three initial monthly injections followed by an as-needed decision to treat (PrONTO, SUSTAIN) obtained very similar BCVA results averaging fewer injections [5–7].

In MARINA [1], ANCHOR [2], and PrONTO [6] trials, 94.6%, 96.4%, and 97.5% of patients prevented the loss of 15 letters (3 lines) BCVA at 2 years of follow-up. In patients who remained stable (with 0 or more earned letters), BCVA was 71%, 78%, and 78%, respectively.

The purpose of this study was to conduct a survival analysis based on the results of the BCVA and the number of intravitreal injections in wet AMD patients treated exclusively with ranibizumab and 3 years of follow-up in normally run vitreoretinal practices, reflecting a "real-life" clinical setting.

2. Methods

2.1. Study Design. It was analytical, observational, longitudinal, retrospective study.

2.2. Inclusion Criteria. Inclusion criteria include

(1) patients >50 years of age;

(2) choroidal neovascularization (CNV) due to AMD diagnosed by fluorescein angiography (FA) with at least 3 years of follow-up, with lesion size no more than 5400 μm in greatest linear diameter in the study eye;

(3) presence of subretinal fluid (SRF), intraretinal fluid (IRF), or central retinal thickness (CRT) >250 microns on spectral domain (SD) optical coherence tomography (OCT);

(4) BCVA of 20/40 to 20/400 (Snellen equivalent determined with the use of a Snellen chart).

2.3. Exclusion Criteria. Exclusion criteria include

(1) use of any other antiangiogenic medication other than ranibizumab;

(2) previous treatment with verteporfin photodynamic therapy, intravitreal steroids, or laser;

(3) any history of uveitis, diabetic retinopathy, or any other retinal disease other than AMD.

2.4. Population. In this cohort, initial treatment consisted of a loading dose of three intravitreal injections of ranibizumab (0.5 mg) at monthly intervals. One month after the third injection, patients underwent a full ophthalmic examination including BCVA, biomicroscopy, and OCT. Disease state was deemed to be still active if BCVA was worse by 5 letters or if there was any clinical or OCT evidence of disease activity (haemorrhage, SRF, or IRF). If this was the case, patients were given another injection of ranibizumab and were instructed to return in one month for another full clinical and OCT evaluation. This was repeated on a monthly basis until disease state was deemed inactive.

Disease state was deemed to be inactive if BCVA was stable or improved and there was no clinical or OCT evidence of disease activity (hemorrhage, SRF, or IRF). If this was the case, ranibizumab injections were suspended, and patients were instructed to return on a monthly basis for a full ophthalmic examination including BCVA, biomicroscopy, and OCT.

If during the patient's monthly examination there was either a 5-letter decrease in BCVA or clinical or OCT evidence of hemorrhage, IRF, or SRF, the patient was deemed to have developed a recurrence of active wet AMD. Monthly injections of ranibizumab were reestablished until the disease state was deemed inactive. If the disease state became inactive again, ranibizumab treatment was suspended again, and the patient was monitored with clinical and OCT examination on a monthly basis until there was a recurrence.

2.5. Study Procedures. The study protocol was approved by the Clinical Research Ethics Committee of Aragón (CEICA), Zaragoza, Spain.

We retrospectively analysed the consecutive charts and FA of three vitreoretinal practices (OR, JL, and CT) at the Miguel Servet University Hospital (Zaragoza, Spain) in patients with naive CNV secondary to AMD who had been treated exclusively with ranibizumab from the first of October 2008 to the first of October 2012.

Baseline data was collected: BCVA, age, gender, slit lamp examination of the anterior segment, intraocular pressure (IOP), dilated fundus examination, FA, and OCT.

The following data was also collected on a quarterly basis: BCVA, CRT measured by OCT, and number of ranibizumab injections.

Snellen visual acuity (VA) was measured by a certified ophthalmic technician. The Snellen value was recalculated to determine the corresponding logarithm of the minimum angle of resolution (logMAR) value for statistical analysis using a formula that reflects the relationship between the two methods [8].

CRT was determined using SD Cirrus OCT (Carl Zeiss Meditec, USA). Scanning with the Cirrus OCT was performed with the 512 × 128 scan pattern where a 6 × 6 mm area on the retina was scanned with 128 horizontal lines, each consisting of 512 A-scans per line (with the total of 65,536 sampled points) within a scan time of 2.4 seconds. All scans were performed by an experienced ophthalmic technician. Only good-quality examinations with a signal strength of ≥6/10 were retained.

2.6. Statistical Analysis. All statistical analyses were performed using IBM's statistical software (SPSS version 19.0; IBM Corporation, Somers, NY).

BCVA and CRT changes were compared every 6 months until the end of the study follow-up: 6, 12, 18, 24, 30, and 36 months (matched t-test).

The main statistical study was a survival analysis, which represents time-to-event data. Subjects were followed over time and observed at the time point at which they experienced the event of interest.

In this study, 2 independent survival analyses were performed: (i) the first event was considered to be a worsening of BCVA (defined as a difference of >0.3 logMAR units or more from baseline) and (ii) the second event was stable or improving BCVA (defined as ≤0.01 logMAR units compared with the baseline). Survival analysis depending on the mean number of ranibizumab injections (cut-off point of 7) was also performed.

Table 1: Demographic and clinical characteristics of the sample.

Age (years)	79.5 ± 7.8
Female (%)	58.8
Right eye (%)	49
High blood pressure (%)	60.8
Pseudophakia (%)	49
Glaucoma (%)	7.8
Type of CNV (FA) (%)	
Classic	48.2
Min. classic	7.4
Occult	44.4
Location of CNV (%)	
Subfoveal	31.8
Juxtafoveal	40.9
Extrafoveal	27.3
IOP (mmHg)	16.16 ± 2.78
BCVA LogMAR (Snellen)	0.68 ± 0.38 (20/95)
CRT (μm)	342.12 ± 121.57
N	51

CNV: choroidal neovascularization; FA: fluorescein angiogram; IOP: intraocular pressure; BCVA: best corrected visual acuity; LogMAR: logarithm of the minimum angle of resolution; CRT: central retinal thickness; *N*: number of subjects.

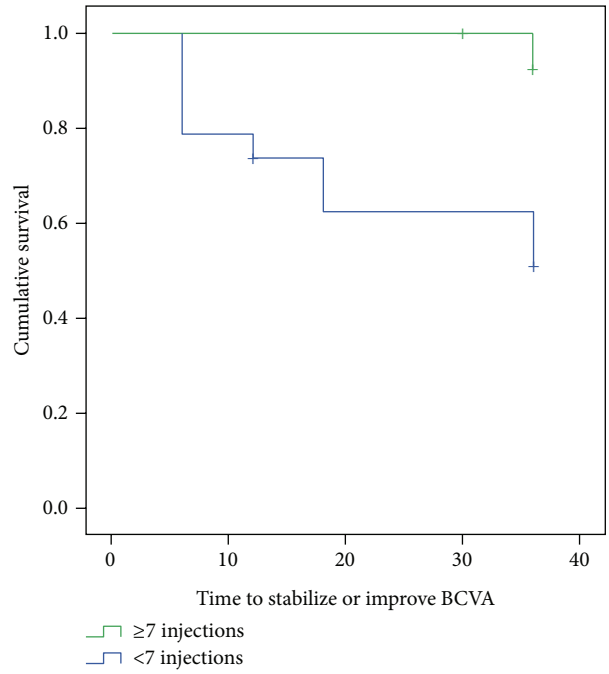

Figure 1: Kaplan-Meier survival plots of stable BCVA (SR was 92.9% in patients who received 7 or more injections versus 51.4% in those treated with <7 treatments ($P = 0.008$; log-rank test)).

Censoring occurred either when the patient attained each event or at the end of the study period (3 years). Differences in the Kaplan-Meier survival plots were calculated by the log-rank test. For all analyses, $P < 0.05$ was considered statistically significant.

3. Results

Of the 122 charts reviewed, 51 eyes (51 patients) met the study inclusion criteria. Baseline demographic and ocular data for both study groups are summarized in Table 1. Mean age was 79.5 ± 7.8 years. Women comprised 58.8% of the cohort, 60.8% of the patients had high blood pressure, and the right eye was treated in 49% of the cases. FA revealed a CNV distribution that was 48.2% predominately classic, 7.4% minimally classic, and 44.4% occult. Locations of these lesions were 31.8% subfoveal, 40.9% Juxtafoveal, and 27.3% extrafoveal. The mean baseline logMAR BCVA was 0.68 (20/95) ± 0.23 and mean CRT by OCT was 342.12 ± 121.57 μm. Mean IOP was 16.16 ± 2.78 mmHg.

Changes in BCVA and CRT from baseline were compared every 6 months up to 3 years (at 6, 12, 18, 24, 30, and 36 months).

BCVA demonstrated a significant logMAR improvement from 0.68 (20/95) to 0.53 ± 0.32 (20/67) ($P < 0.005$) at 6 months and 0.51 ± 0.31 (20/64) ($P < 0.001$) at 12 months. However, no statistical differences were found at 18, 24, 30, and 36 months ($P > 0.05$) (Table 2).

CRT significantly decreased compared to baseline ($P < 0.001$) at 6, 12, 18, 24, 30, and 36 months (Table 2). CRT was also measured using Kaplan-Meier SR analysis after 36 months of follow-up; 74.5% of all patients decreased the CRT compared to baseline during the observational period.

The mean number of ranibizumab injections was 6.98 ± 3.69 [3–20].

At 36 months, Kaplan-Meier SR for the worsening of BCVA was 76.5% (the proportion of patients without a decrease in vision of more than 0.3 logMAR units). According to the number of ranibizumab injections, SR was 88.9% in those who received 7 or more injections versus 69.7% receiving <7 treatments ($P = 0.12$; log-rank test).

The SR calculated for BCVA that remained stable or became better (decrease of 0.01 logMAR units of more) from baseline was 62.7%. According to the number of ranibizumab injections, SR was 92.9% in those who received 7 or more injections versus 51.4% receiving <7 treatments ($P = 0.008$; log-rank test) at 3 years (Figure 1).

4. Discussion

To our knowledge of the currently available data, this is the first study to compare retrospective results of treatment with ranibizumab for 3 years according the number of injections. Although the study is limited by its retrospective nature and small number of patients, the lengthy follow-up period (36 months) allowed us to obtain enough data to make meaningful interpretations, especially considering that this study was conducted in normally run vitreoretinal practices, reflecting a "real-life" clinical setting.

The prevalence of wet AMD increases exponentially with aging [9]. This disease causes a great impact on the quality of life, and patients define the consequences of wet AMD as

Table 2: Comparison of BCVA (LogMAR) and CRT (microns) during the follow-up.

Time (months)	Baseline	6	12	18	24	30	36
BCVA LogMAR (Snellen)	0.68 ± 0.3 (20/95)	0.53 ± 0.3* (20/67)	0.51 ± 0.3** (20/64)	0.59 ± 0.3 (20/77)	0.61 ± 0.3 (20/81)	0.64 ± 0.4 (20/87)	0.67 ± 0.4 (20/93)
CRT (μm)	342 ± 121	297 ± 98**	287 ± 94**	281 ± 85**	288 ± 93**	283 ± 92**	276 ± 88**

Compared to basal value, * $P < 0.005$; ** $P < 0.001$.
BCVA: best corrected visual acuity; LogMAR: logarithm of the minimum angle of resolution; CRT: central retinal thickness; N: number of subjects.

serious as uncontrollable pain or many metastatic or chronic debilitating diseases (severe ischemic transient attack, renal dialysis...). Besides having a devastating effect on the lives of patients, the condition is responsible for a major expense for the economy [10].

Without treatment, exudative AMD causes a significant loss of VA during the first two years of the disease, although most VA loss occurs during the first 3–6 months [11].

One of the primary goals in the management of wet AMD is to halt or delay the progression of visual loss and, if possible, improve VA. The findings of this study confirm the relationship between the number of injections of ranibizumab and the maintenance or improvement of VA. Patients treated with 7 or more injections during the 36-month follow-up showed a better survival rate in both analyses compared with patients who received less than 7 treatments.

Although the SR in worsening BCVA was not statistically significant, there was a clear trend towards a better outcome in the group receiving 7 or more injections (88.9% versus 69.7%, $P = 0.12$).

In the group of stable patients, the difference was even greater and statistically significant (BCVA SR was 92.9% in those who received 7 or more injections of ranibizumab versus 51.4% in those who received <7 treatments, $P = 0.008$).

Recently, Rofagha et al. [12] published the results after 8-year follow-up in 65 patients which participated in the MARINA and ANCHOR [1, 2] trials. To note, 34% worsened their VA (<15 letters) while 43% keep their VA stable or better (≥0 letters) compared to baseline, with a mean number of ranibizumab injections of 6.4 and a mean follow-up of 3.4 years. These results are similar to ours, with a worsening of VA in 23.5% of the patients (>0.3 LogMAR units) whereas 62.7% keep their VA stable or better compared to baseline. They also found that patients who received more intravitreal injections showed better VA outcomes.

In this work, no significant BCVA differences were found at 18, 24, 30, and 36 months ($P > 0.05$), probably because of the insufficient number of injections. Saleh et al. [13] analysed 66 eyes of 60 wet AMD patients treated with ranibizumab with a mean follow-up of 27 months. They did not find a significant VA improvement at the end of the follow-up period ($P > 0.05$) and the percentage of stable patients was 66.6% (compared to 62.7% in our work). Mean number of ranibizumab injections was 5 per year.

The mean number of injections received after 36 months (6.98 ± 3.69) seems to be very low when compared with the previous randomised trials: in the CATT study [14], patients were treated with a mean of 12.6 ± 6.6 ranibizumab injections during 2 years. In the ANCHOR study, the mean number of ranibizumab injections was 21.3 during 24 months of treatment. Such a huge difference in a clinical setting daily routine suggests that although patients are scheduled on a regular basis, the activity of the disease is being undertreated (underestimated) and more aggressive treatment is needed to maintain or improve BCVA during the follow-up.

Unlike this paper, MARINA and ANCHOR [1, 2] trials showed a significant VA improvement after a fixed monthly dosing schedule for intravitreal injections over a two-year period. Despite these impressive results, mostly patients, their families, and clinicians have considerable difficulty to sustain and accept monthly visits, not to mention the economic costs.

Alternate regimens of treatment have evolved in an attempt to provide comparable results in terms of BCVA, but with a fewer number of injections. The "Treat and Extend" (TAE) regimen described by Spaide aims to achieve and maintain a "dry" macula by gradually increasing the length of time between injections in the absence of macular fluid [15]. Growing use of the TAE method with ranibizumab for wet AMD has been described in recent studies with favourable improvements in VA while reducing the number of office visits and injections [16–18]. The 2012 American Society of Retinal Specialists Preferences and Trends survey revealed that the majority of Retinal Specialists members have turned to nonmonthly regimens, with 66.7% using TAE [19].

In conclusion, this study confirms that stable wet AMD patients after 3-year follow-up showed a significantly better BCVA SR (92.9%) if they received 7 or more injections versus those treated with fewer number of ranibizumab injections (51.4%) ($P = 0.008$).

Conflict of Interests

The authors declare that there is no conflict of interests regarding the publication of this paper.

Acknowledgment

The authors acknowledge Novartis Pharma, S.A, for the financial support.

References

[1] P. J. Rosenfeld, D. M. Brown, J. S. Heier et al., "Ranibizumab for neovascular age-related macular degeneration," *The New England Journal of Medicine*, vol. 355, no. 14, pp. 1419–1431, 2006.

[2] D. M. Brown, M. Michels, P. K. Kaiser, J. S. Heier, J. P. Sy, and T. Ianchulev, "Ranibizumab versus verteporfin photodinamic

therapy for neovascular age-related macular degeneration: two-year results of the ANCHOR study," *Ophthalmology*, vol. 116, no. 1, pp. 57.e5–65.e5, 2009.

[3] C. D. Regillo, D. M. Brown, P. Abraham et al., "Randomized, double-masked, sham-controlled trial of ranibizumab for neovascular age-related macular degeneration: PIER Study year 1," *American Journal of Ophthalmology*, vol. 145, no. 2, pp. 239–248, 2008.

[4] U. Schmidt-Erfurth, B. Eldem, R. Guymer et al., "Efficacy and safety of monthly versus quarterly ranibizumab treatment in neovascular age-related macular degeneration: the EXCITE study," *Ophthalmology*, vol. 118, no. 5, pp. 831–839, 2011.

[5] A. E. Fung, G. A. Lalwani, P. J. Rosenfeld et al., "An optical coherence tomography-guided, variable dosing regimen with intravitreal ranibizumab (Lucentis) for neovascular age-related macular degeneration," *The American Journal of Ophthalmology*, vol. 143, no. 4, pp. 566–e2, 2007.

[6] G. A. Lalwani, P. J. Rosenfeld, A. E. Fung et al., "A variable-dosing regimen with intravitreal ranibizumab for neovascular age-related macular degeneration: year 2 of the PrONTO Study," *American Journal of Ophthalmology*, vol. 148, no. 1, pp. 43–58, 2009.

[7] F. G. Holz, W. Amoaku, J. Donate et al., "Safety and efficacy of a flexible dosing regimen of ranibizumab in neovascular age-related macular degeneration: the SUSTAIN Study," *Ophthalmology*, vol. 118, no. 4, pp. 663–671, 2011.

[8] J. T. Holladay and T. C. Prager, "Snellen equivalent for the Bailey-Lovie acuity chart," *Archives of Ophthalmology*, vol. 107, no. 7, p. 955, 1989.

[9] C. A. Korb, U. B. Kottler, C. Wolfram et al., "Prevalence of age-related macular degeneration in a large European cohort: results from the population-based Gutenberg Health Study," *Graefe's Archive for Clinical and Experimental Ophthalmology*, vol. 252, no. 9, pp. 1403–1411, 2014.

[10] M. M. Brown, G. C. Brown, J. D. Stein, Z. Roth, J. Campanella, and G. R. Beauchamp, "Age-related macular degeneration: economic burden and value-based medicine analysis," *Canadian Journal of Ophthalmology*, vol. 40, no. 3, pp. 277–287, 2005.

[11] T. Y. Wong, U. Chakravarthy, R. Klein et al., "The natural history and prognosis of neovascular age-related macular degeneration: a systematic review of the literature and meta-analysis," *Ophthalmology*, vol. 115, no. 1, pp. 116–126, 2008.

[12] S. Rofagha, R. B. Bhisitkul, D. S. Boyer, S. R. Sadda, and K. Zhang, "Seven-year outcomes in ranibizumab-treated patients in ANCHOR, MARINA, and HORIZON: a multicenter cohort study (SEVEN-UP)," *Ophthalmology*, vol. 120, no. 11, pp. 2292–2299, 2013.

[13] M. Saleh, M. Kheliouen, E. Tebeanu et al., "Retreatment by series of three intravitreal injections of ranibizumab in neovascular age-related macular degeneration: long-term outcomes," *Graefe's Archive for Clinical and Experimental Ophthalmology*, vol. 251, no. 8, pp. 1901–1907, 2013.

[14] D. F. Martin, M. G. Maguire, S. L. Fine et al., "Ranibizumab and bevacizumab for treatment of neovascular age-related macular degeneration: two-year results," *Ophthalmology*, vol. 119, no. 7, pp. 1388–1398, 2012.

[15] R. Spaide, "Ranibizumab according to need: a treatment for age-related macular degeneration," *The American Journal of Ophthalmology*, vol. 143, no. 4, pp. 679–680, 2007.

[16] M. Engelbert, S. A. Zweifel, and K. B. Freund, "'Treat and extend' dosing of intravitreal antivascular endothelial growth factor therapy for type 3 neovascularization/retinal angiomatous proliferation," *Retina*, vol. 29, no. 10, pp. 1424–1431, 2009.

[17] M. Engelbert, S. A. Zweifel, and K. B. Freund, "Long-term follow-up for type 1 (subretinal pigment epithelium) neovascularization using a modified 'treat and extend' dosing regimen of intravitreal antivascular endothelial growth factor therapy," *Retina*, vol. 30, pp. 1368–1375, 2010.

[18] O. P. Gupta, G. Shienbaum, A. H. Patel, C. Fecarotta, R. S. Kaiser, and C. D. Regillo, "A treat and extend regimen using ranibizumab for neovascular age-related macular degeneration: clinical and economic impact," *Ophthalmology*, vol. 117, no. 11, pp. 2134–2140, 2010.

[19] R. A. Mittra and J. S. Pollack, *Preferences and Trends Membership Survey*, American Society of Retina Specialists, Las Vegas, Nev, USA, 2012.

Hindawi Publishing Corporation
Journal of Ophthalmology
Volume 2015, Article ID 424783, 6 pages
http://dx.doi.org/10.1155/2015/424783

Research Article

The Measurement of Intraocular Biomarkers in Various Stages of Proliferative Diabetic Retinopathy Using Multiplex xMAP Technology

Stepan Rusnak,[1] Jindra Vrzalova,[2,3] Marketa Sobotova,[1] Lenka Hecova,[1] Renata Ricarova,[1] and Ondrej Topolcan[2,3]

[1]*Department of Ophthalmology, University Hospital Pilsen, Alej Svobody 80, 304 60 Plzen, Czech Republic*
[2]*Department of Nuclear Medicine, Laboratory of Immunoanalysis, University Hospital Pilsen, Dr. E. Benese 13, 305 99 Plzen, Czech Republic*
[3]*Central Radioisotopic Laboratory, Faculty of Medicine in Pilsen, Charles University in Prague, Dr. E. Benese 13, 305 99 Plzen, Czech Republic*

Correspondence should be addressed to Marketa Sobotova; sobotovam@fnplzen.cz

Received 19 December 2014; Accepted 27 February 2015

Academic Editor: Ricardo Giordano

Purpose. To determine the intraocular levels of growth factors and cytokines in patients with various degrees of severity of proliferative diabetic retinopathy (PDR) using multiplex xMAP technology. *Methods*. A prospective cohort study of 61 eyes from 56 patients who were divided into 3 groups based on the severity of PDR. Patients in group number 1 are those who presented PDR with no need of repeated surgical intervention; patients in group number 2 had repeated vitreous bleeding; and patients in group number 3 had refractory neovascular glaucoma. The concentrations of proangiogenic, antiangiogenic, inflammatory, and neurotrophic factors were measured in intraocular fluid. The results were also compared with levels of factors measured in 50 eyes from 50 patients prior to senile cataract surgery (control group). *Results*. Patients with refractory neovascular glaucoma (the highest clinical severity group) had higher levels of interleukin 6 (IL-6) (median1 37.19; median3 384.74; $P = .00096$), transforming growth factor beta 1 (TGFβ-1) (median1 49.00; median3 414.40; $P = .0017$), and vascular endothelial growth factor (VEGF) (median1 211.62; median3 352.82; $P = .0454$) compared with other PDR patients. *Conclusions*. Results of our study imply that levels of IL-6, TGFβ-1, and VEGF correlate with the severity of PDR.

1. Introduction

Diabetes mellitus is one of the most common endocrine disorders in the world; it affected roughly 6% of the global population ca. in the year 2000, and it is estimated that it will affect 300 million people in 2025 [1]. Diabetic retinopathy affects 35% of the patients in the diabetic population [2] and is the main cause of permanent vision loss in the working population [3]. Proliferative diabetic retinopathy (PDR) is characterized by the pathological formation of retinal blood vessels. Despite progress in diagnostics and therapies, PDR leads to a terminal stage of therapeutically unmanageable neovascularization that is characterized by the development of secondary neovascular glaucoma in a number of cases.

Retinal hypoxia is a major driving force for retinal neovascularization that increases hypoxia inducible factor (HIF) levels and launches a cascade of the production of cytokines and growth factors. Since the discovery of the proangiogenic role of vascular endothelial growth factor (VEGF) in PDR, changes in the levels of a number of other proangiogenic factors, such as those in the insulin-like growth factor family (IGF), hepatocyte growth factor (HGF), basic fibroblast growth factor (b-FGF), platelet-derived growth factor (PDGF), proinflammatory cytokines, and angiopoietin, have been demonstrated. However, the intraocular synthesis of angiogenic factors is counterbalanced by the synthesis of antiangiogenic factors, including γ-interferon inducible protein 10 (IP-10), the pigment epithelium-derived factor

(PEDF), transforming growth factor beta (TGFβ), thrombospondin (TSP), endostatin, angiostatin, and somatostatin [4, 5]. Fluorescein angiography, or more recently ultra wide-field fluorescein angiography, is used to determine the scope of neovascularization or ischemia [6]. This method is an image-processing technique for angiographic mapping of the retina. It enables the most recent stage of retinal angiogenesis to be described, but it is not an objective risk assessment technique. The measurement of intraocular biomarkers is emerging as a novel possibility for patient stratification. Because neovascularization results from an imbalance in proangiogenic and antiangiogenic factors, a multiplex analytical tool for monitoring the levels of several factors in a small sample volume is necessary to describe this process. A combination of immunoanalysis and flow cytometry [7], called xMAP technology, is one of the most promising multiplex technologies in clinical research to date.

In our study, the concentration levels of epidermal growth factor (EGF), interleukin 6 (IL-6), VEGF, tumor necrosis factor alfa (TNF-α), interleukin 8 (IL-8), IP-10, monocyte chemoattractant protein 1 (MCP-1), PDGF, TGFβ-1, fractalkine, interleukin 10 (IL-10), interferon gamma (IFN-γ), fibroblast growth factor 2 (FGF-2), brain-derived neurotrophic factor (BDNF), ciliary neurotrophic factor (CNTF), and RANTES in samples of the aqueous humour from a group of PDR patients were measured using xMAP technology. The PDR cohort was further divided into three subgroups on the basis of clinical severity and these subgroups were compared with a control group. Our aim was to demonstrate that a biomarker panel measurement using multiplex immunoanalysis is applicable as a diagnostic and prognostic method in ophthalmology.

2. Materials and Methods

2.1. Patient Cohort. Patients undergoing treatment for PDR at the University Hospital in Pilsen during 2008–2010 were enrolled in this institutional prospective cohort study.

The patients with PDR were divided into groups according to the severity of their pathologies. Group 1 included 41 eyes from 37 patients with PDR who had no need for repeated surgical intervention (for better understanding, this group consists of 26 patients with PDR and vitreous bleeding, 5 patients with PDR and tractional retinal detachment, 5 patients with PDR, vitreous bleeding, and tractional retinal detachment, 4 patients with PDR and exudative maculopathy, and 1 patient with PDR with fibroproliferation), group 2 was composed of 11 eyes of nine patients who had repeated vitreous bleeding, and group 3 included 10 eyes from 10 patients with refractory neovascular glaucoma, which represents the most severe stage of the disease. The control group (group 0) was composed of 50 eyes from 50 preoperative senile cataract patients. Small samples (approximately 50 μL) of intraocular fluid from the aqueous humour of each participant were obtained under topical anesthesia from the anterior chamber of each eye by means of aspiration using a fine 30-gauge needle that was attached to a syringe.

2.2. Multiplex Analysis. All specimens were frozen immediately. Samples were stored at −80°C until they were analyzed. No more than one freeze-thaw cycle was allowed prior to analysis. The protein concentrations in the aqueous humour were measured using multiplex xMAP technology on a Luminex 100 instrument with commercially available panels from Millipore Corporation (Billerica, MA, USA), MILLIPLEX MAP Human Cytokine/Chemokine Panel, and MILLIPLEX MAP TGFβ-1. The procedures were performed according to the manufacturer's instructions, and the control samples that were provided within the kits were assayed in each analysis. The xMAP technology that was applied is a combination of immunoanalysis and flow cytometry based on bead particles that can be distinguished by internal dyes, as described, for example, by Kellar and Iannone [7]. In our study, the levels of EGF, IL-6, VEGF, TNF-α, IL-8, IP-10, MCP-1, PDGF AA, TGFβ-1, fractalkine, PDGF AB/BB, IL-10, IFN-γ, FGF-2, CNTF, BDNF, and RANTES were studied.

2.3. Statistical Methods. A descriptive statistic was calculated for each of the markers. The results under the calibration curve ranges were stated as the value of the lowest calibration point. The Mann-Whitney U test (independent samples) and Kruskal-Wallis test were used to compare marker levels between groups. Borderline significance was determined to be reflected by P values ranging from 0.05 to 0.0001, and significance was reflected by P values below 0.0001. MedCalc 11.2 statistics software was used for analysis.

3. Results

The median, lower, and upper quartile values for all of the markers within each group are listed in Table 1. When comparing the groups, significantly higher levels of IL-6, IL-8, IP-10, PDGF AA, and VEGF were found among PDR patients compared with patients in the control group. The concentrations of TGFβ-1 were higher in PDR patients compared with the control group. Patients in group 3 (those with neovascular glaucoma that was refractory to treatment) had higher levels of IL-6, TGFβ-1, and VEGF compared with patients in PDR group 1 and PDR group 2 (the nonneovascular glaucoma groups). The differences in concentrations were all of borderline significance (see Tables 1 and 2). No significant differences in marker levels were found between PDR group 1 (with no complications) and PDR group 2 (with repeated vitreous bleeding). No differences between groups were found in the levels of BDNF, CNTF, EGF, and MCP-1. See Table 2 for the results of the group comparisons. Boxplots of the VEGF concentrations in each of the groups are provided in Figure 1, and boxplots of the markers for which levels in control eyes differed significantly from levels in the eyes of patients in PDR group 1 are shown in Figure 2. Because the vast majority of patients had intraocular fluid concentrations of fractalkine, PDGFAB/BB, IL-10, IFN-γ, TNF-α, FGF-2, and RANTES that were below the detection limit of the panels that were used, the results from assays for these markers are not presented. Although the concentration of TGFβ-1 was below the detection limit in the control group,

Table 1: Descriptive statistics. Median values and 5th and 95th percentile values in pg/mL for all markers and groups are shown. Proliferative diabetic retinopathy (PDR) patients were divided into groups. Group 1: PDR patients with no need for repeated surgical intervention; group 2: PDR patients with repeated vitreous bleeding, which is a less serious complication of PDR; group 3: PDR patients with refractory neovascular glaucoma, which is a serious complication of PDR; group 0: control group.

	Groups							
	0		1		2		3	
	Median	5–95 P	Median	5–95 P	Median	5–95 P	Median	5–95 P
BDNF	12.00	12.00–59.67	12.00	12.00–49.37	12.00	12.00–103.23	30.00	12.00–81.43
CNTF	122.00	122.00–2667.92	393.19	122.00–1787.45	276.19	122.00–573.63	388.29	197.96–578.61
EGF	24.88	13.893–115.99	36.22	14.02–133.31	96.47	4.23–120.42	37.48	3.95–114.20
IL-6	3.20	3.200–196.312	37.19	3.992–4577.38	25.22	3.37–299.13	384.74	22.63–9982.69
IL-8	3.20	3.20–15.49	25.28	13.21–184.62	27.96	13.84–53.67	33.76	20.04–96.37
IP-10	105.92	12.93–307.68	460.68	159.49–2237.28	365.35	150.90–758.61	874.06	463.94–1698.36
MCP-1	962.59	3.20–2931.63	2772.21	353.18–3249.45	2336.77	2020.39–2653.15	661.23	3.20–2881.94
PDGFAA	111.26	5.85–212.85	227.96	104.57–756.34	208.36	151.58–344.62	192.66	79.91–316.61
TGFβ-1	49.00	49.00-49.00	49.00	49.00–220.41	49.00	49.00–84.71	414.40	119.85–955.58
VEGF	69.85	16.00–200.63	211.62	48.10–1990.98	187.96	4.28–523.25	352.82	132.84–7052.89

BDNF: brain-derived neurotrophic factor; CNTF: ciliary neurotrophic factor; EGF: epidermal growth factor; IL: interleukin; IP-10: γ-interferon inducible protein 10; MCP-1: monocyte chemoattractant protein 1; PDGF AA: platelet-derived growth factor AA; TGFβ-1: transforming growth factor beta 1; VEGF: vascular endothelial growth factor.
P: percentile.

Table 2: Comparison of biomarker levels between groups. *P* values are listed.

	Kruskal-Wallis	Mann-Whitney *U* 0 × 1	Mann-Whitney *U* 1 × 2	Mann-Whitney *U* 2 × 3	Mann-Whitney *U* 1 × 3
BDNF	NS	NS	NS	NS	NS
CNTF	NS	NS	NS	NS	NS
EGF	NS	NS	NS	NS	NS
IL-6	<0.0001	<0.0001	NS	0.0088	0.0096
IL-8	<0.0001	<0.0001	NS	NS	NS
IP-10	<0.0001	<0.0001	NS	NS	NS
MCP-1	NS	NS	NS	NS	NS
PDGFAA	<0.0001	<0.0001	NS	NS	NS
TGFβ-1	<0.0001	0.0027	NS	0.0037	0.0017
VEGF	<0.0001	<0.0001	NS	0.0265	0.0454

BDNF: brain-derived neurotrophic factor; CNTF: ciliary neurotrophic factor; EGF: epidermal growth factor; IL: interleukin; IP-10: γ-interferon inducible protein 10; MCP1: monocyte chemoattractant protein 1; PDGF AA: platelet-derived growth factor AA; TGFβ-1: transforming growth factor beta 1; VEGF: vascular endothelial growth factor.
NS: nonsignificant.

TGFβ-1 levels in some of the PDR patients were measureable; thus, the results are presented.

4. Discussion

Biomarkers in disease detection and management have become important tools in modern clinical medicine, and their application to retinal disease should be no exception. Because multiplex analysis based on xMAP technology allows for the analysis of tens of analytes in a small sample volume (10–50 μL), this is a potent technology for introducing laboratory medicine into ophthalmology.

In this study, we have confirmed that the patients with PDR have higher intraocular concentrations of proangiogenic, antiangiogenic, and inflammatory cytokines compared with nonPDR patients. Intraocular levels of IL-6, IL-8, IP-10, PDGF AA, TGFβ-1, and VEGF were increased in patients with PDR. Today, many studies compare the intraocular concentrations of various cytokines in PDR patients versus patients who do not have PDR. Maier et al. found that mean cytokine levels of IP-10, MCP-1, and VEGF in the vitreous humour were significantly higher compared to those of normal controls [8]. Murugeswari et al. documented that levels of IL-6, IL-8, MCP-1, and VEGF in the vitreous were

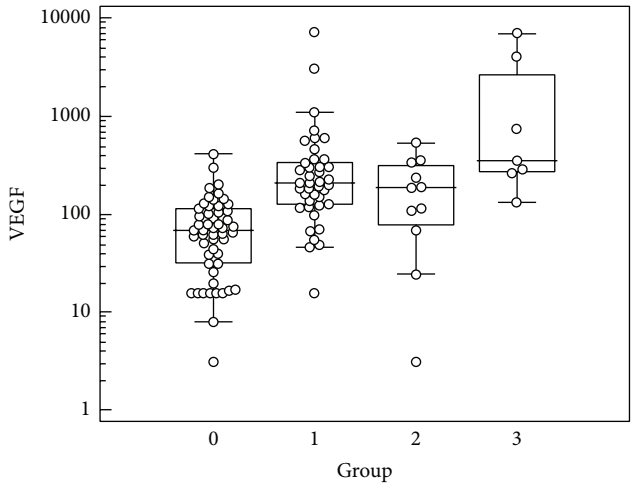

Figure 1: Vascular endothelial growth factor levels for each group. Group 1: proliferative diabetic retinopathy (PDR) patients with no need for repeated surgical intervention; group 2: PDR patients with repeated vitreous bleeding, which is a less serious complication of PDR; group 3: PDR patients with refractory neovascular glaucoma, which is a serious complication of PDR; group 0: control group.

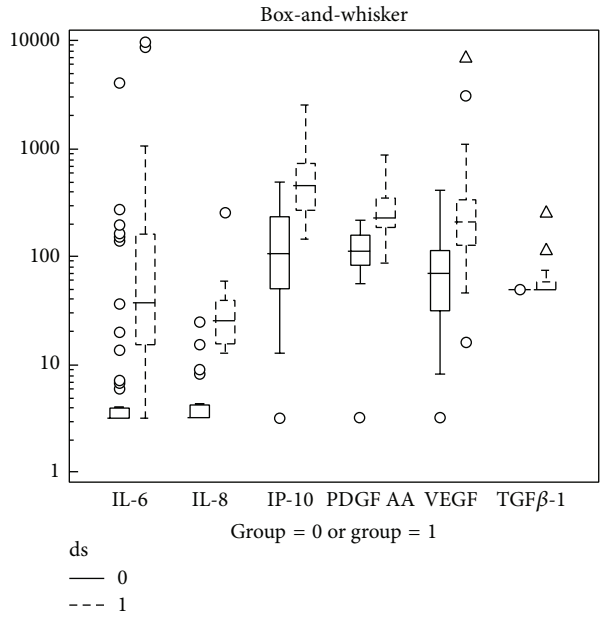

Figure 2: Levels of biomarkers for which significant differences between the levels in control group 0 and those in proliferative diabetic retinopathy group 1 were found. IL: interleukin; IP-10: γ-interferon inducible protein 10; PDGF AA: platelet-derived growth factor AA; VEGF: vascular endothelial growth factor; TGFβ-1: transforming growth factor beta 1.

significantly higher in PDR patients compared with levels in macular hole patients. Conversely, the vitreous level of PEDF was significantly reduced in patients with PDR [9]. Yoshimura et al. performed a comprehensive analysis of mediators in the vitreous fluids in PDR patients and in patients with other ocular diseases, and they found elevated levels of VEGF, MCP-1, IL-8, and IL-6 compared with control patients [10]. We found similar results in this study, but we have not demonstrated that the concentration of MCP-1 increases in patients with PDR. However, we have shown that higher intraocular concentrations of PDGF AA and nonmeasurable values of PDGF AB/BB can be seen in PDR patients. Contrary to our result, Freyberger et al. published results showing that PDGF AB levels are elevated in patients with PDR [11].

In a clinical environment, it is essential to further stratify the PDR patients; however, only a few studies that compare the levels of biomarkers in PDR patients with differing disease severities exist. Funatsu et al. divided PDR patients into subgroups based on disease progression and regression. The vitreous levels of VEGF and IL-6 were significantly higher in the eyes of patients in the progression group than they were in eyes with PDR regression. Multivariate logistic regression analysis showed that higher vitreous levels of VEGF were associated with the progression of PDR following vitreous surgery. A high vitreous level of VEGF was identified as a significant risk factor in determining the outcome of vitreous surgery in patients with PDR [12]. Freyberger et al. studied 23 patients with PDR, four of whom had rubeosis iridis, which is an indicator of very high vasoproliferative activity. Significantly elevated concentrations of PDGF AB were found among individuals with PDR; even higher levels were found in conjunction with rubeosis iridis [11]. In our study, patients with neovascular glaucoma that was refractory to treatment showed higher levels of IL-6, TGFβ-1, and VEGF than other PDR patients, which implies that the levels of these three factors are correlated with the severity of PDR. No differences in biomarker levels were found between patients who belonged to group 2 (those with repeated vitreous bleeding) and those who belonged to group 1 (those who had no complications).

The novel multiplex technology that we proposed not only saves time, labor, and costs of immunoanalysis, but it also rapidly reduces the sample volume requirements compared to a traditional immunoanalysis method (single ELISA) while allowing the full comparability of all studied parameters. The last two points are critical when entering laboratory measurements into the diagnostic and risk assessment process in ophthalmology. One limitation of xMAP technology could be that it is limited in its ability to detect some factors. In the present study, we were not able to detect fractalkine, PDGF AB/BB, IL-10, IFN-γ, TNF-α, FGF-2, and RANTES in the aqueous humour. Similarly, Yoshimura et al. found that the intraocular concentrations of IL-1β, IL-2, IL-4, IL-5, IL-10, IL-17, IFN-γ, TNF-α, eotaxin, MIP-1α, RANTES, EGF, and FGF-2 were lower than the detection level [10].

We have chosen three works as examples of studies that have shown the potency of xMAP technology in ophthalmology. Curnow et al. measured a panel of cytokines in the aqueous humour, and from the spectra of cytokines that they studied, they used random forest analysis to show that only IL-6, IL-8, MCP-1, IL-13, IL-2, and TNF-α are required to distinguish between noninflammatory control and idiopathic uveitis with 100% classification accuracy [13]. Funding et al. used xMAP technology to simultaneously quantify and compare the concentrations of 17 immune

mediators in aqueous humour samples from patients with corneal rejection and patients with a noninflammatory condition in the anterior chamber. Their results underscore both the complex immunological interactions of the rejection process and the need for multiplex laboratory measurements based on small sample volumes [14]. Rusnak et al. measured the levels of 12 cytokines in the aqueous humour in 27 eyes that were undergoing vitrectomies for retinal detachment with various degrees of severity of proliferative vitreoretinopathy. According to this study MCP-1 and VEGF may participate in pathogenesis of retinal detachment and proliferative vitreoretinopathy [15].

Sohn et al. have shown that multiplex measurements of cytokine and growth factor concentrations also enable treatment monitoring. After intravitreal injections of 2 antiangiogenic drugs (triamcinolone and bevacizumab), the clinical effects and differences in biomarker levels in the aqueous humour were monitored. A more effective treatment modality was linked to decreases in the concentrations of IL-6, IP-10, MCP-1, PDGF AA, and VEGF compared with those resulting from a less effective treatment; the latter treatment was only connected with a decrease in the concentration of VEGF [16].

The Sohn et al. study [16], in conjunction with our findings in patients with neovascular glaucoma refractory to treatment, shows that biomarkers have a strong potential for use in patient stratification and in determining personalized medical needs. Tailored treatments are necessary due to the introduction and costs of novel treatment. The vast majority of novel types of therapy are based on the inhibition of VEGF. A number of anti-VEGF agents have been introduced into clinical use and are widely used for the treatment of many ocular diseases, but the widespread use of these agents raises new questions. It has been proposed that anti-VEGF agents may have negative effects on retinal cells. Animal studies have shown that systemic neutralization of VEGF with soluble VEGF receptors results in a reduction of the thicknesses of both the inner and the outer nuclear layers in adult mouse retinas. These results indicate that endogenous VEGF plays an important role in the maintenance and function of neuronal cells in the adult retina and suggest that anti-VEGF therapies should be administered with caution [17]. Because of the risks associated with using anti-VEGF therapies, it is absolutely necessary to select patients who can benefit from anti-VEGF treatment despite the risk of adverse effects. In our study, we have shown that certain complications, such as neovascular glaucoma that is refractory to conventional treatment, are correlated with high concentrations of certain biomarkers; in the future, we can use these to justify more aggressive therapies. Our findings suggest that patients could be selected for repeat intravitreal injections of VEGF inhibitors, corticosteroids, more aggressive panretinal laser photocoagulation, cyclocryodestruction, or cyclophotodestruction on the basis of biomarker concentrations. Another study that shows that measuring protein concentrations in the aqueous humour has potential future benefits for treatment monitoring was conducted by Campochiaro et al.; they measured concentrations of VEGF, IL-6, IL-1 beta, tumor necrosis factor, and ranibizumab [18].

Another problem in patients who have been treated with anti-VEGF therapies is determining the concentration of VEGF. The determination of the VEGF concentration is influenced by treatment with anti-VEGF inhibitors via direct interaction in the immunoanalysis, which we verified in our laboratory (data not presented). The interaction requires an adjustment to the approach to determining the intraocular concentrations of VEGF in these patients; the half-life of anti-VEGF therapies in the eye was established as being 9.8 days [19]. Only patients who had never received anti-VEGF treatment or, in advanced cases, had received their most recent administrations of anti-VEGF therapy more than two months prior to aqueous humour sampling for this study were included. With the expansion of anti-VEGF therapy, it is clear that multifactor monitoring, that is, introducing other biomarkers in addition to VEGF, is important. Both our study and others show that there are several possible candidate biomarkers. As more PDR biomarkers are identified, a panel of them has the potential to be effective for identifying high-risk individuals, monitoring disease progression, and evaluating the efficacy of therapeutic interventions.

In conclusion, the results of our study suggest that the concentrations of IL-6, TGFβ-1, and VEGF correlate with the severity of PDR. In future, assessment of PDR biomarkers in intraocular fluid could be effective method for treatment monitoring and early detection of PDR progression.

Consent

Each participant signed informed consent approved by the Institutional Review Board.

Conflict of Interests

The authors declare that there is no conflict of interests regarding the publication of this paper.

Acknowledgment

This study was supported by the government granting agency IGA MZ NS10251-3.

References

[1] E. Adeghate, P. Schattner, and E. Dunn, "An update on the etiology and epidemiology of diabetes mellitus," *Annals of the New York Academy of Sciences*, vol. 1084, pp. 1–29, 2006.

[2] R. Klein and B. Klein, The Beaver Dam Eye Study, 1987–2010, http://www.bdeyestudy.org/.

[3] B. E. K. Klein, "Overview of epidemiologic studies of diabetic retinopathy," *Ophthalmic Epidemiology*, vol. 14, no. 4, pp. 179–183, 2007.

[4] R. Simó, E. Carrasco, M. García-Ramírez, and C. Hernández, "Angiogenic and antiangiogenic factors in proliferative diabetic retinopathy," *Current Diabetes Reviews*, vol. 2, no. 1, pp. 71–98, 2006.

[5] R. F. Gariano and T. W. Gardner, "Retinal angiogenesis in development and disease," *Nature*, vol. 438, no. 7070, pp. 960–966, 2005.

[6] R. F. Spaide, "Peripheral areas of nonperfusion in treated central retinal vein occlusion as imaged by wide-field fluorescein angiography," *Retina*, vol. 31, no. 5, pp. 829–837, 2011.

[7] K. L. Kellar and M. A. Iannone, "Multiplexed microsphere-based flow cytometric assays," *Experimental Hematology*, vol. 30, no. 11, pp. 1227–1237, 2002.

[8] R. Maier, M. Weger, E.-M. Haller-Schober et al., "Multiplex bead analysis of vitreous and serum concentrations of inflammatory and proangiogenic factors in diabetic patients," *Molecular Vision*, vol. 14, pp. 637–643, 2008.

[9] P. Murugeswari, D. Shukla, A. Rajendran, R. Kim, P. Namperumalsamy, and V. Muthukkaruppan, "Proinflammatory cytokines and angiogenic and anti-angiogenic factors in vitreous of patients with proliferative diabetic retinopathy and eales' disease," *Retina*, vol. 28, no. 6, pp. 817–824, 2008.

[10] T. Yoshimura, K.-H. Sonoda, M. Sugahara et al., "Comprehensive analysis of inflammatory immune mediators in vitreoretinal diseases," *PLoS ONE*, vol. 4, no. 12, Article ID e8158, 2009.

[11] H. Freyberger, M. Bröcker, H. Yakut et al., "Increased levels of platelet-derived growth factor in vitreous fluid of patients with proliferative diabetic retinopathy," *Experimental and Clinical Endocrinology & Diabetes*, vol. 108, no. 2, pp. 106–109, 2000.

[12] H. Funatsu, H. Yamashita, T. Mimura, H. Noma, S. Nakamura, and S. Hori, "Risk evaluation of outcome of vitreous surgery based on vitreous levels of cytokines," *Eye*, vol. 21, no. 3, pp. 377–382, 2007.

[13] S. J. Curnow, F. Falciani, O. M. Durrani et al., "Multiplex bead immunoassay analysis of aqueous humor reveals distinct cytokine profiles in uveitis," *Investigative Ophthalmology and Visual Science*, vol. 46, no. 11, pp. 4251–4259, 2005.

[14] M. Funding, T. K. Hansen, J. Gjedsted, and N. Ehlers, "Simultaneous quantification of 17 immune mediators in aqueous humour from patients with corneal rejection," *Acta Ophthalmologica Scandinavica*, vol. 84, no. 6, pp. 759–765, 2006.

[15] S. Rusnak, J. Vrzalova, L. Hecová, M. Kozova, O. Topolcan, and R. Ricarova, "Defining the seriousness of proliferative vitreoretinopathy by aspiration of cytokines from the anterior chamber," *Biomarkers in Medicine*, vol. 7, no. 5, pp. 759–767, 2013.

[16] H. J. Sohn, D. H. Han, I. T. Kim et al., "Changes in aqueous concentrations of various cytokines after intravitreal triamcinolone versus bevacizumab for diabetic macular edema," *American Journal of Ophthalmology*, vol. 152, no. 4, pp. 686–694, 2011.

[17] M. Saint-Geniez, A. S. R. Maharaj, T. E. Walshe et al., "Endogenous VEGF is required for visual function: evidence for a survival role on Müller cells and photoreceptors," *PLoS ONE*, vol. 3, no. 11, Article ID e3554, 2008.

[18] P. A. Campochiaro, D. F. Choy, D. V. Do et al., "Monitoring ocular drug therapy by analysis of aqueous samples," *Ophthalmology*, vol. 116, no. 11, pp. 2158–2164, 2009.

[19] T. U. Krohne, N. Eter, F. G. Holz, and C. H. Meyer, "Intraocular pharmacokinetics of bevacizumab after a single intravitreal injection in humans," *The American Journal of Ophthalmology*, vol. 146, no. 4, pp. 508–512, 2008.

Hindawi Publishing Corporation
Journal of Ophthalmology
Volume 2015, Article ID 102582, 8 pages
http://dx.doi.org/10.1155/2015/102582

Clinical Study

Outcomes and Prognostic Factors of Intravitreal Bevacizumab Monotherapy in Zone I Stage 3+ and Aggressive Posterior Retinopathy of Prematurity

Simona Delia Nicoară,[1] Constanța Nascutzy,[2] Cristina Cristian,[1] Iulian Irimescu,[3] Anne Claudia Ștefănuț,[4] Gabriela Zaharie,[5] and Tudor Drugan[6]

[1]*Department of Ophthalmology, "Iuliu Haţieganu" University of Medicine and Pharmacy, 8 Victor Babeş Street, 400012 Cluj-Napoca, Romania*
[2]*"Alfred Rusescu" Institute for Mother and Child Care, 120 Lacul Tei Boulevard, 020395 Bucharest, Romania*
[3]*Department of Neuroscience, "Iuliu Haţieganu" University of Medicine and Pharmacy, 8 Victor Babeş Street, 400012 Cluj-Napoca, Romania*
[4]*Department of Ophthalmology, Emergency County Hospital, 3-5 Clinicilor Street, 400006 Cluj-Napoca, Romania*
[5]*Department of Neonatology, "Iuliu Haţieganu" University of Medicine and Pharmacy, 8 Victor Babeş Street, 400012 Cluj-Napoca, Romania*
[6]*Department of Medical Informatics and Biostatistics, "Iuliu Haţieganu" University of Medicine and Pharmacy, 8 Victor Babeş Street, 400012 Cluj-Napoca, Romania*

Correspondence should be addressed to Simona Delia Nicoară; simonanicoara1@gmail.com

Received 8 December 2014; Revised 7 March 2015; Accepted 23 March 2015

Academic Editor: Juliana L. Dreyfuss

Purpose. This study aims to evaluate the regression of retinopathy of prematurity (ROP) after one intravitreal injection of bevacizumab and the factors that influenced it. *Methods*. This retrospective case series was carried out at the "Iuliu Haţieganu" University of Medicine and Pharmacy, Cluj-Napoca, Romania. It includes all the consecutive infants treated for ROP with one intravitreal bevacizumab injection, from January 1, 2009, throughout July 31, 2013. The follow-up continued for 60 weeks after injection. We recorded ROP classification, regression, gender, gestational age, birth weight, postnatal age and postmenstrual age at treatment, and pregnancy type. Regression was analyzed according to each of the abovementioned factors, with the program IBM SPSS 20 (Chicago, Illinois, USA). *Results*. This study includes 74 eyes of 37 infants of which 52 had aggressive posterior ROP (70.27%) and 22 had zone I stage 3+ ROP (29.72%). One week after the bevacizumab injection, ROP regressed in 63 eyes (85.13%), with a statistically significant higher rate in zone I stage 3+ ROP (100%), as compared with aggressive posterior ROP (78.84%) ($P = 0.03$). We recorded no complications subsequent to the intravitreal injections of bevacizumab. We identified no late retinal detachment. *Conclusion*. ROP regression rate after one intravitreal bevacizumab injection was 85.13%. This trial is registered with trial registration number IRCT2014101618966N2.

1. Introduction

Bevacizumab (Avastin; Genentech Inc., San Francisco, California, USA) is a full anti-VEGF human monoclonal antibody approved in 2004 by the FDA for the treatment of metastatic colon cancer and used off label in the treatment of neovascular retinal diseases, such as retinopathy of prematurity (ROP) [1, 2]. The first reports on the use of bevacizumab for ROP were published in 2007 and they presented the experience in aggressive posterior ROP (AP-ROP) [3–5]. This severe form of ROP progresses rapidly to retinal detachment and often has an unfavorable outcome with standard laser treatment [6–10]. The reports on bevacizumab in AP-ROP included a small number of infants, but the finding that the outcomes

were better in comparison with the ones of laser brought them into the spotlight.

The first prospective case series was published in 2008 and proved neovascular regression after bevacizumab injection, in 17 of the 18 eyes included in the study [11].

BEAT-ROP (Bevacizumab Eliminates the Angiogenic Threat of Retinopathy of Prematurity) was the first prospective, controlled, randomized trial that investigated the effect of one dose of bevacizumab (0.625 mg) for stage 3+ ROP, without combining laser and bevacizumab in the same infant. The recurrence rate in infants following bevacizumab was significantly lower as compared to the laser recurrence rate, 4% versus 22%. Benefits of bevacizumab over laser were statistically significant in zone I ROP. Another important observation of the BEAT-ROP study was that the injection of bevacizumab allows continued peripheral vascularization into avascular retina. However, the BEAT-ROP study has some unresolved issues: safety, long-term outcomes, and appropriate dosage [12].

In a previous study, we reported an AP-ROP regression rate of 54.16%, following laser treatment [10]. Disappointed by these outcomes and encouraged by the results mentioned above, we started to use bevacizumab injections to treat AP-ROP and zone I stage 3+ ROP.

We report our experience with intravitreal bevacizumab over a 55-month period for the treatment of ROP.

2. Materials, Subjects, and Methods

This is a retrospective case series.

Main Outcome Measures. ROP regression and the outcome associated with the intravitreal injection of bevacizumab.

2.1. Setting. The work was conducted in accordance with the Declaration of Helsinki (1964). All the intravitreal injections were carried out by the same ophthalmologist in the Departments of Neonatology and Ophthalmology belonging to the "Iuliu Haţieganu" University of Medicine and Pharmacy from Cluj-Napoca and in the Departments of Neonatology belonging to the "Saint Pantelimon" and "Polizu" Hospitals from Bucharest, Romania. The patients were enrolled after obtaining the informed consent from the parents/tutors. The study was approved by the Ethics Committee of the "Iuliu Haţieganu" University of Medicine and Pharmacy.

2.2. Study Sample. We analyzed retrospectively the files of all the consecutive infants with AP-ROP and zone I stage 3+ ROP who were treated by one intravitreal bevacizumab injection, from January 1, 2009, throughout July 31, 2013.

2.3. Screening Protocol. The treated premature infants came from a screening program that included the preterm newborns who met the following criteria: gestational age (GA) less than or equal to 33 weeks or birth weight (BW) less than or equal to 1500 grams. In the screening for ROP the premature infants with GA of more than 33 weeks and with BW of more than 1500 grams were also included, if other risk factors were associated: prolonged oxygen administration with saturation over 93%, repeated transfusions, sepsis, and necessity of more than 6 days of mechanical ventilation for the cardiorespiratory support. The first eye exam was performed at 4 weeks after birth in all the premature infants.

2.4. ROP Classification. We classified our cases according to the ICROP revisited [13]. This classification keeps the ICROP elaborated in 1984 [14], which takes into account the zone, the extension, the stage, and the presence/absence of "plus" disease and adds the definition of "pre-plus" disease and of the aggressive posterior ROP (AP-ROP). AP-ROP was defined as extreme vessel dilation and tortuosity in 4 quadrants, direct arteriovenous shunting, flat neovascularization, and rapid evolution, without following stage 1 to 3 progression [13].

2.5. Medical Intervention. A dose of bevacizumab of 0.625 mg in 0.025 mL was injected in each eye from the study sample, according to the following protocol: the pupils were dilated with a mixture of tropicamide 0.5% and phenylephrine 0.5%. Anesthesia was achieved with 0.5% proparacaine hydrochloride administered topically, 3 times, every 2 minutes before the injection. Every eye was prepared in a sterile manner using 5% povidone iodine which was also instilled in the eye 3 minutes prior to the injection. A nurse held the infant's head during the procedure and 0.025 mL of bevacizumab (0.625 mg) was injected in pars plicata, 1.5–1.75 mm away from the limbus, with a 30 G needle, perpendicularly on the globe initially and then slightly directed toward the center of the eyeball. After the injection, the patients received topical tobramycin, 5 times/day, for 3 days. The patients were reexamined the next day and then every week to monitor the regression of the disease. The follow-up continued for 60 weeks, every 2 weeks initially and then every 3 weeks, until full vascularization of the retina was observed. Full vascularization was defined as follows: vascularization as far as it would develop without an active component or clinically significant tractional elements. All the patients were followed by the pediatricians for long-term systemic complications. All the intravitreal injections were carried out by the same ophthalmologist and the examinations were performed by three ophthalmologists experienced in ROP.

We considered the following to be signs of regression: the pupil dilation, the disappearance or decrease of retinal vessel tortuosity and neovascularization, and the growth of the normal retinal vessels toward the peripheral retina. The treatment failure of ROP was defined according to the following criteria: the persistence/reappearance of plus disease and of retinal neovascularization and the progression toward retinal detachment. In all these latter situations, conventional laser photocoagulation of the retina was carried out.

Pictures of the retina before and after bevacizumab injections were taken with a Ret Cam (Clarity Medical System, Pleasanton, California, USA).

The following data were recorded: gender, GA, BW, zone and stage of ROP, other ocular findings (persistence of fetal vasculature, vitreous hemorrhage, and undilated pupil), postnatal age (PNA) and postmenstrual age (PMA) at treatment,

Table 1: Demographic and clinical characteristics of the premature infants who received intravitreal bevacizumab as primary therapy for ROP.

Eyes (patients)	74 (37)
Male/female	17/20
Unique/multiple pregnancy	29/8
Mean gestational age (wk)	28.89
Mean birth weight (g)	1218.35
Mean injection time (postmenstrual age/postnatal age, wk)	35.11/6.22
Number of eyes (%) with regression after bevacizumab injection alone	63 (85.13)

Table 2: Classification of ROP in the eyes treated with intravitreal injections of bevacizumab.

ROP classification	Eyes (number)	Eyes (%)
AP-ROP*	52	70.27
Stage 3 zone I with "plus"	22	29.72

*AP-ROP = aggressive posterior ROP.

type of pregnancy (unique, multiple), complications, and follow-up period.

2.6. Visual Outcome Assessment. Visual acuity (VA) testing was performed at 60 weeks by a trained pediatric ophthalmologist using Teller acuity cards (Stereo Optical Company, Inc., Chicago, IL) at a test distance of 40 cm. VA data were compared with available data of normal VA ranges for full-term infants. We considered as normal a VA within one or two octaves or greater than two octaves of the lower limit of the normal range. In cases with ROP progression towards retinal detachment, VA was categorized as unrecordable.

2.7. Statistical Analysis. We performed statistical analysis with the program IBM SPSS 20. Chi-square test was performed in order to verify the observed distributions in the contingency tables. If the theoretical distribution had less than 2 cases per cell we preferred the P value calculated with Fisher's exact test. The P value < 0.05 was considered statistically significant. Means comparisons were performed with Student's t-test because data were normally distributed and the number of cases was relatively low. Variance was tested with Levene's test.

3. Results

3.1. Demographic and Clinical Characteristics of the Study Sample. Our study was performed on 74 eyes with zone I stage 3+ ROP and AP-ROP belonging to 37 premature infants, treated by intravitreally injected bevacizumab (Table 1). The demographic and clinical characteristics of the premature infants are presented in Table 1.

All of the infants had a history of supplemental oxygen and mechanical ventilation use. None of the infants had a history of laser prior to the bevacizumab injection. Within the study sample, 17 infants were males (45.94%), 20 were females (54.05%), 29 were coming from unique pregnancies (78.37%), and 8 were coming from multiple pregnancies (21.62%). The mean GA was 28.89 ± 1.88 weeks (range 26–34 weeks) and the mean BW was 1218.35 ± 326.33 grams (range 800–2300 grams) (Table 1).

The ROP classification within the study sample is presented in Table 2.

Of the 37 prematures, 26 had bilateral aggressive posterior disease (AP-ROP) (70.27%) and 11 had bilateral zone I stage 3+ ROP (29.72%). We noted the persistence of fetal vasculature in 10 eyes (13.51%), undilated pupil in 7 eyes (9.45%), and vitreous hemorrhage in 4 eyes (5.71%), all within the AP-ROP group.

The most important data of each preterm newborn included in this study are illustrated in Table 3.

3.2. Outcomes of ROP after Intravitreal Bevacizumab Injections. One week after the bevacizumab injection, ROP regressed in 63 eyes (85.13%) (Table 1). ROP regressed bilaterally in 30 cases (81.08%), regressed unilaterally in 3 cases (8.10%), and progressed bilaterally in 4 cases (10.81%).

3.2.1. Structural Outcomes at 60 Weeks. In all of the 11 eyes that failed to regress after one intravitreal injection of bevacizumab, laser photocoagulation was carried out at 7–10 days after the intravitreal bevacizumab, with good evolution in 9 of the 11 eyes. At 60 weeks, retina was attached completely in 72 eyes (97.29%) and totally detached (stage V) in 2 eyes (2.70%). None of the cases in this series progressed towards bilateral retinal detachment.

3.2.2. Functional Outcomes at 60 Weeks. From the 72 eyes with good structural outcomes at 60 weeks, 68 had VA within normal limits (94.44%). All the 4 eyes with lower than normal VA come from the AP-ROP subgroup with laser addition.

3.3. Individual Factors Associated with the Outcomes after Bevacizumab Injections. We analyzed the following individual factors in correlation with the evolution after the intravitreal injection of bevacizumab: ROP type, gender, type of pregnancy, GA, and BW. Bevacizumab administered as one intravitreal injection was followed by ROP regression in all the 22 eyes with zone I stage 3+ ROP (100%) and in 41 of the 52 eyes with AP-ROP (78.84%) (Table 3). Fischer's exact test proved that the success rate was significantly higher in stage 3 zone I ROP, as compared to AP-ROP ($P = 0.03$).

Within the group of girls (40 eyes), ROP regressed in 33 eyes (82.50%) and within the group of boys (34 eyes), ROP regressed in 30 eyes (88.23%). The difference between genders was not statistically significant ($P > 0.05$).

Of the 37 pregnancies, 29 were unique and 8 were multiple. Within the unique pregnancies group (58 eyes), ROP regressed in 47 eyes (81.03%) and within the multiple pregnancies group (18 eyes), ROP regressed in all the 16 eyes (100.00%). The difference was not statistically significant ($P > 0.05$).

Table 3: Data of each premature infant treated by intravitreal injections of bevacizumab.

Case	Gender	GA (w)	BW (g)	ROP (OD/OS)	PNA (w)	PMA (w)	Outcome (OD/OS)
1	M	28	900	AP*/AP	8	36	Good/bad
2	F	28	1000	AP/AP	5	33	Good/good
3	F	32	1800	AP/AP	4	36	Good/good
4	M	34	2300	3 I**/3 I	4	38	Good/good
5	F	27	995	AP/AP	7	34	Good/good
6	F	30	1400	3 I/3 I	4	34	Good/good
7	M	30	1500	3 I/3 I	4	34	Good/good
8	F	26	1100	AP/AP	5	31	Good/good
9	F	28	990	AP/AP	6	34	Good/good
10	M	30	1650	3 I/3 I	7	37	Good/good
11	F	28	2050	3 I/3 I	6	34	Good/good
12	F	27	1100	AP/AP	8	35	Good/good
13	F	29	1140	AP/AP	8	37	Good/bad
14	M	30	1200	3 I/3 I	7	37	Good/good
15	F	27	970	AP/AP	6	33	Good/good
16	F	29	1070	AP/AP	6	35	Good/good
17	F	28	990	AP/AP	7	35	Good/good
18	M	28	1000	AP/AP	6	34	Good/good
19	F	31	1200	3 I/3 I	5	36	Good/good
20	F	31	1100	3 I/3 I	5	36	Good/good
21	F	30	1030	AP/AP	6	36	Good/good
22	M	28	990	AP/AP	7	35	Good/good
23	M	28	1100	AP/AP	7	35	Good/good
24	M	28	985	AP/AP	7	35	Good/good
25	M	31	1400	AP/AP	4	35	Bad/bad
26	M	32	1500	3 I/3 I	5	37	Good/good
27	M	31	1240	AP/AP	5	36	Good/good
28	F	31	1499	AP/AP	7	38	Bad/bad
29	M	27	1010	AP/AP	7	34	Good/good
30	F	26	1100	AP/AP	8	34	Bad/bad
31	F	27	950	AP/AP	7	34	Bad/bad
32	M	27	980	AP/AP	5	32	Good/good
33	M	28	1550	3 I/3 I	8	36	Good/good
34	F	27	800	AP/AP	10	37	Good/good
35	M	28	1390	AP/AP	7	35	Good/bad
36	F	31	1550	3 I/3 I	6	37	Good/good
37	M	28	1050	AP/AP	6	34	Good/good

*AP = aggressive posterior; **3 I = stage 3 zone I.

An independent t-test was conducted to determine if there was a difference between the mean GA of the premature infants with favorable or unfavorable outcome after bevacizumab injections. The results of Levene's test $F(72) = 0.43$, $P = 0.51$ indicate that the variances of the two populations (with favorable and unfavorable outcome) were approximately equal. Thus, the t-tests assuming equal variations were used. There was no statistically significant difference between the mean GA of the premature infants with favorable ($n = 63$; $M = 28.94$; SD = 1.86) and unfavorable ($n = 11$; $M = 28.64$; SD = 2.06) outcome, $t(72) = 0.48$, $P = 0.62$. The 95 confidence interval was −0.934 to 1.534.

An independent t-test was conducted to determine if there was a difference between the mean BW of the premature infants with favorable or unfavorable outcome after bevacizumab injections. The results of Levene's test $F(72) = 0.66$, $P = 0.41$ indicate that the variances of the two populations (with favorable and unfavorable outcome)

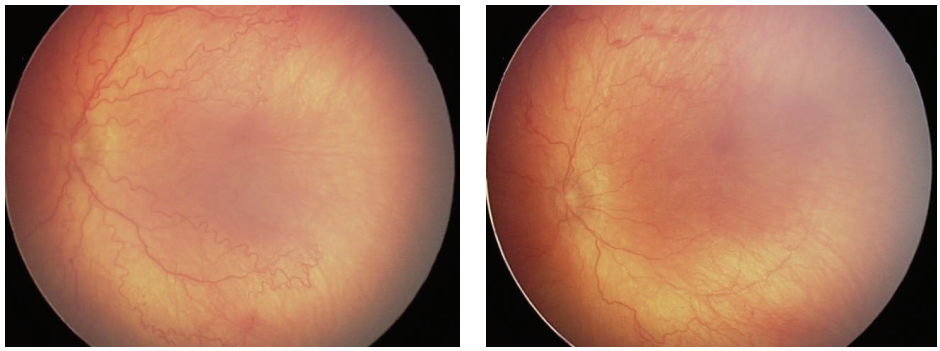

(a) (b)

Figure 1: (a) AP-ROP prior to the bevacizumab injection: male infant, BW 1000 g, GA 28 w, treated with intravitreal bevacizumab at PMA of 34 weeks and PNA of 6 weeks. (b) Fundus photography 5 days after bevacizumab injection with venous dilatation and arteriolar tortuosity improvement in the posterior pole, showing plus disease regression.

were approximately equal. Thus, the t-tests assuming equal variations were used. There was no statistically significant difference between the mean BW of the infants with favorable ($n = 63$; $M = 1219.52$ g; SD = 341.75 g) and unfavorable ($n = 11$; $M = 1211.64$; SD = 230.65) outcome after bevacizumab therapy, $t(72) = 0.73$, $P = 0.94$. The 95 confidence interval was −206.153 to 221.928.

3.4. Timing of Bevacizumab Injections. We evaluated the moment of bevacizumab injections according to two parameters: PNA and PMA at treatment. PNA at the moment of bevacizumab injection varied on our series between 4 and 10 weeks (mean 6.22 ± 1 weeks) (Table 1). An independent t-test was conducted in order to determine if the mean PNA at treatment was significantly different between the favorable and unfavorable outcome subgroups. The results of Levene's test $F(72) = 0.05$, $P = 0.82$ indicate that the variances of the two populations (with favorable and unfavorable outcome) were equal. Thus, the t-tests assuming equal variations were performed. The PNA at treatment did not differ significantly between the favorable ($n = 63$; $M = 6.11$ w; SD = 1.38 w) and unfavorable ($n = 11$; $M = 6.82$ w, SD = 1.47 w) outcome subgroups, $t(72) = -1.55$, $P = 0.12$. The 95 confidence interval was −1.615 to 0.201. PMA at treatment varied between 31 and 38 weeks (mean 35.11 ± 2 weeks) (Table 2). An independent t-test was conducted in order to determine if the mean PMA at treatment was significantly different between the favorable and unfavorable outcome subgroups. The results of Levene's test $F(72) = 0.02$, $P = 0.88$ indicate that the variances of the two populations (with favorable and unfavorable outcome) were assumed to be approximately equal. Thus, the t-tests assuming equal variations were used. The PMA at treatment did not differ significantly between the favorable ($n = 63$; $M = 35.05$ w; SD = 1.59 w) and unfavorable ($n = 11$; $M = 35.45$ w; SD = 1.57 w) outcome subgroups, $t(72) = -0.78$, $P = 0.43$. The 95 confidence interval was −1.441 to 0.628.

Figures 1(a) and 1(b) illustrate a case of AP-ROP just prior to the bevacizumab injection (a) and 5 days after the injection (b).

The immediate good outcome of this case is revealed by the significant improvement of "plus" disease and the decrease of retinal vessel tortuosity.

Figure 2 presents a case with zone I disease prior to the injection of bevacizumab (a) and 8 weeks after the injection (b). "Plus" disease disappeared, the ridge regressed, and the retinal vessels continued their normal growth towards the periphery.

We recorded no systemic complication subsequent to the intravitreal administration of bevacizumab in our series. No cataracts, endophthalmitis, or retinal detachments produced by the intraocular injections were identified in our series. The final anatomic outcome (after having added the laser photocoagulation of the retina) proved the bilateral attached retina in 35 cases (94.59%) and the unilateral attached retina in 2 cases (5.40%). No case ended up with bilateral retinal detachment.

4. Discussion

4.1. Rationale for Anti-VEGF Treatment in ROP. The basis for the intravitreal administration of anti-VEGF agents as treatment for ROP is the evidence that the concentration of VEGF is increased in the vitreous of infants with ROP [15, 16]. Bevacizumab blocks the molecules of VEGF already in the vitreous and it also inhibits the production of new ones. This explains the better and more rapid outcomes as compared to laser [1]. It was shown that ROP ceases within 48 h after the intravitreal administration of bevacizumab [17]. We observed the regression of "plus" disease even at 24 hours after the injection in our series. Bevacizumab is less destructive and more oriented towards the pathogenesis of ROP as compared to laser [18]. Unlike with laser, the retinal vascularization continues after the intravitreal injection of bevacizumab. We followed all the patients for 60 weeks and we observed the development of retinal vessels up to the periphery in all our cases with good outcomes after bevacizumab intravitreal injections. Moreover, according to the BEAT-ROP study, the intravitreal administration of bevacizumab is not associated

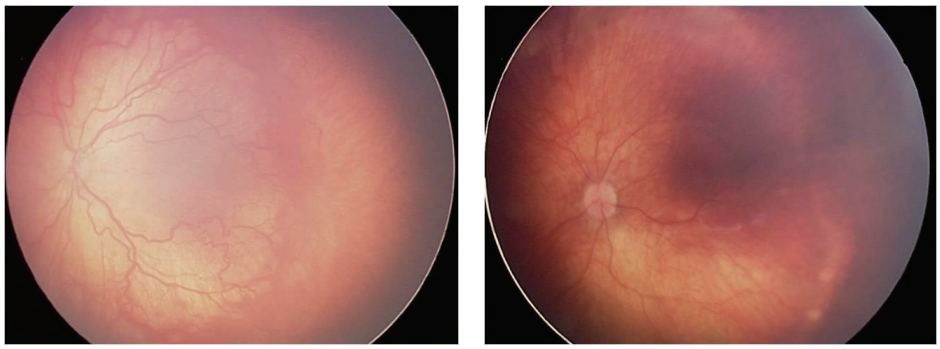

(a) (b)

Figure 2: (a) Zone I disease prior to the bevacizumab injection: female infant, BW 2050 g, GA 28 w, treated with intravitreal bevacizumab at PMA of 34 weeks and PNA of 6 weeks. (b) The same case as in (a), 8 weeks after the intravitreal injection of bevacizumab showing ROP regression.

with cystoid macular edema [12]. This finding is confirmed by our series.

As opposed to the laser treatment, the intravitreal injection of bevacizumab is shorter, easier, accessible, and less expensive; it can be performed if the pupils are small and/or vitreous hemorrhage is associated and it is more efficient than laser in zone I ROP. It was not our goal to compare the results of bevacizumab with laser. However, we found that the primary intravitreal injection of 0.025 mL (0.625 mg) of bevacizumab was followed by the regression of ROP in 78.84% of the AP-ROP eyes. In the lasered AP-ROP cases, we found regression in 53.84% [10].

4.2. Indications of Intravitreal Bevacizumab in ROP according to Our Experience. In our series, we used bevacizumab intravitreally in AP-ROP and in zone I stage 3+ ROP. In AP-ROP, our choice was motivated by our poor outcomes following laser treatment. As mentioned above, in our previous study, we registered regression rates of AP-ROP after laser treatment of 53.84% [10].

In zone I stage 3+ ROP, we used bevacizumab instead of laser, despite the good results of the laser treatment that we previously reported [10]. Our choice was motivated by the much longer duration of the laser treatment and its association with significant loss of visual field in this posterior location of the disease.

4.3. Demographic and Clinical Characteristics of the Study Sample. ROP is rare in infants with BW > 2000 g. On our series, we identified 2 infants with severe ROP, with BW over 2000 g. Also, 6 infants had BW over 1500 g, outside the screening criteria for ROP that are used in the USA. Nine of the 37 prematures had GA higher than 30 weeks, which is the limit for screening in the USA. This observation proves that, in each region, specific criteria for ROP screening must be applied. Older and bigger babies in developing and middle-income countries are known to develop significant ROP and possibly oxygen-induced retinopathy [19]. Larger and more mature babies developed severe forms of ROP disease in our series compared to screening criteria used in other countries (USA, Canada, and UK). This may suggest that possibly other predisposing factors not described in this study play a role in this aggressive presentation of ROP disease.

4.4. Timing of Intravitreal Bevacizumab Injections for ROP. The exact therapeutic window during which intravitreal bevacizumab is effective is not precisely known. The most important decisional factors are the PMA at treatment and the degree of membrane formation [18]. The PMA helps us evaluate the likely proportion between the angiogenic and fibrotic growth factors [18]. If intravitreal bevacizumab is administered too late, the contraction of membranes with subsequent acceleration of retinal detachment can result [20]. In all the premature infants included in this series, the initial eye exam had been done at 4 weeks after birth. None of the severe cases can be attributed to the failure in early diagnosis. In our series, the mean PMA at treatment was 35.11 weeks, with no statistically significant difference between the favorable (35.05 weeks) and unfavorable (35.45 weeks) outcome groups.

In the neovascular retinal diseases of the adult (age-related macular degeneration and diabetic retinopathy), there is a continuous release of VEGF [1]. As opposed to this situation, in ROP there is a single burst of VEGF that initiates the retinal neovascularization. Therefore, the repeat of injection appears unnecessary in ROP [1]. In all the cases included in this series, we performed one single bevacizumab injection in each eye.

4.5. Outcomes. The only factor that influenced the outcomes of bevacizumab monotherapy in our series was the ROP type. ROP regressed in all the eyes with zone I stage 3+ ROP (100%) and in 78.84% of the eyes with AP-ROP after one intravitreal bevacizumab injection ($P = 0.03$). The outcomes in our series were not influenced by gender, type of pregnancy (unique or multiple), GA, BW, and PNA and PMA at treatment.

Recent studies proved that VEGF is not the only growth factor upregulated in the eye and therefore its inhibition may not induce the ROP regression in all cases. Other growth factors involved in ROP pathogeny are insulin-like growth

factor, angiopoietin-1, and angiopoietin-2 [2, 16]. These data could partially explain the failures in our series.

Within the group of eyes with good structural outcomes (72 eyes), 94.44% had normal VA at 60 weeks. This observation allows us to affirm that if the structural result was successful, the potential for normal VA development was high in our series.

4.6. Safety. All the patients in the study sample were followed by pediatricians for systemic side effects related to bevacizumab, regarding the development of the brain, lungs, kidneys, and skeleton, and no abnormalities were reported. No local side effects, such as cataract, endophthalmitis, vitreous hemorrhage, and retinal detachment related to the intraocular injection, were identified in our series. ROP progression in 11 AP-ROP eyes was probably not due to the bevacizumab injection but to its inefficacy.

Still, there are concerns regarding the long-term effects of bevacizumab, the probability of the substance to leave the eye and the delayed-onset retinal detachment [15, 21].

In the eye, VEGF is not only an angiogenic factor, but also a neural survival one. Therefore, the suppression of the normal development of neural retinal components by the anti-VEGF therapy is suspected [15]. Histopathological studies, performed both on a rabbit model and in a very premature infant, proved that bevacizumab had no adverse effect on the growing and development of the eye [22, 23].

In the eyes with ROP, there is the breakdown of the blood-retinal barrier. As a consequence, the anti-VEGF substances might leave the vitreous and get into the systemic circulation, reducing the serum VEGF level [15]. Laser photocoagulation of the retina destroys the natural retinal barrier, enhancing the exit of bevacizumab from the choroidal vessels into the blood. Subsequently, these infants are at a higher risk of systemic effects [1]. This is the reason why we used bevacizumab as the first-choice treatment, not subsequently to the laser therapy. At the moment when anti-VEGF therapy is administered, the infant is still in the process of organogenesis and the VEGF is necessary for the development of the brain, lungs, kidneys, and skeleton. Therefore, the injection of the minimal effective dose and the use of an anti-VEGF agent with the most rapid systemic clearance are recommended [15]. A 2007 report on the pharmacokinetics of bevacizumab found that the half-life of 1.25 mg is 4.32 days in a rabbit eye. In addition, small amounts were detected in the serum and the fellow eye. However, humans have a larger serum compartment than rabbits and, therefore, systemic exposure may be less [24]. In adults, the intrinsic serum elimination half-life of bevacizumab is 20 days. In children this is not known, but it is probably longer [25]. When we compare the dosage of bevacizumab which is used for the premature infants with the one in adults, we find that the concentration for bodyweight is very large in infants. The appropriate dosage that should be used is not well known [21].

Even if there has been no report on the possible systemic side effects of intravitreally administered bevacizumab, we do not know for sure the long-term side effects on a developing child. Larger and longer studies are needed, in order to fully address the systemic toxicity issues.

Bevacizumab changes the natural evolution of ROP; despite the initial resolution there are chances of recurrence that we must be aware of. The delayed-onset retinal detachment, 4–4.5 months after the injection, is explained by the incomplete regression of the fibrovascular proliferation that develops slowly into a tractional complex [26]. The practical conclusion of this observation is the necessity to extend the follow-up period. We followed all the infants in this series for 60 weeks after the intravitreal injection of bevacizumab. We report no late retinal detachment.

A recent study documented significant vascular and macular abnormalities at the age of 9 months, in the eyes that received intravitreal bevacizumab for ROP [27]. These findings were not identified in the laser treated eyes. Long-lasting implications of these abnormalities for visual function of the child need further investigation [27].

The limitations of our study are its retrospective nature and the lack of a concomitant control group. On the ground of our results, currently, bevacizumab is our treatment of choice in AP-ROP and zone I disease. We follow each patient for 15 months after the injection, in order to identify late onset retinal detachment. We still have questions to be answered, regarding the optimal dosing, timing, avoidance of unnecessary treatment, long-term effects, and safety.

5. Conclusion

ROP regression rate after one intravitreal bevacizumab injection was 85.13%. Our study proves that 100% of patients with zone I stage 3+ ROP and 78.84% of patients with AP-ROP regressed with a single injection of bevacizumab, without ocular or systemic complications. Eyes with zone I stage 3+ ROP were more likely to have regression of ROP with a single injection of bevacizumab than those with AP-ROP.

Conflict of Interests

The authors declare that there is no conflict of interests regarding the publication of this paper.

Acknowledgments

This paper was performed within the frame of the Program "Partnerships in priority domains, PN II, with the support of the National Education Ministry, UEFISCDI, Project no. 134."

References

[1] J. A. Micieli, M. Surkont, and A. F. Smith, "A systematic analysis of the off-label use of bevacizumab for severe retinopathy of prematurity," *American Journal of Ophthalmology*, vol. 148, no. 4, pp. 536.e2–543.e2, 2009.

[2] C. Lin, S. Chen, C. Tseng, Y. Chang, and J. Hwang, "Effects of ranibizumab on very low birth weight infants with stage 3 retinopathy of prematurity: a preliminary report," *Taiwan Journal of Ophthalmology*, vol. 2, no. 4, pp. 136–139, 2012.

[3] A. Travassos, S. Teixeira, P. Ferreira et al., "Intravitreal bevacizumab in aggressive posterior retinopathy of prematurity,"

Ophthalmic Surgery Lasers and Imaging, vol. 38, no. 3, pp. 233–237, 2007.

[4] E. J. Chung, J. H. Kim, H. S. Ahn, and H. J. Koh, "Combination of laser photocoagulation and intravitreal bevacizumab (Avastin) for aggressive zone I retinopathy of prematurity," *Graefe's Archive for Clinical and Experimental Ophthalmology*, vol. 245, no. 11, pp. 1727–1730, 2007.

[5] S. Kusaka, C. Shima, K. Wada et al., "Efficacy of intravitreal injection of bevacizumab for severe retinopathy of prematurity: a pilot study," *British Journal of Ophthalmology*, vol. 92, no. 11, pp. 1450–1455, 2008.

[6] M. O'Keefe, B. Lanigan, and V. W. Long, "Outcome of zone 1 retinopathy of prematurity," *Acta Ophthalmologica Scandinavica*, vol. 81, no. 6, pp. 614–616, 2003.

[7] Z. Récsán, R. Vámos, and G. Salacz, "Laser treatment of zone I prethreshold and stage 3 threshold retinopathy of prematurity," *Journal of Pediatric Ophthalmology and Strabismus*, vol. 40, no. 4, pp. 204–207, 2003.

[8] A. Kychenthal, P. Dorta, and X. Katz, "Zone I retinopathy of prematurity: clinical characteristics and treatment outcomes," *Retina*, vol. 26, no. 7, supplement, pp. S11–S15, 2006.

[9] Early Treatment for ROP Cooperative Group, "Revised indications for the treatment of retinopathy of prematurity: results of the early treatment for retinopathy of prematurity randomized trial," *Archives of Ophthalmology*, vol. 121, no. 12, pp. 1684–1694, 2003.

[10] S.-D. Nicoară, C. Cristian, I. Irimescu, A.-C. Stefanut, and G. Zaharie, "Diode laser photocoagulation for retinopathy of prematurity: outcomes after 7 years of treatment," *Journal of Pediatric Ophthalmology and Strabismus*, vol. 51, no. 1, pp. 39–45, 2014.

[11] H. Quiroz-Mercado, M. A. Martinez-Castellanos, M. L. Hernandez-Rojas, N. Salazar-Teran, and R. V. P. Chan, "Antiangiogenic therapy with intravitreal bevacizumab for retinopathy of prematurity," *Retina*, vol. 28, no. 3, pp. S19–S25, 2008.

[12] H. A. Mintz-Hittner, K. A. Kennedy, and A. Z. Chuang, "Efficacy of intravitreal bevacizumab for stage 3+ retinopathy of prematurity," *The New England Journal of Medicine*, vol. 364, no. 7, pp. 603–615, 2011.

[13] International Committee for the Classification of Retinopathy of Prematurity, "The international classification of retinopathy of prematurity revisited," *Archives of Ophthalmology*, vol. 123, no. 7, pp. 991–999, 2005.

[14] A. Garner, I. Ben-Sira, and A. Deutman, "An international classification of retinopathy of prematurity," *British Journal of Ophthalmology*, vol. 68, no. 10, pp. 690–697, 1984.

[15] C.-H. Yang, "Anti-vascular endothelium growth factor therapy for retinopathy of prematurity: a continuing debate," *Taiwan Journal of Ophthalmology*, vol. 2, no. 4, pp. 115–116, 2012.

[16] T. Sato, C. Shima, and S. Kusaka, "Vitreous levels of angiopoietin-1 and angiopoietin-2 in eyes with retinopathy of prematurity," *The American Journal of Ophthalmology*, vol. 151, no. 2, pp. 353–357, 2011.

[17] H. A. Mintz-Hittner and R. R. Kuffel Jr., "Intravitreal injection of bevacizumab (avastin) for treatment of stage 3 retinopathy of prematurity in zone i or posterior zone II," *Retina*, vol. 28, no. 6, pp. 831–838, 2008.

[18] H. A. Mintz-Hittner, "Avastin as monotherapy for retinopathy of prematurity," *Journal of AAPOS*, vol. 14, no. 1, pp. 2–3, 2010.

[19] C. Gilbert, A. Fielder, L. Gordillo et al., "Characteristics of infants with severe retinopathy of prematurity in countries with low, moderate, and high levels of development: implications for screening programs," *Pediatrics*, vol. 115, supplement 2, pp. e518–e525, 2005.

[20] L. J. Faia and M. T. Trese, "Retinopathy of prematurity," S. Ryan, A. Schachat, C. Wilkinson, D. Hinton, and P. Wiedemann, Eds., vol. 2, pp. 1920–1932, Elsevier, New York, NY, USA, 5th edition, 2013.

[21] A. Mataftsi, S. A. Dimitrakos, and G. G. W. Adams, "Mediators involved in retinopathy of prematurity and emerging therapeutic targets," *Early Human Development*, vol. 87, no. 10, pp. 683–690, 2011.

[22] L. Kong, H. A. Mintz-Hittner, R. L. Penland, F. L. Kretzer, and P. Chévez-Barrios, "Intravitreous bevacizumab as anti–vascular endothelial growth factor therapy for retinopathy of prematurity: a morphologic study," *Archives of Ophthalmology*, vol. 126, no. 8, pp. 1161–1163, 2008.

[23] R. Axer-Siegel, Z. Herscovici, M. Hasanreisoglu, I. Kremer, Y. Benjamini, and M. Snir, "Effect of intravitreal bevacizumab (Avastin) on the growing rabbit eye," *Current Eye Research*, vol. 34, no. 8, pp. 660–665, 2009.

[24] S. J. Bakri, M. R. Snyder, J. M. Reid, J. S. Pulido, and R. J. Singh, "Pharmacokinetics of intravitreal bevacizumab (Avastin)," *Ophthalmology*, vol. 114, no. 5, pp. 855–859, 2007.

[25] R. L. Avery, "Bevacizumab (Avastin) for retinopathy of prematurity: wrong dose, wrong drug, or both?" *Journal of AAPOS*, vol. 16, no. 1, pp. 2–4, 2012.

[26] S. Y. Jang, K. S. Choi, and S. J. Lee, "Delayed-onset retinal detachment after an intravitreal injection of ranibizumab for zone 1 plus retinopathy of prematurity," *Journal of AAPOS*, vol. 14, no. 5, pp. 457–459, 2010.

[27] D. Lepore, G. E. Quinn, F. Molle et al., "Intravitreal bevacizumab versus laser treatment in type 1 retinopathy of prematurity," *Ophthalmology*, vol. 121, no. 11, pp. 2212–2219, 2014.

Hindawi Publishing Corporation
Journal of Ophthalmology
Volume 2015, Article ID 412903, 8 pages
http://dx.doi.org/10.1155/2015/412903

Review Article

Individualized Therapy with Ranibizumab in Wet Age-Related Macular Degeneration

Alfredo García-Layana,[1,2,3] Marta S. Figueroa,[2,3,4,5] Luis Arias,[2,3,6] Javier Araiz,[2,3,7] José María Ruiz-Moreno,[2,3,8] José García-Arumí,[2,3,9] Francisco Gómez-Ulla,[2,3,10] María Isabel López-Gálvez,[2,3,11] Francisco Cabrera-López,[2,12] José Manuel García-Campos,[2,13] Jordi Monés,[2,14] Enrique Cervera,[2,15] Felix Armadá,[2,16] and Roberto Gallego-Pinazo[2,17]

[1] *Clínica Universidad de Navarra, Avenida de Pío XII 36, 31008 Pamplona, Spain*
[2] *Sociedad Española de Retina y Vítreo (SERV), C/ Xosé Chao Rego 8, 15705 Santiago de Compostela, Spain*
[3] *RETICS OFTARED (RD12/0034) "Prevention Early Detection and Treatment of the Prevalent Degenerative and Chronic Ocular Pathology", Institute of Health Carlos III, C/ Sinesio Delgado 4, 28029 Madrid, Spain*
[4] *Hospital Universitario Ramon y Cajal, Carretera de Colmenar, km 9, 28034 Madrid, Spain*
[5] *Vissum Madrid, Santa Hortensia 58, 28002 Madrid, Spain*
[6] *Hospital de Bellvitge, C/ Feixa Llarga s/n, L'Hospitalet de Llobregat, 08907 Barcelona, Spain*
[7] *Hospital de San Eloy, Avenida Antonio Miranda 5, 48902 Baracaldo, Spain*
[8] *Hospital Universitario de Albacete, Avenida de Almansa s/n, 02006 Albacete, Spain*
[9] *Hospital Vall D'Hebron, Passeig de la Vall d'Hebron 119–129, 08035 Barcelona, Spain*
[10] *Instituto Oftalmológico Gómez-Ulla, Calle Maruja Mallo 3, 15706 Santiago de Compostela, Spain*
[11] *IOBA, Hospital Clínico Universitario de Valladolid, Paseo de Belén 17, 47011 Valladolid, Spain*
[12] *Complejo Hospitalario Universitario Insular Materno Infantil de Gran Canaria, Avenida Marítima del Sur s/n, 35016 Las Palmas de Gran Canaria, Spain*
[13] *Hospital Universitario Virgen de la Victoria, Campus de Teatinos s/n, 29010 Málaga, Spain*
[14] *Institut de la Macula i de la Retina, Carrer de Vilana 12, 08022 Barcelona, Spain*
[15] *Hospital General de Valencia, Avenida Tres Cruces 2, 46014 Valencia, Spain*
[16] *Hospital la Paz, Paseo de la Castellana 261, 28046 Madrid, Spain*
[17] *Hospital la Fe, Avenida de Fernando Abril Martorell 106, 46026 Valencia, Spain*

Correspondence should be addressed to Alfredo García-Layana; aglayana@unav.es

Received 13 October 2014; Accepted 10 March 2015

Academic Editor: Juliana L. Dreyfuss

Individualized treatment regimens may reduce patient burden with satisfactory patient outcomes in neovascular age-related macular degeneration. Intravitreal anti-VEGF drugs are the current gold standard. Fixed monthly injections offer the best visual outcome but this regimen is not commonly followed outside clinical trials. A PRN regimen requires monthly visits where the patient is treated in the presence of signs of lesion activity. Therefore, an early detection of reactivation of the disease with immediate retreatment is crucial to prevent visual acuity loss. Several trials suggest that "treat and extend" and other proactive regimens provide a reasonable approach. The rationale of the proactive regimens is to perform treatment anticipating relapses or recurrences and therefore avoid drops in vision while individualizing patient followup. Treat and extend study results in significant direct medical cost savings from fewer treatments and office visits compared to monthly treatment. Current data suggest that, for one year, PRN is less expensive, but treat and extend regimen would likely be less expensive for subsequent years. Once a patient is not a candidate to continue with treatment, he/she should be sent to an outpatient unit with adequate resources to follow nAMD patients in order to reduce the burden of specialized ophthalmologist services.

1. Early Diagnosis and Treatment Initiation

Age-related macular degeneration (AMD) is the leading cause of blindness among the elderly in the Western world [1–3]. Currently, there is no cure for the disease; however, intravitreal antivascular endothelial growth factor (anti-VEGF) agents have significantly improved visual outcomes in patients with neovascular age-related macular degeneration (nAMD) [4–7]. These new therapeutic approaches have been shown to prevent and in some cases reverse visual damage caused by nAMD in clinical trials. Early diagnosis is obviously essential in order to take action as promptly as possible to obtain the best result from therapy [8]. Therefore, primary care physicians who suspect nAMD should directly refer their patients to an ophthalmologist [9]. It is advisable to establish a referral protocol based on signs and symptoms in order to maximize efficiency and utilization of health resources.

Based on clinical evidence, most protocols recommend administering three consecutive monthly intravitreal injections of ranibizumab [8, 10, 11]. The pivotal studies MARINA [4] and ANCHOR [5] and later Pronto [12], SUSTAIN [13], and IVAN [14] scheduled three loading doses of ranibizumab as initial treatment. Their results have shown that visual acuity (VA) improves plateaus after the first three injections. The current summary of product characteristics of ranibizumab recommends initiating the treatment with a loading phase consisting of a monthly injection of 0.5 mg ranibizumab during three consecutive months. However, more recently CATT [6] protocol found that after the first year ranibizumab given as needed without the use of three mandatory loading doses was equivalent to ranibizumab given monthly. Therefore, although most clinical protocols recommend a loading phase, we still do not have conclusive data to support the superiority of three mandatory monthly initial doses over one dose.

These results have also been endorsed recently with the use of aflibercept in the VIEW-1 and VIEW-2 studies which have established its indication for the treatment of nAMD with a recommended regimen of 2 mg injection every 8 weeks during the first year following a loading phase of three injections [7].

Furthermore, the response to the initial loading dose constitutes a very important parameter to assess the possible progression of the patient, to establish a profile for future response to treatment, and to individualize the therapy [15, 16]. Thus, following the loading dose in the SUSTAIN study, 53% maintain what was gained in the first three months, 21% do not maintain it, and 26% did not gain vision [13].

As far as bevacizumab is concerned, some studies also recommend a loading dose [17, 18], but in CATT study, the comparison between bevacizumab given as needed without loading phase and bevacizumab given monthly was inconclusive, so neither no inferiority nor inferiority was established between the two study groups [6].

2. Individualized Treatment Protocols

Intravitreal ranibizumab based on a PRN (*Pro Re Nata* or "as needed") regimen where retreatment is given in the presence of signs of activity is frequently used for the management of neovascular age-related macular degeneration. However, strict monthly monitoring is required to obtain the best results. This represents a huge burden for both the ophthalmologist and the patient, though some patients do not need to be monitored monthly. Individualization of the treatment and followup is a key to ensure optimal clinical outcomes for those patients.

In the pivotal MARINA and ANCHOR trials, ranibizumab was administered monthly for two years in patients with nAMD. With this treatment protocol, mean VA improved 6.6 letters and 10.7 letters, respectively [4, 5]. In the VIEW trials, bimonthly aflibercept 2.0 mg showed very similar visual results compared to monthly ranibizumab 0.5 mg [7].

The Pronto study pioneered retreatment based on optical coherence tomography (OCT) findings. In this study, 40 patients were monitored monthly after receiving a loading dose of three consecutive ranibizumab injections. Retreatment was mainly administered in the presence of VA loss and persistent or recurrent intraretinal or subretinal fluid on OCT scans. At 24 months, mean VA improved 11 letters and 43% of patients gained 15 or more letters, with an average of 9.9 injections [12]. However, the promising results of the Pronto study could not be reproduced in the larger SUSTAIN trial with a similar treatment regimen [13]. These studies laid the foundations of the so-called PRN regimen. Notwithstanding, strict monthly monitoring is required to achieve a good clinical outcome with no tolerance to the presence of macular fluid detected on OCT, which has been demonstrated in the CATT trial [6]. The CATT study concluded that ranibizumab and bevacizumab were equivalent in terms of VA results when given under the same treatment protocol; however, ranibizumab better corrected anatomic pathologies as demonstrated by OCT. At two years, monthly injections of each treatment were found to be superior to their respective PRN regimens. Importantly, this study has also shown that patients receiving monthly injections with either ranibizumab or bevacizumab during the first year who are then rerandomized to PRN treatment during the second year had similar VA results as patients treated with a PRN regimen from the start. Therefore, an aggressive approach at the beginning of the disease does not seem to be a key factor for a better long-term outcome.

It seems that the key to the success of monthly dosing may possibly lie in treating before further disease progression, that is, treatment being administered even when the lesion is inactive. In this approach, the treatment has the advantage—not the disease. If this theory was correct, the ideal treatment would be one that anticipates and prevents disease but at the same time avoids the burden and risks of the monthly injections. The proactive regimens such as treat and extend or the Fusion regimens seek this goal.

In the "inject and extend" or "treat and extend" regimens, the intervals between reinjections are progressively extended if there is no fluid, thereby "titrating" a patient's individual maximal treatment-free interval [19, 20]. The visual results of these regimens gave satisfactory results. The 1-year results of the LUCAS trial, the largest and best performed treat

and extend study, showed equivalent effectiveness in the VA scores with ranibizumab (8.2 letters) and bevacizumab (8 letters). These results were achieved with a mean of eight injections in the ranibizumab group and a mean of 8.8 injections in the bevacizumab group. The difference in the number of injections reached significance ($P = 0.002$) [19]. In addition, a small retrospective nonrandomized case series showed more favourable results with the treat and extend regimen than with PRN, probably because patients in the PRN group were only examined 8.8 times a year instead of the 12 times initially expected [20]. According to the ASRS PAT survey, treat and extend regimen is preferred by most physicians (communication at the American Academy Meeting in New Orleans, November 2013). In the treat and extend regimen, the patients are treated regardless of the presence of fluid or neovascular activity. In the absence of neovascular activity, the patient receives the treatment at each visit; however, the interval between subsequent visits will continually be extended several weeks unless disease activity returns. In this manner, the treatment anticipates and avoids the relapses. In the case of the PRN regimen, the treatment tries to catch up to the relapses but has no chance by definition to prevent them. Randomized prospective studies comparing the two methods are now needed to establish the best reinjection strategy for patients treated with anti-VEGF drugs, as the one currently in progress sponsored by the Spanish Vitreoretinal Society (*In Eye study*, EudraCT number 2012-003431-37).

The Fusion regimen combines the PRN approach with fixed injections after certain periods of (apparent) inactivity [21, 22]. In the second year of the VIEW study, a similar approach was followed and was termed capped-PRN [7]. The Fusion regimen consists of three steps. First, a loading phase of three consecutive monthly injections is given. If CNV activity is resolved at the first follow-up visit, the loading phase can be reduced to two monthly injections. Second, a PRN regimen is established on demand, and intravitreal injections are given if CNV activity is present. After cessation of CNV activity, patients still receive one injection. Third, after cessation of CNV activity, patients receive fixed injections every 2 months for two courses and every 3 months for two courses. At the intermediate visits, between the preplanned fixed injections, patients are treated according to PRN criteria [22].

Though conceptually different, the Fusion regimen has some similarities with the proposed "treat and extend" regimen [23, 24] because both regimens aim at the prevention of disease recurrence. The main differences between the Fusion and "treat and extend" regimens are that in the latter the periods between treatments are extended in a continuous linear form and that there are no visits in between these periods.

In summary, the rationale of the proactive regimens is to perform treatment anticipating the relapses or recurrences and therefore avoid drops in vision while individualizing patient followup. The objective is to avoid irreversible loss of vision at recurrences despite reactive treatment. Proactive regimens not only reduce the number of injections and their associated risks as do PRN regimens but also minimize the number of visits and their associated costs and inconvenience. Treat and extend has the potential to be most cost-effective regimen, by reducing the frequency of injections compared to monthly regimen, as well as the number of visits compared to PRN. Due to the proactivity of the treatment, this reduced cost does not compromise clinical benefit or efficacy.

The main weakness so far is that these regimens have not yet been validated in larger, controlled, randomized trials.

3. Socioeconomical Burden

Different challenges must be faced in the long-term treatment of nAMD with intravitreal injections of ranibizumab. One of the major problems is how to manage a high number of patients who require frequent monitoring visits and retreatments. It is known that monthly visits are mandatory during the initial period after the onset of the disease to optimize the results that can be obtained with the treatment. However, these follow-up visits can be progressively extended if the lesion remains stable. Currently, there is lack of evidence to recommend a "treat and extend" regimen instead of a PRN regimen. The percentage of patients gaining 15 or more letters and the mean VA change are not as good in studies performed in a "real-world" context as in clinical trials. This could be due to the wide range of lesions treated in clinical practice compared to the strictly selected ones in randomized trials. Furthermore, although flexible regimens may reduce the burden of visits and injections, they might offer a less favourable long-term outcome.

The goal of OCT-driven treatment protocols is to achieve a "dry macula" with repeated injections. Nevertheless, some residual fluid may be left untreated if VA is stable during several follow-up visits. This might be relevant to save some extra injections making the treatment more cost-effective.

4. Signs of Activity and Retreatment Criteria in Individualized Therapies

Initially, it should be established that there is no structural damage defined as longstanding fibrosis or atrophy in the foveal area, significant chronic disciform scar, or other severe ocular diseases like vitreous hemorrhage or rhegmatogenous retinal detachment. It is also recommended that treatment with ranibizumab should not be commenced if there is evidence or suspicion of hypersensitivity to this drug [11].

The choroidal neovascular membrane should be considered active if it presents any of the following features: abnormal retinal thickness, particularly if there is evidence of accumulated intraretinal or subretinal fluid, or fluid under the RPE, confirmed by OCT; presence or recurrence of intraretinal fluid and/or subretinal fluid or subretinal hemorrhage; new or persistent leakage detected with angiography fluorescein; choroidal neovascular membrane growth detected with angiography fluorescein; and VA deterioration, considered to represent deterioration of the choroidal neovascular membrane [25].

Choroidal neovascular membrane disease progression is defined by the Institute for Health and Clinical Excellence

[26] as the appearance of sight-threatening choroidal neovascular membrane which was not previously suspected or thought to be present or evidence of new hemorrhage and/or subretinal fluid or a documented recent visual decline in the choroidal neovascular membrane or an increase in the lesion size between visits.

The disease should be considered to have become inactive when there is [11] persistence or absence of fluid with absence of fluorescein leakage or other signs of disease activity like increasing lesion size, new haemorrhages, or exudates; no deterioration in vision that can be attributed to choroidal neovascular membrane activity; no lesion growth or new signs of disease activity on subsequent followup following recent discontinuation of treatment; and no worsening of OCT indicators of choroidal neovascular membrane disease.

Retreatment criteria from Pronto study [12] are defined if any of the following changes were observed: VA loss of at least 5 letters or 1 EDTRS line; an increase in OCT of at least 100 m; new macular hemorrhage; new area of classic neovascular choroidal membrane; or evidence of persistent fluid on OCT one month after injection. Detachment of pigment epithelium was recorded as an OCT finding but was not included as retreatment criteria. This decision was based on the observations from phase I/II extension Pronto study with ranibizumab. In this study, little correlation between the presence of pigment epithelium detachment and VA was observed. During the second year of the study, retreatment criteria were changed to include any qualitative modifications in the OCT that suggested fluid in the macular area. These changes included the appearance of retinal cysts or subretinal fluid or an enlargement of the pigment epithelium detachment. Any of these qualitative changes alone was sufficient to permit retreatment [12].

In the SUSTAIN [13] study, retreatment was based on VA and OCT findings indicating loss of more than five letters of VA from the previous highest VA score and OCT criteria ≥100 m increase from the previous lowest measurement.

It is important to remember that some degenerative retinal changes observed with OCT can be presented as hyporeflective images and may not correspond to fluid but structural changes like the residual internal layers pseudocysts or the outer retinal tabulations [27]. In these cases we must rule out the possibility that the fluid is not representing disease activity.

5. Nonresponder and Therapeutical Approach

There is not an accepted definition of nonresponders to nAMD treatment. However, in clinical practice, some patients do not respond adequately to the treatment. Even with monthly injections of ranibizumab at the 2-year followup, 9% of the patients in the MARINA study and 10% of patients in the ANCHOR study lost more than 15 letters of VA [28]. Patients with good VA at baseline might have difficulty improving 3 lines of VA compared with the greater likelihood of losing 3 lines of VA. The opposite is likely true for patients with poor VA at baseline. It may be impossible for a patient with poor VA at baseline to lose an additional 3 lines of VA, whereas there is a greater likelihood of improving 3 lines once treatment is initiated [28]. If vision loss is associated with a suppressed CNV without leakage but is associated with pigmentary abnormalities and geography atrophic scar, it does not seem that a shift to another treatment would allow any improvement.

In addition, the failure of anti-VEGF monotherapy to provide a long-lasting resolution of intraretinal or subretinal fluid is frequently observed even in clinical trials. In the CATT study, the proportion of patients without fluid on OCT in the ranibizumab monthly group, where the best anatomical results were obtained, was 45.5% after two years of followup [6].

Therefore, both functional and anatomical aspects must be considered when we define a nonresponder, and we must consider both the short time and the long time after beginning the treatment, in order to decide the management of these patients.

In the short term, the SUSTAIN study identified three groups of responders to ranibizumab therapy after the loading doses [13]: those who gained vision (one or more letters) in the initial 3 months and maintained that vision in the maintenance phase (53%); those who gained vision in the initial 3 months but did not maintain it through the maintenance phase and stabilized at the baseline VA level (21%); and those who had no initial vision gain and no gain during the PRN phase. In that group, rather a decrease in BCVA was observed during the follow-up period (26%). In this third group, if VA gets worse and fluid is still present in the OCT, we can consider the patient a "real nonresponder." If the patient has a bad VA and a disciform scar, probably no additional treatment should be provided, although this can be reconsidered if it is the eye with the best VA of the patient.

If the patient has still a useful vision, additional tests should be used to determine different macular diseases that should be treated in a different way. Diagnosis of polypoidal choroidal vasculopathy (PCV) should be based on early phase hyperfluorescent hot spots visualized using indocyanine green angiography (ICG). Treatment of PCV is usually performed with combined therapy using ICG-guided verteporfin photodynamic therapy plus three doses of ranibizumab intravitreal injections 1 month apart [29].

Differentiating long-standing central serous chorioretinopathy (CSC) from nAMD can sometimes be difficult. Chronic CSC patients often develop in old patients, with RPE hyperplasia or atrophy, subretinal fluid and cystoid edema in the OCT, and hyperfluorescence on fluorescein and ICG. CSC can also be diagnosed with the help of enhanced depth imaging on OCT. In addition, some patients presenting with choroidal neovascularization have a missed background of CSC and the etiology is erroneously ascribed to nAMD. Atrophic changes in RPE are better seen with fundus autofluorescence imaging and midphase. ICG showing bilateral choroidal hyperpermeability can also help with the diagnosis. In the OCT, subretinal fluid and hypertrophic outer retinal changes are more common but intraretinal fluid is less frequent. Choroidal thickness is also increased in CSC. Chronic CSC is better treated with ICG-guided verteporfin photodynamic therapy and ranibizumab may be also added if CNV has also complicated the process [30].

Those who gained vision in the initial 3 months but did not maintain it must be considered "responders" although the type of response is not so good. Some studies suggest that patients treated with repeat intravitreal bevacizumab and ranibizumab injections may demonstrate tachyphylaxis over time [31]. When a patient does not respond adequately to the drug of choice, the question arises whether a shift in therapy to another VEGF inhibitor will be useful. Shifting patients to ranibizumab after insufficient response to bevacizumab has shown that most patients improved the anatomic status of the macula on OCT (32% complete resolution of fluid and 39% with partial response). However, the mean VA did not change after shifting treatment, with individual changes ranging from loss of 4 lines to gain of 2 lines [32]. When patients are transitioned from bevacizumab, ranibizumab, or both to aflibercept, 7% gained 2 lines or more and 85% showed stable VA. Again, an improvement in the anatomic outcomes was observed in the OCT after the change to aflibercept with 5% showing complete resolution of baseline exudative fluid and 49% showing partial resolution [33].

Finally, another group of responders are those who gain and maintain visual improvement but need almost continuous monthly injections, because there is always fluid in the OCT during the follow-up visits. As previously mentioned, in these cases we must rule out the possibility that the fluid is not representing disease activity, like the residual internal layers pseudocysts or the outer retinal tabulations [27]. In addition, a follow-up visit may be scheduled two weeks after the intravitreal injection in order to know if a patient has an initial improvement of the fluid after treatment, which then rapidly recurs with one month's time [34]. In these cases, treatment every two weeks, change of anti-VEGF drug, or combined therapy with verteporfin and anti-VEGF may be postulated [23, 33, 34]. Recently, some steroids and slow-delivered steroid implants combined with anti-VEGF have been postulated as an alternative option in eyes with refractory nAMD [24, 35].

6. Criteria for Patient Follow-Up Externalization

Interruption of the treatment can be considered in two ways: temporary suspension of anti-VEGF injections whilst still maintaining periodic controls or definite interruption of both the injections and patient followup [36].

Just as in one way or another, the Pronto study has shown that in certain cases the treatment with ranibizumab can be suspended, at least temporarily without showing a loss of the benefits obtained [12]. At the same time, it is observed that up to 30% of the cases did not require additional treatment [36].

Meanwhile, the decision of suspending anti-VEGF treatment in nAMD may result in very different situations. In favourable situations, the treatment is interrupted due to the long-term resolution of exudation and stability of vision; in unfavourable situations, the interruption is fundamentally due to the development of a fibrotic macular disciform scar, chronic macular edema, or macular atrophy. The SEVEN-UP study has shown that, approximately 7 years after ranibizumab therapy, one-third of patients demonstrated good visual outcomes, whereas another third had poor outcomes. Active exudative disease was detected by spectral-domain OCT in 68% of study eyes, and 46% were receiving ongoing ocular anti-VEGF treatments. Macular atrophy was detected by fundus autofluorescence in 98% of eyes and the area of atrophy correlated significantly with poor visual outcome [37].

For these reasons, we can conclude by affirming that once the patient with nAMD is not a candidate to continue with treatment, he/she should be sent to AMD outpatients units, where a periodic followup can be carried out by a specialist in macular disease who can perform the following tests: measurement of VA, fundus examination, and macular OCT [8]. At the same time, the aforementioned could be complimented with the referral of certain patients to low vision units (teams formed by ophthalmologists, opticians, rehabilitation technicians, social workers, and psychologists), thus increasing the use of units that are underused at present [38]. All of this would contribute to reducing the healthcare burden in hospitals and assuring a satisfactory control of nAMD patients.

The creation of an AMD outpatient unit would therefore signify a clear advance in assuring a better quality of life for a chronic patient and reducing the healthcare burden of the ophthalmologist services in an illness that has a strong tendency for periodic visits (closer periods versus spaced out checkups) and a growing demand due to demographic factors [39].

7. Real-Life Practice Results of Anti-VEGF in nAMD

Apart from clinical trials, several studies have explored different regimens for the treatment of nAMD with ranibizumab in the "real world." Most of them are based on a PRN scheme but with more flexible criteria than in clinical trials to reduce the burden of injections and follow-up visits [40]. However, overall results of these studies are not as good as those obtained following the more rigid protocols of clinical trials. The PRN regimens performed outside clinical trials have many potential sources of noncompliance. Therefore, the risk of an even worse outcome is higher and it remains controversial whether initial good results can be maintained over time [41]. Therefore, despite the ophthalmology community's joy at new developments in the treatment of nAMD in 2005 [4–7], the inconvenience of monthly injections or at least monthly followup remained. In addition, when analysing different patient responses across clinical trials, individualization of the treatment and the followup is needed. In the Lumiere study performed in France, the mean VA gain at 12 months was 3.2 ± 14.8 ETDRS letters [42]. Fewer than 40% of patients received the recommended treatment of initial 3 monthly injections, 50% patients had to wait more than 8 days for the initial anti-VEGF treatment, and the average number of injections was 5.1 during the 12-month period.

The retrospective pooled analysis of four European registries (Wave/Germany; Helios/Netherlands; Helios/Belgium; Sweden) within the LUMINOUS program has shown that the mean improvement in ETDRS letters at 12 months

was 0, 5.6, 2.5, and 1 with a mean number of 4.3, 5.5, 5.0, and 4,7 injections, respectively [43].

In the AURA multinational study, the mean improvement from baseline in France was 0.8 letters and 0.1 at 1 year and 2 years, respectively [44]. In Germany, these figures were −0.4 and −2.4, respectively. The mean number of injections in years 1 and 2 was 4.4 and 1.9 in France and 4.2 and 1.1 in Germany [44].

In Spain, a study has evaluated the degree of compliance by Spanish retinal specialists with the Spanish Vitreoretinal Society Guidelines for Management of AMD [45]. This multicenter retrospective observational study included 346 patients. Adherence to SERV guidelines was high for the diagnosis (96,8%), medium for initial treatment (84,4%), and low for followup and retreatment (46,9%). In the first year, follow-up visits were made every 2 months or more frequently in 66.2% of patients. In the second year, followup was even less frequent: every 3 months or more in 70.2% of patients.

Another study in 12 sites across Spain, which included 208 patients followed for 24 months, has shown that the average number of follow-up visits was 9 (5.4 and 3.6 during the first and second year), the mean number of injections was 6.1 (4.5 and 1.6 during the first and second year), and the mean VA gain was 2.4 ± 16.6 letters at 12 months and 3.1 ± 19.6 at 24 months [46].

Treatment with intravitreal anti-VEGF injections in real-life practice produces, on average, poorer-than-expected visual outcomes, probably due to fewer injections per year and less than monthly monitoring. Recently, a Delphi study to detect deficiencies in real-life treatment of nAMD was performed in one hundred members of the Spanish Vitreoretinal Society [47]. Recommendations were developed after analyzing the differences between the results and the SERV guidelines recommendations. Consensus statements to reduce the burden of the disease included the use of treat and extend regimen and reducing the amount of diagnostic tests during the loading phase and training technical staff to perform these tests and reducing the time between relapse detection and reinjection, as well as establishing patient referral protocols to outside general ophthalmology clinics.

In conclusion, ranibizumab demonstrates a favourable clinical effectiveness and dramatically improves outcomes in nAMD, although some actions must be implemented in order to enhance results in real-world practice. The positioning of ranibizumab in nAMD will be defined more accurately in the future, when data for existing and new therapies become available.

Disclosure

This review has not been previously published by the authors.

Conflict of Interests

The authors declare that there is no conflict of interests regarding the publication of this paper.

Acknowledgments

This work has been developed by members of the Spanish Vitreoretinal Society (SERV), the RETICs (RD07-0062) "Age Related Ocular Diseases, Quality of Life and Vision," and RETICS OFTARED (RD12/0034) "Prevention, Early Detection and Treatment of the Prevalent Degenerative and Chronic Ocular Pathology" from the Instituto de Salud Carlos III from the Ministerio de Economía y Competitividad, Spain. This work has been partly funded by the PN I+D+i 2008–2011, ISCIII, Subdireccion General de Redes y Centros de Investigación Cooperativa, and the European Program FEDER.

References

[1] R. Klein, B. E. K. Klein, S. C. Tomany, and S. E. Moss, "Ten-year incidence of age-related maculopathy and smoking and drinking: the Beaver Dam Eye study," *The American Journal of Epidemiology*, vol. 156, no. 7, pp. 589–598, 2002.

[2] C. Sainz-Gómez, P. Fernández-Robredo, Á. Salinas-Alamán et al., "Prevalence and causes of bilateral blindness and visual impairment among institutionalized elderly people in Pamplona, Spain," *European Journal of Ophthalmology*, vol. 20, no. 2, pp. 442–450, 2010.

[3] J. Ambati, B. K. Ambati, S. H. Yoo, S. Ianchulev, and A. P. Adamis, "Age-related macular degeneration: etiology, pathogenesis, and therapeutic strategies," *Survey of Ophthalmology*, vol. 48, no. 3, pp. 257–293, 2003.

[4] P. J. Rosenfeld, D. M. Brown, J. S. Heier et al., "Ranibizumab for neovascular age-related macular degeneration," *The New England Journal of Medicine*, vol. 355, no. 14, pp. 1419–1431, 2006.

[5] D. M. Brown, P. K. Kaiser, M. Michels et al., "Ranibizumab versus verteporfin for neovascular age-related macular degeneration," *The New England Journal of Medicine*, vol. 355, no. 14, pp. 1432–1444, 2006.

[6] D. F. Martin, M. G. Maguire, G.-S. Ying, J. E. Grunwald, S. L. Fine, and G. J. Jaffe, "Ranibizumab and bevacizumab for neovascular age-related macular degeneration," *The New England Journal of Medicine*, vol. 364, no. 20, pp. 1897–1908, 2011.

[7] G. Trichonas and P. K. Kaiser, "Aflibercept for the treatment of age-related macular degeneration," *Ophthalmology and Therapy*, vol. 2, no. 2, pp. 89–98, 2013.

[8] J. M. Ruiz-Moreno, L. Arias-Barquet, F. Armadá-Maresca et al., "Guidelines of clinical practice of the SERV: treatment of exudative age-related macular degeneration (AMD)," *Archivos de la Sociedad Espanola de Oftalmologia*, vol. 84, no. 7, pp. 333–344, 2009.

[9] N. M. Bressler, "Early detection and treatment of neovascular age-related macular degeneration," *The Journal of the American Board of Family Practice*, vol. 15, no. 2, pp. 142–152, 2002.

[10] A. F. Cruess, A. Berger, K. Colleaux et al., "Canadian expert consensus: optimal treatment of neovascular age-related macular degeneration," *Canadian Journal of Ophthalmology*, vol. 47, no. 3, pp. 227–235, 2012.

[11] W. Amoaku, "Ranibizumab: the clinician's guide to commencing, continuing, and discontinuing treatment," *Eye*, vol. 23, no. 11, pp. 2140–2142, 2009.

[12] G. A. Lalwani, P. J. Rosenfeld, A. E. Fung et al., "A variable-dosing regimen with intravitreal ranibizumab for neovascular

age-related macular degeneration: year 2 of the PrONTO study," *The American Journal of Ophthalmology*, vol. 148, no. 1, pp. 43.e1–58.e1, 2009.

[13] F. G. Holz, W. Amoaku, J. Donate et al., "Safety and efficacy of a flexible dosing regimen of ranibizumab in neovascular age-related macular degeneration: the SUSTAIN study," *Ophthalmology*, vol. 118, no. 4, pp. 663–671, 2011.

[14] U. Chakravarthy, S. P. Harding, C. A. Rogers et al., "Alternative treatments to inhibit VEGF in age-related choroidal neovascularisation: 2-year findings of the IVAN randomised controlled trial," *The Lancet*, vol. 382, no. 9900, pp. 1258–1267, 2013.

[15] M. Menghini, M. M. Kurz-Levin, C. Amstutz et al., "Response to ranibizumab therapy in neovascular AMD. An evaluation of good and bad responders," *Klinische Monatsblätter für Augenheilkunde*, vol. 227, no. 4, pp. 227–248, 2010.

[16] H. J. Shin, H. Chung, and H. C. Kim, "Correlation of foveal microstructural changes with vision after anti-vascular endothelial growth factor therapy in age-related macular degeneration," *Retina*, vol. 33, no. 5, pp. 964–970, 2013.

[17] M. L. Bidot, L. Malvitte, S. Bidot, A. Bron, and C. Creuzot-Garcher, "Etude preliminaire sur l'efficacité de trois injec-tions intravitreennes de bevacizumab dans le traitement de la degenrescence maculaire lieé à l'agê exsudative," *Journal Français d'Ophtalmologie*, vol. 34, no. 6, pp. 376–381, 2011.

[18] P. J. Mekjavic, A. Kraut, M. Urbancic, E. Lenassi, and M. Hawlina, "Efficacy of 12-month treatment of neovascular age-related macular degeneration with intravitreal bevacizumab based on individually determined injection strategies after three consecutive monthly injections," *Acta Ophthalmologica*, vol. 89, no. 7, pp. 647–653, 2011.

[19] K. Berg, T. R. Pedersen, L. Sandvik, and R. Bragadóttir, "Comparison of ranibizumab and bevacizumab for neovascular age-related macular degeneration according to LUCAS treat-and-extend protocol," *Ophthalmology*, vol. 122, no. 1, pp. 146–152, 2015.

[20] H. Oubraham, S. Y. Cohen, S. Samimi et al., "Inject and extend dosing versus dosing as needed: a comparative retrospective study of ranibizumab in exudative age-related macular degeneration," *Retina*, vol. 31, no. 1, pp. 26–30, 2011.

[21] J. Monés, "A review of ranibizumab clinical trial data in exudative age-related macular degeneration and how to translate it into daily practice," *Ophthalmologica*, vol. 225, no. 2, pp. 112–119, 2011.

[22] J. Monés, M. Biarnés, F. Trindade, and R. Casaroli-Marano, "FUSION regimen: ranibizumab in treatment-naïve patients with exudative age-related macular degeneration and relatively good baseline visual acuity," *Graefe's Archive for Clinical and Experimental Ophthalmology*, vol. 250, no. 12, pp. 1737–1744, 2012.

[23] G. Seidel, C. Werner, M. Weger, I. Steinbrugger, and A. Haas, "Combination treatment of photodynamic therapy with verteporfin and intravitreal ranibizumab in patients with retinal angiomatous proliferation," *Acta Ophthalmologica*, vol. 91, no. 6, pp. 482–485, 2013.

[24] P. Calvo, A. Ferreras, F. Al Adel, Y. Wang, and M. H. Brent, "Dexamethasone intravitreal implant as adjunct therapy for patients with wet age-related macular degeneration with incomplete response to ranibizumab," *British Journal of Ophthalmology*, 2014.

[25] P. Mitchell, J.-F. Korobelnik, P. Lanzetta et al., "Ranibizumab (Lucentis) in neovascular age-related macular degeneration: evidence from clinical trials," *British Journal of Ophthalmology*, vol. 94, no. 1, pp. 2–13, 2010.

[26] W. M. K. Amoaku, "The Royal College of Ophthalmologists interim recommendations for the management of patients with age-related macular degeneration," *Eye*, vol. 22, no. 6, pp. 864–868, 2008.

[27] S. A. Zweifel, M. Engelbert, K. Laud, R. Margolis, R. F. Spaide, and K. B. Freund, "Outer retinal tubulation a novel optical coherence tomography finding," *Archives of Ophthalmology*, vol. 127, no. 12, pp. 1596–1602, 2009.

[28] P. J. Rosenfeld, H. Shapiro, L. Tuomi, M. Webster, J. Elledge, and B. Blodi, "Characteristics of patients losing vision after 2 years of monthly dosing in the phase III ranibizumab clinical trials," *Ophthalmology*, vol. 118, no. 3, pp. 523–530, 2011.

[29] A. H. C. Koh, L.-J. Chen, S.-J. Chen et al., "Polypoidal choroidal vasculopathy: evidence-based guidelines for clinical diagnosis and treatment," *Retina*, vol. 33, no. 4, pp. 686–716, 2013.

[30] A. N. Stangos, J. S. Gandhi, J. Nair-Sahni, H. Heimann, C. J. Pournaras, and S. P. Harding, "Polypoidal choroidal vasculopathy masquerading as neovascular age-related macular degeneration refractory to ranibizumab," *The American Journal of Ophthalmology*, vol. 150, no. 5, pp. 666–673, 2010.

[31] S. Schaal, H. J. Kaplan, and T. H. Tezel, "Is there tachyphylaxis to intravitreal anti-vascular endothelial growth factor pharmacotherapy in age-related macular degeneration?" *Ophthalmology*, vol. 115, no. 12, pp. 2199–2205, 2008.

[32] S. J. R. De Geus, M. J. Jager, G. P. M. Luyten, and G. Dijkman, "Shifting exudative age-related macular degeneration patients to ranibizumab after insufficient response to bevacizumab," *Acta Ophthalmologica*, vol. 91, no. 5, pp. e411–e413, 2013.

[33] S. Y. Ho, S. Yeh, T. W. Olsen et al., "Short-term outcomes of aflibercept for neovascular age-related macular degeneration in eyes previously treated with other vascular endothelial growth factor inhibitors," *American Journal of Ophthalmology*, vol. 156, no. 1, pp. 23–e2, 2013.

[34] M. W. Stewart, P. J. Rosenfeld, F. M. Penha et al., "Pharmacokinetic rationale for dosing every 2 weeks versus 4 weeks with intravitreal ranibizumab, bevacizumab, and aflibercept (vascular endothelial growth factor Trap-eye)," *Retina*, vol. 32, no. 3, pp. 434–457, 2012.

[35] T. M. Ranchod, S. K. Ray, S. A. Daniels, C. J. Leong, T. D. Ting, and A. Z. Verne, "LUCEDEX: a prospective study comparing ranibizumab plus dexamethasone combination therapy versus ranibizumab monotherapy for neovascular age-related macular degeneration," *Retina*, vol. 33, no. 8, pp. 1600–1604, 2013.

[36] A. Gaudric and S. Y. Cohen, "When should anti-vascular endothelial growth factor treatment be stopped in age-related macular degeneration?" *The American Journal of Ophthalmology*, vol. 149, no. 1, pp. 4.e2–6.e2, 2010.

[37] S. Rofagha, R. B. Bhisitkul, D. S. Boyer, S. R. Sadda, and K. Zhang, "Seven-year outcomes in ranibizumab-treated patients in ANCHOR, MARINA, and HORIZON: a multicenter cohort study (SEVEN-UP)," *Ophthalmology*, vol. 120, no. 11, pp. 2292–2299, 2013.

[38] J. Monés and F. Gómez-Ulla, *Degeneración Macular Asociada a la Edad*, Prous Science, Barcelona, Spain, 2005.

[39] L. Arias, *Actualización de Terapia Anti-VEGF en las Enfermedades de la Retina y Coroides*, Elsevier España, 2010.

[40] L. Arias, I. Roman, C. Masuet-Aumatell et al., "One-year results of a flexible regimen with ranibizumab therapy in macular degeneration: relationship with the number of injections," *Retina*, vol. 31, no. 7, pp. 1261–1267, 2011.

[41] M. A. Singer, C. C. Awh, S. Sadda et al., "HORIZON: an open-label extension trial of ranibizumab for choroidal neovascularization secondary to age-related macular degeneration," *Ophthalmology*, vol. 119, no. 6, pp. 1175–1183, 2012.

[42] S. Y. Cohen, G. Mimoun, H. Oubraham et al., "Changes in visual acuity in patients with wet age-related macular degeneration treated with intravitreal ranibizumab in daily clinical practice: the lumiere study," *Retina*, vol. 33, no. 3, pp. 474–481, 2013.

[43] P. Mitchel, "Ranibizumab in age-related macular degeneration: a pooled analysis of European registries included in the LUMINOUS program," in *Proceedings of the WOC Meeting*, 2012.

[44] C. B. Hoyng and AURA Steering Committee, "Retrospective analysis of the real world utilization of ranibizumab in AMD," in *Proceedings of the World Congress on Controversies in Ophthalmology (COPHy '13)*, Budapest, Hungary, April 2013.

[45] J. D. López, "Adherencia a las recomendaciones de la SERV para el manejo de pacientes con DMAE exudativa por parte de los especialistas retinologos," in *Actas del 17th Congreso de la Sociedad Española de Retina y Vitreo*, Madrid, Spain, 2013.

[46] R. Casaroli-Marano, R. Gallego-Pinazo, C. T. Fernández-Blanco et al., "Age-related macular degeneration: clinical findings following treatment with antiangiogenic drugs," *Journal of Ophthalmology*, vol. 2014, Article ID 346360, 6 pages, 2014.

[47] A. García-Layana, L. Arias, M. S. Figueroa et al., "A Delphi study to detect deficiencies and propose actions in real life treatment of neovascular age-related macular degeneration," *Journal of Ophthalmology*, vol. 2014, Article ID 595132, 10 pages, 2014.

Hindawi Publishing Corporation
Journal of Ophthalmology
Volume 2015, Article ID 731461, 6 pages
http://dx.doi.org/10.1155/2015/731461

Clinical Study

Aqueous Levels of Pigment Epithelium-Derived Factor and Macular Choroidal Thickness in High Myopia

Wei Chen,[1] Yubo Guan,[1] Guanghui He,[1] Zhiwei Li,[2] Hui Song,[1] Shiyong Xie,[1] and Quanhong Han[1]

[1] *Clinical College of Ophthalmology, Tianjin Medical University, No. 4, Gansu Road, Tianjin 300020, China*
[2] *Department of Ophthalmology, Shandong Provincial Hospital Affiliated to Shandong University, Jinan 250000, China*

Correspondence should be addressed to Quanhong Han; hanquanhong1968@163.com

Received 14 July 2014; Revised 1 October 2014; Accepted 21 October 2014

Academic Editor: Ricardo Giordano

Purpose. To investigate the correlation between aqueous and serum levels of pigment epithelium-derived factor (PEDF) and macular choroidal thickness in high myopia patients, both with and without choroidal neovascularization (CNV). *Methods*. Serum and aqueous levels of PEDF were measured by enzyme-linked immunosorbent assay in 36 high myopia patients (36 eyes) with no CNV (non-CNV group), 14 high myopia patients (14 eyes) with CNV (CNV group), and 42 nonmyopia patients (42 eyes) (control group). Macular choroidal thickness was measured by enhanced-depth imaging optical coherence tomography. *Results*. Aqueous levels of PEDF were significantly higher in CNV group compared with non-CNV ($P < 0.001$) and control ($P < 0.001$) groups. Macular choroidal thicknesses were significantly decreased in the non-CNV and CNV groups compared with the control ($P < 0.001$) group. A statistically significant difference ($P = 0.012$) was found between the CNV and non-CNV groups. There was a positive correlation between aqueous PEDF and macular choroidal thickness in the non-CNV group ($P = 0.005$), but no correlation with the CNV group. No correlation between serum PEDF and macular choroidal thickness was detected in the three groups. *Conclusion*. Variations in aqueous PEDF levels coincide with changes in macular choroidal thickness in high myopia patients with no CNV, while no such relationship exists in high myopia patients with CNV.

1. Introduction

High myopia, which accounts for 27–33% of all myopia, is a major cause of legal blindness in numerous developed countries worldwide [1], with a prevalence of ~2% in the general population. Pathologically, myopia is characterized by excessive and progressive elongation of the globe (axial length, >26.5 mm) [2] and is associated with degenerative changes of the retina, choroid, and sclera at the posterior segment [3]. Myopic chorioretinal atrophy and choroidal neovascularization (CNV) are common causes of visual loss in high myopes. Since prevention of myopia is presently unachievable, it is of great importance to investigate the underlying mechanisms of and morphological changes associated with chorioretinal atrophy and CNV in highly myopic eyes.

Pigment epithelium-derived factor (PEDF), a secreted 50 kDa glycoprotein belonging to the superfamily of serine protease inhibitors, was first identified in conditioned media of cultured fetal human retinal pigment epithelial (RPE) cells [4]. PEDF not only is a more potent inhibitor of angiogenesis in the eye than are other endogenous antiangiogenic molecules [5], but also has neurotrophic/neuroprotective functions, playing roles in retinal differentiation, survival, and maintenance. Measurable variations in levels of aqueous PEDF in high myopia—with and without CNV—may indirectly reflect the nature and pathogenesis of these two phases of high myopia.

A new technique was recently implemented for improving depth imaging by optical coherence tomography (OCT). This technique—enhanced-depth imaging- (EDI-) OCT—has been shown to produce reliable images of full-thickness choroid [6]. EDI-OCT is, therefore, a most valuable tool for measuring choroidal thickness in highly myopic eyes. Wang et al. reported choroidal thickness to be a better indicator classifying myopic maculopathy than is either axial length or

refractive error [7]. Using EDI-OCT, Ohsugi et al. revealed that choroidal thickness in all regions of highly myopic eyes was significantly reduced compared with normal refractive eyes [8].

Whether aqueous levels of PEDF are reflective of stages of chorioretinal atrophy and CNV in high myopia remains to be elucidated. The aim of our study was to determine how changes in choroidal thickness in high myopia contribute to the formation of myopic lesions in CNV. We investigated variations in aqueous and serum levels of PEDF in high myopia patients (with and without CNV) and correlated these variations with macular choroidal thickness. Results are expected to clarify the role of PEDF in the pathophysiology and morphology of high myopia.

2. Materials and Methods

2.1. Subjects. This observational, comparative, prospective study was carried out at the Tianjin Eye Hospital, Tianjin, China, between August and November 2013. The study conformed to the Declaration of Helsinki tenets for research involving human subjects and was approved by the Institutional Review Board of Tianjin Eye Hospital. Informed consent was obtained from all participants. Patients who had had surgery on both eyes were only enrolled at the time of the first surgery.

Patients were divided into groups based on myopia with and without CNV. The *non-CNV group* comprised 36 high myopia patients ($n = 36$ eyes) (with no CNV) who were in need of cataract surgery. Inclusion criteria included patients with eyes of axial lengths of ≥26.5 mm (Miller and Singerman, 2001) [9], refractive errors of >6 diopters (D), and no apparent macular abnormalities (e.g., choroidal neovascularization, macular holes) and who were 50–70 years of age. Exclusion criteria included poor image quality on OCT as a result of unstable fixation, severe cataract, previous ocular surgery, use of immunosuppressive drugs, eye diseases (e.g., glaucoma, age-related macular degeneration, and retinal detachment), and systemic diseases like serious heart, lung, liver, or kidney dysfunction. Patients with eyes in which the choriosclera interface could not be clearly visualized were also excluded. The *CNV group* comprised 14 high myopia patients ($n = 14$ eyes) who were in need of intravitreal injections of ranibizumab (Lucentis, Novartis, Switzerland). Inclusion criteria comprised patients with eyes of axial lengths of ≥26.5 mm, refractive errors of >6 D, and choroidal neovascularization by fundus fluorescein angiography (FFA) and who were 50–70 years of age. Exclusion criteria were the same as those for the non-CNV group. Patients with secondary choroidal neovascular diseases, for example, angioid streaks and ocular trauma, were also excluded. All cases of CNV were confirmed by FFA. The *control group* comprised 42 normal patients ($n = 42$ eyes) who were in need of cataract surgery. Inclusion criteria comprised patients with healthy eyes with spherical equivalents of −3D–+3D. Exclusion criteria were the same as for the other groups.

2.2. Aqueous and Serum Samples. Samples of undiluted aqueous humor (100–200 μL) were collected by aspiration into a 1 mL syringe at the start of cataract surgery or before a single 0.05 mL intravitreal injection of ranibizumab. Serum specimens were collected prior to surgery. The levels of PEDF in aqueous humor and serum were measured using enzyme-linked immunosorbent assay (ELISA), according to the manufacturer's instructions (ChemiKine, Temecula, California, USA).

2.3. Ophthalmic Examination. All patients underwent a complete ophthalmic examination, including assessment of visual acuity (VA), refractive error, intraocular pressure (IOP), and axial length; OCT; dilated fundus examination by indirect ophthalmoscopy; and color fundus photographic assessment of myopic maculopathy. FFA was performed on all high myopia patients to confirm the presence or absence of CNV.

2.4. Measurements

2.4.1. Choroidal Thickness. The scan protocol of the Cirrus OCT (Carl Zeiss Meditec, Jena, Germany) generates a cube of data through a 9 mm line consisting of 4,096 A-scans around the macular region via a HD 5-line raster mode. EDI-OCT protocols have been described elsewhere [10]. Using the software-provided caliper system, choroidal thickness was measured from the outer surface of the hyperreflective line ascribed to the retinal pigment epithelium (RPE) to the hyperreflective line of the inner scleral border (Figure 1). Choroidal thicknesses were measured at the fovea, 3 mm superior and inferior to the fovea in vertical sections, and 3 mm temporal and nasal to the fovea in horizontal sections. The mean overall choroidal thickness, recorded as macular choroidal thickness, was obtained by calculating average choroidal thickness measurements from all measured areas. Two independent observers manually measured each choroidal thickness; both sets of measurements were averaged for analysis.

2.4.2. Axial Length, Refractive Error, and IOP. Axial length was measured using the Intraocular Lens Master (IOL-Master; Carl Zeiss Meditec, Dublin, CA). Refractive error was measured by autorefractometry (RK-3; Canon, Tokyo, Japan). IOP was measured by noncontact tonometry (TX-20 model; Canon, Tokyo, Japan).

2.5. Statistical Analysis. Statistical analyses were performed using version 17.0 SPSS software (SPSS, Inc., Chicago, IL, USA). All data were described as mean ± standard deviation (SD), with a 95% confidence interval (CI). An unpaired t-test was used to compare two independent groups with normal distribution; the Mann-Whitney U test was used to compare two independent groups without normal distribution; the Kruskal-Wallis H-test was used to compare variables among different groups; Fisher's exact t-test was used to compare noncontinuous variables; and Pearson's correlation test was used to analyze the correlation between aqueous PEDF concentrations, macular choroidal thickness, and serum PEDF

Table 1: Demographic and clinical characteristics.

Variables	Control group ($n = 42$)	High myopia without CNV group ($n = 36$)	High myopia with CNV group ($n = 14$)	P value
Mean age (years)	58.5 ± 5.3	59.6 ± 4.9	57.6 ± 5.4	0.573*
Axial length (mm)	24.3 ± 0.6	28.5 ± 1.1	29.6 ± 1.3	<0.001*
Refractive error (D)	−0.29 ± 1.42	−12.3 ± 4.7	−15.2 ± 3.1	<0.001*
Male gender (%)	42.9	44.4	42.9	0.916**
IOP (mmHg)	14.5 ± 2.8	15.8 ± 2.6	15.5 ± 3.2	0.357*

*Kruskal-Wallis H-test, compared among control, high myopia without CNV (non-CNV), and high myopia with CNV (CNV) groups.
**Fisher's exact t-test compared between control, non-CNV, and CNV groups.
CNV, choroidal neovascularization; D, diopters; IOP, intraocular pressure.

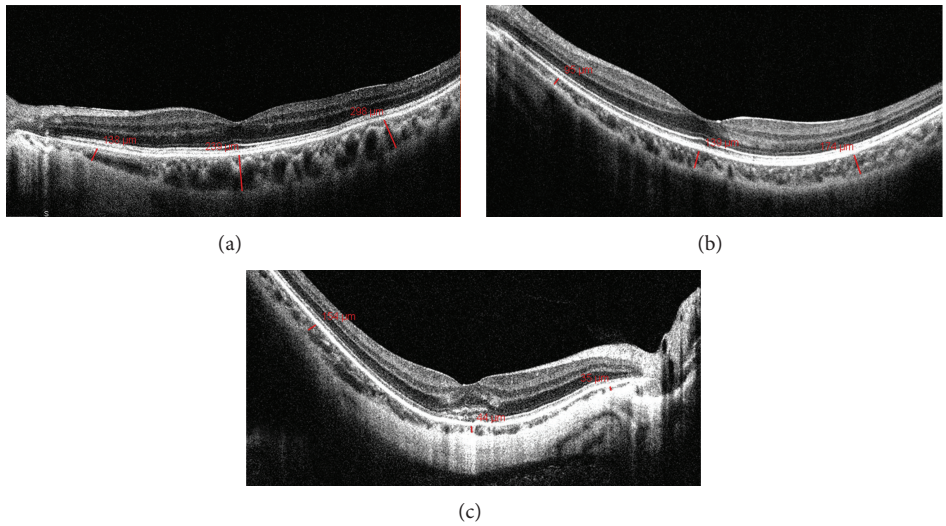

(a) (b) (c)

Figure 1: Optical coherence tomography (OCT) images using enhanced-depth imaging. The choroidal thickness (red line) is defined as the vertical from the outer surface of the hyperreflective line ascribed to the retinal pigment epithelium (RPE) to the hyperreflective line of the inner sclera border (a). Representative scan of a control individual (b). Representative scan of an individual with high myopia without choroidal neovascularization (CNV); note that the choroid is thinner than in the control but thicker than in high myopia with CNV (c). Representative scan of an individual with high myopia with CNV; note that the choroid is thinner than that of control or high myopia without CNV.

concentrations for the three groups. A $P < 0.05$ was considered statistically significant.

3. Results

Table 1 summarizes demographic and clinical characteristics. Average axial globe lengths were 24.3 ± 0.6, 28.5 ± 1.1, and 29.6 ± 1.3 mm for the control, non-CNV, and CNV groups, respectively. Average refractive errors (spherical equivalent refraction) were −0.29 ± 1.42, −12.3 ± 4.7, and −15.2 ± 3.1 D for the control, non-CNV, and CNV groups, respectively. Significant differences among the three groups were seen in axial length and refractive error ($P < 0.001$). Diffuse chorioretinal atrophy was present in 28 of 36 (77.8%) highly myopic eyes in the non-CNV group.

Aqueous levels of PEDF were significantly decreased in the non-CNV group (3.6 ± 1.3 ng/mL) compared with the control group (4.8 ± 1.8 ng/mL) ($P = 0.001$) and were significantly elevated in the CNV group (17.0 ± 5.8 ng/mL) compared with the other two groups ($P < 0.001$) (Figure 2). Mean serum concentrations of PEDF were 5.8 ± 1.3, 5.4 ± 1.2, and 6.1 ± 1.5 μg/mL in the control, non-CNV, and CNV groups, respectively, with no statistically significant differences ($P = 0.632$). Aqueous levels of PEDF were significantly lower than serum levels of PEDF in all three groups ($P < 0.001$). Mean macular choroidal thicknesses were 230.6 ± 81.8, 111.1 ± 45.0, and 77.2 ± 26.9 μm in the control, non-CNV, and CNV groups, respectively. Differences were statistically significant for the non-CNV and CNV groups compared with the control group ($P < 0.001$), while a significant difference ($P = 0.012$) was also found between the non-CNV and CNV groups (Figure 2).

We studied the correlation between aqueous PEDF levels and macular choroidal thickness for the non-CNV group and found a significant, positive correlation ($R^2 = 0.211$, $P = 0.005$) (Figure 3), while no correlation was found for the CNV group ($R^2 = 0.108$, $P = 0.214$) (Figure 4). Conversely, no correlation between serum PEDF and macular choroidal

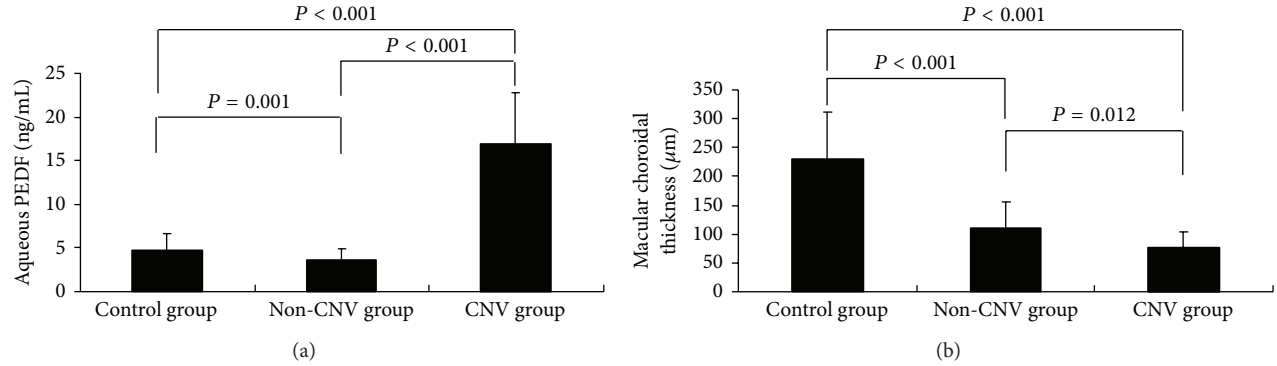

Figure 2: Aqueous pigment epithelium-derived factor (PEDF) levels in control and non-CNV groups (a) and in high myopia with CNV group. (b) Macular choroidal thickness in control, non-CNV, and CNV groups. Results are geometric mean (95% CI).

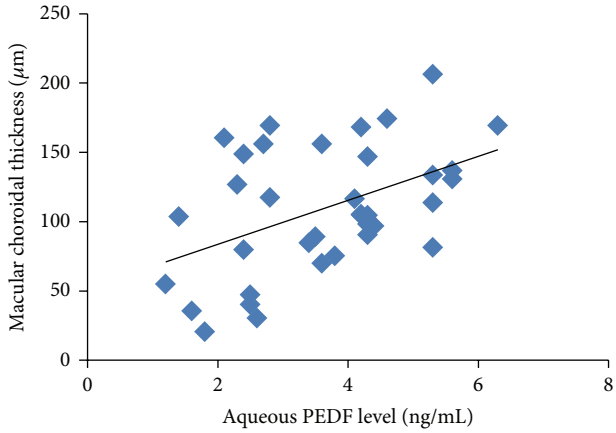

Figure 3: Scatterplots of aqueous PEDF levels and macular choroidal thickness in the non-CNV group show a significant positive correlation ($R^2 = 0.211$; $y = 15.852x + 51.986$; $P = 0.005$).

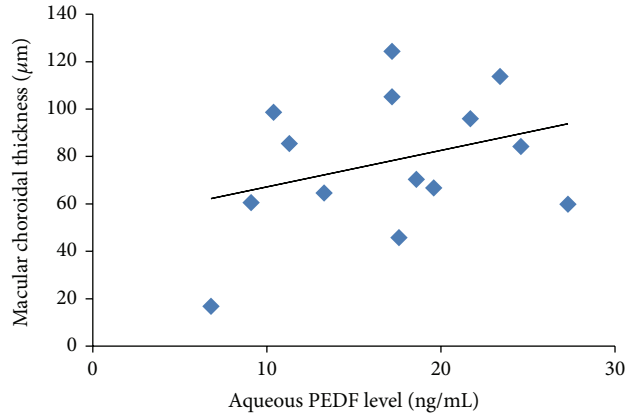

Figure 4: Scatterplots of aqueous PEDF levels and macular choroidal thickness in the CNV group show no correlation ($R^2 = 0.108$; $y = 1.5162x + 51.404$; $P = 0.214$).

thickness was detected for the non-CNV and CNV groups ($R^2 = 0.078$, $P = 0.674$; $R^2 = 0.0064$, $P = 0.720$, resp.). Also no correlation was found between aqueous and serum concentrations of PEDF for the non-CNV and CNV groups ($R^2 = 0.017$ and $R^2 = 0.0054$, resp.). There were also no correlations between aqueous PEDF, serum PEDF, and macular choroidal thickness for the control group.

4. Discussion

Pathologic myopia with progressive and excessive elongation of the eyeball results in a number of chorioretinal changes, including posterior staphyloma, chorioretinal atrophy, and pathologic CNV. Although the mechanisms underlying the development of chorioretinal atrophy and CNV remain unknown, dysfunctional RPE and RPE retraction—in the direction of radial traction line from its underlying glial tissue—are important contributors [11].

PEDF is synthesized and secreted by RPE and retinal ganglion cells and diffuses into the vitreous and aqueous humors [12]. In high myopia, the mechanical tissue strain caused by axial elongation could lead to the development of choroidal ischemia, followed by RPE atrophy. There is a trend toward fewer photoreceptor cells and decreased RPE cell density in eyes with pathological myopia [13]. In addition, age-related functional deterioration of the RPE could result in altered PEDF expression, consequently decreasing inhibition of CNV growth [14].

In the present study, we found that levels of aqueous PEDF in non-CNV eyes were significantly lower (3.6 ± 1.3 ng/mL) than in the control group ($P = 0.001$). Ogata et al. also found the mean aqueous PEDF levels in high myopia to be significantly lower than in eyes with cataract alone [15]. However, Shin et al. reported that PEDF concentrations in highly myopic eyes did not differ significantly from those of control eyes [16]. We speculate that there are two reasons for the decrease found in the non-CNV group. First, because of the elongated axial length of highly myopic eyes, PEDF concentrations may be diluted as a result of the larger vitreous cavity, leading to decreased aqueous concentrations. Second, with chorioretinal atrophy-associated high myopia, decreased PEDF production may be a consequence of degenerated RPE and retinal ganglion cells, its two main sources in the eye.

Vascular endothelial growth factor (VEGF) and PEGF are two major cytokines in angiogenesis. VEGF not only is the major stimulator of neovascular growth and vascular permeability, but also maintains normal functions in many normal adult tissues. The aqueous level of VEGF has been analyzed in high myopia in another study of our group. We found aqueous levels of VEGF from non-CNV high myopia patients were significantly lower compared with those from control persons ($P < 0.001$); meanwhile aqueous levels of VEGF were significantly associated with both macular choroidal thickness ($P < 0.001$) and axial length ($P < 0.001$) [17]. Interestingly, in a similar study, Shin et al. reported that aqueous levels of VEGF in high myopia without CNV were significantly lower than levels in normal eyes [16].

Aqueous levels of PEDF were significantly increased in the CNV group compared with the non-CNV and control groups ($P < 0.001$). Ogata et al. demonstrated increased expression of both VEGF and PEDF in retinas with experimentally induced CNV [18]. However, Holekamp et al. demonstrated lower PEDF, but not VEGF, levels in the vitreous of patients with active CNV resulting from age-related macular degeneration (AMD) [19].

In the present study, we found no significant differences in serum PEDF levels among groups. Furthermore, there were no significant correlations between concentrations of aqueous and serum PEDF for the non-CNV and CNV groups. These findings suggest that, in high myopia, aqueous concentrations of PEDF are not determined by serum concentrations but, rather, by alterations in intraocular synthesis of PEDF.

In our study, macular choroidal thicknesses were 111.1 ± 45.0 and 77.2 ± 26.9 μm in the non-CNV and CNV groups, respectively, both significantly thinner than that of the control group ($P < 0.001$). In addition, Ikuno et al. reported that eyes with myopic CNV have a thinner choroid in comparison to the contralateral eye without CNV [20]. Chung et al. also speculated that a thinner choroid is a risk factor for CNV in eyes with high myopia [21]. We found that choroidal thickness differed significantly ($P = 0.012$) between highly myopic eyes with CNV and those with no CNV. Ikuno et al. also found choroidal thinning to be more prominent in eyes with myopic CNV compared with non-CNV eyes [20]. The association of choroidal thinning with development of myopic CNV is, as yet, unknown. One hypothesis is that choroidal thinning at the fovea leads to outer retinal hypoxic changes, resulting in release of VEGF—a critical mediator of angiogenesis in the eye [22].

To ensure consistency and to minimize any potential influence from diurnal fluctuation, we measured choroidal thickness between 9:00 a.m. and 12:00 p.m. Studies have shown the choroid to be thickest near midnight and thinnest near noon [23]. Using regression analysis, Margolis and Spaide reported an approximate decrease in choroidal thickness of 15 μm every 10 years [24]. Thus, in order to reduce the influence of age, we chose patients who were 50–70 years old.

Although the primary regulatory role of the choroid in ocular physiology is well known, the in vivo clinical association of choroidal thickness with aqueous PEDF levels is unclear. We examined scatterplots of aqueous PEDF levels and macular choroidal thickness and found positive correlations for the non-CNV (Figure 3), but not the CNV (Figure 4), groups. There was no correlation for the CNV group, because PEDF could not be derived from the atrophic RPE cells in this stage.

Several limitations of our study should be mentioned. First, patients undergoing cataract surgery may differ from patients in general or high myopia patients and, accordingly, it is unclear whether the patients included in our study were representative of normal and high myopia patients. Second, choroidal thickness measurements were performed manually, as there exists no automated device for such measurements. In the present study, two masked readers performed measurements, with open negotiation if there was a difference of >15%. Third, RPE autofluorescence was not evaluated but may be an interesting variable to add to future studies.

In summary, variations in aqueous PEDF levels coincide with changes in macular choroidal thickness in high myopia patients with no CNV, while no such relationship exists in high myopia patients with CNV. Our findings suggest that in vivo macular choroidal thickness may be indicative of aqueous PEDF concentration in high myopia with no CNV, but no indication in high myopia with CNV. Nevertheless, based on previous studies showing that age, refractive error, and/or axial length could significantly influence choroidal thickness, the use of macular choroidal thickness as an indirect assessment of aqueous PEDF concentration might be of limited clinical application. Large-scale studies are recommended, particularly to examine the potential prognostic value of aqueous PEDF levels and choroidal changes.

Disclosure

Wei Chen and Yubo Guan are co-first authors.

Conflict of Interests

The authors declare that there is no conflict of interests regarding the publication of this paper.

References

[1] J. H. Kempen, "The prevalence of refractive errors among adults in the United States,Western Europe, and Australia," *Archives of Ophthalmology*, vol. 122, no. 4, pp. 495–505, 2004.

[2] Verteporfin in Photodynamic Therapy (VIP) Study Group, "Photodynamic therapy of subfoveal choroidal neovascularization in pathologic myopia with verteporfin: 1-year results of a randomized clinical trial VIP report no. 1," *Ophthalmology*, vol. 108, no. 5, pp. 841–852, 2001.

[3] J. M. Ruiz-Moreno, L. Arias, J. Montero, A. Carneiro, and R. Silva, "Intravitreal anti-VEGF therapy for choroidal neovascularisation secondary to pathological myopia: 4-year outcome," *The British Journal of Ophthalmology*, vol. 97, no. 11, pp. 1447–1450, 2013.

[4] J. Tombran-Tink and L. V. Johnson, "Neuronal differentiation of retinoblastoma cells induced by medium conditioned by human

RPE cells," *Investigative Ophthalmology and Visual Science*, vol. 30, no. 8, pp. 1700–1707, 1989.

[5] D. W. Dawson, O. V. Volpert, P. Gillis et al., "Pigment epithelium-derived factor: a potent inhibitor of angiogenesis," *Science*, vol. 285, no. 5425, pp. 245–248, 1999.

[6] D. S. Dhoot, S. Huo, A. Yuan et al., "Evaluation of choroidal thickness in retinitis pigmentosa using enhanced depth imaging optical coherence tomography," *British Journal of Ophthalmology*, vol. 97, no. 1, pp. 66–69, 2013.

[7] N.-K. Wang, C.-C. Lai, H.-Y. Chu et al., "Classification of early dry-type myopic maculopathy with macular choroidal thickness," *American Journal of Ophthalmology*, vol. 153, no. 4, pp. 669.e2–677.e2, 2012.

[8] H. Ohsugi, Y. Ikuno, K. Oshima, and H. Tabuchi, "3-D choroidal thickness maps from EDI-OCT in highly myopic eyes," *Optometry and Vision Science*, vol. 90, no. 6, pp. 599–606, 2013.

[9] D. G. Miller and L. J. Singerman, "Natural history of choroidal neovascularization in high myopia," *Current Opinion in Ophthalmology*, vol. 12, no. 3, pp. 222–224, 2001.

[10] N. Kara, N. Sayin, D. Pirhan et al., "Evaluation of subfoveal choroidal thickness in pregnant women using enhanced depth imaging optical coherence tomography," *Current Eye Research*, vol. 39, no. 6, pp. 642–647, 2014.

[11] N. Kitaya, S. Ishiko, T. Abiko et al., "Changes in blood-retinal barrier permeability in form deprivation myopia in tree shrews," *Vision Research*, vol. 40, no. 17, pp. 2369–2377, 2000.

[12] S. P. Becerra, R. N. Fariss, Y. Q. Wu, L. M. Montuenga, P. Wong, and B. A. Pfeffer, "Pigment epithelium-derived factor in the monkey retinal pigment epithelium and interphotoreceptor matrix: apical secretion and distribution," *Experimental Eye Research*, vol. 78, no. 2, pp. 223–234, 2004.

[13] H. E. Grossniklaus and W. R. Green, "Pathologic findings in pathologic myopia," *Retina*, vol. 12, no. 2, pp. 127–133, 1992.

[14] F. C. Delori, D. G. Goger, and C. K. Dorey, "Age-related accumulation and spatial distribution of lipofuscin in RPE of normal subjects," *Investigative Ophthalmology & Visual Science*, vol. 42, no. 8, pp. 1855–1866, 2001.

[15] N. Ogata, M. Imaizumi, M. Miyashiro et al., "Low levels of pigment epithelium-derived factor in highly myopic eyes with chorioretinal atrophy," *American Journal of Ophthalmology*, vol. 140, no. 5, pp. 937–939, 2005.

[16] Y. J. Shin, W. H. Nam, S. E. Park, J. H. Kim, and H. K. Kim, "Aqueous humor concentrations of vascular endothelial growth factor and pigment epithelium-derived factor in high myopic patients," *Molecular Vision*, vol. 18, no. 8, pp. 2265–2270, 2012.

[17] W. Chen, H. Song, S. Xie, Q. Han, X. Tang, and Y. Chu, "Correlation of macular choroidal thickness with concentrations of aqueous vascular endothelial frowth factor in high myopia," *Current Eye Research*. In press.

[18] N. Ogata, M. Wada, T. Otsuji, N. Jo, J. Tombran-Tink, and M. Matsumura, "Expression of pigment epithelium-derived factor in normal adult rat eye and experimental choroidal neovascularization," *Investigative Ophthalmology & Visual Science*, vol. 43, no. 4, pp. 1168–1175, 2002.

[19] N. M. Holekamp, N. Bouck, and O. Volpert, "Pigment epithelium-derived factor is deficient in the vitreous of patients with choroidal neovascularization due to age-related macular degeneration," *The American Journal of Ophthalmology*, vol. 134, no. 2, pp. 220–227, 2002.

[20] Y. Ikuno, Y. Jo, T. Hamasaki, and Y. Tano, "Ocular risk factors for choroidal neovascularization in pathologic myopia," *Investigative Ophthalmology & Visual Science*, vol. 51, no. 7, pp. 3721–3725, 2010.

[21] S. E. Chung, S. W. Kang, J. H. Lee, and Y. T. Kim, "Choroidal thickness in polypoidal choroidal vasculopathy and exudative age-related macular degeneration," *Ophthalmology*, vol. 118, no. 5, pp. 840–845, 2011.

[22] N. Ogata, M. Nishikawa, T. Nishimura, Y. Mitsuma, and M. Matsumura, "Unbalanced vitreous levels of pigment epithelium-derived factor and vascular endothelial growth factor in diabetic retinopathy," *American Journal of Ophthalmology*, vol. 134, no. 3, pp. 348–353, 2002.

[23] G. I. Papastergiou, G. F. Schmid, C. E. Riva, M. J. Mendel, R. A. Stone, and A. M. Laties, "Ocular axial length and choroidal thickness in newly hatched chicks and one-year-old chickens fluctuate in a diurnal pattern that is influenced by visual experience and intraocular pressure changes," *Experimental Eye Research*, vol. 66, no. 2, pp. 195–205, 1998.

[24] R. Margolis and R. F. Spaide, "A pilot study of enhanced depth imaging optical coherence tomography of the choroid in normal eyes," *American Journal of Ophthalmology*, vol. 147, no. 5, pp. 811–815, 2009.

Hindawi Publishing Corporation
Journal of Ophthalmology
Volume 2015, Article ID 706404, 9 pages
http://dx.doi.org/10.1155/2015/706404

Research Article

Suppression of *In Vivo* Neovascularization by the Loss of TRPV1 in Mouse Cornea

Katsuo Tomoyose,[1] Yuka Okada,[1] Takayoshi Sumioka,[1] Masayasu Miyajima,[2] Kathleen C. Flanders,[3] Kumi Shirai,[1] Tomoya Morii,[1] Peter S. Reinach,[4] Osamu Yamanaka,[1] and Shizuya Saika[1]

[1] *Department of Ophthalmology, Wakayama Medical University, 811-1 Kimiidera, Wakayama 641-0012, Japan*
[2] *Laboratory Animal Center, Wakayama Medical University, 811-1 Kimiidera, Wakayama 641-0012, Japan*
[3] *Laboratory of Cell Regulation and Carcinogenesis, National Cancer Institute, National Institutes of Health, Bethesda, MD, USA*
[4] *Wenzhou Medical University School of Ophthalmology and Optometry, Wenzhou, China*

Correspondence should be addressed to Yuka Okada; yokada@wakayama-med.ac.jp

Received 10 December 2014; Revised 6 March 2015; Accepted 16 March 2015

Academic Editor: Caio V. Regatieri

To investigate the effects of loss of transient receptor potential vanilloid receptor 1 (TRPV1) on the development of neovascularization in corneal stroma in mice. Blocking TRPV1 receptor did not affect VEGF-dependent neovascularization in cell culture. Lacking TRPV1 inhibited neovascularization in corneal stroma following cauterization. Immunohistochemistry showed that immunoreactivity for active form of TGFβ1 and VEGF was detected in subepithelial stroma at the site of cauterization in both genotypes of mice, but the immunoreactivity seemed less marked in mice lacking TRPV1. mRNA expression of VEGF and TGFβ1 in a mouse cornea was suppressed by the loss of TRPV1. TRPV1 gene ablation did not affect invasion of neutrophils and macrophage in a cauterized mouse cornea. Blocking TRPV1 signal does not affect angiogenic effects by HUVECs *in vitro*. TRPV1 signal is, however, involved in expression of angiogenic growth factors in a cauterized mouse cornea and is required for neovascularization in the corneal stroma *in vivo*.

1. Introduction

The cornea is a unique ocular tissue of avascularity and transparency for proper vision. It is susceptible to neovascularization-inducing intervention, that is, microbial infection or ocular surface damage. Such unfavorable neovascularization potentially impairs vision. The process of the new vessel formation in an injured cornea is orchestrated by a complex system of various growth factor signaling [1–5]. Resident corneal cells and inflammatory cells invaded to an injured tissue express growth factors and cytokines involved in injury-induced neovascularization. Such factors include vascular endothelial growth factor (VEGF), transforming growth factor β (TGFβ), and fibroblast growth factor (FGF) [6–10].

Members of the transient receptor potential (TRP) channel superfamily are polymodal receptors that are activated by a host of stimuli to mediate sensory transduction. The family is divided into 7 different subfamilies and composed of 28 different genes [11–14]. TRP vanilloid subtype 1 (TRPV1), the capsaicin receptor, is a nociceptor and one of the prototypes of TRPV subfamily. It elicits responses to a variety of noxious stimuli including chemical irritants besides capsaicin, inflammatory mediators, tissue injury, an alteration in pH, and moderate heat (≥43°C). TRPV1 activation leads to nociception and evokes pain or pain-related behaviors and reportedly induces release of tachykinin neuropeptides from sensory nerves, inducing neurogenic inflammation in the surrounding area [15–17]. Various nonneuronal cell linages, that is, epidermal keratinocyte or corneal epithelium and keratocytes, also express TRPV1, which presumably exerts a variety of biological responses to external stimuli [18–24]. We previously reported that lacking TRPV1 counteracted inflammatory and fibrogenic reactions in corneal

stroma following an alkali burn [24]. The phenotype of less-inflammation/fibrosis was found to depend on the loss of keratocytes in the affected stroma, but not on inflammatory cells as revealed by reciprocal bone marrow transplantation experiments. Stromal neovascularization is also a component of the biological reaction observed in an injured cornea. In our previous study on an alkali-burned cornea, however, we failed to extract the effects of the loss of TRPV1 on injury-induced neovascularization in an alkali-burned cornea due to complex tissue reaction in the stroma. It was reported that capsiate and piperine, both TRPV1 agonists, suppress angiogenic behaviors of vascular endothelial cells cultured in the absence of inflammatory components *in vitro* [25, 26]. *In vivo* role of TRPV1 signal in modulation of neovascularization is to be assessed in *in vivo* condition. In the present study we examined the roles of TRPV1 signal in the activity of neovascularization development by using TRPV1-null (KO) mice and *in vitro* human umbilical vein endothelial cell (HUVEC) culture model of neovascularization.

2. Materials and Methods

In vivo experiments were approved by the DNA Recombination Experiment Committee and the Animal Care and Use Committee of Wakayama Medical University and performed in accordance with the Association for Research in Vision and Ophthalmology Statement for the Use of Animals in Ophthalmic and Vision Research.

2.1. Coculture Experiment of Tube-Like Structure Formation by HUVECs. We first employed *in vitro* assay of angiogenic activity of HUVECs. The degree of tube-like structure formation by HUVECs on a fibroblast feeder layer was employed to assess the effects of each agent on neovascularization activity of the cells. The detailed procedure was reported in our previous publications [8, 27]. HUVECs were seeded on the fibroblast feeder layer as the manufacture suggested (NV kit, Kurabo, Tokyo, Japan). Then the culture was maintained in the routine culture condition in the presence of vascular endothelial cell growth factor- (VEGF-) A (10.0 ng/ml, Kurabo, Tokyo, Japan) as an angiogenesis inducer in the presence or absence of a TRPV1 antagonist, SB366791 (10 μM, Sigma-Aldrich). HUVECs did not develop tube-like structure in the absence of VEGF (data not shown). Eight wells were prepared for each culture condition. After 11 days of culture the cells were processed for immunohistochemistry for CD31 (a marker for vascular endothelium) according to the manufacture's protocol. Color development was performed by 3,3′-diaminobentidine (DAB) reaction [8, 27]. Average length and the average number of bifurcations (the number of branching points) were counted in three central fields in each well in a blinded fashion by an investigator. The mean value of the data from these three fields represented the data of each well. Statistical analysis of the data from eight wells was conducted by employing Tukey-Kramer test and $p < 0.05$ was taken as significant.

2.2. Induction of Stromal Neovascularization by Cauterization of the Central Cornea in Mice. We then performed an *in vivo* neovascularization assessment experiment by using a wild-type (WT) of C57Bl/6 ($n = 52$) or KO mouse of C57Bl/6 background ($n = 65$) as previously reported [8]. KO mice were healthy without any obvious general abnormalities and were fertile. There was no difference in the histological findings in an uninjured cornea between a WT and KO mice as previously reported [24]. Corneal stromal neovascularization from the limbal vessels was induced by cauterization of the central cornea of an eye of both WT and KO mice by disposable cauterization tool as previously reported [8].

We first observed the morphology of neovascularization at day 3 after cauterization in whole-mounted specimens by using CD34 immunostaining. Four WT and 4 KO mice were used. Mice were sacrificed at day 3 after cauterization in the central cornea by CO_2 asphyxia. The eye was enucleated, processed for whole-mounted immunostaining. The eyes were fixed in 4% paraformaldehyde for 48 hrs. After washing in phosphate-buffered saline (PBS), the specimens were treated in 0.5% Triton X for 1 hr to facilitate the antibody penetration into the tissue. After rinsing in PBS, the samples were allowed to react with a monoclonal anti-CD31 antibody (1 : 100 in PBS, Santa Cruz Biotechnology Inc., Santa Cruz, CA, USA) for 24 hrs at 4°C. After washing the antibody the tissues were then treated with a FITC-labeled secondary antibody (Southern Biotechnology, Birmingham, Alabama, USA) for 12 hrs at 4°C, mounted in Fluoromount-G after another wash in PBS, and observed under Carl Zeiss Apotome. 2 AxioVision 4.8 fluorescence microscopy.

We then examined the length of neovascularization from limbus toward the center of the cornea following cauterization in histological section. For this purpose, 15, 16, or 8 WT mice and 21, 21, or 10 KO mice were used for assessment at day 3, 7, or 14, respectively. Mice were sacrificed at days 3, 7, and 14 after cauterization in the central cornea by CO_2 asphyxia. The eye was enucleated, processed for cryosections, and used for immunohistochemistry for CD31 (monoclonal, 1 : 100 in PBS, Santa Cruz Biotechnology Inc.) as previously reported [28]. The length of corneal stromal neovascularization was measured as follows: length between limbus and the tip of neovascularization was measured in both sides of the limbus in three cryosections produced from one eye. The average value of the six data represented the neovascularization in one cornea. Statistical analysis was conducted with the use of Mann-Whitney U test, and $p < 0.05$ was taken as significant.

2.3. Immunohistochemistry. Cornea of three eyes of each genotype of mice was also cauterized and then processed for paraffin section immunohistochemistry for active form of TGFβ1, VEGF, substance P, and F4/80 macrophage antigen as previously reported. As described below we semiquantified mRNA expression of TGFβ1 in treated corneas and TGFβ1 exerts its action after processing to the active form. We therefore used an antibody that reacts the active, but not inactive, form of TGFβ1 in the current study [24, 29].

2.4. Gene Expression Analysis. We examined the expression of mRNAs of neovascularization-related growth factors and the degree of inflammation in *in vivo* mouse cornea. We considered mRNA level quantification was essential because our

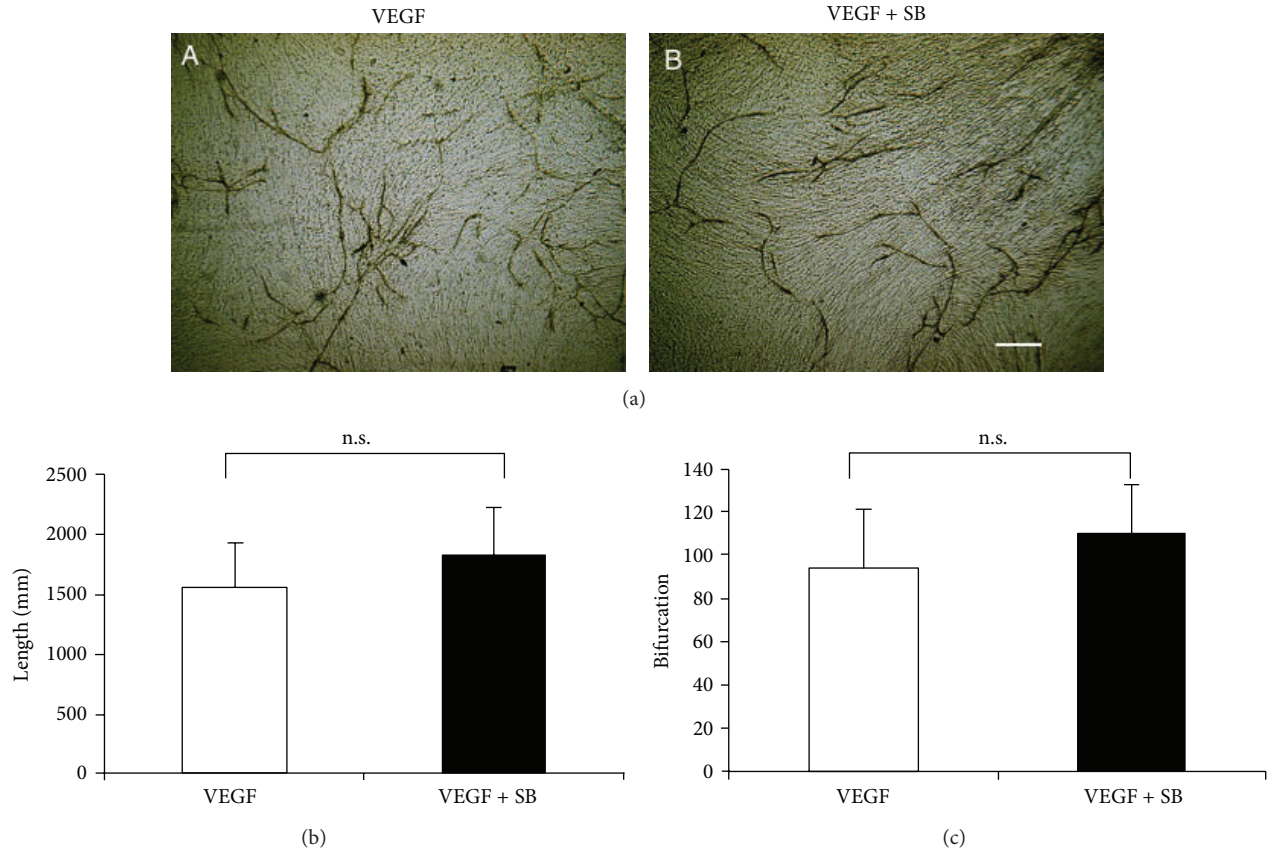

Figure 1: Tube-like structure formation by human umbilical vein endothelial cells (HUVECs). (a) The HUVEC culture on fibroblast feeder was processed for CD31 immunocytochemistry at day 11. In control vascular endothelial growth factor- (VEGF-) plus, culture HUVEC forms CD31-labeled tube-like tissue (A). VEGF action of tube-like structure formation is not affected by supplementation of a TRPV1 antagonist, SB366791 (10 μM) (B). Measurement of total length (b) and the number of branching points (c) of CD31-labeled structure coincide with the findings shown in frame (a). $^{*}p < 0.05$, bar, 1 mm.

preliminary immunohistochemistry for VEGF and TGFβ1 showed very faint staining with minimal difference of the staining in central corneal stroma between a WT and a KO mouse. Centrally cauterized cornea (n = 6 in each of WT or KO group) was excised at day 3. Total RNA was extracted from these tissues and processed for TaqMan real-time reverse transcription-polymerase chain reaction (RT-PCR) for VEGF, TGFβ1, myeloperoxidase (MPO) and F4/80 macrophage antigen and as previously reported [24]. Delta/delta CT method by Applied Biosystem Inc. was employed with the internal control of glyceraldehyde 3-phosphate dehydrogenase (GAPDH) expression. Primers (Applied Biosystem Inc.) used were described in the following list. Data were statistically analyzed by employing Mann-Whitney U test.

Primers Used (Applied Biosystem Inc.). Consider

vascular endothelial growth factor: Mm01281447_ml;

transforming growth factor β1: Mm03024053_ml;

substance P: Mm01166996_ml;

interleukin-6: Mm01210732_gl;

myeloperoxidase: Mm01298422_gl;

F4/80: Mm00802524_ml.

3. Results

3.1. In Vitro Experiment of Tube-Like Structure Formation by HUVECs. Dense CD31 immunoreactivity was detected in tissue where HUVECs formed a vessel-like tube structure. Without exogenous VEGF, HUVECs grown on the fibroblast feeder layer did not form a vessel-like tube tissue. The HUVEC culture was processed for CD31 immunocytochemistry at day 11 (Figure 1(a)). The angiogenic behaviors of HUVECs were evaluated by measurement of the mean total length of the structure (Figure 1(b)) and of the men number of bifurcations (Figure 1(c)) in randomly selected fields of the culture as described above. In the culture with VEGF-A (10 μg/ml) CD31-labeled tube-like structure was observed. Supplementation of a TRPV1 antagonist, SB366791 (10 μM), did not affect VEGF-A action on tube-like structure formation by HUVECs (Figure 1).

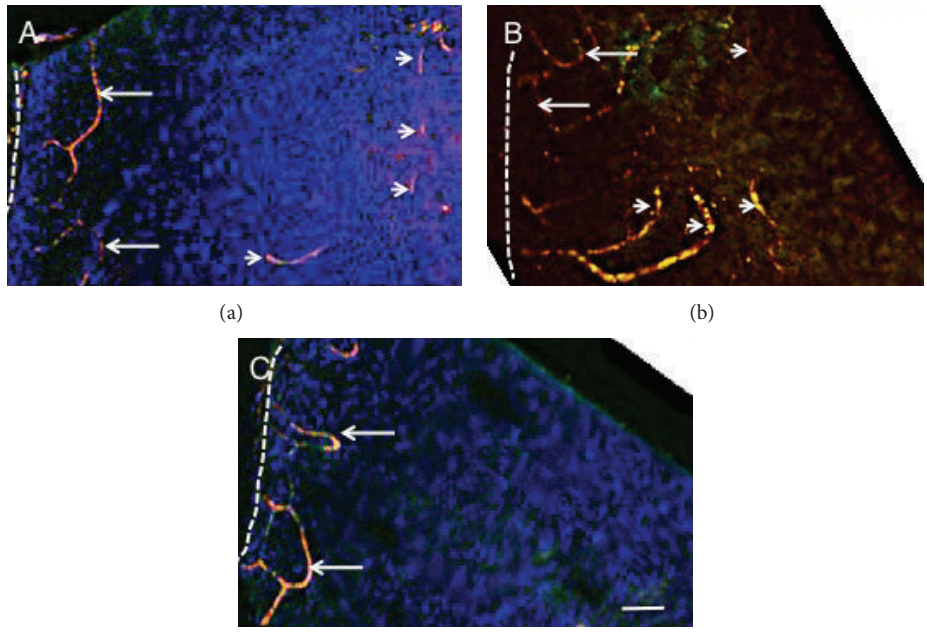

(a) (b)

(c)

Figure 2: Neovascularization in corneal stroma as observed in whole-mounted specimens. We first observed the morphology of neovascularization in whole-mounted specimens by employing CD34 immunostaining. WT ((a), (b)) and KO (c) corneas at day 3 show loop-like distribution of blood limbal vasculature (arrows in (a), (b), and (c)). In WT corneas neovascularization was observed in the stroma apart from the limbus (arrowheads in (a) and (b)), although the staining procedure did not figure the continuous elongation of the vessels. Dotted lines, limbal corneoscleral border; bar, 100 μm.

3.2. Neovascularization in Corneal Stroma. We first observed the morphology of neovascularization in whole-mounted specimens by employing CD31 immunostaining. Figure 2 shows the morphology of limbal vasculature of WT and KO corneas at day 3. In both WT (Figures 2(a) and 2(b)) and KO (Figure 2(c)) corneas loop-like distributions of blood vessels were observed. In WT corneas neovascularization was observed in the stroma apart from the limbus, although the staining procedure did not figure the continuous elongation of the vessels (Figures 2(a) and 2(b)).

We then measured the length of neovascularization in the stroma in histology section. CD31 immunostaining was performed in cryosections of the mouse cornea (Figure 3(a)). In WT mouse corneas, development of the CD31-labeled neovascularization from the limbus in the corneal stroma was detected in the peripheral cornea as early as at day 3 (Figure 3(a)). The length of the neovascularization between the limbus (arrowheads) and the tip (arrows) of new vessels in the corneal stroma was measured at each timepoint.

The length of neovascularization was shorter in KO mice as compared with WT mice at day 3 and day 7, but not at day 14 (Figure 3(b)).

3.3. Expression of Inflammatory and Angiogenic Components in Centrally Cauterized Cornea. Immunohistochemistry showed that active forms of TGFβ1, VEGF, and substance P were not detected in untreated cornea of both genotypes of mice (not shown). Active form of TGFβ1 was detected in stroma just beneath the epithelium in the area of cauterization at days 3 and 7 in WT mice (Figures 4(a) and 4(c)). Its immunoreactivity was quite less marked in cornea of KO mice (Figures 4(b) and 4(d)). VEGF was also not detected in uninjured corneas of both genotypes of mice. At day 1 after cauterization very faint VEGF immunoreactivity was observed in basal cells of corneal epithelia in cauterization area of both WT and KO mice (Figures 4(e) and 4(f)). At day 3 the basal epithelial cells with VEGF immunoreactivity were more frequently observed in a WT cornea as compared with a KO mouse (Figures 4(g) and 4(h)). Immunoreactivity for substance P was detected in basal layer of corneal epithelium with no obvious difference in intensity between WT and KO mice at days 1 and 3 (Figures 4(i), 4(j), 4(k), and 4(l)).

We then examined mRNA expression of VEGF and TGFβ1, the major two growth factors reportedly involved in corneal neovascularization in day 3 specimens by using real-time RT-PCR. Expression of mRNAs of both VEGF (Figure 5(a)) and TGFβ1 was significantly less in a KO cornea as compared with a WT cornea at day 3 (Figure 5(b)). TRPV1 signal is reportedly involved in expression of substance P and interleukin-6 (IL-6), both involved in local tissue inflammation. However, in the present study the loss of TRPV1 did not affect mRNA expression level of substance P (Figure 5(c)) and IL-6 (Figure 5(d)) in the centrally cauterized cornea at this timepoint.

3.4. Expression of Inflammatory Cell Markers in Centrally Cauterized Cornea. We previously reported that cauterization in the central cornea induced inflammation in the affected area

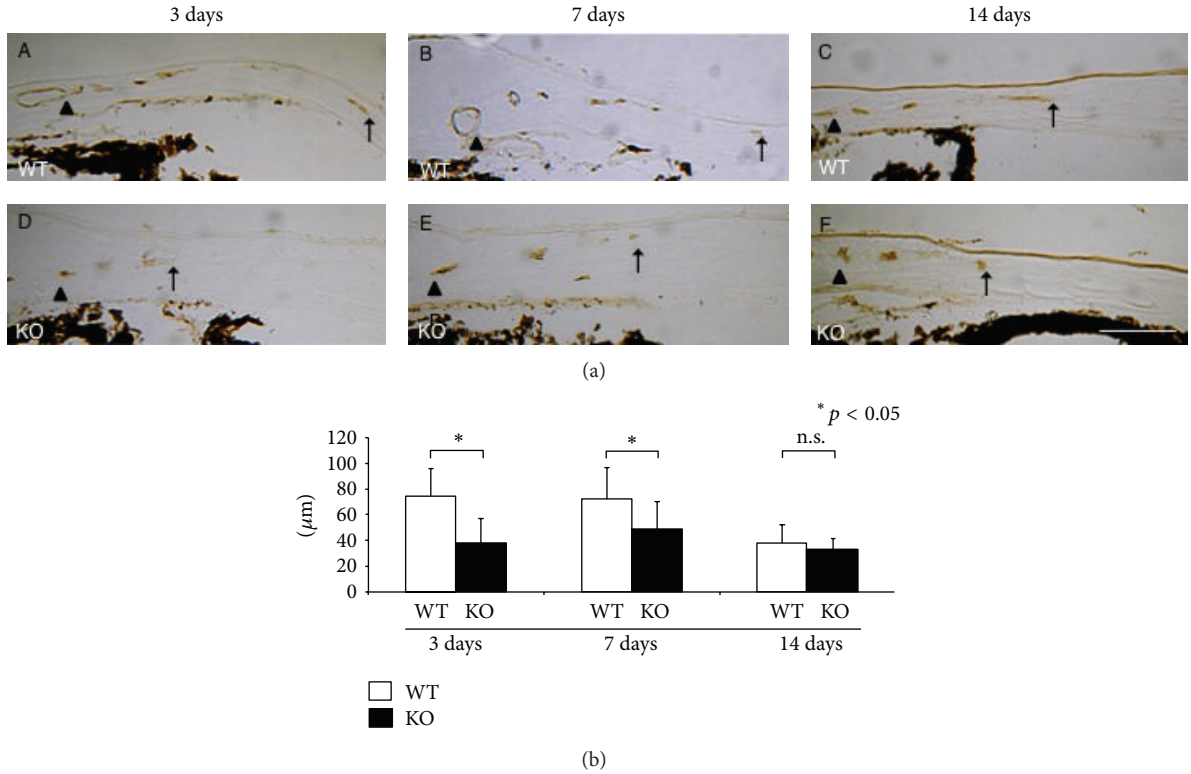

Figure 3: Neovascularization in corneal stroma in histology and evaluation of its length. (a) CD31 immunostaining was performed in cryosections of the mouse cornea. In WT mouse corneas, formation of CD31-labeled neovascularization (arrows) from the limbal vessels (arrowheads) in the corneal stroma was detected in the peripheral cornea at days 3 and 7. The length of the neovascularization was less in KO mice as compared with WT mice at day 3 and day 7 (b). $^{*}p < 0.05$; n.s.: not significant. Bar, 100 μm.

of tissues. We therefore first examined distribution of F4/80-labeled macrophages by using immunohistochemistry and saw difference of distribution of F4/80-labeled macrophages (Figure 6(a)). We then semiquantified the invasion of neutrophils and macrophages in tissues by conducting real-time RT-PCRs for mRNAs of MPO, a neutrophil marker, and F4/80. The loss of TRPV1 exhibited no remarkable effect on mRNA expression of these cell markers (Figures 6(b) and 6(c)).

4. Discussion

The present experiments first showed that lacking TRPV1 cation channel receptor suppressed stromal neovascularization in an *in vivo* mouse cornea following receiving a cauterization injury at the central cornea. Neovascularization was found to sprout from the loop-shaped vessels of the limbus toward the center of the corneal stroma in whole-mounted samples of WT tissues, while such neovascularization was much less in a KO cornea at day 3. The distance between limbus and the tip of the neovascularization in the stroma was significantly shorter in a KO cornea and compared with a WT mouse. Cell culture experiment showed that blockage of TRPV1 receptor did not affect VEGF angiogenic action on HUVECs. HUVECs do not reportedly express TRPV1 [26], and thus the present *in vivo* finding of less angiogenesis observed in a KO cornea was not attributed to the direct effects of the loss of TRPV1 on vascular endothelial cells. Although various growth factors that potentially affect neovascularization activity are expressed in an injured cornea during tissue repair [29–32], expression of such components is reportedly modulated by ion channel receptor signaling, that is, signaling derived from TRP family members.

To analyze the mechanism of antiangiogenic effect of lacking TRPV1 in *in vivo* corneal stroma we conducted further experiments. Because TRPV1 signal is involved in inflammation in response to external stimuli, which potentially affect formation of neovascularization, we ran real-time RT-PCR for inflammatory/angiogenic growth factors and inflammation/wound healing-related components. The results showed that mRNA expression of VEGF and TGFβ1 in cauterized cornea was suppressed by lacking TRPV1, but expression of mRNA of IL-6 was not affected by the loss of TRPV1. Immunohistochemistry also showed that deposition of active form of TGFβ1 in the stroma beneath the regenerated epithelium and VEGF expression in the basal epithelial cells in the central cornea both seemed less in amount in a KO tissue as compared with a WT mouse. We reported that TGFβ1 is expressed in corneal epithelium and is deposited in stroma beneath the regenerated epithelium as an active form [33]. Thus, reduced accumulation of active form of TGFβ1 in the KO cornea might be attributable to the suppression

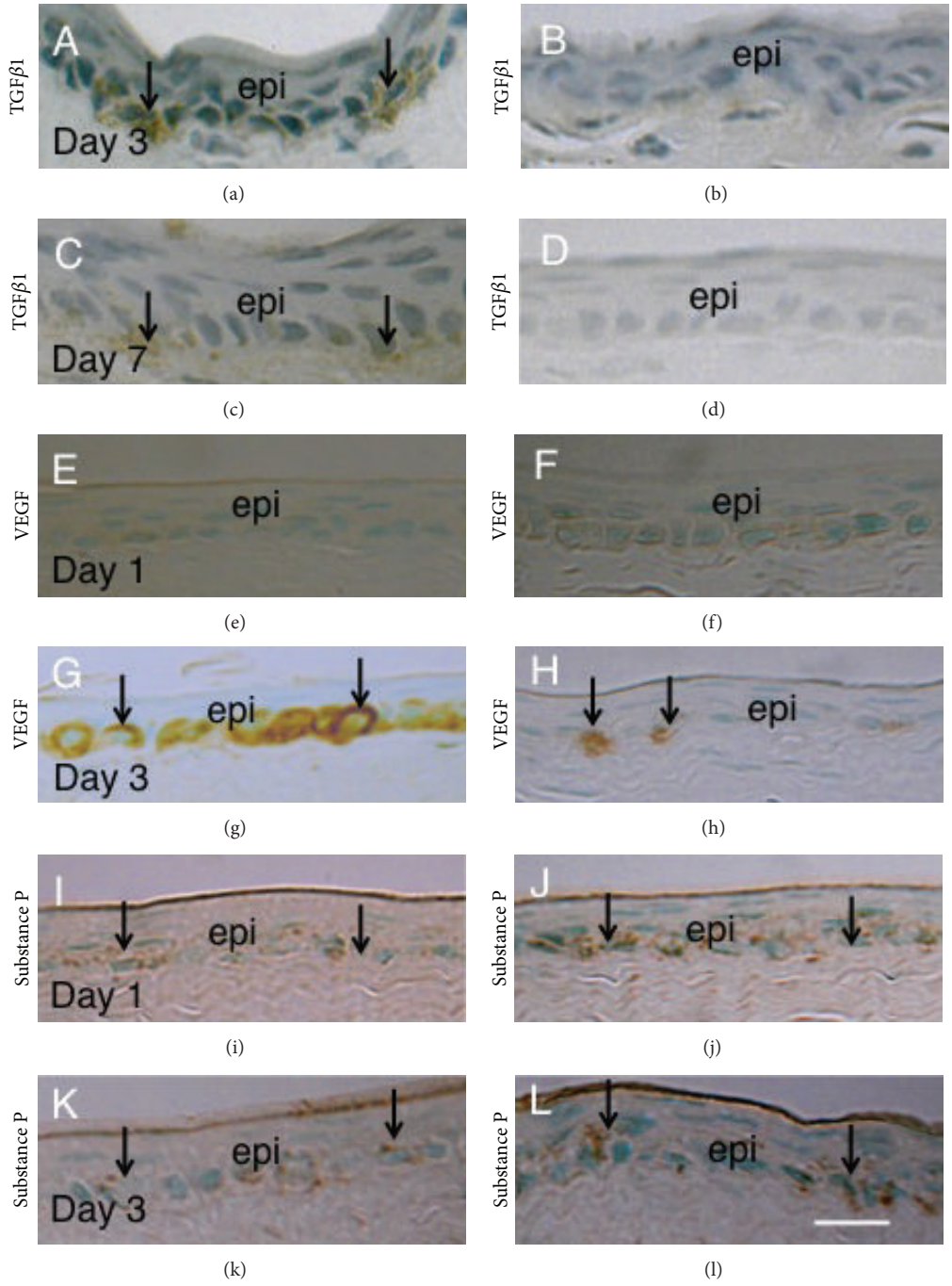

Figure 4: Immunohistochemical detection of angiogenic or inflammatory components in centrally cauterized cornea. Active form of TGFβ1 was detected in stroma just beneath the epithelium in the area of cauterization at days 3 and 7 in WT mice (arrows in (a) and (c)). Its immunoreactivity was quite less marked in cornea of KO mice ((b) and (d)). At day 1 after cauterization very faint VEGF immunoreactivity was observed in basal cells of corneal epithelia in cauterization area of both WT (e) and KO (f) mice. At day 3 the basal epithelial cell with VEGF immunoreactivity was more frequently observed in a WT cornea (e) as compared with a KO mouse (f). Immunoreactivity for substance P was detected in basal layer of corneal epithelium with no obvious difference in intensity between WT and KO mice at days 1 and 3 ((g)–(l)). Bar, 20 μm.

of TGFβ1 expression in epithelium after cauterization by the loss of TRPV1. Similarly, postcauterization VEGF expression in corneal epithelium was suppressed by lacking TRPV1. IL-6 was not detected by immunohistochemistry presumably because the protein might be secreted out from the cells.

We also examined the level of inflammation in cornea. Immunohistochemistry did not show difference of F4/80-labeled macrophage infiltration. We then ran semiquantification by real-time RT-PCR. The present assessment of inflammatory cell markers, that is, MPO and F4/40, indicated

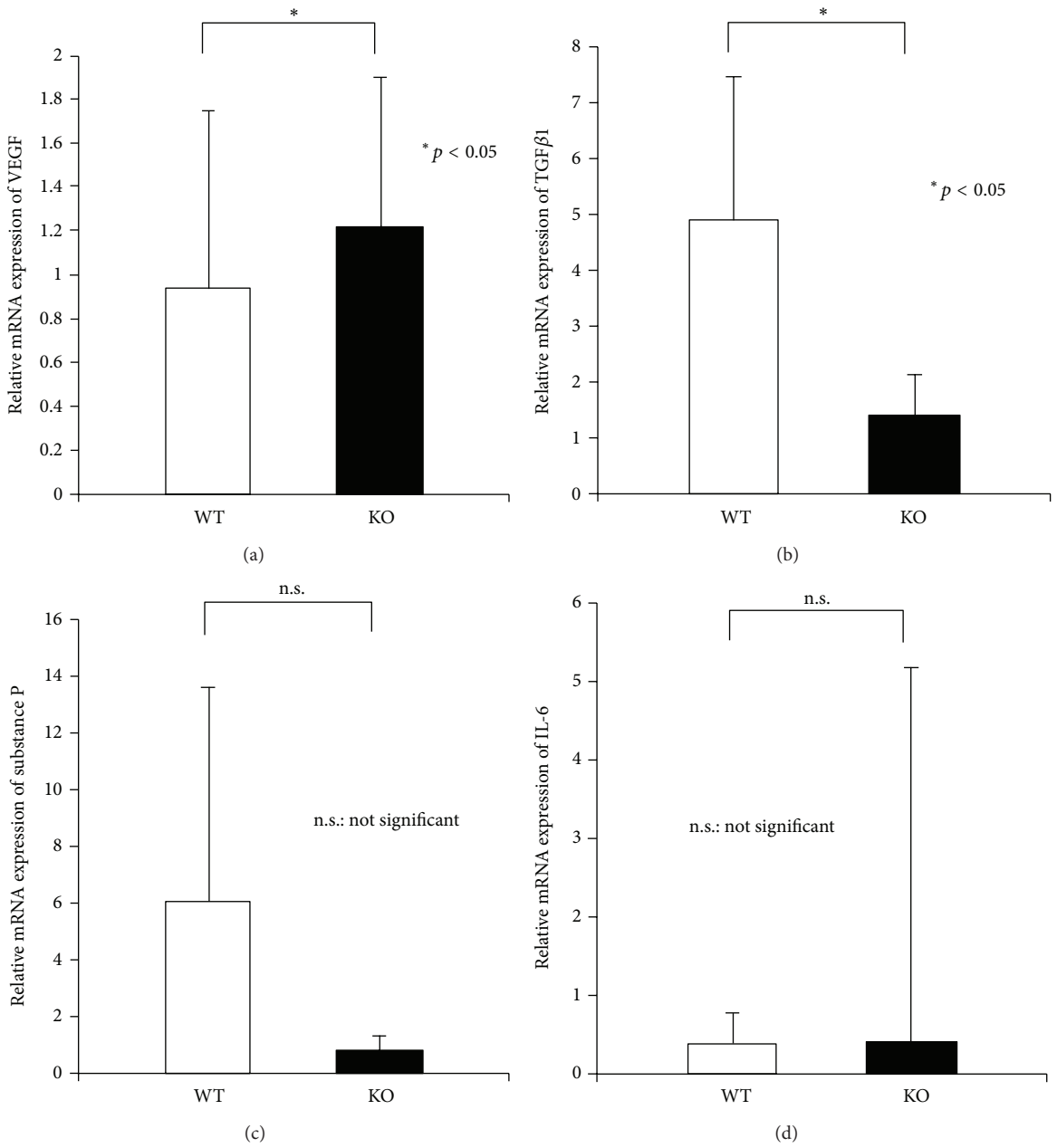

Figure 5: Expression of mRNAs of angiogenic or inflammatory components in centrally cauterized cornea at day 3. mRNA expression of vascular endothelial growth factor (VEGF, (a)) and transforming growth factor β1 (TGFβ1, (b)) mRNAs in the affected cornea of wild-type (WT) was more marked as compared with that in TRPV1-null (KO) mice at day 3 after cauterization. The loss of TRPV1 did not affect mRNA expression level of substance P (c) and IL-6 (d) in the centrally cauterized cornea at this timepoint. $^{*}p < 0.05$; n.s.: not significant.

that following cauterization in the central cornea the loss of TRPV1 did not affect infiltration of neutrophil leukocytes and macrophages. Data from these real-time RT-PCR results suggest that less expression of angiogenic growth factors, that is, VEGF and TGFβ1, is unattributed to the alteration of the level of inflammatory cell infiltration following cauterization in a KO tissue and presumably is dependent on the effects of lacking TRPV1 on the gene expression in resident corneal cells, that is, corneal epithelial cells. Involvement of keratocytes in the suppression of neovascularization in the KO mouse is to be further investigated. TRPV1 in sensory nerve fibers reportedly mediates expression of neuroinflammatory mediators, for example, substance P [34, 35]. In the present study protein and mRNA expressions of substance P were similar in WT and KO corneas after cauterization.

In conclusion, blocking TRPV1 signal might be beneficial in suppression of neovascularization in cornea.

Disclosure

The abstract of the current study was presented by Dr. Tomoyose in the Annual Meeting of the Association for

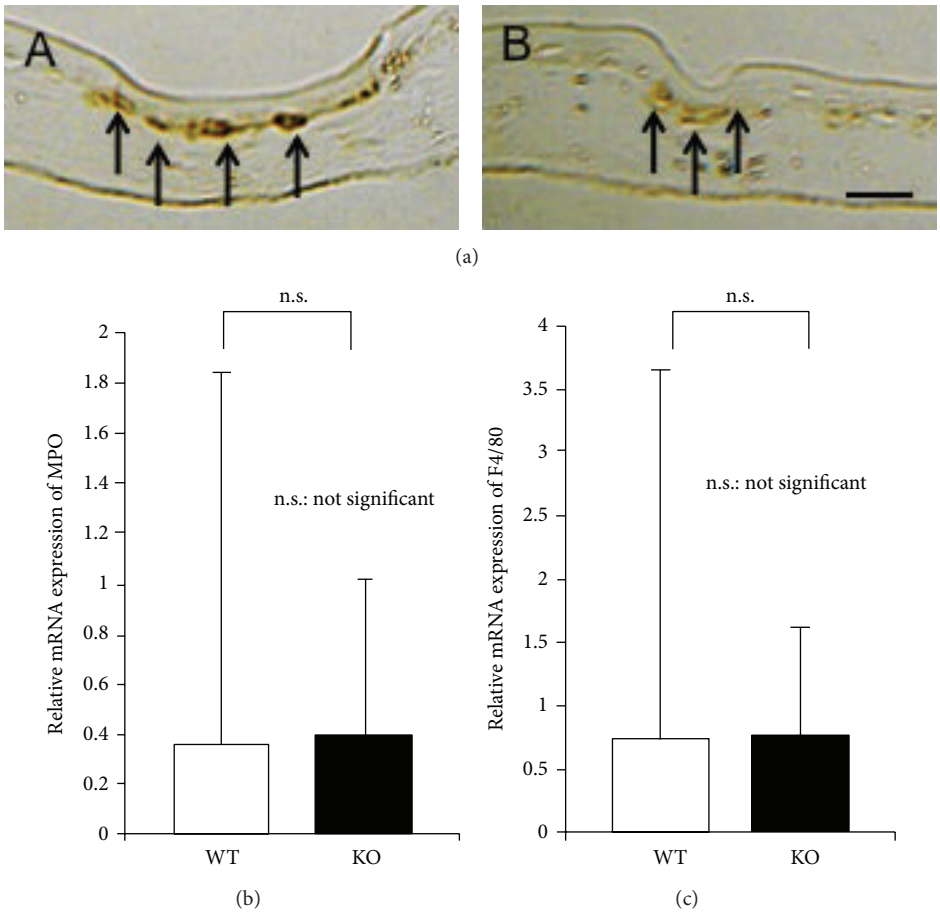

Figure 6: Inflammatory cells in centrally cauterized cornea of WT and KO mice. (a) Immunohistochemistry detected F4/80 labeled macrophages (arrows) beneath the epithelium in the central cornea of both WT (A) and KO (B) corneas at day 7. There is no difference in mRNA expression of myeloperoxidase (MPO), a neutrophil marker (b), and F4/80 macrophage antigen (c) between wild-type (WT) and TRPV1-null (KO) corneas at day 3 after cauterization. n.s.: not significant, bar, 50 μm.

Research in Vision and Ophthalmology (ARVO 2013, Seattle).

Conflict of Interests

The authors have declared that there is no conflict of interests regarding the paper.

Acknowledgment

This study was supported by grant from the Ministry of Education, Science, Sports and Culture of Japan (C40433362 to Takayoshi Sumioka, C21592241 to Yuka Okada, and C19592036 to Shizuya Saika).

References

[1] F. Bock, K. Maruyama, B. Regenfuss et al., "Novel anti(lymph) angiogenic treatment strategies for corneal and ocular surface diseases," *Progress in Retinal and Eye Research*, vol. 34, no. 1, pp. 89–124, 2013.

[2] J. L. Clements and R. Dana, "Inflammatory corneal neovascularization: etiopathogenesis," *Seminars in Ophthalmology*, vol. 26, no. 4-5, pp. 235–245, 2011.

[3] D. Meller, R. T. F. Pires, R. J. S. Mack et al., "Amniotic membrane transplantation for acute chemical or thermal burns," *Ophthalmology*, vol. 107, no. 5, pp. 980–989, 2000.

[4] S. Saika, O. Yamanaka, T. Sumioka et al., "Fibrotic disorders in the eye: targets of gene therapy," *Progress in Retinal and Eye Research*, vol. 27, no. 2, pp. 177–196, 2008.

[5] D. T. Azar, "Corneal angiogenic privilege: angiogenic and antiangiogenic factors in corneal avascularity, vasculogenesis, and wound healing (an American Ophthalmological Society Thesis)," *Transactions of the American Ophthalmological Society*, vol. 104, pp. 264–302, 2006.

[6] M. Papathanassiou, P. G. Theodossiadis, V. S. Liarakos, A. Rouvas, E. J. Giamarellos-Bourboulis, and I. A. Vergados, "Inhibition of corneal neovascularization by subconjunctival bevacizumab in an animal model," *American Journal of Ophthalmology*, vol. 145, no. 3, pp. 424.e1–431.e1, 2008.

[7] S. Saika, "TGFβ pathobiology in the eye," *Laboratory Investigation*, vol. 86, no. 2, pp. 106–115, 2006.

[8] S. Fujita, S. Saika, W. W.-Y. Kao et al., "Endogenous TNFα suppression of neovascularization in corneal stroma in mice,"

Investigative Ophthalmology and Visual Science, vol. 48, no. 7, pp. 3051–3055, 2007.

[9] W. Stevenson, S.-F. Cheng, M. H. Dastjerdi, G. Ferrari, and R. Dana, "Corneal neovascularization and the utility of topical VEGF inhibition: ranibizumab (Lucentis) Vs bevacizumab (Avastin)," *Ocular Surface*, vol. 10, no. 2, pp. 67–83, 2012.

[10] M. E. Francis, S. Uriel, and E. M. Brey, "Endothelial cell-matrix interactions in neovascularization," *Tissue Engineering Part B: Reviews*, vol. 14, no. 1, pp. 19–32, 2008.

[11] S. F. Pedersen, G. Owsianik, and B. Nilius, "TRP channels: an overview," *Cell Calcium*, vol. 38, no. 3-4, pp. 233–252, 2005.

[12] I. S. Ramsey, M. Delling, and D. E. Clapham, "An introduction to TRP channels," *Annual Review of Physiology*, vol. 68, pp. 619–647, 2006.

[13] G. Owsianik, K. Talavera, T. Voets, and B. Nilius, "Permeation and selectivity of TRP channels," *Annual Review of Physiology*, vol. 68, pp. 685–717, 2006.

[14] C. Montell, L. Birnbaumer, and V. Flockerzi, "The TRP channels, a remarkably functional family," *Cell*, vol. 108, no. 5, pp. 595–598, 2002.

[15] M. J. Caterina, M. A. Schumacher, M. Tominaga, T. A. Rosen, J. D. Levine, and D. Julius, "The capsaicin receptor: a heat-activated ion channel in the pain pathway," *Nature*, vol. 389, no. 6653, pp. 816–824, 1997.

[16] M. J. Caterina, A. Leffler, A. B. Malmberg et al., "Impaired nociception and pain sensation in mice lacking the capsaicin receptor," *Science*, vol. 288, no. 5464, pp. 306–313, 2000.

[17] J. B. Davis, J. Gray, M. J. Gunthorpe et al., "Vanilloid receptor-1 is essential for inflammatory thermal hyperalgesia," *Nature*, vol. 405, no. 6783, pp. 183–187, 2000.

[18] F. Zhang, H. Yang, Z. Wang et al., "Transient receptor potential vanilloid 1 activation induces inflammatory cytokine release in corneal epithelium through MAPK signaling," *Journal of Cellular Physiology*, vol. 213, no. 3, pp. 730–739, 2007.

[19] H. Yang, Z. Wang, J. E. Capó-Aponte, F. Zhang, Z. Pan, and P. S. Reinach, "Epidermal growth factor receptor transactivation by the cannabinoid receptor (CB1) and transient receptor potential vanilloid 1 (TRPV1) induces differential responses in corneal epithelial cells," *Experimental Eye Research*, vol. 91, no. 3, pp. 462–471, 2010.

[20] Z. Pan, Z. Wang, H. Yang, F. Zhang, and P. S. Reinach, "TRPV1 activation is required for hypertonicity-stimulated inflammatory cytokine release in human corneal epithelial cells," *Investigative Ophthalmology & Visual Science*, vol. 52, no. 1, pp. 485–493, 2011.

[21] Z. Wang, Y. Yang, H. Yang et al., "NF-κB feedback control of JNK1 activation modulates TRPV1-induced increases in IL-6 and IL-8 release by human corneal epithelial cells," *Molecular Vision*, vol. 17, pp. 3137–3146, 2011.

[22] Y. Yang, H. Yang, Z. Wang et al., "Cannabinoid receptor 1 suppresses transient receptor potential vanilloid 1-induced inflammatory responses to corneal injury," *Cellular Signalling*, vol. 25, no. 2, pp. 501–511, 2013.

[23] Y. M. Lee, S. M. Kang, and J. H. Chung, "The role of TRPV1 channel in aged human skin," *Journal of Dermatological Science*, vol. 65, no. 2, pp. 81–85, 2012.

[24] Y. Okada, P. S. Reinach, K. Shirai et al., "TRPV1 involvement in inflammatory tissue fibrosis in mice," *The American Journal of Pathology*, vol. 178, no. 6, pp. 2654–2664, 2011.

[25] B.-J. Pyun, S. Choi, Y. Lee et al., "Capsiate, a nonpungent capsaicin-like compound, inhibits angiogenesis and vascular permeability via a direct inhibition of Src kinase activity," *Cancer Research*, vol. 68, no. 1, pp. 227–235, 2008.

[26] C. D. Doucette, A. L. Hilchie, R. Liwski, and D. W. Hoskin, "Piperine, a dietary phytochemical, inhibits angiogenesis," *Journal of Nutritional Biochemistry*, vol. 24, no. 1, pp. 231–239, 2013.

[27] K. Fujita, T. Miyamoto, and S. Saika, "Sonic hedgehog: its expression in a healing cornea and its role in neovascularization," *Molecular Vision*, vol. 15, pp. 1036–1044, 2009.

[28] T. Sumioka, N. Fujita, A. Kitano, Y. Okada, and S. Saika, "Impaired angiogenic response in the cornea of mice lacking tenascin C," *Investigative Ophthalmology and Visual Science*, vol. 52, no. 5, pp. 2462–2467, 2011.

[29] S. Saika, T. Miyamoto, O. Yamanaka et al., "Therapeutic effect of topical administration of SN50, an inhibitor of nuclear factor-κB, in treatment of corneal alkali burns in mice," *The American Journal of Pathology*, vol. 166, no. 5, pp. 1393–1403, 2005.

[30] S. Saika, K. Ikeda, O. Yamanaka et al., "Therapeutic effects of adenoviral gene transfer of bone morphogenic protein-7 on a corneal alkali injury model in mice," *Laboratory Investigation*, vol. 85, no. 4, pp. 474–486, 2005.

[31] S. Saika, K. Ikeda, O. Yamanaka et al., "Expression of Smad7 in mouse eyes accelerates healing of corneal tissue after exposure to alkali," *The American Journal of Pathology*, vol. 166, no. 5, pp. 1405–1418, 2005.

[32] S. Saika, K. Ikeda, O. Yamanaka et al., "Loss of tumor necrosis factor α potentiates transforming growth factor β-mediated pathogenic tissue response during wound healing," *American Journal of Pathology*, vol. 168, no. 6, pp. 1848–1860, 2006.

[33] S. Saika, "TGF-β signal transduction in corneal wound healing as a therapeutic target," *Cornea*, vol. 23, no. 8, supplement, pp. S25–S30, 2004.

[34] M. A. Engel, M. Khalil, S. M. Mueller-Tribbensee et al., "The proximodistal aggravation of colitis depends on substance P released from TRPV1-expressing sensory neurons," *Journal of Gastroenterology*, vol. 47, no. 3, pp. 256–265, 2012.

[35] R. J. Steagall, A. L. Sipe, C. A. Williams, W. L. Joyner, and K. Singh, "Substance P release in response to cardiac ischemia from rat thoracic spinal dorsal horn is mediated by TRPV1," *Neuroscience*, vol. 214, pp. 106–119, 2012.

Hindawi Publishing Corporation
Journal of Ophthalmology
Volume 2015, Article ID 343515, 8 pages
http://dx.doi.org/10.1155/2015/343515

Clinical Study

Optical Coherence Tomography Angiography in Retinal Vascular Diseases and Choroidal Neovascularization

Rodolfo Mastropasqua,[1] Luca Di Antonio,[2] Silvio Di Staso,[3] Luca Agnifili,[2] Angela Di Gregorio,[3] Marco Ciancaglini,[3] and Leonardo Mastropasqua[2]

[1]*Ophthalmology Unit, Department of Neurological, Neuropsychological, Morphological and Movement Sciences, University of Verona, 37100 Verona, Italy*
[2]*Ophthalmology Clinic, Department of Medicine and Aging Science, University G. d'Annunzio of Chieti-Pescara, 66100 Chieti, Italy*
[3]*Eye Clinic, Department of Life, Health and Environmental Sciences, University of L'Aquila, 67100 L'Aquila, Italy*

Correspondence should be addressed to Marco Ciancaglini; marco.ciancaglini@cc.univaq.it

Received 17 December 2014; Revised 13 April 2015; Accepted 24 May 2015

Academic Editor: Caio V. Regatieri

Purpose. To assess the ability of optical coherence tomography-angiography (OCT-A) to show and analyze retinal vascular patterns and the choroidal neovascularization (CNV) in retinal vascular diseases. *Methods*. Seven eyes of seven consecutive patients with retinal vascular diseases were examined. Two healthy subjects served as controls. All eyes were scanned with the SD-OCT XR Avanti (Optovue Inc, Fremont CA, USA). Split spectrum amplitude decorrelation angiography algorithm was used to identify the blood flow within the tissue. Fluorescein angiography (FA) and indocyanine green angiography (ICGA) with Spectralis HRA + OCT (Heidelberg Engineering GmbH) were performed. *Results*. In healthy subjects OCT-A visualized major macular vessels and detailed capillary networks around the foveal avascular zone. Patients were affected with myopic CNV (2 eyes), age-related macular degeneration related (2), branch retinal vein occlusion (BRVO) (2), and branch retinal artery occlusion (BRAO) (1). OCT-A images provided distinct vascular patterns, distinguishing perfused and nonperfused areas in BRVO and BRAO and recognizing the presence, location, and size of CNV. *Conclusions*. OCT-A provides detailed images of retinal vascular plexuses and quantitative data of pathologic structures. Further studies are warranted to define the role of OCT-A in the assessment of retinovascular diseases, with respect to conventional FA and ICG-A.

1. Introduction

Fifty years have passed since Novotny and Alvis performed the first fluorescein angiography (FA). This invasive method uses intravenous fluorescein to produce fluorescence images of circulating blood in the human retina [1]. For many years this procedure has been considered the gold standard for imaging the retinal vasculature network [2].

From its commercialization, both time and spectral domain (SD) optical coherence tomography (OCT) modalities have dramatically changed the daily clinical practice in ophthalmology [3, 4]. With the introduction of SD-OCT, acquisition time decreased while the imaging resolution greatly improved. Thus it was possible to generate clinically useful cross-sectional and 3-dimensional (3D) images of the retinal layers [5]. A limit remains in that this imaging modality cannot visualize and thus cannot provide functional information of retinal microcirculation.

Recently, a novel dyeless method of microvasculature imaging called OCT angiography (OCT-A) was introduced. Several prototypes used the normal movement of the red blood cells in the retinal capillaries as intrinsic contrast medium to generate flow imaging. The phase-based and amplitude-based modalities showed feasibility of rendering deeper structural details of retinal and choroidal microvascular structures when motion-based contrast techniques are used [6–9]. Three examples that are currently in use are as follows: Phase Variance OCT (PV-OCT), Phase Contrast OCT (PC-OCT), and Split Spectrum Amplitude Decorrelation Angiography (SSADA) (Angio-OCT). These methods

(a) (b) (c)

Figure 1: Fluorescein angiography image of the central macula in a healthy subject (a). OCT angiography image (3 × 3 mm) of the superficial vascular plexus (b) showing the vascular centripetal distribution "web-like shape" towards the fovea. OCT angiography image (3 × 3 mm) of the deep vascular plexus (c) showing a close-knit pattern of vessels around the foveal avascular zone. OCT angiography identifies more about details of the capillary beds (superficial and deep) than standard Fluorescein Angiography.

were implemented using both SD and swept-source OCT (SS-OCT) imaging systems in order to detect the transverse and axial flow thus differing from Doppler OCT that measures just the axial velocity. Pilot studies that investigated these OCT systems in patients with age-related macular degeneration and glaucoma [10–12] confirmed their utility.

Amplitude-based OCT signal analysis may be advantageous for ophthalmic imaging since it uses a speckle variance method that does not suffer from phase noise artifacts and does not require complex phase correction methods [8]. Both phase-based and amplitude-based OCT provide noninvasive visualization of both larger blood vessels and capillary networks in the retina and choroid [6, 8]. The results obtained with these modalities were comparable to currently used invasive angiographic imaging [6, 8] in addition to being able to separately characterize features of the superficial and deep vascular plexuses, which cannot be distinguished in FA [9]. The aim of this study was to evaluate the ability of OCT-A for imaging retina of subjects affected with vascular diseases to assess perfused and nonperfused areas and choroidal neovascularization (CNV), using XR Avanti AngioVue OCT (Optovue, Inc, Fremont CA, USA).

2. Materials and Methods

This prospective unmasked study adhered to the tenets of the Declaration of Helsinki, and informed consent was obtained from all patients prior to their enrolment. Our local Ethics Board was notified and stated that their approval was not necessary. Seven eyes of seven consecutive Caucasian patients (four males and three females) ranging in age from 54 to 64 years (mean 59.1 years), referred to the Ophthalmic Clinic of University Chieti-Pescara, Italy, for the presence of retinal vascular diseases from October 1 to 31, 2014, were examined. Two healthy subjects with no significant medical history and no signs or symptoms of retinal vascular disease were included as controls. FA was performed in all subjects with the Spectralis HRA + OCT (Heidelberg Engineering GmbH). Indocyanine green angiography (ICGA) was performed only in patients with suspected choroidal neovascularization (CNV). All eyes were also scanned with the SD-OCT XR Avanti (Optovue Inc, Fremont CA, USA), using the following settings: high speed (70,000 A-scans/seconds), 840 nm wavelength (band-width 45 nm), and an axial resolution of 5 μm. Each B-scan contained 216 A-scans. The scanning procedure was described in detail elsewhere [13]. The SSADA algorithm was used to distinguish between static and nonstatic tissue. This algorithm identifies blood flow by calculating the decorrelation of signal amplitude from consecutive B-scans performed at the same retinal acquisition plane.

Decorrelation of OCT signal amplitude between B-scans taken at the same nominal position could be caused by flow, bulk tissue motion, scanner position error, and background noise. To enhance true flow in the images and improve the signal-to-noise ratio for flow detection, the decorrelation due to bulk motion and background noise were eliminated. The SSADA data was separated into retinal and choroidal regions with the dividing boundary set at the retinal pigment epithelium (RPE). The depth (Z position) of the highly reflective RPE was identified through the analysis of the reflectance and reflectance gradient profiles in depth [14]. The region above the RPE was the retinal layer and the region below was the choroidal layer. Since the retina is a laminar structure with a stratified blood supply, *en face* X-Y projection angiograms were produced by selecting the maximum decorrelation value along the axial (Z) direction in each layer. Segmentation of the retina in specific layers provided a simple en face visualization of the corresponding vascular supply for that layer.

Automatic segmentation was used to identify retinal layers. When a retinal pathology was present (i.e., presence of subretinal fluid or serous pigment epithelial detachment), manual correct of the segmentation was necessary in order to avoid both image processing software and segmentation errors [9]. The allowable field of view (FOV) in the retina SSADA scans is 2 × 2, 3 × 3, 6 × 6, and 8 × 8 mm.

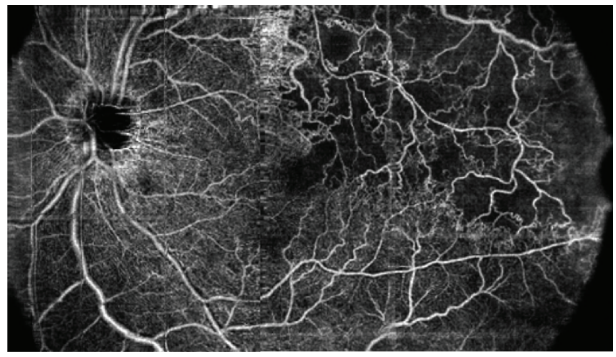

Figure 2: OCT angiography (composition map of three partially overlapping 8 × 8 mm scans) of a 57-year-old woman with branch retinal vein occlusion (BRVO) showing enlargement of foveal avascular zone and retinal nonperfused area (capillary drop-out) at the posterior pole and at the mid periphery with the development of collaterals.

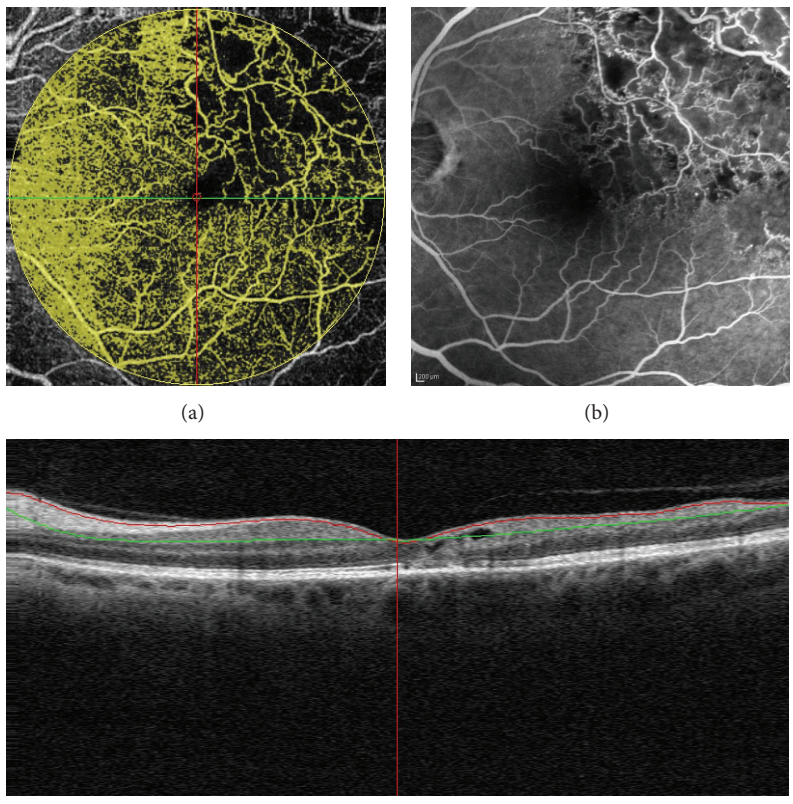

(a) (b)

(c)

Figure 3: Branch retinal vein occlusion (BRVO) of a 53-year-old woman: OCT angiography (8 × 8 mm) showing perfused and nonperfused flow areas of the retina (a) due to capillary drop-out seen in fluorescein angiography (b). Longitudinal B-scan demonstrating the reference lines of the superficial plane (c).

A 3 × 3 mm FOV is the recommended default size for visualization of retinal capillaries. The 6 × 6 or 8 × 8 mm scans are the recommended scans for performing large area scans of the retina.

3. Results

In healthy subjects OCT-A visualized major macular vessels and detailed capillary networks around the foveal avascular zone. The vascular network was similar to those reported using FA (Figure 1(a)). Notably, OCT-A revealed more capillary details compared to FA in the superficial and, especially, in the deep retinal layer (Figures 1(b) and 1(c)).

Patients 1 and 2 were affected with ischemic branch retinal vein occlusion (BRVO). A composite map composed of three 8 × 8 mm scans from patient 1 and an 8 × 8 mm OCT-A scan from patient 2 are shown in Figures 2 and 3(b), respectively. In both cases, OCT-A distinguished perfused and nonperfused

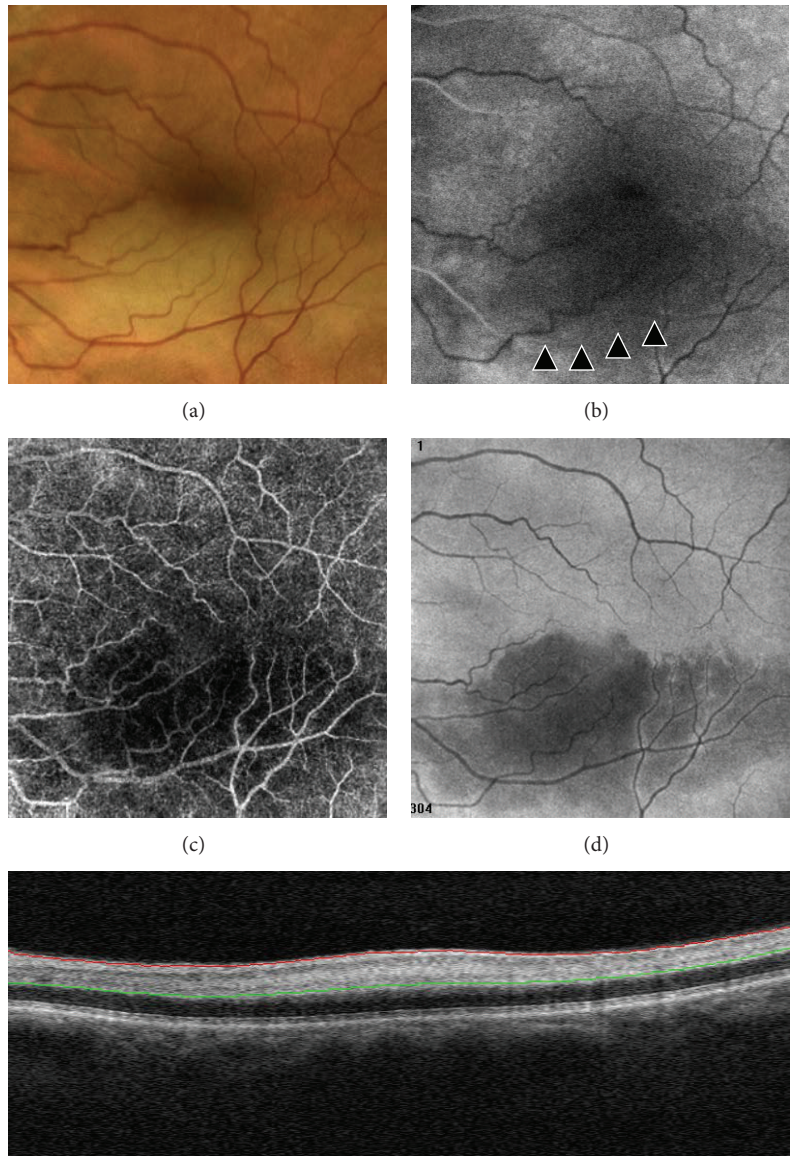

Figure 4: Branch retinal artery occlusion (BRAO) of a 62-year-old man showing a band of retinal whitening extending inferior-temporally from the disc in a color image (a). Delayed filling (about 17 sec) of the arteriole (arrowheads) during the arterial phase in fluorescein angiography (b). Low flow area in OCT-angiography (6 × 6 mm) image (c). Area of hyporeflectivity in high-resolution en face projection adapted to the retinal pigment epithelium surface (d). Focal thickening and hyperreflectivity due to intraretinal edema in the reference plane of B-scan (e).

areas located in both the posterior pole and mid periphery (Figures 2 and 3).

Patient 3 was affected with branch retinal artery occlusion (BRAO). The main finding was the low flow area in OCT-A, which correlated with the area of hypofluorescence in FA due to retinal artery hypoperfusion. Moreover, the en face image adapted to the RPE surface showed the presence of ischemia-induced area of hyporeflectivity and longitudinal B-scan revealed focal thickening and hyperreflectivity within both inner and deep capillary plexuses (Figure 4).

In patient 4, the color-mode OCT-A aided in detecting the vascular network of myopic CNV and in defining specific morphological features (Figure 5). The entire vascular pattern was seen with enhanced details compared to simultaneous FA and ICGA frames. Color-mode OCT-A in patient 5, affected by myopic CNV, showed the response to therapy with intravitreal antivascular endothelial growth factor medications (Figure 6). Analysis of OCT-A changes indicated a reduction in size and flow of CNV and the resolution of subretinal fluid observed in B-scan.

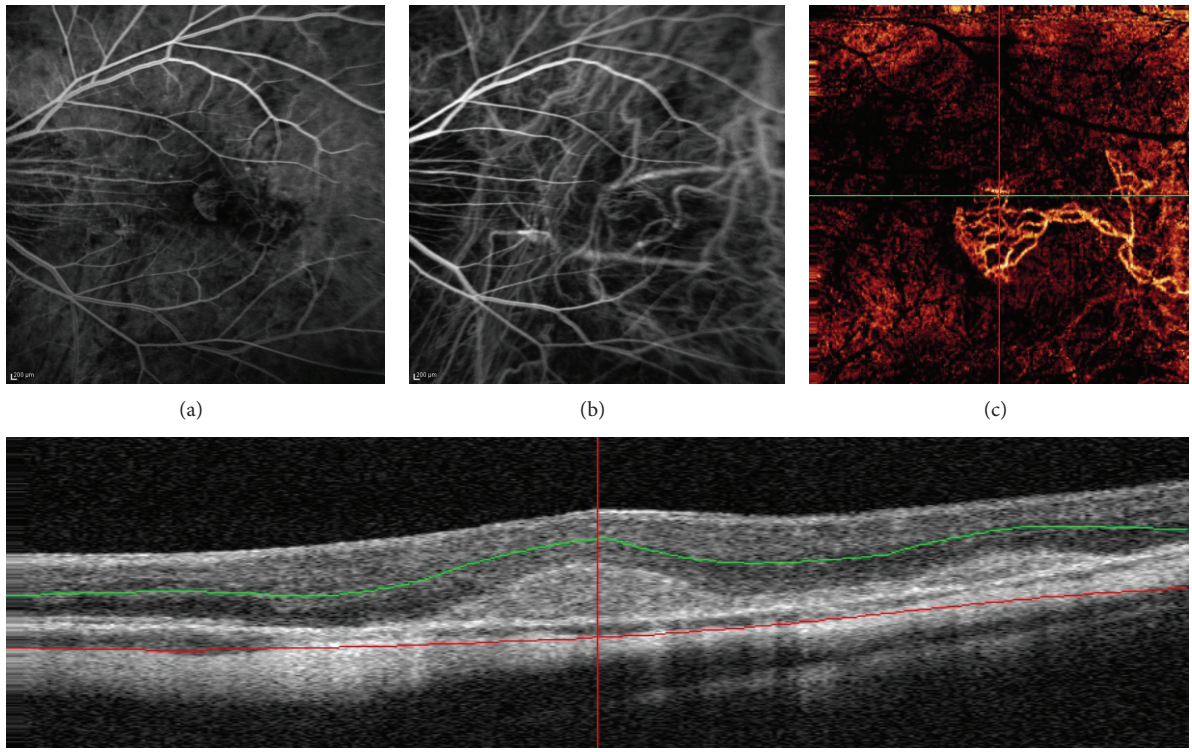

(a) (b) (c)

(d)

Figure 5: Simultaneous fluorescein angiography (a) and Indocyanine green angiography arteriovenous phase (b) showing myopic choroidal neovascularization. Color-mode OCT angiography (3 × 3 mm) image (c) shows both feeder vessels and neovascular network of myopic choroidal neovascularization. B-scan (d) showing reference planes at the level of the outer retina.

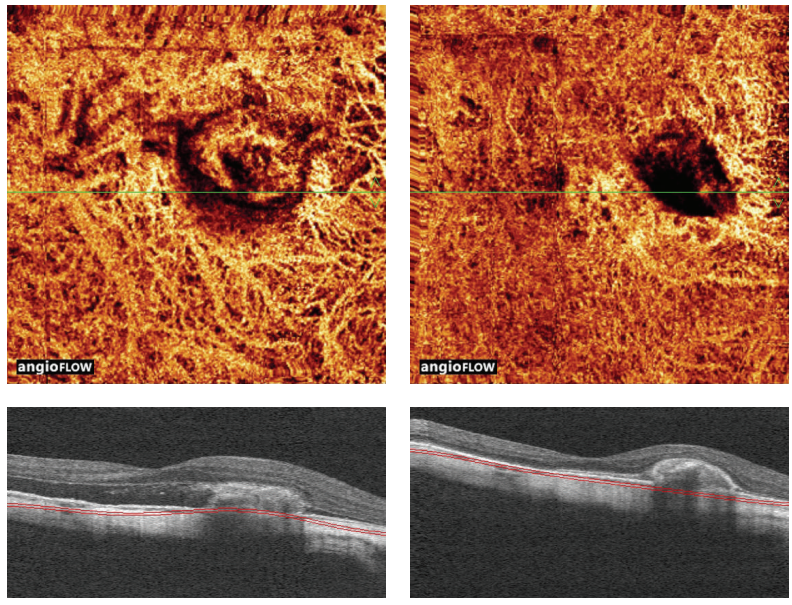

(a) (b)

Figure 6: Angioretina color-mode change analysis. (a) Baseline showing neovascular network of myopic choroidal neovascularization (top) and the presence of subretinal fluid in longitudinal B-scan (bottom). (b) Follow-up showing reduction of both flow and size of neovascular complex after intravitreal injection of anti-VEGF (top) and resolution of SRF in longitudinal B-scan (bottom).

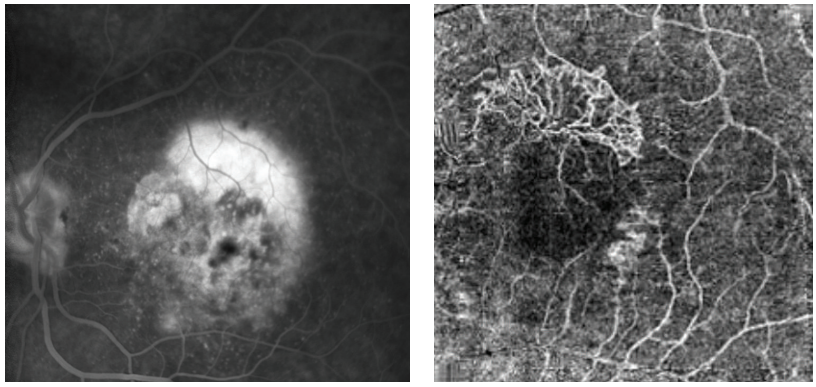

(a) (b)

Figure 7: Fluorescein angiography (a) shows late leakage from classical choroidal neovascularization. OCT angiography (6 × 6 mm) and (b) enhances choroidal new vessels as high-flow network "umbrella like-shape" above retinal pigment epithelium (RPE).

Patients 6 and 7 were affected with CNV secondary to age-related macular degeneration (AMD). Classic CNV (Figure 7) focused on the outer capillary plexus and above the RPE. Retinal angiomatous proliferation (Figure 8) was detected at the level of the deep capillary plexus. By using OCT-A, CNV was clearly recognizable and the rim and area of neovascularization were more easily detectable compared to FA and ICGA.

4. Discussion

This study aimed at examining the ability of OCT-A, a promising and noninvasive imaging modality, to image the vascular modifications within the inner and outer retinal layers in several retinovascular diseases. Currently, FA and ICGA are considered the gold standard for defining functional and morphological features in patients affected with ocular vascular diseases. However, both techniques are invasive since they require intravenous dye injection and are bothersome for some patients who complain of side effects that range from nausea/vomiting to serious anaphylactic reactions (although the latter is rare). Moreover, FA can only show vessels in a nearly transparent structure with a thickness that is on the order of only hundreds of micrometers. This allows a good visualization of the superficial capillary network of the retina but not of the deep capillary layer [15, 16]. On the other hand, OCT angiography obtained with the SSADA algorithm provides images of both the superficial and deep retinal vascular plexuses.

In the present study both OCT-A and FA provided clinically useful images of the inner retinal vascular plexus. This was in accordance with results of Imai et al. [17] who used swept-source OCT in patients with BRVO, reporting a good agreement between FA and OCT-A in assessing the area and colocalization of nonperfused area. The authors concluded that OCT angiography was a valuable alternative imaging modality for studying ischemic diseases in both the diagnostic phase and during follow-up. Currently, the role of the outer retinal plexus in retinal diseases is unclear. In fact, vascular diseases could affect inner and outer plexuses differently. In support of this, vein occlusions and inflammatory vascular diseases may be selectively involved, as suggested by modifications of middle layers in OCT B-scans.

One of the most promising fields for the application of OCT-A is CNV imaging. Other structural OCT imaging modalities cannot directly identify the CNV structure, but only the presence of changes such as abnormal tissue above or below the RPE. Therefore, FA and ICGA are still needed in the initial diagnosis of neovascular AMD.

The present study showed that OCT-A was also valuable in imaging and quantifying CNV in myopia and AMD since the neovascularization was successfully identified in all patients presenting this lesion. The SSADA algorithm was crucial in differentiating CNV from the surrounding outer retinal tissue, RPE, and hemorrhages. This confirmed the preliminary data reported by Jja et al. in a swept-source OCT prototype study [10]. Notably, CNV vascular network patterns were more distinct in OCT-A scans compared to FA and ICGA, particularly in terms of location, size, and presence of feeder vessels.

It is important to keep in mind that subretinal and surrounding CNV fluid appeared as a low flow area in OCT-A (because SSADA identifies only moving flow), whereas it produced a hyperfluorescent pattern in FA; where the fluid outside of the blood vessels generates dye leakage Overall, OCT-A was not completely comparable to FA and ICGA angiograms. In fact, OCT-A provided static images of the vascular flow, without providing dynamic information, which was conversely provided by classical ocular angiographies with dyes. However, the integration of structural and quantitative data obtained with OCT has the potential to be a new useful tool for studying retinal vascular diseases.

Although this pilot study has the weaknesses of limited sample size it showed the potential of OCT-A for providing quantitative data for diagnosis and follow-up of different retinochoroidal diseases without the use of intravenous dyes.

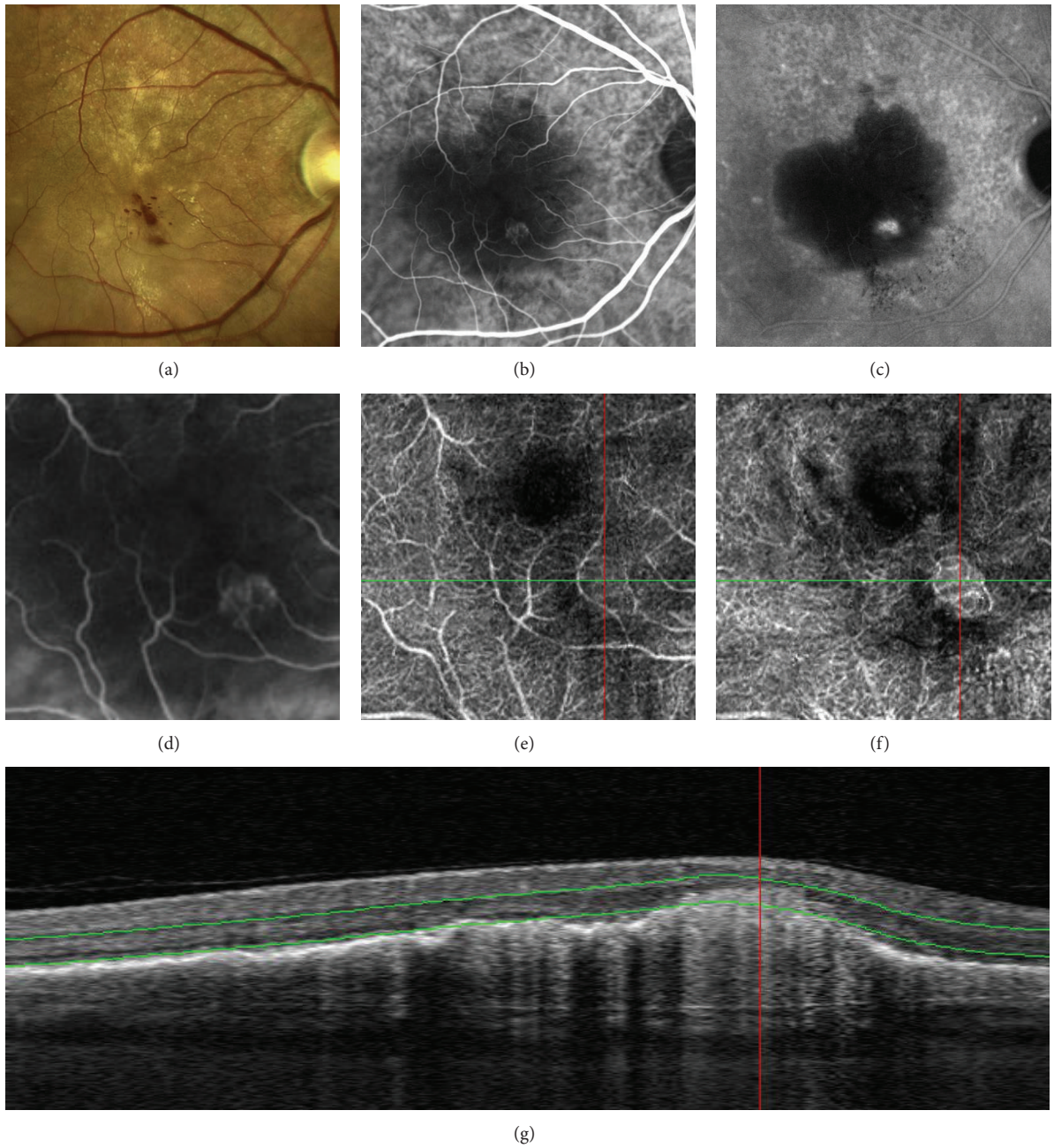

Figure 8: Multimodal retinal imaging of retinal angiomatous proliferation (RAP): color picture (a) showing intraretinal hemorrhages and exudates. Early phase of indocyanine green angiography (ICG-A) (b) revealing typical features such as feeding artery, a focal hyperfluorescence, and draining vein, seen better in the enlarged view (d). Late phase of ICG-A (c) showing a hot-spot within a serous pigment epithelial detachment (PED). OCT-Angiography scan (3 × 3 mm) (e) adapted to inner vascular plexus showing a subtle glomerular network. OCT angiography scan (3 × 3 mm) (f) highlighting glomerular high flow arising from deep capillary plexus. B-scan (g) demonstrating the reference plane at the level of deep capillary plexus.

The first limit of this new technique was that the field of view (3 × 3 mm, 6 × 6 mm and 8 × 8 mm) was smaller than conventional FA. In the future the FOV should increase as scan speeds increase. The second limit was that a precise fixation was required in order to obtain good images, so this technique was not reproducible in patients with low vision. Further investigations will be needed to validate the clinical application of this novel method.

Conflict of Interests

There are no competing interests.

Authors' Contribution

Rodolfo Mastropasqua and Luca Di Antonio equally contributed to this work and share primary authorship.

References

[1] H. R. Novotny and D. L. Alvis, "A method of photographing fluorescence in circulating blood in the human retina.," *Circulation*, vol. 24, pp. 82–86, 1961.

[2] L. Laatikainen, "The fluorescein angiography revolution: a breakthrough with sustained impact," *Acta Ophthalmologica Scandinavica*, vol. 82, no. 4, pp. 381–392, 2004.

[3] D. Huang, E. A. Swanson, C. P. Lin et al., "Optical coherence tomography," *Science*, vol. 254, no. 5035, pp. 1178–1181, 1991.

[4] N. Nassif, B. Cense, B. H. Park et al., "In vivo human retinal imaging by ultrahigh-speed spectral domain optical coherence tomography," *Optics Letters*, vol. 29, no. 5, pp. 480–482, 2004.

[5] M. Wojtkowski, V. Srinivasan, J. G. Fujimoto et al., "Three-dimensional retinal imaging with high-speed ultrahigh-resolution optical coherence tomography," *Ophthalmology*, vol. 112, no. 10, pp. 1734–1746, 2005.

[6] J. Fingler, R. J. Zawadzki, J. S. Werner, D. Schwartz, and S. E. Fraserl, "Volumetric microvascular imaging of human retina using optical coherence tomography with a novel motion contrast technique," *Optics Express*, vol. 17, no. 24, pp. 22190–22200, 2009.

[7] S. M. Motaghiannezam, D. Koos, and S. E. Fraser, "Differential phase-contrast, swept-source optical coherence tomography at 1060 nm for in vivo human retinal and choroidal vasculature visualization," *Journal of Biomedical Optics*, vol. 17, no. 2, Article ID 026011, 2012.

[8] Y. Jia, O. Tan, J. Tokayer et al., "Split-spectrum amplitude-decorrelation angiography with optical coherence tomography," *Optics Express*, vol. 20, no. 4, pp. 4710–4725, 2012.

[9] B. Lumbroso, D. Huang, Y. Jia et al., *Clinical Guide to Angio-OCT—Non Invasive Dyeless OCT Angiography*, Jaypee Brothers Medical Publisher, New Delhi, India, 2015.

[10] Y. Jia, S. T. Bailey, D. J. Wilson et al., "Quantitative optical coherence tomography angiography of choroidal neovascularization in age-related macular degeneration," *Ophthalmology*, vol. 121, pp. 1435–1444, 2014.

[11] Y. Jia, E. Wei, X. Wang et al., "Optical coherence tomography angiography of optic disc perfusion in glaucoma," *Ophthalmology*, vol. 121, no. 7, pp. 1322–1332, 2014.

[12] M. Miura, S. Makita, T. Iwasaki, and Y. Yasuno, "Three-dimensional visualization of ocular vascular pathology by optical coherence angiography in vivo," *Investigative Ophthalmology & Visual Science*, vol. 52, no. 5, pp. 2689–2695, 2011.

[13] R. F. Spaide, J. M. Klancnik Jr., and M. J. Cooney, "Retinal vascular layers imaged by fluorescein angiography and optical coherence tomography angiography," *JAMA Ophthalmology*, vol. 33, no. 1, pp. 45–50, 2015.

[14] L. An and R. K. Wang, "In vivo volumetric imaging of vascular perfusion within human retina and choroids with optical micro-angiography," *Optics Express*, vol. 16, no. 15, pp. 11438–11452, 2008.

[15] R. S. Weinhaus, J. M. Burke, F. C. Delori, and D. M. Snodderly, "Comparison of fluorescein angiography with microvascular anatomy of Macaque retinas," *Experimental Eye Research*, vol. 61, no. 1, pp. 1–16, 1995.

[16] D. M. Snodderly, R. S. Weinbaus, and J. C. Choi, "Neural-vascular relationships in central retina of macaque monkeys (*Macaca fascicularis*)," *Journal of Neuroscience*, vol. 12, no. 4, pp. 1169–1193, 1992.

[17] A. Imai, Y. Toriyama, Y. Iesato, T. Hirano, and T. Murata, "En face swept-source optical coherence tomography detecting thinning of inner retinal layers as an indicator of capillary nonperfusion," *European Journal of Ophthalmology*, vol. 25, no. 2, pp. 153–158, 2015.

Hindawi Publishing Corporation
Journal of Ophthalmology
Volume 2015, Article ID 186946, 14 pages
http://dx.doi.org/10.1155/2015/186946

Research Article

Apelin Protects Primary Rat Retinal Pericytes from Chemical Hypoxia-Induced Apoptosis

Li Chen,[1,2] Yong Tao,[1,2] Jing Feng,[1,2] and Yan Rong Jiang[1,2]

[1] *Department of Ophthalmology, People's Hospital, Peking University, 11 Xizhimen South Street, Xicheng District, Beijing 100044, China*
[2] *Key Laboratory of Vision Loss and Restoration, Beijing Key Laboratory of Diagnosis and Therapy of Retinal and Choroid Diseases, Ministry of Education, 11 Xizhimen South Street, Xicheng District, Beijing 100044, China*

Correspondence should be addressed to Yan Rong Jiang; drjyr@gmail.com

Received 27 November 2014; Revised 24 January 2015; Accepted 10 February 2015

Academic Editor: Juliana L. Dreyfuss

Pericytes are a population of cells that participate in normal vessel architecture and regulate permeability. Apelin, as the endogenous ligand of G protein-coupled receptor APJ, participates in a number of physiological and pathological processes. To date, the effect of apelin on pericyte is not clear. Our study aimed to investigate the potential protection mechanisms of apelin, with regard to primary rat retinal pericytes under hypoxia. Immunofluorescence staining revealed that pericytes colocalized with APJ in the fibrovascular membranes dissected from proliferative diabetic retinopathy patients. In the *in vitro* studies, we first demonstrated that the expression of apelin/APJ was upregulated in pericytes under hypoxia, and apelin increased pericytes proliferation and migration. Moreover, knockdown of apelin in pericyte was achieved via lentivirus-mediated RNA interference. After the inhibition of apelin, pericytes proliferation was inhibited significantly in hypoxia culture condition. Furthermore, exogenous recombinant apelin effectively prevented hypoxia-induced apoptosis through downregulating active-caspase 3 expression and increasing the ratio of B cell lymphoma-2 (Bcl-2)/Bcl-2 associated X protein (Bax) in pericytes. These results suggest that apelin suppressed hypoxia-induced pericytes injury, which indicated that apelin could be a potential therapeutic target for retinal angiogenic diseases.

1. Introduction

Pericytes are a population of contractile cells that surround the endothelial cells of microvessel [1]. Genetic studies have shown that pericytes exert multiple effects on the vasculature: they participate in vascular development, maturation, and remodeling, and they also contribute to normal architecture and regulate permeability [1–3]. Retina, a light sensitive layer lining at the back of the eye, has the highest pericyte density around the body [4]. Recently, pericytes have received considerable attention as an active player in the pathological mechanisms of retinal angiogenic diseases, such as diabetic retinopathy (DR) and retinopathy of prematurity (ROP) [5, 6]. DR is one of the most common and important chronic microvascular complications in individuals with diabetes mellitus, which will give rise to blindness in uncontrolled conditions. Numerous studies have shown that the primary morphological change in the diabetic retina is the dysfunction and loss of pericytes [7]. The absence of pericytes destabilizes retinal vessels, making them more susceptible to hypoxia-induced sprouting [7, 8]. Others showed that pericytes are also involved in pathological retinal angiogenesis in a murine model of ROP [9]. Therefore, pericytes are currently under consideration as therapeutic targets for the treatment of retinal angiogenic diseases.

Apelin, a natural ligand for an orphan G protein-coupled receptor APJ, is widely expressed in various tissues, including brain, heart, lung, kidney, uterus, and ovary [10, 11], and is reported to be involved in the regulation of multiple physiological functions [12]. The studies of apelin-deficient mice and Xenopus laevis embryos indicate that apelin is involved in the regulation of vasculogenesis and angiogenesis [13, 14]. Hara et al. showed that the size of choroidal neovascular membrane lesions was decreased in apelin gene knockout mice [15], and *in vitro* studies have shown that apelin induced proliferation and migration of vascular smooth muscle cells (VSMCs) and suppresses VSMCs apoptosis induced by serum deprivation via APJ/PI3-K/Akt signaling pathways [16, 17]. In endothelial

cells apelin also significantly enhanced migration, proliferation, and capillary-like tube formation [18]. Besides, our previous studies showed that apelin significantly enhanced the viability, migration, and proliferation of Müller cells and retinal pigment epithelium (RPE) cells through the pathway of MAPK/Erk and PI3-K/Akt [19–21].

Hypoxia has been widely used as a typical apoptosis insult to a variety of cell types [22]. Hypoxia has been shown to induce rat pancreatic β-cell apoptosis through Bcl-2/Bax pathway [23]. Previous studies demonstrated that apelin suppressed apoptosis in osteoblastic cell, human osteoblasts, and bone marrow mesenchymal cells through regulation of Bcl-2/Bax via PI3-K pathway [24–26]. Moreover, apelin reduced cytochrome c release from mitochondria to cytoplasm and activation of caspase 3. These results explained apelin protected cells via various mechanisms.

However, whether apelin has protective effects on rat primary pericytes has not been explored. We propose a putative role for apelin in the viability and apoptosis of pericytes and conducted this study to investigate whether apelin could exert protective effects on primary rat retinal pericytes under hypoxia.

2. Materials and Methods

2.1. Reagents. Exogenous recombinant apelin-13 peptide was purchased from Sigma (St. Louis, MO). The makers of pericytes were PDGFR-B (ab69506, Abcam, US), NG2 (SC-20162, Santa Cruz, CA), and Desmin (ab6322, Abcam, US). Anti-apelin and anti-APJ were purchased from Abcam company (ab59469, ab125213, and ab84296, Abcam, US), respectively. CellTiter 96 AQueous One Solution was used in cell Proliferation Assay (Promega, US). Lentiviral vector knockout of apelin was constructed and purchased from GeneChem Co., Ltd. (Shanghai, China). Bcl-2 and Bax antibody were obtained from Cell Signaling Technology (#2870; #2772, CST, US).

2.2. Primary Rat Pericyte Cells Isolation, Culture, and Treatment. All experiments were performed in accordance with the Research Ethics Committees of the People's Hospital, Peking University, China. We isolated primary rat retinal pericyte cells from the retinal microvessel of Sprague-Dawley (SD) rats, using a modified method of previously published articles [27–29]. Briefly, eyes from SD rats (4–6 weeks, 150–200 g) were incubated with cold Dulbecco's phosphate-buffered saline (PBS) containing penicillin-streptomycin antibiotic (500 U/mL) for 10 min. The retinas were removed and cut into 1 × 1 mm small pieces and then incubated with collagenase I (Roche Applied Science, Mannheim, Germany) for 30–45 min at 37°C. The digested retina were filtered through 70 μm and 40 μm nylon mesh (Falcon, BD, US) and then centrifuged. Rat retinal pericytes were purified with Dynabeads Pan Mouse IgG (Invitrogen Dynal AS, Norway) according to the instructions. Before use, we washed the Dynabeads (25 μL) in Dulbecco's Modified Eagle's Media (DMEM) (Hyclone, US), and we added 1 μL mouse anti-desmin monoclonal antibody (ab6322, abcam, US) and then incubated them overnight at 4°C. The cell pellets were suspended in DMEM containing 10% fetal bovine serum (Gibco, US) and incubated with Dynabeads conjugated mouse anti-desmin monoclonal antibody for 30 min at 37°C, with gentle rotation. After washing, the bead-bound pericytes in pericyte medium (Sciencell Inc., US) were suspended at 37°C in a humidified atmosphere of a 5% CO_2 incubator. Pericytes between passages three and five were used throughout the study.

In chemical hypoxia-induced pericytes injury models, 150 μmol $CoCl_2$ was used according to the previous report [21]. In the viability assay, we treated pericytes with different concentrations of apelin (10, 100, and 1000 ng/mL) and knockdown of apelin was performed via lentivirus vector. We incubated control group cells in pericyte medium.

2.3. Immunofluorescent Staining. Immunofluorescent staining of membranes tissue was described in our previous published study [20, 30]. Briefly, 12 fibrovascular membranes with proliferative diabetic retinopathy were surgically obtained during vitrectomy. In a similar manner, 10 macular preretinal membranes were obtained and served as control. Immunofluorescence staining was performed on the frozen sections of the fibrovascular membranes and of the control membranes by staining with rabbit anti-apelin (ab59469, 1 : 100, Abcam, US) or rabbit anti-APJ (ab84296, 1 : 200, Abcam, US). The human patients study protocol was approved by the Ethical Committee and Institutional Review Board of Peking University People's Hospital (Beijing, China) and was conducted in accordance with the Declaration of Helsinki. Written informed consent was obtained from each study subject.

Pericytes which were cultured on cover slides (Fisher, US) were fixed with 4% paraformaldehyde and incubated in 0.3% H_2O_2 and 0.1% triton X-100 to quench endogenous peroxidase activity and penetrate the cytomembrane. Then, the cells were incubated in 3% blocking goat serum for 1 h and then incubated with anti-PDGFR-β (ab69506, 1 : 100, Abcam, US), NG2 (SC-20162, 1 : 100, Santa Cruz, CA), desmin (ab6322, 1 : 200, Abcam, US), apelin (1 : 100, Abcam, US), and APJ (1 : 200, Abcam, US) overnight at 4°C. The following day, pericytes were incubated with the relevant fluorescence-conjugated secondary antibody (1 : 200, Invitrogen, US) for 2 h at room temperature. Images were obtained with Nikon 50i fluorescent microscope (Nikon, Tokyo, Japan) under 200x magnifications.

2.4. Lentivirus-Mediated shRNA Knockdown of Apelin Expression and Transfection. The knockdown of Apelin (Rattus, NM_031612.2, GI:52345441) was induced by a lentivirus-mediated RNA interference vector (GeneChem Co., Ltd., Shanghai, China). The small interfering RNA (siRNA) target sequences were selected: #1, 5′-GAGGAGAGATAGAAACAGA-3′; #2, 5′-GGAGGATGTTGGCTGAGAA-3′; #3, 5′-GTTTGCCTTTCTTGACAAA-3′; and #4, 5′-CAGATGAGTTCTCTTCTCT-3′. The lentivirus-GFP (LV-GFP) which included the GFP gene and did not include the apelin interference sequence served as negative control. For lentivirus transduction, pericytes were cultured at 5×10^4 cells/well into 6-well culture plates. After being grown to 70% confluence, cells were transduced with shRNA lentivirus at

a multiplicity of infection (MOI) of 100. Cells were harvested at 24 hours after infection, and transfection efficiency was evaluated by immunofluorescence staining. The knockdown efficiency of apelin was evaluated by RT-PCR and western blot analysis.

2.5. Cell Viability/Cell Proliferation. Pericyte viability was measured by MTS assay, according to the manufacturer's instructions (CellTiter 96 AQueous One Solution Assay; Promega, Madison, WI, US). 5000 cells/well were seeded into a 96-well plate and incubated with different concentrations of apelin (1, 100, and 1000 ng/mL) for 24 h. At the end of the incubation, 10 μL MTS solution was added into each well and incubated for 1 h. The absorbance wavelength was evaluated with microculture plate reader (Model 550; Bio-Rad, Tokyo, Japan) at 490 nm (OD_{490}). Each experiment was performed in five wells and repeated at least three times.

2.6. Edu Assay. Pericytes proliferation was assessed using a Cell-Light EdU Apollo 643 *in vitro* Imaging Kit (RuiBo. Inc., Guangzhou, China). Briefly, 1×10^4 cells/well, which was pretreated with apelin, was plated in 96-well plates for 24 h. Following the incubation interval, 10 μmol 5-ethynyl-2′-deoxyuridine (Edu) medium was added to each well and incubated for 2 h. After washing twice with PBS, pericytes were fixed with 4% paraformaldehyde for 30 min and washed with 2 mg/mL glycine solution for 5 min in order to neutralize paraformaldehyde and assure a good staining system. The cells were incubated in 100 μL 1x Apollo staining solution for 30 min and the nuclei were dyed with Hoechst 33342. The images were obtained under 10x magnification, using a Nikon 50i fluorescent microscope. Each experiment was performed in five wells and repeated at least three times.

2.7. Cell Migration/Transwell Assay. Transwell assay was used for evaluating cell migration assays. Briefly, 100 μL of pericyte suspension (1×10^5 cells/mL) was added to the upper chamber and 600 μL medium containing apelin, hypoxia medium, or DMEM (control) to the lower chamber, respectively. The chambers were incubated for 6 h at 37°C. The filters were fixed with 4% paraformaldehyde for 15 min and we subjected the nuclei to DAPI staining for 10 min. The remaining cells on the upper surface of the filter were removed by wiping with a cotton swab. The number of migrated cells were quantified by counting in five random fields (10x magnification), using a Nikon 50i fluorescence microscope. The data are shown as the mean ± standard deviation (SD). Each experiment was repeated at least three times.

2.8. TUNEL Assay. Pericyte apoptosis after hypoxia was evaluated by terminal deoxynucleotidyl transferase-mediated dUTP nick end-labeling (TUNEL) assay. TUNEL staining was performed on cell coverslips using a commercial kit (In Situ Cell Death Detection Kit; Roche Applied Science, USA), according to the manufacturer's recommended instructions. TUNEL-positive cell nuclei were visualized as green fluorescence and images performed under 10x magnification. Finally, the percentage of TUNEL-positive cells was calculated in five microscopic fields of each slide.

2.9. Quantitative Real-Time PCR. Total RNA was isolated from cultured pericytes using Trizol reagent (Invitrogen, CA, US), and we determined the concentration and integrity of total RNA with UV spectrophotometry (NANODROP 2000C, Thermo, US). We used the Fermentas reverse transcription system (Fermentas, St. Leon-Rot, Germany) to reverse RNA (1 μg) into first strand cDNA, using a real-time PCR system (PikoReal 96 PCR system, Thermo Scientific). The PCR solution system contained 1 μL of cDNA (1 : 20 diluted), specific primers 1 μL (10 pmol), 3 μL DEPC-water, and 5 μL of SYBR Select Master Mix (Invitrogen), with a final volume of 10 μL. Each sample was measured in triplicate wells. Primers used were as follows: β-actin Forward: 5′-TGGCTCTATCCTGGCCTCACT-3′, β-actin Reverse: 5′-GCTCAGTAACAGTCCGCCTAGAA-3′; rat apelin Forward: 5′-GATGGAGAAAGGCGAAGAAAG-3′, rat apelin Reverse: 5′-GGTGAGAGATGAGACCACTTGT-3′. The standard PCR conditions included 2 min at 50°C and 10 min at 95°C, followed by 35 cycles of extension at 95°C for 15 s, 60°C for 30 s, and 72°C for 30 s. The mRNA expression was normalized to the expression level of ACTB. We calculated the changes in mRNA expression according to the $2^{-\Delta\Delta}$CT method, with $\Delta CT = C_{\text{Target gene}} - CT_{ACTB}$ and $\Delta\Delta CT = \Delta C_{\text{Treatment}} - \Delta CT_{\text{Control}}$. Each experiment was repeated at least three times.

2.10. Western Blot Analysis. Pericytes were harvested and lysed in RIPA buffer (1% Nonidet P-40, 0.5% sodium deoxycholate, 0.1% SDS in PBS) and centrifuged at 15,000 rpm for 15 min at 4°C. The membranes were blocked with 5% nonfat milk for 1 h and then incubated overnight at 4°C with primary antibody: rabbit anti-Bcl-2, (#2870; 1 : 1000, CST); rabbit anti-Bax, (#2772; 1 : 1000; CST); rabbit anti-Apelin (ab125213; 1 : 500; abcam); and rabbit anti-APJ (ab84296; 1 : 1000, abcam). The membranes were incubated with goat anti-rabbit horse-radish peroxidase- (HRP-) conjugated secondary antibody (1 : 3000, DAKO, Japan) for 1 h at room temperature. The density of each band was analyzed with Image J software. Each experiment was repeated at least three times.

2.11. Statistical Analysis. The results were expressed as mean ± SD. Difference between two groups was compared with an independent sample t-test (SPSS17.0 software, Chicago, IL). Two-tailed $P < 0.05$ was considered to indicate statistical significance. Differences among groups were assessed using one-way analysis of variance (ANOVA), followed by Dunnett's test. A value of $P < 0.05$ was considered as significantly different. We repeated all experiments at least three times, and representative experiments are shown.

3. Results

3.1. Immunohistochemical Expression of APJ in Fibrovascular Membranes. Expression of APJ was detected in the specimens of all fibrovascular membranes of the proliferative diabetic retinopathy (PDR) group with strong staining for APJ (Figure 1). Colocalization of pericyte markers desmin and APJ were observed in all specimens of the PDR group

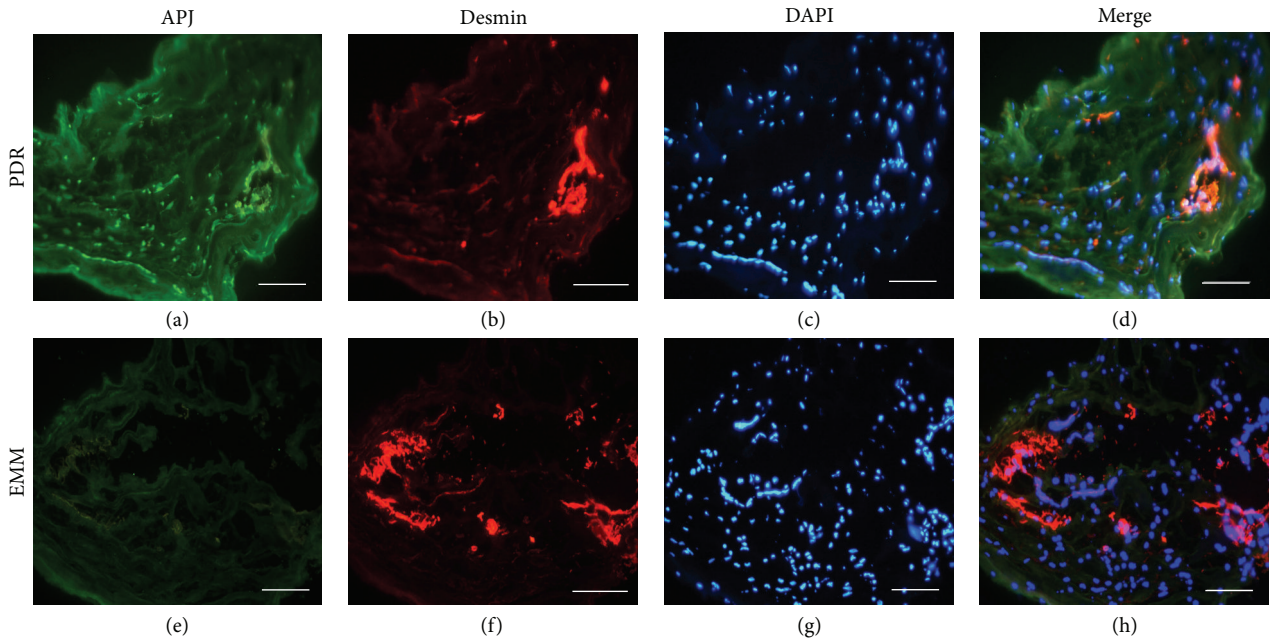

Figure 1: Immunostaining of APJ and pericyte in fibrovascular membranes. (a–d) Immunostaining for APJ (a), pericyte marker desmin (b), and DAPI (c) in fibrovascular membranes from eyes with proliferative diabetic retinopathy. Staining intensities of APJ were strong and were colocalized with pericyte, as identified by desmin. (e–h) Staining of APJ (e), desmin (f), and DAPI (g) in epiretinal macular membranes (EMM) of control patients without diabetic retinopathy. None of APJ (e) and staining of desmin (f) were observed. Scale bar = 100 μm.

($n = 12$) (Figures 1(a)–1(d)). None of the membranes removed from the eyes of the epithelial macular membrane (EMM) group showed specific staining of APJ ($n = 10$) (Figures 1(e)–1(h)). Our previous study also demonstrated that vitreous concentrations of apelin were significantly higher in the PDR group than in the EMM group [30].

3.2. Cultivation and Identification of Primary Rat Retinal Pericytes. Primary rat retinal pericytes were isolated by Magnetic Dynabeads and formed cell clusters floating in cell medium (Figure 2(A)). At day 7, the primary pericytes got adherence, and the colony formed and grew (Figure 2(B)). Generally, primary pericytes confluenced at about day 14. When pericytes were passaged, the growth and adherence became rapid obviously, which got adherence about 4–6 hours and passaged about 4-5 days. Primary rat retinal pericytes showed irregular triangular cell bodies, with thick filaments in the cytoplasm and a plump nucleus (Figure 2(C)). As specific markers for pericyte, desmin, PDGFR-β, and NG2 were used to confirm the purity of cultured primary rat pericyte cells, which was approximately 95% (Figure 3(b)).

3.3. Expression of Apelin and APJ Receptor in Pericytes. Prior to exploring the effects of apelin in rat retinal pericytes, we carried out immunofluorescence staining to detect the expression of apelin/APJ in pericytes. We observed low apelin immunoreactivity in normal pericyte culture, which showed weak and diffuse expression in the cytoplasm (Figure 3(a)-(A), (B)). In similar way, the APJ staining was moderate, which was expressed in cytoplasm membrane (Figure 3(b)-(A), (B)). However, after exposure under hypoxia for 12 h, the expression of apelin represented obvious stronger cytoplasm staining (Figure 3(a)-(C), (D)), accompanied by expanding stronger APJ immunoreactivities in cytoplasm and cytoplasm membrane (Figure 3(b)-(C), (D)). In addition, the results of western blot about apelin and APJ under hypoxia support the change of immunofluorescence staining (Figures 3(c) and 3(d)). The expression of apelin and APJ under hypoxia was upregulated 2.5-fold and 1.9-fold, respectively ($P < 0.05$).

3.4. Detection of Interference Efficacy of Lentivirus-Apelin. Quantitative Real-Time PCR in NRK-52E and IEC6 cells demonstrated that LV-Apelin (#4) was the most efficient shRNA, in which the RNA level of apelin was decreased by more than 70% (data was not shown). Then, we tested the knockdown efficiencies of LV-Apelin in pericytes. When MOI is 100, the result of immunofluorescence staining showed that interference efficacy achieved 90% (Figure 4(a)). After that, the qRT-PCR in pericyte revealed the apelin level was decreased by 75% in LV-apelin group compared to LV-GFP control group ($P < 0.01$) (Figure 4(b)). In a similar way, western blot demonstrated that the apelin level was downregulated by 64% ($P < 0.05$) (Figures 4(c) and 4(d)).

3.5. Apelin-Stimulated Cell Proliferation and Migration in Normoxia. Experiments were performed to evaluate whether apelin had any effect on pericytes proliferation and migration in normoxia. Pericytes were incubated with apelin at different concentrations (1, 10, 100, and 1000 ng/mL) for 24 h. Among the various concentrations, MTS assay results show that 100 ng/mL group significantly increased pericytes viability, compared with the control groups (Figure 5(B)) (100 ng/mL

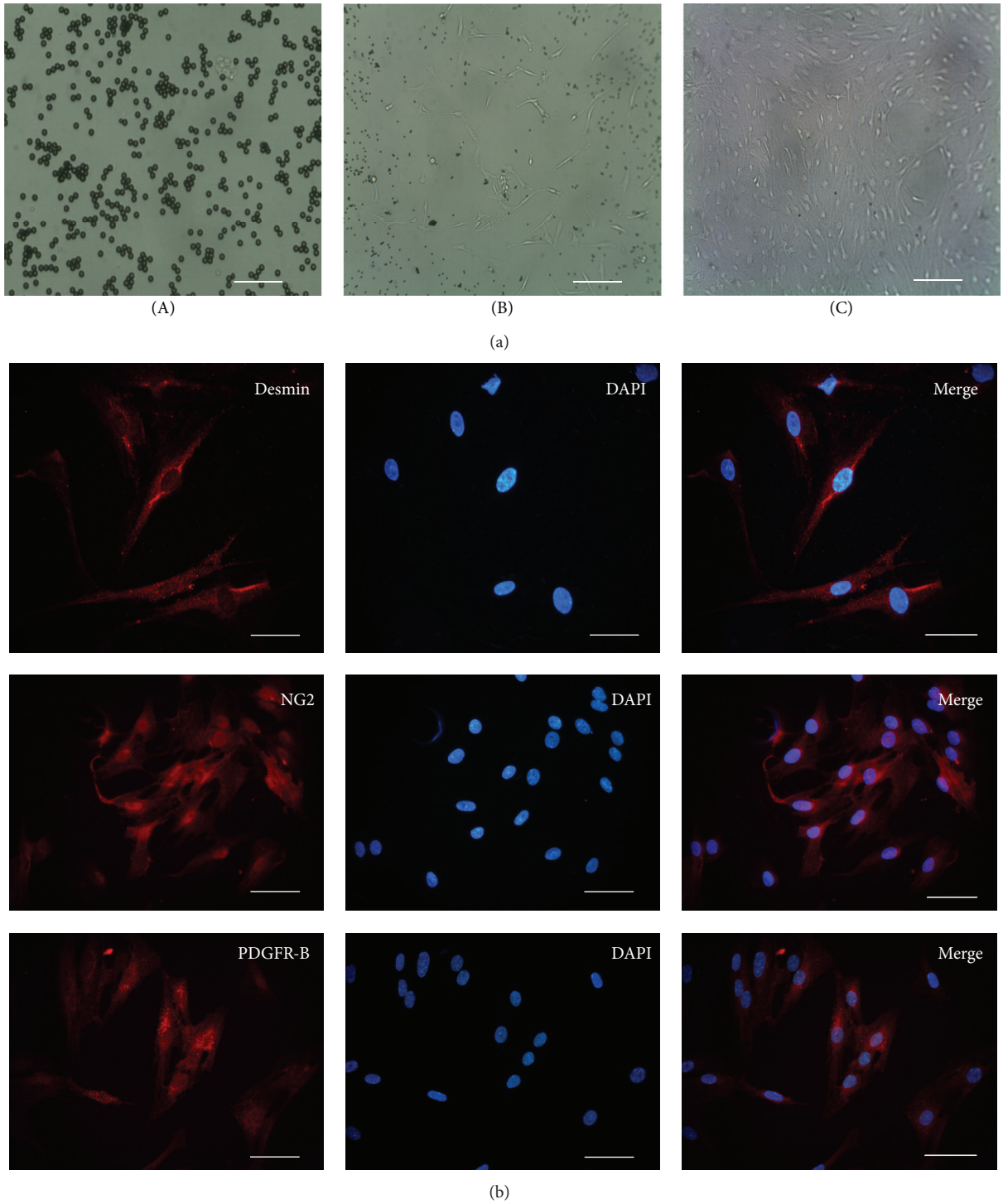

Figure 2: Morphology and immunofluorescent staining were identified in primary rat retinal pericytes. (a) Microscopic image of retinal pericytes, showing cell mass isolated by Dynabeads (A), at 7 days, pericytes got adherence and formed cells cluster (B), at passage 1 non-contact-inhibited growth of pericyte and irregular triangular cell bodies, with thick filaments in the cytoplasm and a plump nucleus (C). Scale bar = 200 μm. (b) Immunofluorescence staining with anti-desmin, NG2, and PDGFR-B antibody for primary rat retinal pericytes, respectively. Scale bar = 100 μm.

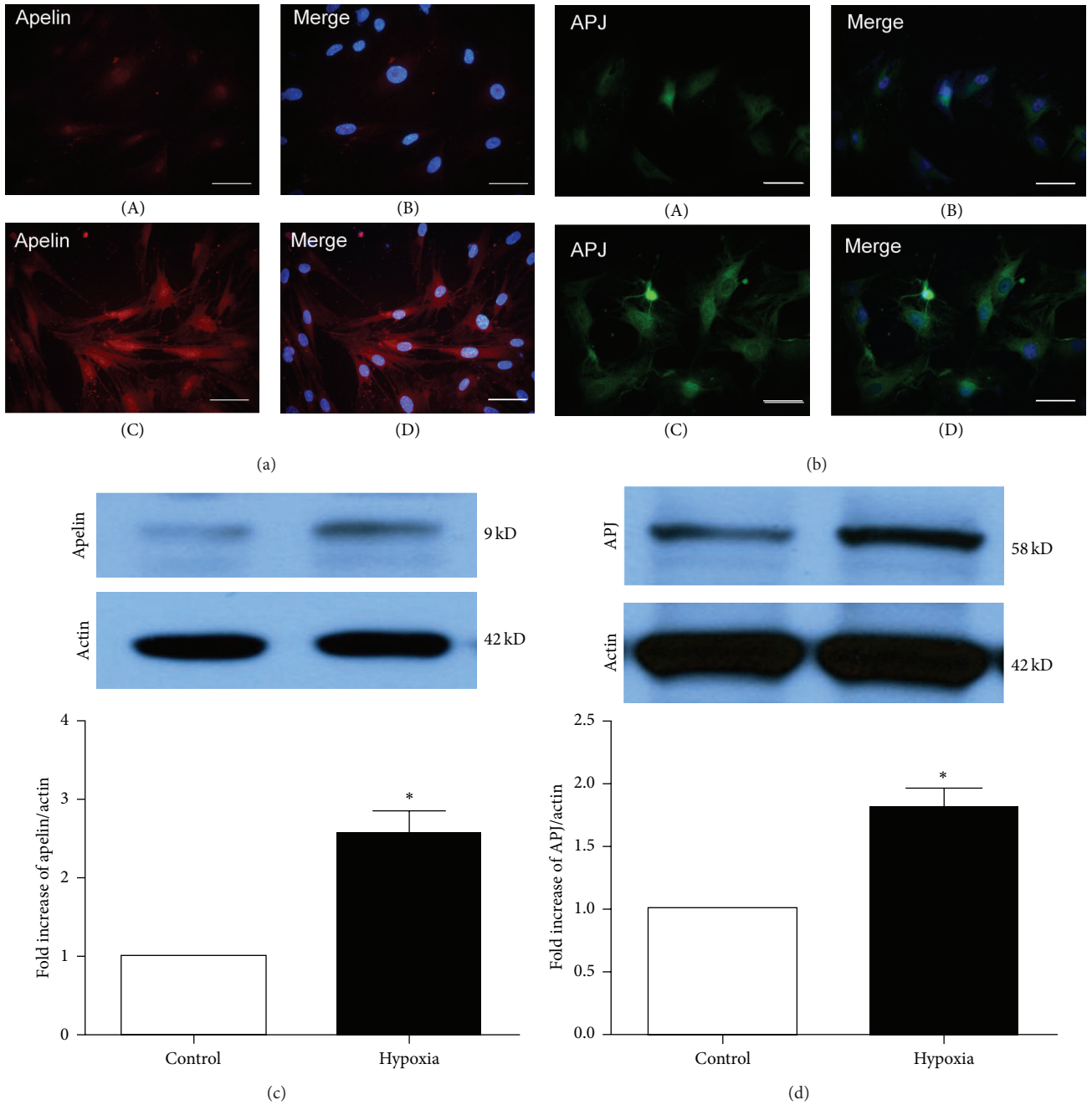

FIGURE 3: The cellular localization of apelin/APJ. (a) Apelin immunoreactivity was found weak and diffused in the cytoplasm of normal (A) but showed more intense cytoplasmic staining in hypoxic pericyte (C). Scale bar = 100 μm. Similarly, (b) compared with restricted cytomembrane expression in normal (A) and hypoxia (C) pericyte, APJ localization expanded and brightened in the cytoplasm and cytoplasm membrane (apelin in red, APJ in green, and DAPI in blue). Scale bar = 100 μm. (c) and (d) Western blot analysis shows that the expression of apelin and APJ under hypoxia was upregulated 2.5-fold and 1.9-fold, respectively ($P < 0.05$).

versus control, $^{**}P < 0.01$; 1000 ng/mL versus control, $^{*}P < 0.05$).

Edu experiment was used to detect pericyte proliferation at different concentrations of apelin (10 ng/mL and 100 ng/mL). The number of proliferative cells was significantly higher in the apelin-treated group, compared with the control group (Figure 5(A)).

In the cell migration assay, cells were measured in a modified Boyden Chamber in which pericytes migrated through a porous membrane. The mean number of migrated pericytes incubated with apelin (1–100 ng/mL) was significantly higher than the mean number of the control group ($P < 0.05$) (Figures 5(C) and 5(D)).

3.6. The Effects of Apelin and Lentivirus Knockdown Apelin for Cell Proliferation and Migration in Hypoxia. Furthermore, we carried out experiment to study the effect of apelin for pericyte under hypoxia. We found that the viability of

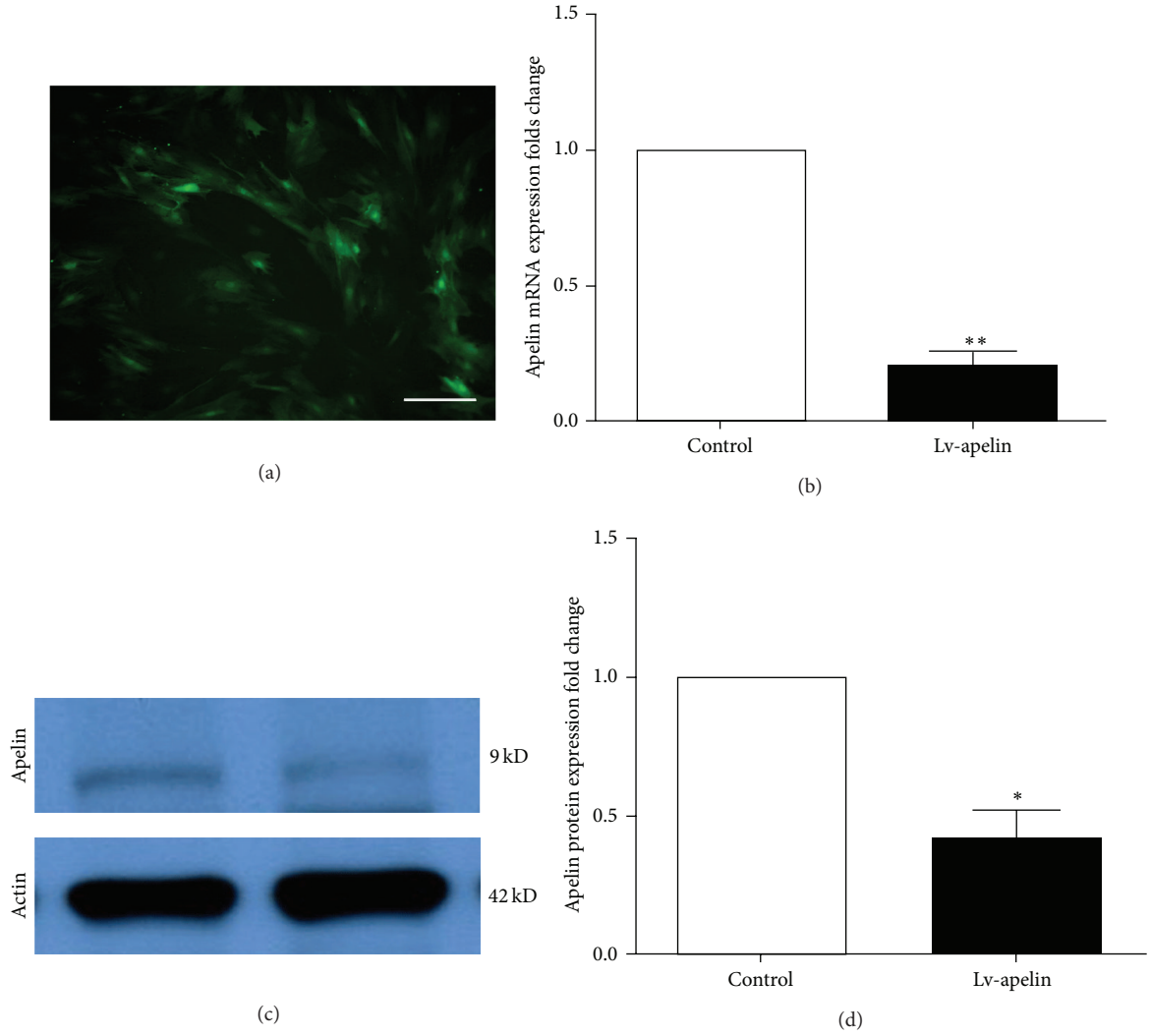

Figure 4: Pericytes transducted with Lentivirus-Apelin. (a) Immunofluorescence staining of LV-apelin infection in pericyte. Interference efficacy arrived about 90%, MOI = 100. Scale bar = 100 μm. (b) The mRNA expression of LV-Apelin was decreased by 75% after blocking by siRNA sequence ($P < 0.01$). (c and d). The western blot analysis shows that protein of expression of LV-Apelin decreased by 64% ($P < 0.05$).

pericytes incubated with $CoCl_2$ was decreased obviously time dependently. The viability of pericytes was reduced by 27% at 6 h and by 40% at 12 h after stimulation by 150 μmol/L $CoCl_2$, respectively. However, the viability of pericytes stimulated by apelin was significantly enhanced, compared with the $CoCl_2$ group (8 h versus control $^{*}P < 0.05$; 12 h versus control $^{**}P < 0.01$) (Figure 6(A)).

Our study showed that under hypoxia the viability of cells treated with apelin was significantly increased. Meanwhile, the viability of cells in the LV-apelin knockout group was significantly reduced ($CoCl_2$ versus apelin, $P < 0.05$; LV-GFP versus LV-apelin, $P < 0.05$; $CoCl_2$ versus LV-apelin, $P < 0.01$), which suggests that apelin can stimulate pericyte viability (Figure 6(B)). We also detected migration of pericytes under hypoxia. Compared with the control group, the mean number of migrated pericytes under hypoxia and combination with LV-apelin knockdown decreased significantly. However, in the group treated with apelin, the mean number of migrated pericytes was increased under hypoxia (Figures 6(C) and 6(D)).

3.7. Apelin Protected Pericytes against Apoptosis Induced by Hypoxia via Bcl-2/Bax Restoration and Caspase 3 Pathway. In the cell viability experiment, hypoxia resulted in a 27% decrease in pericyte viability. However, cell viability increased significantly in pericytes pretreated with 100 ng/mL of apelin for 12 h. To further evaluate the effects of apelin on cell death, we used TUNEL staining to detect DNA fragmentation and cell death in hypoxia-treated pericytes with and without apelin treatment. We pretreated pericytes with apelin for 12 h and then exposed these pericytes to hypoxia for 12 h. In the percentage of apoptotic cells showing green, approximately 30% of cell death was blocked by the apelin treatment (Figure 7).

Active-caspase 3 protein is one of the key executioners of apoptosis. As shown in Figure 8, active-caspase 3 protein

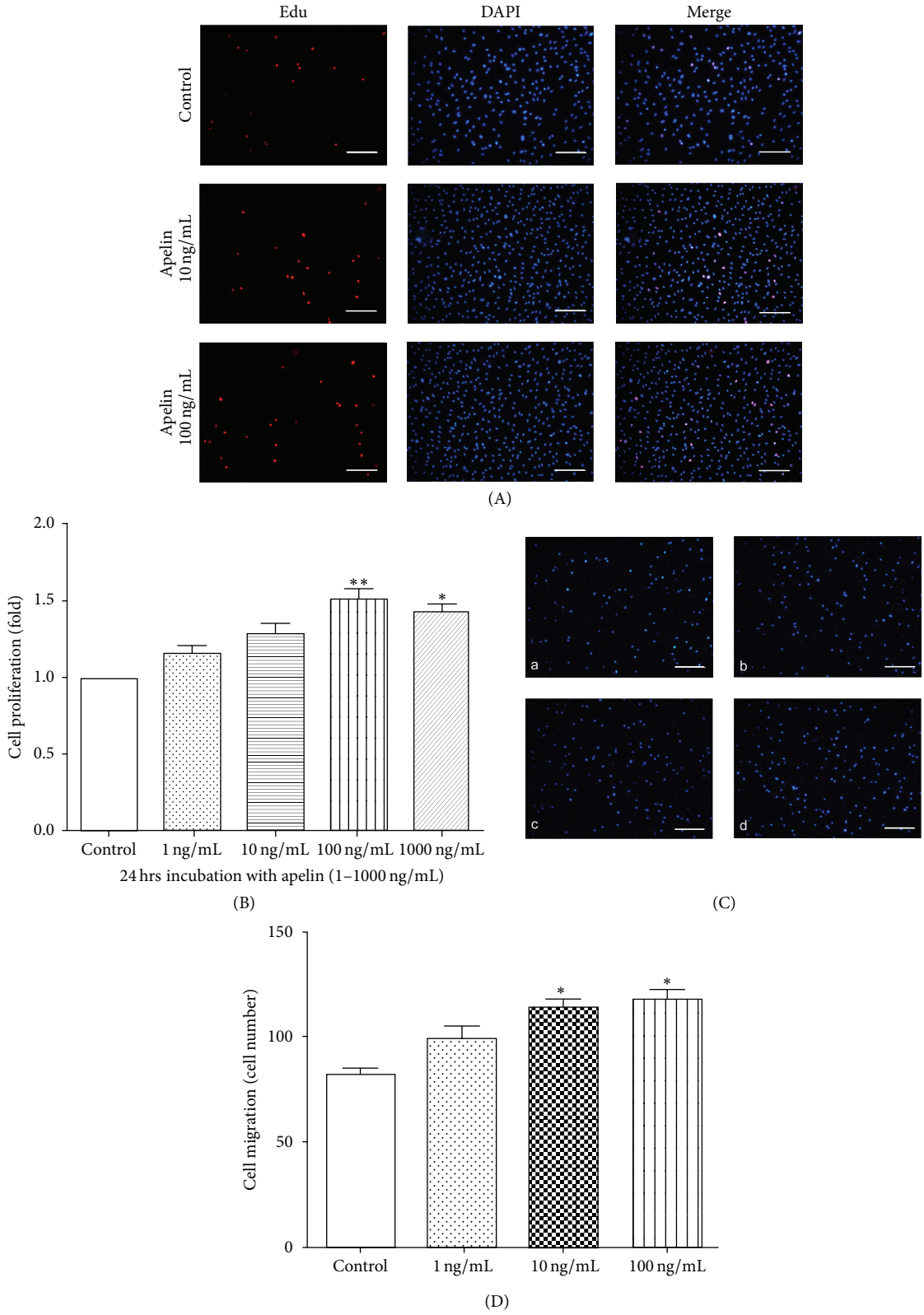

FIGURE 5: Effect of apelin on cell viability and migration under normoxia. (A) The Edu proliferation assay. Apollo staining (red) represents proliferating cells, and DAPI (blue) staining nuclei. Compared with the control group, the number of proliferating cells treated with apelin (10 or 100 ng/mL) increased significantly. Scale bar = 200 μm. (B) The folds of apelin-treated cell viability compared with the control group ($^{*}P < 0.05$, $^{**}P < 0.01$ versus untreated control); (C) and (D) pericyte migration in response to apelin treatment was measured using the transwell assay (a: control; b: 1 ng/mL; c: 10 ng/mL; d: 100 ng/mL, $^{*}P < 0.05$ versus untreated control). The data are expressed as means ± standard deviation (SD). Scale bar = 200 μm.

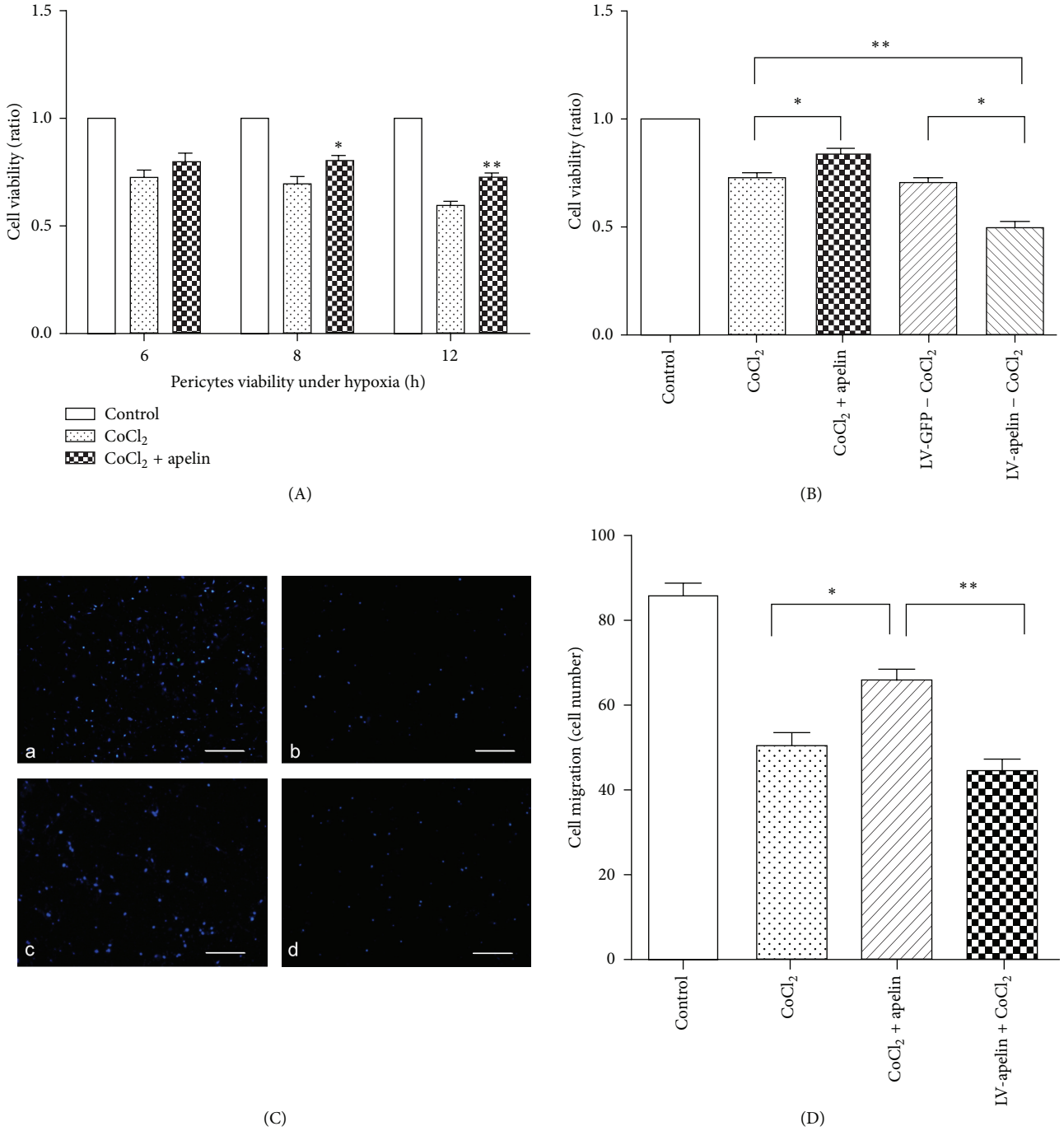

Figure 6: Effect of apelin on cell viability and migration under hypoxia. Cell viability was evaluated by MTS assay and migration was assessed with a transwell cell chamber. (A) In hypoxic pericytes, the viability of cells stimulated by apelin was significantly enhanced during 12 h (8 h versus $CoCl_2$ $^*P < 0.05$; 12 h versus $CoCl_2$ $^{**}P < 0.01$). (B) Viability of pericytes treated with apelin and LV-apelin knockout under hypoxia. Compared with the $CoCl_2$ group, viability was significantly increased in the apelin group ($P < 0.05$). Moreover, cell viability was significantly reduced in the LV-apelin knockout group (LV-GFP versus LV-apelin, $P < 0.05$; $CoCl_2$ versus LV-apelin, $P < 0.05$). (C) and (D) Pericyte migration induced by apelin under hypoxia (a: control; b: $CoCl_2$ 150 μmol; and c: $CoCl_2$ 150 μmol + apelin 100 ng/mL). The number of migrated cells per HPF is shown. Apelin versus $CoCl_2$ $^*P < 0.05$. Scale bar = 200 μm.

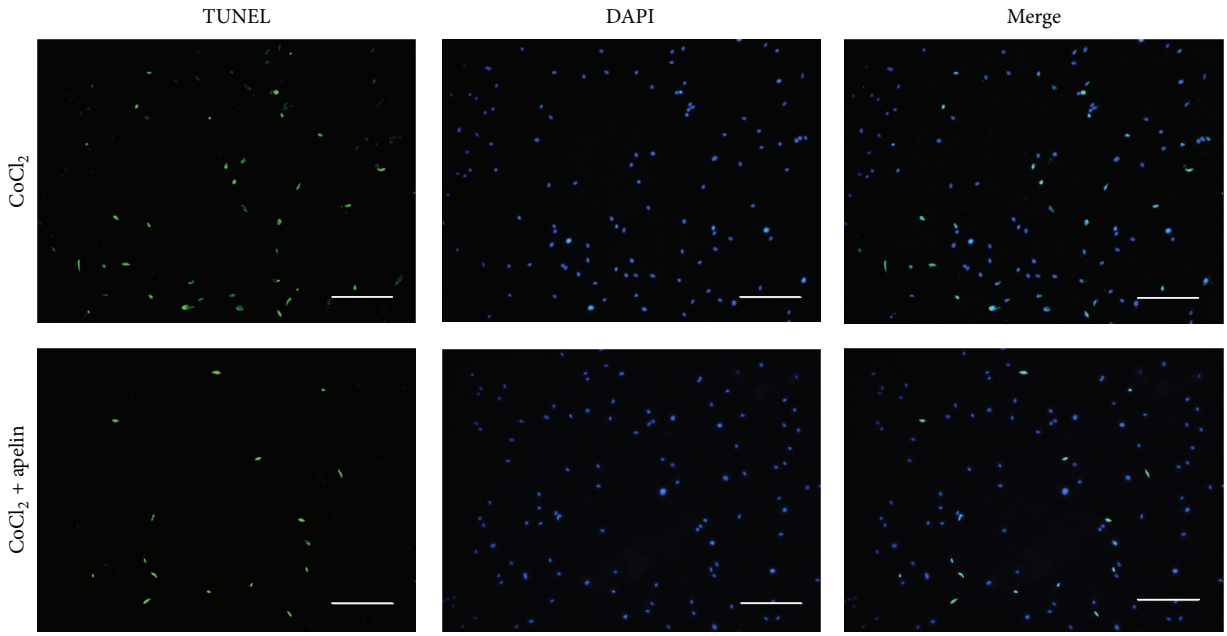

Figure 7: TUNEL staining was used to evaluate hypoxia-induced cell death. Cells were exposed to 100 ng/mL apelin for 12 h and then exposed to hypoxia for 12 h. Apoptotic nuclei were visualized by TdT-mediated dUTP nick end-labeling (TUNEL). Scale bar = 200 μm.

level significantly increased 12 h after hypoxia injury ($P < 0.001$, compared with the control group). Administration of apelin significantly decreased its levels after hypoxia injury ($P < 0.01$, compared with hypoxia group). The expression of active-caspase 3 in hypoxia combination with LV-Apelin knockdown was similar to hypoxia group and its levels significantly increased ($P < 0.01$, compared with control group) (Figures 8(a) and 8(b)).

Likewise, we also detect bcl-2 and Bax expression in pericyte. Western blot analysis showed that apelin dose-dependently induced Bcl-2 protein expression and down-regulated Bax protein expression in pericytes (Figures 8(c) and 8(d)). The antiapoptotic effect of apelin was through increased expression of Bcl-2 and reduced expression of Bax. In hypoxia group, the ratio of Bcl-2/Bax decreased 36% and LV-apelin group has a similar ratio ($P < 0.001$, compared with con. group). However, the ratio of Bcl-2/Bax in treatment with apelin group was significantly increased ($P < 0.001$, compared with hypoxia group) (Figures 8(e) and 8(f)).

4. Discussion

Apelin interacts with its specific receptor APJ, has multiple biological activities, and had been characterized in various tissues [31]. Previously, we proved that vitreous concentrations of apelin were significantly higher in the proliferative diabetic retinopathy (PDR) group. Likewise, apelin and APJ also colocalized with endothelial cells maker CD 31 in PDR [30]. In the present study, we further demonstrated that APJ was strong expressed in fibrovascular membranes of the PDR and was colocalized with pericytes. Therefore, apelin/APJ system was possibly involved in the pathological progression of PDR. However, the effect of apelin on apoptosis of primary retinal pericytes remains unknown. In order to study the effects of apelin in pericyte, primary rat pericytes were used here. Based on the current results, we proved the expression of apelin and APJ in pericytes and demonstrated that apelin and APJ are upregulated in hypoxia cultured condition. Knockdown of apelin inhibits proliferation and migration of pericytes. Moreover, exogenous recombinant apelin effectively prevented hypoxia-induced apoptosis through down-regulating the expression of active-caspase 3 and increased the ratio of Bcl-2/Bax in pericyte. These results establish the foundation for further study of diseases associated with ischemia and hypoxia.

As we all know, rodent is similar to human in genetic background. In previous published studies, primary cultured pericytes were mostly originated from bovine retina, which restricted further *in vivo* studies [32]. In the present study, we established a rodent- (rat-) based primary pericyte *in vitro* model. By using a magnetic beads isolation method, we obtained primary rat retinal pericytes successfully in the purity of 90%. As for marker of pericytes, alpha smooth muscle actin (α-SMA), tropomyosin desmin, nestin, sulfatide or nerve/glial antigen-2 (NG2) proteoglycan, platelet-derived growth factor receptor-B (PDGFR-B), aminopeptidase N (CD13), and the regulator of G-signaling 5 (RG5) are common pericyte markers [4, 33]. However, no single entirely pericyte-specific marker is known to date, and all markers currently used are dynamic in their expression and may be up- or downregulated in conjunction with developmental states, pathological reactions, and *in vitro* culturing conditions [4]. For example, pericytes on normal capillaries typically express desmin, but not SMA, whereas smooth muscle cells on arterioles and pericytes on venues are immunoreactive for both [34]. Therefore, we select three markers that sufficiently

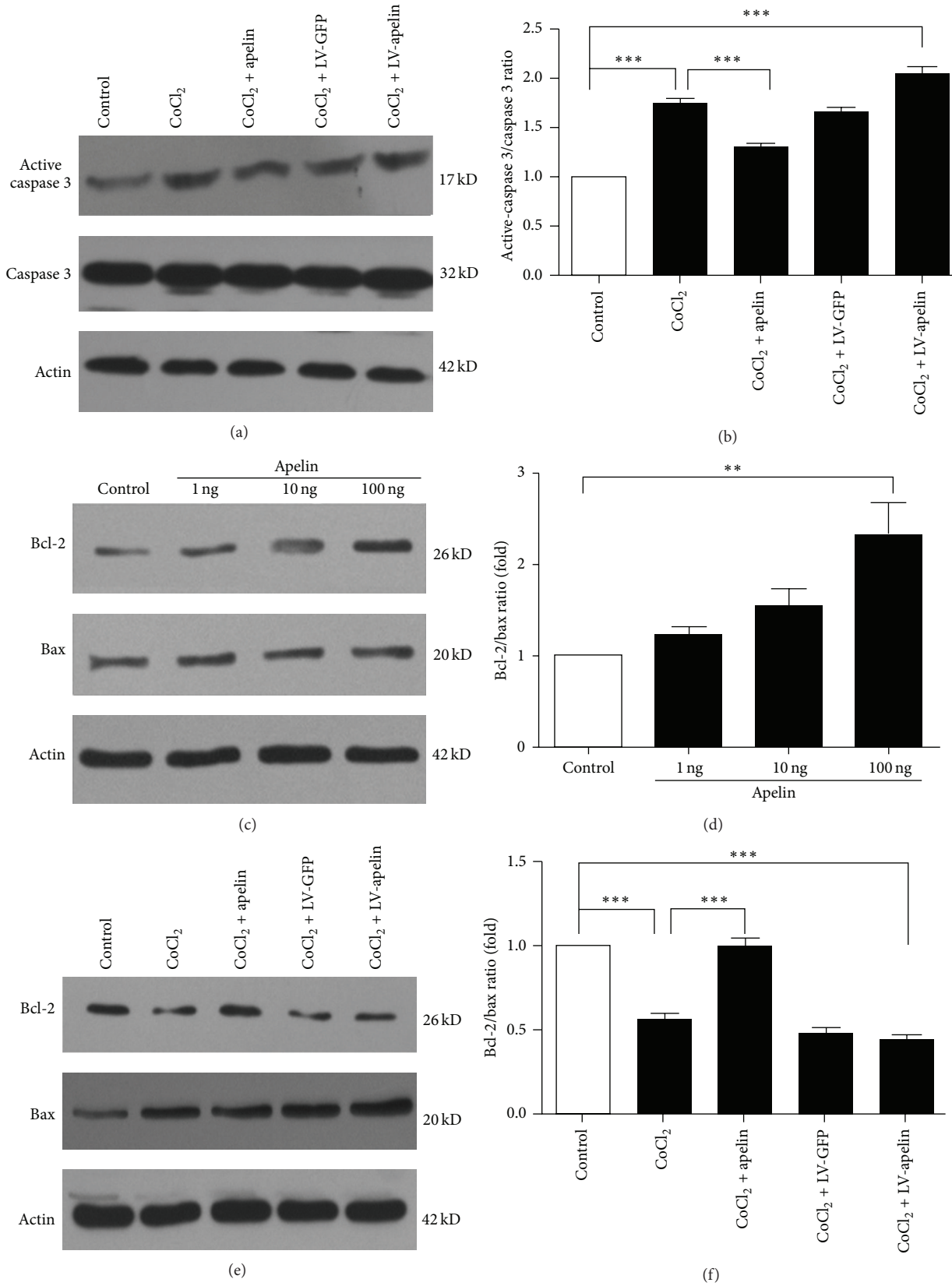

Figure 8: Effect of apelin on hypoxia-induced apoptosis in rat retinal pericytes. (a) Active-caspase 3 protein level significantly increased 12 h after hypoxia injury ($P < 0.001$). Apelin significantly decreased its levels after hypoxia injury ($P < 0.01$). (c and e) Effects of apelin on Bcl-2 and Bax protein expression in rat retinal pericytes. Cells were incubated with apelin and LV-apelin knockout under hypoxia. Western blot analysis was quantitated by densitometry of autoradiographs, and the relative mean ratio of Bcl-2/Bax was increased in apelin group ($P < 0.001$ versus con.) and reduced in Lv-apelin knockdown group ($P < 0.001$ versus con.).

identify pericytes in order to obtain highly pure rat retinal pericytes. In present study, pericytes uniformly expressed the cellular markers PDGFR-β, NG2 and desmin. Our results are consistent with Liu's study, who also proved these markers expressed in pericytes isolated from rats by mechanical morcellation and collagenase digestion [29].

Apelin/APJ is localized in a wide variety of tissues, including the endothelial cells of the primary blood vessels, neurons, and oligodendrocytes [18]. The lines of evidence show that apelin exerts its biological functions through its interaction with APJ. Knockout of apelin or APJ leads to the inhibition of both hypoxia-induced endothelial cell proliferation *in vitro* and hypoxia-induced vessel regeneration in the caudal fin regeneration of Fli-1 transgenic zebrafish [35]. Therefore, location of APJ in cells or tissues is very important with regard to apelin exerting its diverse functions. In the present study, through immunofluorescence staining, we first confirmed the expression of APJ in pericytes and hypoxia-induced upregulation of apelin and APJ. The results of this study showed that the expression of APJ was positive in pericytes, which is essential for apelin/APJ system and plays a role in pathological and physiological condition. This suggested that apelin might be involved in pericyte physiology and pathology.

Apelin was shown to have angiogenic activity in retinal endothelial cells, both *in vitro* and *in vivo* [18]. In our previous studies, we showed that apelin can enhance proliferation and migration of Müller cells and RPE cells [19, 21]. Eyries identified apelin as a hypoxia-inducible factor-1 (HIF-1) target gene and demonstrated that, under hypoxia, HIF-1 binds to the first intron of apelin, leading to upregulation of apelin expression [35]. In the present study, we observed that the viability and migration of pericytes incubated with various concentrations of apelin were enhanced. Under hypoxia exposure, pericytes viability decreased significantly with time-dependent manner and apelin can protect pericytes viability. Furthermore, knockdown of apelin led to a significant decrease in pericyte viability. These results further support the hypothesis that apelin is sensitive to hypoxia, playing a key role in hypoxia-induced pericyte proliferation and migration.

Many *in vitro* and *in vivo* insults, such as hypoxia and ischemia, trigger mixed cell death composed of both necrosis and apoptosis [31, 36]. Hypoxia-induced Bax upregulation, Bcl-2 downregulation, and caspase 3 activation in variety of cells were reversed by HIF-1 overexpression and lead to the acquisition of antiapoptotic properties [37–39]. The ratio of antiapoptotic to proapoptotic proteins, especially the Bcl-2/Bax ratio, determines susceptibility to apoptosis [40]. We therefore investigated whether these pathways were involved in the antiapoptotic effects of apelin in pericytes. Our result was consistent with previous studies, which indicated that Bcl-2/Bax apoptotic signaling pathways mediate the protective effects of the apelin/APJ system in vascular smooth muscle cells and osteoblasts [17, 24]. Caspases, cysteine proteases with aspartate specificity, are important mediators of apoptosis. Caspase 3 is effector caspase that is responsible for cleaving nucleases in addition to cellular substrates. We also revealed that apelin reduced caspase 3 activity, which suggests that apelin inhibits pericyte apoptosis through regulation of activity of caspase 3 and Bcl-2/Bax expression. Therefore, there is a growing consensus that apelin may be a promising therapeutic target against hypoxia/ischemia in the future.

In conclusion, this study demonstrated that apelin/APJ was expressed in PDR patient's membranes and in rat retinal pericytes. Apelin can protect pericytes against hypoxia-induced apoptosis through regulation of activation of caspase 3 and Bcl-2/Bax expression. These results indicated that apelin could be a potential therapeutic target for retinal angiogenic diseases.

5. Conclusion

Pericytes are a population of cells that are involved in normal vessel architecture and contraction and regulated blood flow. Hypoxia causes decreasing of pericytes viability in a time-dependent manner and induced pericytes apoptosis. However, apelin regulated function of pericytes under hypoxia inversely in a concentration-dependent manner and effectively prevented hypoxia-induced apoptosis through downregulating active-caspase 3 expression and increasing the ratio of Bcl-2/Bax.

Conflict of Interests

The authors declare that there is no conflict of interests regarding the publication of this paper.

Acknowledgments

This work has been supported by the National Natural Science Foundation of China (no. 81271027), EFSD/CDS/Lilly Grant (nos. 90561 and 94410), the Program for New Century Excellent Talents in University (no. NCET-12-0010), and Fok Ying Tong Education Foundation (Hong Kong).

References

[1] M. Hellström, H. Gerhardt, M. Kalén et al., "Lack of pericytes leads to endothelial hyperplasia and abnormal vascular morphogenesis," *The Journal of Cell Biology*, vol. 153, no. 3, pp. 543–554, 2001.

[2] P. Lindahl, B. R. Johansson, P. Levéen, and C. Betsholtz, "Pericyte loss and microaneurysm formation in PDGF-B-deficient mice," *Science*, vol. 277, no. 5323, pp. 242–245, 1997.

[3] P. Levéen, M. Pekny, S. Gebre-Medhin, B. Swolin, E. Larsson, and C. Betsholtz, "Mice deficient for PDGF B show renal, cardiovascular, and hematological abnormalities," *Genes & Development*, vol. 8, no. 16, pp. 1875–1887, 1994.

[4] A. Armulik, G. Genové, and C. Betsholtz, "Pericytes: developmental, physiological, and pathological perspectives, problems, and promises," *Developmental Cell*, vol. 21, no. 2, pp. 193–215, 2011.

[5] D. von Tell, A. Armulik, and C. Betsholtz, "Pericytes and vascular stability," *Experimental Cell Research*, vol. 312, no. 5, pp. 623–629, 2006.

[6] A. P. Hall, "Review of the pericyte during angiogenesis and its role in cancer and diabetic retinopathy," *Toxicologic Pathology*, vol. 34, no. 6, pp. 763–775, 2006.

[7] H.-P. Hammes, J. Lin, O. Renner et al., "Pericytes and the pathogenesis of diabetic retinopathy," *Diabetes*, vol. 51, no. 10, pp. 3107–3112, 2002.

[8] Y. Feng, F. vom Hagen, F. Pfister et al., "Impaired pericyte recruitment and abnormal retinal angiogenesis as a result of angiopoietin-2 overexpression," *Thrombosis and Haemostasis*, vol. 97, no. 1, pp. 99–108, 2007.

[9] S. Hughes, T. Gardiner, L. Baxter, and T. Chan-Ling, "Changes in pericytes and smooth muscle cells in the kitten model of retinopathy of prematurity: Implications for plus disease," *Investigative Ophthalmology and Visual Science*, vol. 48, no. 3, pp. 1368–1379, 2007.

[10] Y. Kawamata, Y. Habata, S. Fukusumi et al., "Molecular properties of apelin: tissue distribution and receptor binding," *Biochimica et Biophysica Acta—Molecular Cell Research*, vol. 1538, no. 2-3, pp. 162–171, 2001.

[11] M. de Falco, L. de Luca, N. Onori et al., "Apelin expression in normal human tissues," *In Vivo*, vol. 16, no. 5, pp. 333–336, 2002.

[12] A. Reaux, K. Gallatz, M. Palkovits, and C. Llorens-Cortes, "Distribution of apelin-synthesizing neurons in the adult rat brain," *Neuroscience*, vol. 113, no. 3, pp. 653–662, 2002.

[13] H. Kidoya, M. Ueno, Y. Yamada et al., "Spatial and temporal role of the apelin/APJ system in the caliber size regulation of blood vessels during angiogenesis," *The EMBO Journal*, vol. 27, no. 3, pp. 522–534, 2008.

[14] C. M. Cox, S. L. D'Agostino, M. K. Miller, R. L. Heimark, and P. A. Krieg, "Apelin, the ligand for the endothelial G-protein-coupled receptor, APJ, is a potent angiogenic factor required for normal vascular development of the frog embryo," *Developmental Biology*, vol. 296, no. 1, pp. 177–189, 2006.

[15] C. Hara, A. Kasai, F. Gomi et al., "Laser-induced choroidal neovascularization in mice attenuated by deficiency in the apelin-APJ system," *Investigative Ophthalmology and Visual Science*, vol. 54, no. 6, pp. 4321–4329, 2013.

[16] Q.-F. Liu, H.-W. Yu, L. You, M.-X. Liu, K.-Y. Li, and G.-Z. Tao, "Apelin-13-induced proliferation and migration induced of rat vascular smooth muscle cells is mediated by the upregulation of Egr-1," *Biochemical and Biophysical Research Communications*, vol. 439, no. 2, pp. 235–240, 2013.

[17] R.-R. Cui, D.-A. Mao, L. Yi et al., "Apelin suppresses apoptosis of human vascular smooth muscle cells via APJ/PI3-K/Akt signaling pathways," *Amino Acids*, vol. 39, no. 5, pp. 1193–1200, 2010.

[18] A. Kasai, N. Shintani, M. Oda et al., "Apelin is a novel angiogenic factor in retinal endothelial cells," *Biochemical and Biophysical Research Communications*, vol. 325, no. 2, pp. 395–400, 2004.

[19] D. Qin, X.-X. Zheng, and Y.-R. Jiang, "Apelin-13 induces proliferation, migration, and collagen I mRNA expression in human RPE cells via PI3K/Akt and MEK/Erk signaling pathways," *Molecular Vision*, vol. 19, pp. 2227–2236, 2013.

[20] Q. Lu, Y.-R. Jiang, J. Qian, and Y. Tao, "Apelin-13 regulates proliferation, migration and survival of retinal Müller cells under hypoxia," *Diabetes Research and Clinical Practice*, vol. 99, no. 2, pp. 158–167, 2013.

[21] X.-L. Wang, Y. Tao, Q. Lu, and Y.-R. Jiang, "Apelin supports primary rat retinal Müller cells under chemical hypoxia and glucose deprivation," *Peptides*, vol. 33, no. 2, pp. 298–306, 2012.

[22] A. Sendoel and M. O. Hengartner, "Apoptotic cell death under hypoxia," *Physiology*, vol. 29, no. 3, pp. 168–176, 2014.

[23] Y. Fang, Q. Zhang, J. Tan, L. Li, X. An, and P. Lei, "Intermittent hypoxia-induced rat pancreatic beta-cell apoptosis and protective effects of antioxidant intervention," *Nutrition & Diabetes*, vol. 4, no. 9, article e131, 2014.

[24] H. Xie, L.-Q. Yuan, X.-H. Luo et al., "Apelin suppresses apoptosis of human osteoblasts," *Apoptosis*, vol. 12, no. 1, pp. 247–254, 2007.

[25] S.-Y. Tang, H. Xie, L.-Q. Yuan et al., "Apelin stimulates proliferation and suppresses apoptosis of mouse osteoblastic cell line MC3T3-E1 via JNK and PI3-K/Akt signaling pathways," *Peptides*, vol. 28, no. 3, pp. 708–718, 2007.

[26] X. Zeng, S. P. Yu, T. Taylor, M. Ogle, and L. Wei, "Protective effect of apelin on cultured rat bone marrow mesenchymal stem cells against apoptosis," *Stem Cell Research*, vol. 8, no. 3, pp. 357–367, 2012.

[27] O. S. Kim, J. Kim, C.-S. Kim, N. H. Kim, and J. S. Kim, "KIOM-79 prevents methyglyoxal-induced retinal pericyte apoptosis in vitro and in vivo," *Journal of Ethnopharmacology*, vol. 129, no. 3, pp. 285–292, 2010.

[28] J. Cai, O. Kehoe, G. M. Smith, P. Hykin, and M. E. Boulton, "The angiopoietin/Tie-2 system regulates pericyte survival and recruitment in diabetic retinopathy," *Investigative Ophthalmology and Visual Science*, vol. 49, no. 5, pp. 2163–2171, 2008.

[29] G. Liu, C. Meng, M. Pan et al., "Isolation, purification, and cultivation of primary retinal microvascular pericytes: a novel model using rats," *Microcirculation*, vol. 21, no. 6, pp. 478–489, 2014.

[30] Y. Tao, Q. Lu, Y.-R. Jiang et al., "Apelin in plasma and vitreous and in fibrovascular retinal membranes of patients with proliferative diabetic retinopathy," *Investigative Ophthalmology & Visual Science*, vol. 51, no. 8, pp. 4237–4242, 2010.

[31] A. Y. Xiao, L. Wei, S. Xia, S. Rothman, and S. P. Yu, "Ionic mechanism of ouabain-induced concurrent apoptosis and necrosis in individual cultured cortical neurons," *The Journal of Neuroscience*, vol. 22, no. 4, pp. 1350–1362, 2002.

[32] E. Beltramo, E. Berrone, S. Giunti, G. Gruden, P. C. Perin, and M. Porta, "Effects of mechanical stress and high glucose on pericyte proliferation, apoptosis and contractile phenotype," *Experimental Eye Research*, vol. 83, no. 4, pp. 989–994, 2006.

[33] M. Krueger and I. Bechmann, "CNS pericytes: concepts, misconceptions, and a way out," *Glia*, vol. 58, no. 1, pp. 1–10, 2010.

[34] S. Morikawa, P. Baluk, T. Kaidoh, A. Haskell, R. K. Jain, and D. M. McDonald, "Abnormalities in pericytes on blood vessels and endothelial sprouts in tumors," *The American Journal of Pathology*, vol. 160, no. 3, pp. 985–1000, 2002.

[35] M. Eyries, G. Siegfried, M. Ciumas et al., "Hypoxia-induced apelin expression regulates endothelial cell proliferation and regenerative angiogenesis," *Circulation Research*, vol. 103, no. 4, pp. 432–440, 2008.

[36] L. Wei, D. J. Ying, L. Cui, J. Langsdorf, and S. Ping Yu, "Necrosis, apoptosis and hybrid death in the cortex and thalamus after barrel cortex ischemia in rats," *Brain Research*, vol. 1022, no. 1-2, pp. 54–61, 2004.

[37] B. Yang, K. He, F. Zheng et al., "Over-expression of hypoxia-inducible factor-1 alpha in vitro protects the cardiac fibroblasts from hypoxia-induced apoptosis," *Journal of Cardiovascular Medicine*, vol. 15, no. 7, pp. 579–586, 2014.

[38] B.-F. Wang, X.-J. Wang, H.-F. Kang et al., "Saikosaponin-D enhances radiosensitivity of hepatoma cells under hypoxic conditions by inhibiting hypoxia-inducible factor-1alpha," *Cellular Physiology and Biochemistry*, vol. 33, no. 1, pp. 37–51, 2014.

[39] A. Nishimoto, N. Kugimiya, T. Hosoyama, T. Enoki, T.-S. Li, and K. Hamano, "HIF-1α activation under glucose deprivation plays a central role in the acquisition of anti-apoptosis in human colon cancer cells," *International Journal of Oncology*, vol. 45, no. 6, pp. 2077–2084, 2014.

[40] Z. N. Oltvai, C. L. Milliman, and S. J. Korsmeyer, "Bcl-2 heterodimerizes in vivo with a conserved homolog, Bax, that accelerates programed cell death," *Cell*, vol. 74, no. 4, pp. 609–619, 1993.